MINISTRY OF EDUCATION AND SCIENCE UKRAINE

ODESSA I. I. MECHNIKOV NATIONAL UNIVERSITY

ФОТОЭЛЕКТРОНИКА

PHOTOELECTRONICS
INTER-UNIVERSITIES SCIENTIFIC ARTICLES

Founded in 1986

Number 25

ODESSA
ONU
2016

«PHOTOELECTRONICS»
№ 2 5 – 2 0 1 6

INTER-UNIVERSITIES SCIENTIFIC ARTICLES

Founded in 1986

Certificate of State Registration
KB № 15953

«ФОТОЭЛЕКТРОНИКА»
№ 25–2016

МЕЖВЕДОМСТВЕННЫЙ НАУЧНЫЙ СБОРНИК

Основан в 1986 г.

Свидетельство о Государственной регистрации
KB № 15953

UDC 621.315.592:621.383.51:537.221

The results of theoretical and experimental studies in problems of the semiconductor and micro-electronic devices physics, opto- and qantum electronics, quantum optics, spectroscopy and photophysics of nucleus, atoms, molecules and solids are presented in the issue. New directions in the photoelectronics, stimulated by problems of the super intense laser radiation interaction with nuclei, atomic systems and substance, are considered. Scientific articles «Photoelectronics» collection abstracted in ВИНИТИ and «Джерело»

Scientific articles «Photoelectronics» collection abstracted in ВИНИТИ and «ДЖЕРЕЛО»,and are in scientificmetric base INDEX COPERNICUS.

The issue is introduced to the List of special editions of the Ukrainian Higher Certification Com-mission in physics-mathematics and technical sciences.

For lecturers, scientists, post-graduates and students.

У збірнику наведено результати теоретичних і експериментальних досліджень з питань фізики напівпровідників та мікроелектронних приладів, опто- та квантової електроніки, квантової оптики, спектроскопії та фотофізики ядра, атомів, молекул та твердих тіл. Розглянуто нові напрямки розвитку фотоелектроніки, пов'язані із задачами взаємодії надінтенсивного лазерного випромінювання з ядром, атомними системами, речовиною.

Збірник включено до Переліку спеціальних видань ВАК України з фізико-математичних та технічних наук. Збірник «Photoelectronics» реферується у ВІНІТІ (Москва) та «Джерело» (Київ) і знаходиться у науковометричній базі INDEX COPERNICUS

Для викладачів, наукових працівників, аспіранітв, студентів

В сборнике приведены результаты теоретических и экспериментальных исследований по вопросам физики полупроводников и микроэлектронных приборов, опто- и квантовой электроники, квантовой оптики, спектроскопии и фотофизики ядра, атомов, молекул и твердых тел. Рассмотрены новые направ¬ления развития фотоэлектроники, связанные с задачами взаимодействия сверхинтенсивного лазерного излучения с ядром, атомными системами, веществом.

Сборник включен в Список специальных изданий ВАК Украины по физико-математическим и тех¬ническим наукам. Сборник «Photoelectronics» реферируется в ВИНИТИ (Москва) и «Джерело» (Киев) и находится в наукометричной базе INDEX COPERNICUS

Для преподавателей, научных работников, аспирантов, студентов

Address of editorial board:

Odessa I. I. Mechnikov National University 42, Pasteur str., Odessa, 65026, Ukraine
Information is on the site: http://phys.onu.edu.ua/journals/photoele/
http://experiment.onu.edu.ua/exp_ru/files/. photoelectronics@onu.edu.ua

TABLE OF CONTENTS:

UDC 621.315.592

V. I. Irkha, V. E. Gorbachev, I. M. Vikulin

Odessa National Academy of Communications named after A.S. Popov,
1, Kuznechna Str., Odessa, 65020, Ukraine
e-mail: phys@onat.edu.ua

SENSOR OF MAGNETIC FIELD BASED ON A LIGHT-EMITTING DIODE

New effects of modification of spectrum of radiation of light-emitting diode in magnetic field, which give the chance to use a LED as an optoelectronic magnetic field sensor, are discovered. Physical phenomena that appear in light-emitting diodes in a magnetic field are considered.

Amplitude-modulated by a magnetic field the optical signal can be obtained if to use a LED with narrow base, where it is possible to gain 50 % magnification of energy of an emission light in a magnetic field. If a LED with long vary-band base is being used as magneto-sensitive element, the magnetic field will shift effective region of recombination to a section with other energy gap, and the LED's radiated frequency will change. Thus, we obtain a frequency-modulated by a magnetic field optical signal, which is resistant to noises in optical channels.

Such detectors of magnetic field are expedient for using in systems with optical processing methods of the

1. Introduction

Development of the modern informational technologies and communication systems requires diversification of elements of optoelectronics, development of new and improvement of existing electronic devices of generation, receiving and storage of the optical information. Though optoelectronic devices are principal components of telecommunication webs, however even more often they are used in industrial measurements, in data reduction systems, etc. Expansion of application area of optoelectronic systems gives the chance to use specified devices as sensors of certain physical quantities, in particular - of magnetic field [1, 2].

In the paper the new effects of modification of spectrum of radiation of light-emitting diode (LED) in magnetic field, which give the chance to use a LED as an optoelectronic magnetic field sensor, are investigated. Physical phenomena that appear in light-emitting diodes in a magnetic field are considered.

2. Discussion of outcomes of experiment

During the moving of charge carriers in semiconductor sample in magnetic field, transversal to the direction of movement, the Lorentz force acts on them. It deflects charge carriers to one of the sides of semiconductor, consequently their concentration there increases, and decreases on the opposite side. Therefore, in the semiconductor, that is placed in transversal magnetic field, at electric current passing because of acting Lorentz force curvature of current line happens. However, as a result of spatial separation of charges, an electric field, that will impede charges separation, arises, and as soon as force, produced by this field, becomes equal to Lorentz force, further separation of charges by magnetic field stops and current lines straighten out. Thus, in semiconductor sample placed into magnetic field the transversal Hall's voltage appears, that depends on both charge carriers' concentration and size of magnetic field. Owing to this Hall's effect different sensors of magnetic field are constructed.

If we place diode into magnetic field, then it is possible to determine three main physical phenomena:

Firstly, in consequence of magnetoresistance effect, charge carriers' mobility decreases, and, subsequently, diode conductivity strongly decreases. Meanwhile the magnetoresistance effect will be increasing in tens and hundreds times due to the change of injection of charge carriers.

Secondly, curvature of current lines increases concentration of charge carriers on one side and decreases on another side. Since effective lifetime of carriers in thin plat is determined by surface recombination, then redistribution of carriers leads to change of role of surface recombination and effective lifetime of carriers. Role of recombination on the side, to which the charge carriers deflect, increases, and recombination on another side almost doesn't play any role.

Thirdly, since concentrations of electrons and holes nearby p-n junction are practically identical, the Hall's electric field will be absent. That's why current lines will always be curved. Elongation of current line leads to reduction of penetration depth of unbalanced carriers and extra reduction of modulation of base region conductivity by injected carriers.

Such phenomena were also observed in magnetotransistors. It is obvious that in transistor, placed into magnetic field, increasing of average path, which charge carriers pass in base region, happens as well. That leads to increase of quantity of charge carriers, whic h will recombine in transistor's base region. Current transmission coefficient increases.

First two phenomena are well studied. We researched magnetic field impact on characteristics of semiconductor radiating heterostructures, taking into account

As a sensing element of optoelectronic's sensor of some physical quantity it is possible to use either a LED, or a light guide, or a photodetector. The operating principle of the majority optoelectronic sensors is based on a changing of absorption coefficient at light transiting through medium or on a modification of a transmission factor of light during the reflection from interfaces of mediums.

Magneto-sensitive properties of light-emitting diodes we tested in papers [3]. We have obtained, that intensity and spectrum of radiation of a light-emitting diodes varies in a crosswise magnetic field.

The emission intensity of light-emitting diodes in a magnetic field can be either increased up to 50 % or decreased depending on diode structure.

Only in light-emitting diodes with vary-band structure a changing of spectrum of radiation is detected. For these light-emitting diodes the energy of a maximum of a spectrum of radiation in a magnetic field with an induction 0.4 Tesla shifts on 10-15 % relative to the position in lack of a magnetic field.

We experimentally researched the AlAsGa triple-compound light-emitting diodes doped by silicon with a heterojunction as an injecting contact. Samples have been made on substrates of gallium arsenide on which the epitaxial method spliced two stratums: light-emitting p-layer from $Ga_{1-x}Al_xAs<Ge>$ and electrons-injecting n-layer from $Ga_{1-y}Al_yAs<Te>$, where x=0,5…0,6 and y=0,22…0,25. The radiating layer had a thickness 4,9 μm, and injecting layer - 11,2 μm. Traversal sizes of samples were 500×500 μm. The working current of light-emitting diode samples had value 10 mA. We applied a magnetic field with an induction up to 0.4 Tesla across to a direction of motion of the injected charge carriers in light-emitting diodes.

Two types of samples with various structure of base were investigated. For the first type of samples, the semiconductor had an equal energy gap on all volume of base. Base length W was less, than a diffusion length L of injected charge carriers. In this case the injected charge carriers recombine with radiation in whole bulk of base. But a part of charge carriers near the lateral surface of base, through which there is a radiation, recombine without radiation through the surface states.

The transverse magnetic field bends a mechanical trajectory of the injected charge carriers, deflecting them from a surface. The angle φ on which the injected charge carriers are being deviated from an electric field direction, is being defined as

$$\mathrm{tg}\varphi = \mu B, \qquad (1)$$

where μ – mobility of injected charge carriers; B – induction of external magnetic field.

Thus in an optimum case the linear deviation of the injected charge carriers from an electric field direction

$$D = L\cos\varphi = L\cos[\mathrm{arctg}(\mu B)] , \qquad (2)$$

as only on this area of p-region equal to diffusion length L there is light generation.

At big values of D only the passive part of p-region is being increased, that leads to decrease of efficiency of LED. Recombination rate of the injected charge carriers near the current-carrying contact of p-region is essential more than in its volume. Therefore near the contact there is no accumulation of charge carriers.

At a forward bias of the light-emitting diode there is an injection of electrons from n-region to a p-region where they radiative recombine with holes. The radiation output is carried out through n-region perpendicular to plane of p-n- junction. In a traversal magnetic field the trajectory of the injected charge carriers is bent, therefore their path through radiating area of p-region is increased, that is equivalent to increasing of effective length of radiating area. Thus, the amount of recombined electrons in radiating field is increased.

The part of a surface nonradiative recom-bination decreases, that leads to growing of effective diffusion length L of injected carriers and to increasing of intensity of radiation of LED. In this case for light-emitting diodes with small length W of base the radiation spectrum does not vary.

The other type of light-emitting diodes had variband base with decreasing of an energy gap from n – region to p – region, and length of base W turned out more than diffusion length L. Therefore the injected charge carriers recombine in a narrow section of base with a certain energy gap (see fig. 1).

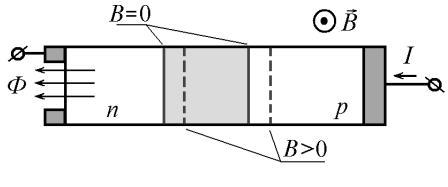

Fig. 1. Structure of magneto-sensitive LED with variband base in a magnetic field

Effect of the surface recombination was insignificant in contrast to light-emitting diodes with small length of base. At turning on of a magnetic field we have obtained some decreasing of radiant intensity of these light-emitting diodes. Obviously, because of the elongated shape of base, the magnetic field presses the injected charge carriers to one of surfaces of base, where they nonradiatively recombine.

In light-emitting diodes with variband base in a transversal magnetic field we observed phenomenon of displacement of a maximum of a spectrum of radiation relative to its position in lack of a magnetic field (fig. 2). It can be explained that the region of a recombination of charge carriers is being translated along base (on fig. 1 is marked out by a dot line $B>0$), therefore charge carriers will radiatively recombine in the region of base with other energy gap E.

As diffusion length L in a magnetic field is being decreased, we expected that the spectrum of radiation of a LED will become narrower. However experimental measurements have shown that the half-width of a spectrum of radiation in a magnetic field does not vary.

In some samples at turning on of a magnetic field we have obtained displacement of a spectrum of radiation in other side. As the half-width of a spectrum of radiation of a LED in a magnetic field does not vary, therefore the displacement to one or another side of electron-hole plasma in a magnetic field we explain by a change of sign of bipolar mobility. This phenomenon is observed in p-n-junctions with high-resistance base [4].

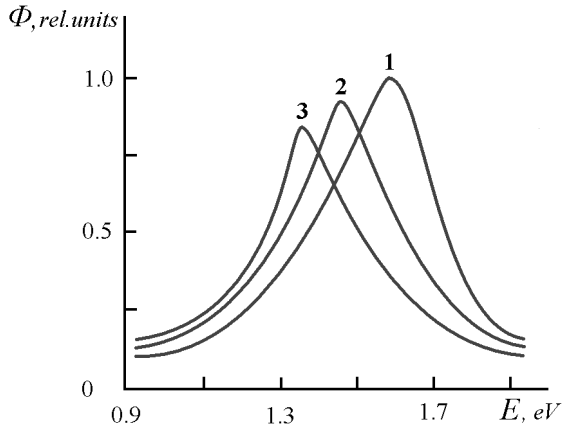

Fig. 2. Spectrums of an electroluminescence of a LED with variband base without a magnetic field (1) and at affecting of a magnetic field (2 – 0.37 Tesla, 3 – 0.4 Tesla)

On fig. 2 the dependence from magnetic induction B of relative photon energy in a maximum of radiation E and relative intensity of radiation Φ for a LED with variband base are presented. We can see that the effect of displacement of frequency of photon energy in a maximum of a spectrum of radiation is more essential, than decreasing of intensity of radiation of a LED at magnetic field turning on.

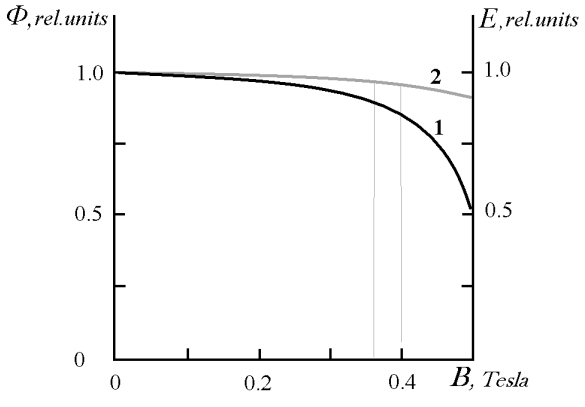

Fig. 3 Dependence of photon energy in a maximum of radiation (1) and intensity of radiation (2) of a LED with variband base from magnetic induction

As seen on fig. 2 and 3, key parameter depending on a magnetic field can be either light intensity, or frequency of radiation. Advantage of using of light intensity as an informative parameter is a simplicity of registration of its variations by a usual photodetector. However, in this case certain difficulty arises if it is necessary to consider absorption of light during its transmission through a light guide, especially at switching of optical channels.

If one uses the frequency of radiation as informative parameter, then necessity of consideration of properties of a LED and optical channels disappears, but transformation of a variation of frequency of radiation to a variation of amplitude of an output current of a photodetector is more difficult, than light intensity transformation.

3 Conclusion

We have considered two possibilities of making optoelectronic magnetic field detectors.

At first we used a usual LED with narrow base. The transversal magnetic field deflects the injected charge carriers from a base surface where they recombine without radiation through the superficial states. In volume of base the charge carriers recombine with radiation therefore radiation intensity of a LED is being increased. If one correctly uses features of structure of such light-emitting diodes, it is possible to obtain 50 % magnification of energy of radiation in a magnetic field. For photoelectric registration of a variation of radiant intensity it is possible to use usual the photodetector. For production of such magneto-optical devices a special manufacturing methods is not required, therefore they are low-price. However at using of such devices in optical information processing systems it is necessary to consider absorption in transmission channels.

For elimination of influence of absorption in optical channels on the level of useful signal it is possible to use more complex structure of the detector in which magnetic field changes frequency of radiation. As a magneto-sensitive device we suggest a LED with long base along which an energy gap of the semiconductor should be various. At such structure the radiation recombination of charge carriers happens in narrow region of base with a certain energy gap. The magnetic field shifts the effective field of a recombination along the base on a section with other energy gap, as a result the frequency of radiation will be changed. Thus, we obtain a frequency-modulated by a magnetic field optical signal, which resistant to noise in optical channels. However, for monitoring of modifications of frequency the special photodetector or the multiplexer in this case is required.

Such detectors of magnetic field are expedient for using in systems with optical processing methods of the information.

References

1. 1. Kai X.Dezhi Y.and all. Magnetic field effects on electroluminescence in phosphorescence organic light emitting diodes// Organic Electronics, –2014, V.15, N.2, –P. 590-594.
2. 2. Sun L., Jiang S., Marciante J. R. All-fiber optical magnetic-field sensor based on Faraday rotation in highly terbium-doped fiber// Optics express, –2010,

V.18, N. 6. – P. 5407-5412.
3. V. Irkha, V. Gorbachev, I. Vikulin. Light-emitting diode as a magnetic field sensor. / Proceedings of XIII International Conference TCSET'2016, Lviv, February 23-26, 2016. P. 79-81.
4. Vikulin I.M., Stafeev V.I. Physics of Semiconducting Devices. – M.: Radio and communications. 1998. -264 p.

This article has been received in April 2016

UDC 621.315.592

V. I. Irkha, V. E. Gorbachev, I. M. Vikulin

SENSOR OF MAGNETIC FIELD BASED ON A LIGHT-EMITTING DIODE

Summary

New effects of modification of spectrum of radiation of light-emitting diode in magnetic field, which give the chance to use a LED as an optoelectronic magnetic field sensor, are discovered. Physical phenomena that appear in light-emitting diodes in a magnetic field are considered. Amplitude-modulated by a magnetic field the optical signal can be obtained if to use a LED with narrow base, where it is possible to gain 50 % magnification of energy of an emission light in a magnetic field. If a LED with long vary-band base is being used as magneto-sensitive element, the magnetic field will shift effective region of recombination to a section with other energy gap, and the LED's radiated frequency will change. Thus, we obtain a frequency-modulated by a magnetic field optical signal, which is resistant to noises in optical channels. Such detectors of magnetic field are expedient for using in systems with optical processing methods of the information.

Keywords: magneto-optical sensor, LED, vary-band structure, magnetic field, frequency-modulated light.

УДК 621.315.592

В. І. Ірха, В. У. Горбачов, І. М. Вікулін

ДАТЧИК МАГНІТНОГО ПОЛЯ НА ОСНОВІ СВІТЛОВИПРОМІНЮЮЧОГО ДІОДА

Резюме

Виявлені нові ефекти зміни спектру випромінювання світлодіода в магнітному полі, які дають можливість використати світлодіод, як оптоелектронний датчик магнітного поля. Розглядаються фізичні явища, які відбуваються у світлодіодах під дією магнітного поля. У роботі досліджені нові фізичні механізми для створення оптоелектронного магнитодатчика і процеси, що протікають у світлодіодах під дією магнітного поля. Амплітудно-модульований магнітним полем оптичний сигнал можна отримати, якщо використати звичайний світлодіод з вузькою базою, де можна отримати 50% збільшення енергії випромінювання в магнітному полі. Якщо в якості магниточутливого елементу використати світлодіод з варізонною довгою базою, то магнітне поле зрушуватиме ефективну область рекомбінації на ділянку з іншою

шириною забороненої зони, і частота випромінювання світлодіода зміниться. Таким чином, ми отримуємо частотно-модульований магнітним полем оптичний сигнал стійкий до перешкод в оптичних каналах. Такі датчики доцільно використовувати в системах з оптичними методами обробки інформації.

Ключові слова: магнітооптичний сенсор, світлодіод, варізонна структура, магнітне поле, частотно-модульоване світло.

УДК 621.315.592

В. И. Ирха, В. Э. Горбачев, И. М. Викулин

ДАТЧИК МАГНИТНОГО ПОЛЯ НА ОСНОВЕ СВЕТОИЗЛУЧАЮЩЕГО ДИОДА

Резюме

Обнаружены новые эффекты изменения спектра излучения светодиода в магнитном поле, которые дают возможность использовать светодиод, как оптоэлектронный датчик магнитного поля. Рассматриваются физические явления, которые происходят в светодиодах под действием магнитного поля. В работе исследованы новые физические механизмы для создания оптоэлектронного магнитодатчика и процессы, протекающие в светодиодах под действием магнитного поля. Амплитудно-модулированный магнитным полем оптический сигнал можно получить, если использовать обычный светодиод с узкой базой, где можно получить 50% увеличение энергии излучения в магнитном поле. Если в качестве магниточувствительного элемента использовать светодиод с варизонной длинной базой, то магнитное поле будет сдвигать эффективную область рекомбинации на участок с другой шириной запрещенной зоны, и частота излучения светодиода изменится. Таким образом, мы получаем частотно модулированный магнитным полем оптический сигнал устойчивый к помехам в оптических каналах. Такие датчики целесообразно использовать в системах с оптическими методами обработки информации.

Ключевые слова: магнитооптический сенсор, светодиод, варизонная структура, магнитное

UDC 539.182

A. V. Glushkov

Odessa State Environmental University, L'vovskaya str.15, Odessa-16, 65016, Ukraine
E-mail: dirac13@mail.ru

RELATIVISTIC THEORY OF THE NEGATIVE MUON CAPTURE BY AN ATOM

We reviewed an effective consistent approach to determination of the cross-section for the negative muon capture by an atomic system. The approach is based on the relativistic many-body perturbation (PT) theory with using the Feynman diagram technique and a generalized relativistic energy approach in a gauge-invariant formulation. The corresponding capture cross-section is connected with an imaginary (scattering) part of the electron subsystem energy shift ImδE (till the QED perturbation theory order). The some calculation results for cross-section of the negative muon μ - capture by He atom are listed and reviewed. The theoretical and experimental studying the muon-γ-nuclear interaction effects opens prospects for nuclear quantum optics, probing the structural features of a nucleus and muon spectroscopy in atomic and molecular photophysics.

1. Introduction

Muonic atoms have always been useful tools for nuclear (atomic) spectroscopy employing atomic-physics techniques. Electrons, muons (other particles such as kaons, pions etc) originally in the ground state of the target atom can be excited reversibly either to the bound or continuum states. With appearance of the intensive neutron pencils, laser sources studying the γ-μ-nuclear interactions is of a great importance [1-20]. The rapid progress in laser technology even opens prospects for nuclear quantum optics via direct laser-nucleus coupling [19-26]. It is known that a negative muon μ^- captured by a metastable nucleus may accelerate a discharge of the latter by many orders of magnitude [18-22]. The μ-atom system differs advantageously of the usual atom; the relation r_n/r_a (r_n is a radius of a nucleus and r_a is a radius of an atom) can vary in the wide limits in dependence upon the nuclear charge. The estimates of probabilities for discharge of a nucleus with emission of γ quantum and further muon or electron conversion are presented in ref. [2-4,19,20,22]. Despite the relatively long history, studying processes of the muon-atom and muon-nucleus interactions hitherto remains very actual and complicated problem. Theoretical estimates in different models differ significantly [1-4,22]. According to Mann & Rose, the μ capture occurs mainly at the energies of E~10κeV, but according to Bayer, muons survive till thermal energies [2,20]. In many papers different authors predicted the μ capture energies in the range from a few dozens to thousands eV. The standard theoretical approach to problem bases on the known Born approximation with the plane or disturbed wave functions and the hydrogen-like functions for the discrete states. In papers by Vogel etal and Leon-Miller the well-known Fermi-Teller model is used (the atomic electrons are treated as an electron gas and a muon is classically described) [2-4]. In paper by Cherepkov and Chernysheva [2] the Hartree-Fock (HF) method is used to calculate the cross-sections of the capture, elastic and inelastic scattering of the negative μ on the He atom. In recent years more advanced approaches using the fermion molecular dynamics method are used to solve the scattering and capture problem [4,5]. The Kravtsov-Mikhailov model [4] describes transition of a muon from the excited muonic H to He based on quasimolecular concept. The series of papers by Ponomarev et al on treating the muonic nuclear catalysis use ideas of Alvarets et al [5]. More sophisticated methods of the relativistic (QED) PT should be used for correct treating the muon capture effects by multielectron atoms (nuclei). In Refs. [20] it has been presented the theoretical basis of a new relativistic energy

formalism. Here we reviewed some aspects of this approach to calculation of the cross-section of the negative muon capture by atoms, using relativistic many-body PT [20,24-27] and listed some computing results for the cross-section of μ^- capture by the He atom.

2. Relativistic energy approach to the muon-atom interaction

2.1. General Formalism

In atomic theory, a convenient field procedure is known for calculating the energy shifts ΔE of the degenerate states. Secular matrix M diagonalization is used. In constructing M, the Gell-Mann and Low adiabatic formula for ΔE is used. A similar approach, using this formula with the QED scattering matrix, is applicable in the relativistic theory [20,24-27]). In contrast to the non-relativistic case, the secular matrix elements are already complex in the PT second order (first order of the inter-electron interaction). Their imaginary parts relate to radiation decay (transition) probability. The total energy shift of the state is usually presented as follows:

$$\Delta E = \mathrm{Re}\Delta E + \mathrm{i}\ \mathrm{Im}\Delta E, \tag{1a}$$

$$\mathrm{Im}\ \Delta E = -\Gamma/2, \tag{1b}$$

where Γ is interpreted as the level width, and the decay possibility $P=\Gamma$. The whole calculation of energies and decay probabilities of a non-degenerate excited state is reduced to calculation and diagonalization of the complex matrix M. To start with the Gell-Mann and Low formula it is necessary to choose the PT zero-order approximation. Usually, the one-electron Hamiltonian is used, with a central potential that can be treated as a bare potential in the formally exact QED PT. There are many well-known attempts to find the fundamental optimization principle for construction of the bare one-electron Hamiltonian (for free atom or atom in a field) or (what is the same) for the set of the one-quasiparticle (QP) functions, which represent such a Hamiltonian [24-27]. Here we consider closed electron shell atoms (ions). For example, the ground state $1s^2$ of the He atom or He-like ion. As the bare potential, one usually includes the electric nuclear potential V_N and some parameterized screening potential V_C. The parameters of the bare potential may be chosen to generate the accurate eigen-energies of all two-QP states. In the PT second order the energy shift is expressed in terms of the two-QP matrix elements [20,24-27]:

$$V(1,2;4,3) = \sqrt{(2\mathrm{j}_1+1)(2\mathrm{j}_2+1)(2\mathrm{j}_3+1)(2\mathrm{j}_4+1)}\cdot$$

$$\cdot(-1)^{j_1+j_2+j_3+j_4+m_1+m_2}\cdot \tag{2}$$

$$\times\sum_{\lambda,\nu}(-1)^{\nu}\begin{bmatrix} j_1 \ldots\ldots j_3 \ldots \lambda \\ m_1 \ldots -m_3 \ldots \nu \end{bmatrix}\begin{bmatrix} j_2 \ldots\ldots j_4 \ldots \lambda \\ m_2 \ldots -m_4 \ldots \nu \end{bmatrix} Q_\lambda^{Qul}$$

Here Q_λ^{Qul} is corresponding to the Coulomb inter-particle interaction:

$$Q_\lambda^{Qul} = \{R_\lambda(1243)S_\lambda(1243) + R_\lambda(\tilde{1}24\tilde{3})S_\lambda(\tilde{1}24\tilde{3}) + \\ + R_\lambda(1\tilde{2}\tilde{4}3)S_\lambda(1\tilde{2}\tilde{4}3) + R_\lambda(\tilde{1}\tilde{2}\tilde{4}\tilde{3})S_\lambda(\tilde{1}\tilde{2}\tilde{4}\tilde{3})\}, \tag{3}$$

where $R_\lambda(1,2;4,3)$ is the radial integral of the Coulomb inter-QP interaction with large radial Dirac components; the tilde denotes a small Dirac component; S_λ is the angular multiplier (see details in Refs.[20,24-30]). To calculate all necessary matrix elements one must have the 1QP relativistic functions. Further we briefly outline the main idea using, as an example, the negative muon capture by He atom: $((ls)^2[J_iM_i],\ \varepsilon_{in}^{\mu})\rightarrow(ls\varepsilon l,\varepsilon_{nl}^{\mu})$. Here J_i is the total angular moment of the initial target state; indices ε_{in}^{μ} and ε_{fk}^{μ} are the incident and discrete state energies, respectively to the incident and captured muons. Further it is convenient to use the second quantization representation. In particular, the initial state of the system "atom plus free muon" can be written as $a_{n}^{+\mu}\Phi_0$ state. The final state is that of an atom with the discrete state electron, removed electron and captured muon; in further $|I\rangle$ represents one-particle (1QP) state, and $|F\rangle$ represents the three-quasiparticle (3QP) state. The imaginary (scattering) part of the energy shift $Im\ \Delta E$ in the atomic PT second order (fourth order of the QED PT) is as follows [20,24,25]:

$$\mathrm{Im}\Delta E = \pi G(\varepsilon_{iv}, \varepsilon_{ie}, \varepsilon^{\mu}_{in}, \varepsilon^{\mu}_{fk}), \quad (4)$$

where indices *e,v* are corresponding to atomic electrons and *G* is a definite squired combination of the two-QP matrix elements (2). The value σ=*-2 Im*ΔE represents the capture cross-section if the incident muon eigen-function is normalized by the unit flow condition. The different normalization conditions are used for the incident and captured state QP wave functions. The details of the whole numerical procedure of calculation of the cross-sections can be found in Refs. [20,24-27].

2.2 The Dirac-Kohn-Sham Relativistic Wave Functions

Usually, a multielectron atom is defined by a relativistic Dirac Hamiltonian(the a.u. used):

$$H = \sum_i h(r_i) + \sum_{i>j} V\left(r_i r_j\right). \quad (5)$$

Here, *h(r)* is one-particle Dirac Hamiltonian for electron in a field of the finite size nucleus and *V* is potential of the inter-electron interaction. The relativistic inter electron potential is as follows [20,24,25]:

$$V\left(r_i r_j\right) = exp\left(i\omega_{ij} r_{ij}\right) \cdot \frac{\left(1 - \alpha_i \alpha_j\right)}{r_{ij}}, \quad (6)$$

where ω_{ij} is the transition frequency; α_i ,α_j are the Dirac matrices. The Dirac equation potential includes the electric potential of a nucleus and exchange-correlation potential. One of the variants is the Kohn-Sham-like (KS) exchange relativistic potential, which is obtained from a Hamiltonian having a transverse vector potential describing the photons, is as follows [31]:

$$V_X[\rho(r), r] = V_X^{KS}(r) \cdot \{\frac{3}{2} \ln \frac{[\beta + (\beta^2 + 1)^{1/2}]}{\beta(\beta^2 + 1)^{1/2}} - \frac{1}{2}\}, \quad (7)$$

where

$$\beta = [3\pi^2 \rho(r)]^{1/3} / c \quad (8)$$

The corresponding correlation functional is [20,31]:

$$V_C[\rho(r), r] = -0.0333 \cdot b \cdot \ln[1 + 18.3768 \cdot \rho(r)^{1/3}], \quad (9)$$

where *b* is the optimization parameter (see details in Refs. [20,27,32]). Earlier it has been shown [27-32] that an adequate description of the atomic characteristics requires using an optimized base of the wave functions. In Ref. [24b] a new ab initio optimization procedure is proposed. It is reduced to minimization of the gauge dependent multielectron contribution $Im\Delta E_{ninv}$ of the lowest QED PT corrections to the radiation widths of atomic levels. In the fourth order of QED PT (the second order of the atomic PT) there appear the diagrams, whose contribution to the $Im\Delta E_{ninv}$ accounts for correlation effects. This contribution is determined by the electromagnetic potential gauge (the gauge dependent contribution). All the gauge dependent terms are multielectron by their nature. The dependent contribution to imaginary part of the electron energy is obtained after involved calculation, as [24b]:

$$Im\delta E_{ninv}(\alpha - s \mid b) = -C\frac{e^2}{4\pi}\iiint dr_1 dr_2 dr_3 dr_4 \sum_{n>f, m\le f} \left(\frac{1}{\omega_{mn} + \omega_{\alpha s}} + \frac{1}{\omega_{mn} - \omega_{\alpha s}}\right)$$
$$\times \Psi^+_{\alpha}(r_1)\Psi^+_m(r_2)\Psi^+_s(r_4)\Psi^+_n(r_3) \cdot [(1 - \alpha_1\alpha_2)/r_{12}] \cdot \{[\alpha_3\alpha_4 - (\alpha_3 n_{34})(\alpha_4 n_{34})]/r_{34}$$
$$\times \sin[\omega_{\alpha n}(r_{12} + r_{34})] + [1 + (\alpha_3 n_{34})(\alpha_4 n_{34})]\omega_{\alpha n}\cos[\omega_{\alpha n}(r_{12} + r_{34})]\}$$
$$\times \Psi_m(r_3)\Psi_{\alpha}(r_4)\Psi_n(r_2)\Psi_s(r_1). \quad (10)$$

Here, *C* is the gauge constant, *f* is the boundary of the closed shells; $n \ge f$ indicating the vacant band and the upper continuum electron states; $m \le f$ indicates the finite number of states in the atomic core). The minimization of the $Im\Delta E_{ninv}$ leads to the Dirac-like equations. In concrete calculation it is sufficient to use the simplified procedure, which is reduced to the functional minimization using the variation of the parameter *b* in Eq.(9) [20,25].

2.3 Capture of negative muons by helium atom

The results of calculation of the cross-section for the negative muon capture by atom of He are shown in Figures 1-3. The scheme includes 2×10^3 points till distance $25a_B$ (a_B is the Bohr radius). The main contribution to the capture cross-section is provided by transitions with the moment *l*=0-3.

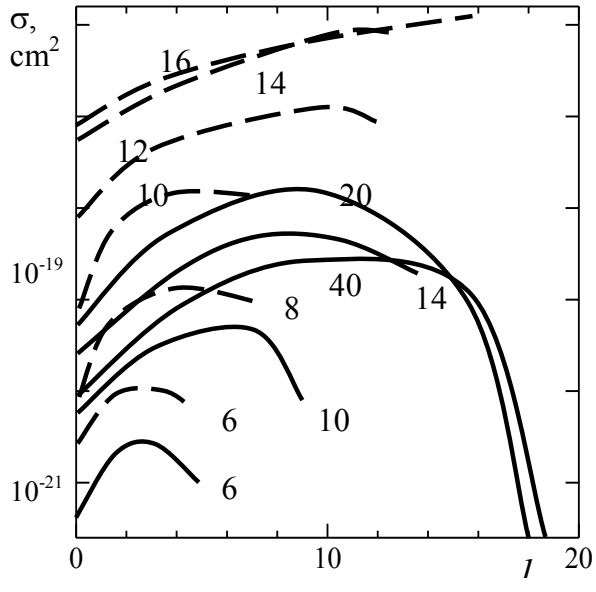

Figure 1. The calculated dependences of the Auger capture cross-section (solid line– E=50eV; dotted line - E=20eV) on orbital number *l* for different *n* values for incident μ^- energies 20, 50 eV (from Refs. [2-4,20]).

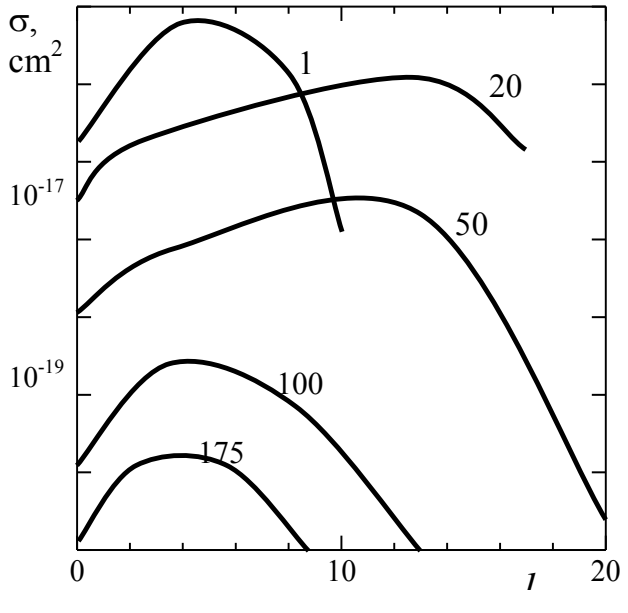

Figure 2. The capture cross-sections in dependence on the orbital number l after summation on the n number (digits in figure – the muon energies in eV; from Refs. [2-4,20]).

First we studied the behaviour of curves of the μ^- capture cross-section in dependence on the principal quantum number *n* with summation on the orbital moments *l* for several values of the muon initial energy. In whole our curves are lying a little higher than the corresponding curves of Refs. [1-3]. The analysis shows that for the incident μ energies 16 and 50eV the capture cross-section begins to decrease for all *n* with growth of the *l* number (*l*>10). The states with large *l* for the muon energies (lower or higher in comparison with the atomic ionization potential value) are populated less probably than in a case of the μ^- energy of the ionization potential order. In figure 1we present the calculated dependences of the Auger capture cross-section on the orbital number *l* for different *n* values for the incident μ energies of 20 and 50 eV. In figure 2 we present the calculated capture cross-section in the dependence on the *l* number after summation on *n*.

In figure 3 we present the total capture cross-section in terms of energy (with summation on all *n,l*): data on the Auger capture cross-section – curve 7 (elastic and inelastic scattering cross-sections) – curves 2,3 [20]. We also present the results by Copenman and Rogova in the Born approximation with using the hydrogen-like wave functions (curve 5) and the HF data [2] (curve 1), the inelastic scattering cross-section by Rosenberg (curve 4), the transport cross-section (x symbol) [2,3,20]. The analysis of the results shows that the data [2-4, 20] are in physically reasonable agreement. But, there is an essential difference of the Mann-Rose and Bayer data [1-3].

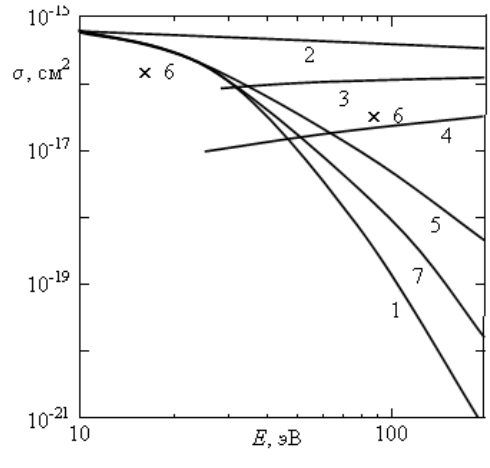

Figure 3. Total cross-section of μ^- capture in dependence on an energy: the Auger capture cross-section – curve 7; elastic and inelastic scattering cross-sections – curves 2,3 by Glushkov et al; cross-section of capture by Copenman and Rogova (curve 5); the HaF data by Cherepkov-Chernysheva – curve 1; inelastic scattering cross-section by Rosenberg – curve 4; the transport cross-section – x (from Refs. [2-4,20]).

The relativistic corrections were to found to be small here, but computing heavy atoms (nuclei) requires a proper treatment for both relativistic and correlation effects.

3 Concluding Remarks and Future Perspectives

We have presented a new relativistic approach to calculation of the cross-section of the negative μ capture by atoms. The approaches are based upon the relativistic many-body PT theory, energy approach. Note that further development of electron-μ-nuclear spectroscopy of atoms (nuclei) is of a great theoretical and practical interest. The development of new approaches [2-6,21-23] to studying the cooperative e-,μ-γ-nuclear processes promises the rapid progress in our understanding of the nuclear decay. Such an approach is useful, providing perspective for search for new cooperative effects on the boundary of atomic and nuclear physics, carrying out new methods for treating (the muonic chemistry tools) the spatial structure of molecular orbitals, studying the chemical bond nature and checking different models in quantum chemistry and atomic physics [3-8,18-23,49].

References

1. J.J.Tiomno, J.A.Weller, Rev.Mod. Phys. **21**, 153 (1999); D. F. Zaretsky, V. Novikov, Nucl.Phys. **14**,540 (1990); L.L.Foldi, J.D.Walecka, Nuovo. Cim. **34**, 1026 (1994).
2. R. Mann, M.Rose, Phys.Rev.**121**, 293 (1961); M.Leon, J.Miller, Nucl. Phys. A**282**,461 (1997); N.Cherepkov, L.Chernysheva, J.Nucl.Phys. **32**, 709 (1980); J.Cohen, M.Leon, Phys.Rev. Lett. **55**, 52 (1995).
3. P. Haff, T. Tombrello, Ann. Phys. **86**, 178 (1994); P.Vogel, P. Haff, V. Akylas, A.Winther, Nucl.Phys.A. **254**,445 (1995).
4. R.A.Naumannm G.Schmidt, J.D.Knight, L.F.Mausner, C.J.Orth, M.E.Schillaci, Phys. Rev. A **21**, 639 (1990); N. Auerbach, A.Klein, Nucl. Phys. A **422**, 480 (1994); E.Kolbe, K. Langanke, P. Vogel, Phys.Rev.C **62**, 055502 (2006).
5. L.Ponomarev, S.Gerstain, Y.Petrov,Phys.- Usp. **160**, 3 (1990);A. Kravtsov, V. Mikhailov, Phys. Rev.A **49**, 3566 (1994).
6. B.Lauss, Nucl.Phys.A **827,** 401 (2009); D.Gazit, Nucl.Phys.A **827**, 408 (2009).
7. I.G. Kaplan, V.N. Smutny, Adv. Quantum Chem. **19**, 289 (1998); I.G. Kaplan, A.P. Markin, JETP **69**, 9 (1995).
8. K.Takahashi, R.Boyd, G.Mathews, K.Yokoi, Phys.Rev.C **36**, 1522 (1997); V.Mikheev, V. Morozov, N.Morozova, Phys. Part. Nucl. Lett. **5**, 371 (2008); V.I. Vysotskii, Phys. Rev.C **58**, 337 (1998).
9. R. M Mössbauer, Z. Phys. A: Hadrons and Nuclei **151**, 124 (1958); L. Szilard, T. Chalmers, Nature. **134**, 462 (1934).
10. A.B. Migdal, J. Phys. USSR **4**, 449 (1941); J.S. Levinger, Phys. Rev. **90**, 11 (1953).
11. G. Ciocchetti, A. Molinari, Nuovo Cim. **40**, 69 (1995); Th. Carlson, C.W. Nestor, T.C. Tucker, F.B. Malik, Phys. Rev. **169**, 27 (1998)
12. P. Amudsen, P.H. Barker, Phys. Rev. C **50**, 2466 (1994); R. Anholt, P. Amundsen, Phys. Rev. A **25**, 169 (1992).
13. R.L. Wolfgang, R. Anderson, R.W. Dodson, J. Chem. Phys. **24**, 16 (1956); R.L. Martin, J.S. Cohen, Phys. Lett. A **110**, 95 (1995).
14. J.Hansen, Phys.Rev.A**9**,40(1994); J. Law, Nucl. Phys. A **286**, 339 (1997); J. Law, J.Campbell, Phys. Rev. C **25**, 514 (1992)
15. T. Mukoyama, Sh. Ito, Phys. Lett. A **131**, 182 (1988); T. Mukoyama, S. Shimizu, J. Phys. G: Nucl. Part. **4**, 1509 (1998)
16. P.Kienle, Phys.Scr. **46**,81 (1993); L. Wauters, N.Vaeck, Phys.Rev. C **53**,497 (1996).
17. A.V. Glushkov, I. Makarov, E. Nikiforova etal Astroparticle Phys. **4**, 15 (1995); A. Glushkov, L.Dedenko, M. Pravdin, I.Sleptsov, JETP **99**, 123 (2004).
18. G.G. Baldwin, J.C. Salem, V.I. Gol'dansky, Rev. Mod. Phys. **53,** 687 (1991); V.S. Letokhov, In *Application*

of Lasers in Atomic, Molecular and Nuclear Physics, ed. by A.M. Prokhorov, V.S. Letokhov (Nauka, Moscow, 1999), p. 412
19. V.S. Letokhov, V. Gol'dansky, JETP. **67**, 513 (1974); L.N. Ivanov, V.S. Letokhov, Com. Mod. Phys. D **4**, 169 (1995);
20. Glushkov A.V., Khetselius O.Yu., Svinarenko A.A., *Advances in the Theory of Quantum Systems in Chemistry and Physics.* Series: Frontiers in Theoretical Physics and Chemistry, Eds. P.Hoggan, E.Brandas, J.Maruani, G. Delgado-Barrio, P.Piecuch (Berlin, Springer).-2011.-Vol.22.-P.51-70; A.V. Glushkov, O.Yu. Khetselius, L. Lovett, L., in: *Advances in the Theory of Atomic and Molecular Systems Dynamics, Spectroscopy, Clusters, Nanostructures*. Series: Progr. Theor. Chem.& Phys., vol. **20**, ed. by P.Piecuch, J. Maruani, G. Delgado-Barrio, S. Wilson (Springer, Berlin, 2010), pp.125-172.
21. A.Glushkov, O. Khetselius, S. Malinovs-kaya, Europ.Phys. Journ. ST **160**, 195 (2008); Molec. Phys. **106**, 1257 (2008). *Frontiers in Quantum Systems in Chemistry and Physics*, *Progr. Theor. Chem.& Phys.* , vol. **18**, ed. by S.Wilson, P.J.Grout, J. Maruani, G. Delgado-Barrio, P. Piecuch (Springer, Berlin, 2008), p. 523;
22. A.V. Glushkov, S. Malinovskaya, L. Vitavetskaya, Yu. Dubrovskaya, in *Recent Advances in Theoretical Physics and Chemistry Systems, Progr. Theor. Chem.& Phys.*, vol. **15**, ed. by J.-P. Julien, J. Maruani, D. Mayou, S. Wilson, G. Delgado-Barrio (Springer, Berlin, 2006), p. 301-318; A. Glushkov, S. Malinovskaya, E. Gurnitskaya, O. Khetselius, J. Phys.CS. **35**, 426 (2006)
23. A.Shahbaz, C.Müller, T.J.Bürvenich, C.H.Keitel, Nucl.Phys.A **821**, 106 (2009); Shahbaz, C. Müller, A. Staudt, T.J. Burnevich, C.H. Keitel, Phys. Rev. Lett. **98**, 263901 (2007); T.J. Burnevich, J. Evers, C.H. Keitel, Phys. Rev. C **74**, 044601 (2006).
24. A.V. Glushkov, L.N. Ivanov, E.P Ivanova, *Autoionization Phenomena in Atoms*, (Moscow University Press, Moscow, 1996); A.V. Glushkov, L.N. Ivanov, Phys. Lett. A **170**, 33 (1992); A.V. Glushkov, JETP Lett. **55**, 97 (1992); L.N. Ivanov, E.P. Ivanova, L. Knight, Phys. Rev. A **48,** 4365 (1993); E. Ivanova, L. Ivanov, JETP **83**, 258 (1996).
25. E.P. Ivanova, L.N. Ivanov, A.V. Glushkov, A. Kramida, Phys. Scripta **32**, 512 (1985); A.V. Glushkov, E.P. Ivanova, J. Quant. Spectr. Rad. Tr. **36**, 127 (1996).
26. A.V. Glushkov, O.Yu. Khetselius, A.V.Loboda, A.A.Svinarenko, in *Frontiers in Quantum Systems in Chemistry and Physics*, *Progr. Theor. Chem.& Phys.*, vol. **18**, ed. by S. Wilson, P.J. Grout., J. Maruani, G. Delgado-Barrio, P. Piecuch (Springer, Berlin, 2008), p. 541; A.V. Glushkov, A.Loboda, E.Gurnitskaya, A.Svinarenko, Phys. Scr.T **134**, 137740 (2009)
27. A.V. Glushkov, S.V. Malinovskaya, A.V. Loboda, E.P. Gurnitskaya, D.A. Korchevsky, J. Phys.: Conf. Ser. **11**, 188 (2005); A.V. Glushkov, S.V. Ambrosov, A.V. Loboda, E.P. Gurnitskaya, G.P. Prepelitsa, Int.J. Quant.Ch.. **104**, 562 (2005); A. Glushkov, S. Malinovskaya, G. Prepelitsa, V. Ignatenko, J. Phys.CS. **11**, 199 (2004)
28. A.V. Glushkov, Opt. Spectr. (USSR). **66**, 31 (1989); **70**, 952 (1991); **71**, 395 (1991); **72,** 55 (1992); **72,** 542 (1992); Rus. J. Phys. Chem. **66**, 589 (1992); **66**, 1259 (1992); Rus. J. Struct. Chem. **32**, 11 (1992); **34**, 3 (1993).
29. A.V. Glushkov, S.V. Ambrosov, A.V. Loboda, E.P. Gurnitskaya, O.Yu. Khetselius, in *Recent Advances in Theoretical Physics and Chemistry Systems, Progr. Theor. Chem.& Phys.*, vol.**15**, eds. J.-P. Julien, J. Maruani, D. Mayou, S. Wilson, G. Delgado-Barrio (Springer, Berlin, 2006), p. 285.
30. A. Glushkov, S. Malinovskaya, A. Loboda, G. Prepelitsa, J. Phys.: Conf. Ser. **35**, 420 (2006); A.V. Glushkov, S.V. Malinovskaya, Yu.G. Chernyakova,

A.A. Svinarenko, Int.J. Quant.Ch.. **99**, 889 (2004); Int.J. Quant.Ch.. **104**, 496 (2005).
31. W. Kohn, L.J. Sham, Phys. Rev. A **140**, 1133 (1964); P. Hohenberg, W. Kohn, Phys. Rev. B **136**, 864 (1964); D.Feller, E.R.Davidson, J.Chem.Phys. **74**, 3977 (1991).
32. O. Gunnarsson, B. Lundqvist, Phys. Rev. B. **13**, 4274 (1976); M. Das, M. Ramana, A.Rajagopal, Phys. Rev. **22,** 9 (1990); R.M. Dreizler, E.K.U. Gross, *Density Functional Theory* (Springer, Berlin, 1990).
33. M.Hehenberger, H.McIntosh, E.Brändas, Phys.Rev.A**10**,1494 (1994); A. Glushkov, L.Ivanov, J. Phys. B: At. Opt.Phys. **26,** L379 (1993); A.Glushkov, S.Ambrosov, A. Ignatenko, D. Korchevsky, Int.J.Quant.Ch.. **99**, 936 (2004).
34. A.Glushkov, in Meson-Nucleon Physics and the Structure of the Nucleon, eds.S. rewald, H. Machner (IKP, Juelich, Germany), SLAC eConf C070910 (Menlo Park, CA, USA) **2**, 111 (2007); A.Glushkov, L. Lovett, O. Khetselius et al, Int.J.Modern Phys. A. **24**, 611 (2009).
35. A. Glushkov, V. Rusov, S. Ambrosov, A. Loboda, in *New Projects and New Lines of Research in Nuclear Phys.*, ed. by G. Fazio and F. Hanappe (World Sci., Singapore, 2003) p.126; V. Zagrebaev, Yu. Oganessian, M. Itkis, W. Greiner, Phys. Rev. C **73**, 031602 (2006).
36. J.Behr, G.Gwinner, J.Phys.G: Nucl. Part. **36**,033101 (2009); K.Kettner, H.Becker, F. Strieder, C. Rolfs, J. Phys. G: Nucl. Part. **32**, 489 (2006); S. Godovikov, Izv. RAN, Ser. Phys. **65**, 1063 (2001); N. Zinner, Nucl. Phys.A **781**, 81 (2007).
37. A.V.Glushkov, S.V.Malinovskaya, in *New Projects and New Lines of Research in Nuclear Physics*, ed. by G. Fazio and F. Hanappe (World Sci., Singapore, 2003) p.242; A.V.Glushkov, in *Low Energy Antiproton Physics,* vol. **796**, ed. by D. Grzonka, R. Czyzykiewicz, W. Oelert, T. Rozek, P. Winter (AIP, Melville, NY, 2005), p. 206.

This article has been received in April 2016

UDC 539.182

A. V. Glushkov

RELATIVISTIC ENERGY APPROACH TO THE NEGATIVE MUON CAPTURE BY AN ATOM

Abstract

We reviewed a new effective consistent approach to determination of the cross-section for the negative muon capture by an atomic system. The approach is based on the relativistic many-body perturbation (PT) theory with using the Feynman diagram technique and a generalized relativistic energy approach in a gauge-invariant formulation. The corresponding capture cross-section is connected with an imaginary (scattering) part of the electron subsystem energy shift ImδE (till the QED perturbation theory order). The some calculation results for cross-section of the negative muon μ^- capture by He atom are listed and reviewed. The theoretical and experimental studying the muon-γ-nuclear interaction effects opens prospects for nuclear quantum optics, probing the structural features of a nucleus and muon spectroscopy in atomic and molecular photophysics.

Key words: Cooperative muon-γ-nuclear processes, muon capture by an atom, Relativistic energy formalism

УДК 539.182

А. В. Глушков

РЕЛЯТИВИСТСКИЙ ЭНЕРГЕТИЧЕСКИЙ ПОДХОД К ОПИСАНИЮ ПРОЦЕССА ЗАХВАТА ОТРИЦАТЕЛЬНОГО МЮОНА АТОМОМ

Резюме

В работе обзорно изложены основы нового эффективного подхода к определению сечений захвата отрицательного мюона атомной системой, основанного на релятивистской многочастичной теории возмущения с использованием фейнмановской диаграммной техники и обобщенном релятивистском энергетическом формализме в калибровочно-инвариантной формулировке. Соответствующее сечение захвата отрицательного мюона атомом определяется мнимой частью энергетического сдвига ImδE электронной подсистемы. Обзорно представлены результаты некоторых расчетов сечения захвата отрицательного мюона атомом He. Теоретическое и экспериментальное изучение эффектов мюон-гамма-ядерных взаимодействий открывает перспективы развития новой области квантовой оптики, а именно, ядерной квантовой оптики, возможности зондирования структурных особенностей ядра (атома) и дальнейшего развития направления мюонной спектроскопии в атомной и молекулярной физике.

Ключевые слова: кооперативные мюон-гамма-ядерные процессы, захват мюона атомом, релятивистский энергетический формализм

УДК 539.182

О. В. Глушков

РЕЛЯТИВІСТСЬКИЙ ЕНЕРГЕТИЧНИЙ ПІДХІД ДО ОПИСУ ПРОЦЕСА ЗАХОПЛЕННЯ НЕГАТИВНОГО МЮОНА АТОМОМ

Резюме

У роботі оглядово викладені основи нового ефективного підходу до визначення перетинів захоплення негативного мюона атомної системою, заснованого на релятивістській багаточастинковій теорії збурень з використанням фейнманівськох діаграмної техніки і узагальненому релятивістському енергетичному формалізмі у калібрувально-інваріантному формулюванні. Відповідний перетин захоплення негативного мюона атомом визначається уявною частиною енергетичного зсуву ImδE електронної підсистеми. Оглядово представлені результати деяких розрахунків перетину захоплення негативного мюона атомом гелія. Теоретичне і експериментальне вивчення ефектів мюон-гамма-ядерних взаємодій відкриває перспективи розвитку нової галузі квантової оптики, а саме, ядерної квантової оптики, нові можливості зондування структурних особливостей ядра (атома) і подальшого розвитку напрямку мюонної спектроскопії в атомній і молекулярної фотофізиці.

Ключові слова: кооперативні мюон-гамма-ядерні процеси, захоплення мюона атомом, релятивістський енергетичний формалізм

UDC 621.315.592

Yu. F. Vaksman, Yu. A. Nitsuk, A. V. Korenkova

I. I. Mechnikov Odesa National University
e-mail: nitsuk@onu.edu.ua

STUDY OF THE IMPURITY PHOTOCONDUCTIVITY AND LUMINESCENCE IN ZnTe:V CRYSTALS

The photoconductivity and photoluminescence spectra of ZnTe:V crystals in the visible spectral region are studied. It is established that the high-temperature impurity photoconductivity of ZnTe:V crystals is controlled by the optical transitions of electrons from the ground state 4T1(F) to high-energy excited states, with subsequent thermally activated transitions of electrons to the conduction band. A photoconductivity band associated with the photoionization of V impurities is revealed. The intracenter luminescence of ZnTe:V crystals is efficiently excited with light corresponding to the intrinsic absorption region of V2+ ion

Introduction

In the last few years, ZnTe crystals doped with transition metals have been extensively used as materials for various laser- and nonlinear-optical applications. ZnTe:Cr crystals were used to achieve lasing at 2.5 μm [1]. ZnTe:Fe crystals served as a basis for the production of tunable lasers emitting in the wavelength range from 4.35 to 5.45 μm [2]. The use of ZnTe:V crystals for attaining lasing in the IR region is hindered by the problem of the observation of IR luminescence at temperatures higher than 150 K [3].

At the same time, the above-mentioned crystals can be used as photodetectors for visible and microwave radiation [4]. Therefore, studies of the photoconductivity and luminescence of ZnTe:V crystals in the visible spectral region present a topical problem.

In this study, we explore and identify structural features of the photoconductivity and luminescence spectra of ZnTe:V crystals in the visible spectral region. It is shown that, in the spectra, there are photoconductivity and luminescence bands associated with the V impurity.

The goals of this study is to identify structural features of the photoconductivity and luminescence spectra of ZnTe:V crystals in the visible spectral region.

Experimental

The samples to be studied were produced by the diffusion doping of initially pure ZnTe crystals with V. The nominally undoped crystals were produced by the free growth method on a ZnSe single crystal substrate oriented in the (111) plane. The advantage of diffusion doping is the possibility of obtaining specified impurity concentrations and doping profiles. The V content in the crystals was determined from the variation in the band gap of ZnTe crystals under variations in the V impurity concentration. The vanadium concentration varies from $3 \cdot 10^{17}$ to $3 \cdot 10^{19}$ cm^{-3}. For reference samples, we used specially produced and studied ZnTe samples subjected to heat treatments at the same temperatures as those of the treatments of V-doped crystals.

The photoconductivity spectra were recorded with an MUM-2 monochromator with a 1200 grove mm^{-1} diffraction grating. A halogen lamp served as the source of light. The power of the light flux from the lamp was kept constant at different wavelengths.

The photoluminescence (PL) spectra were recorded with an ISP-51 prism spectrograph. The emission was detected with an FEU-100 photoelectric multiplier. The luminescence signal was excited with Edison Opto Corporation light-emitting diodes (LEDs) and an ILGI-503 nitrogen pulse laser. The photon energies corresponding to the emission peak of the LEDs were 3.1, 2.69 and 2.25 eV, and the photon energy of laser emission was 3.74 eV.

Analysis of the photoconductivity spectra

The undoped ZnTe crystals exhibit only one photoconductivity band with a peak at 2.26 eV at 300 K (Fig. 1, curve *1*). This band arises from interband optical transitions. On doping of the crystals with vanadium, this band shifts to lower energies. As the V concentration is increased, the shift increases and corresponds to a change in the band gap determined from the optical absorption spectra.

Doping with vanadium brings about the appearance of series photoconductivity bands in the photon energy range from 1.4 to 2.1 eV (Fig.1, curves *2–3*). The intensity of these bands increases, as the V concentration is increased. In the spectra, we can distinguish bands at 1.47, 1.55, 1.7, 1.8, 1.87 and 2.09 eV. It is established that the 2.09 eV band changes position under variations in the V concentration. The position of other bands remains unchanged, as the degree of doping is increased.

At the temperature T = 77 K, only one interband photoconductivity band is observed in all of the crystals under study. As the temperature is elevated from 77 to 350 K, the impurity photoconductivity makes a weightier contribution to the spectrum. We observed a similar effect previously in studying the photoconductivity of ZnSe crystals doped with Fe, Ni, Cr [5,6].

As the temperature is elevated from 300 to 350 K the 2.09 eV photoconductivity band shifts to lower photon energies by 20 meV. Such shift corresponds to the temperature change in the band gap of ZnTe. Other impurity photoconductivity bands do not change their position with temperature, suggesting that the corresponding transitions are of intracenter character. In addition, the position of the above mentioned bands agrees well with the position of optical absorption bands detected for these crystals previously. In [7] visible absorption bands were attributed to intracenter optical transitions that occur within the V^{2+} ions. The above result suggests that these photoconductivity bands are due to the same optical transitions as those involved in optical absorption. The energies and identification of optical transitions are given in the table. The table summarizes the data obtained in studies of optical absorption, photoconductivity and luminescence.

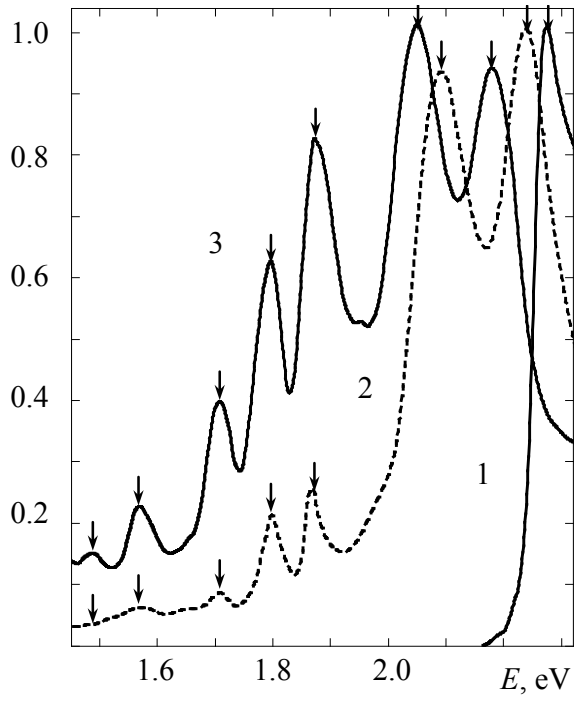

Fig. 1. Photoconductivity spectra of (1) ZnTe and (2, 3) ZnTe:V crystals. The V dopant concentrations are [V] = (2) 5·1018 and (3) 3·1019 cm–3.

The photoconductivity process in the crystals under study occurs in the manner briefly described below. The 2.09 eV photoconductivity band is associated with optical transitions from the $^4T_1(F)$ ground state of the V^{2+} ion into the conduction band. Comparison of the photon energy corresponding to the peak of this photoconductivity band with the energy position of the intrinsic photoconductivity peak for the crystals with the V concentration [V] = $5\cdot10^{18}$cm^{-3} (2.23 eV) allows us to believe that the level of the ground state of the V^{2+} ion is 140 meV above the top of the valence band.

Energies of optical transitions in ZnTe:V crystals

Line No	Absorption		Photoconductivity, *E*, eV	Luminescence, *E*, eV	Stokes shift, E, meV
	E, eV	Transition			
1	---	$^4T_1(F) \rightarrow {}^3A_2(F) + e^-_{c.b}$	2.09	---	---
2	2.19	$^4T_1(F) \rightarrow {}^2E(D)$	---	2.13	60
3	2.08	$^4T_1(F) \rightarrow {}^2E(G)$	---	2.06	20
4	1.87	$^4T_1(F) \rightarrow {}^2T_2(D)$	1.87	1.85	20
5	1.80	$^4T_1(F) \rightarrow {}^2T_1(P)$	1.80	1.78	20
6	1.70	$^4T_1(F) \rightarrow {}^2T_1(H)$	1.7	1.67	30
7	1.54	$^4T_1(F) \rightarrow {}^2E(H)$	1.55	1.52	20
8	1.46	$^4T_1(F) \rightarrow {}^2T_1(H)$	1.47	1.42	40
9	1.36	$^4T_1(F) \rightarrow {}^2T_2(H)$	---	1.33	30
10	1.26	$^4T_1(F) \rightarrow {}^4T_1(P)$	---	1.24	20
11	1.23	$^4T_1(F) \rightarrow {}^2T_2(G)$	---	1.20	30

The other photoconductivity bands are formed in a two-stage process. Initially, the intracenter optical transitions of electrons from the $^4T_1(F)$ ground state to the higher excited states of the V^{2+} ions (table) occur; then thermally activated transitions of these electrons to the conduction band are observed. As a result the local centers transit to the V^{3+} charged state. Later the V^{3+} centers trap electrons and the centers transit to their initial V^{2+} state.

It should be noted that the results of studies of the thermoelectric power are indicative of the electron photoconductivity of the ZnTe:V crystals.

Analysis of luminescence properties

The PL spectra were studied in the temperature range from 77 to 300 K. The PL spectra of undoped crystals excited with nitrogen laser radiation (λ =337 nm) at T = 77 K exhibit one emission band with peak at 2.31 eV (Fig. 2, curve 1). In previous studies the 2.31 eV emission band was attributed to emission of excitons localized at neutral zinc vacancies [6].

Upon doping of the crystals with vanadium, the excitonic emission bands shift to lower energies (Fig. 2, curve 2). The shift corresponds to the change in the band gap with the vanadium concentration [V] in ZnTe.

Doping of the crystals with vanadium brings about a series of long-wavelength emission lines with peaks at 1.20, 1.24, 1.33, 1.42, 1.52, 1.67, 1.78, 1.85, 2.06, 2.13 eV (Fig. 2, curve 2). As the V concentration is increased, the intensity of these emission lines increases, whereas their position remains unchanged.

Figure 2 (curve 3) shows the absorption spectrum of the ZnTe:V crystals at T = 77 K. The spectrum involves lines that correlate with the emission lines observed in this study. As can be seen from the table, the Stokes shifts of the PL lines with respect to the corresponding absorption lines are in the range 20–60 meV.

It is established that the relative luminescence intensity of the ZnTe:V crystals heavily depends on the photon energy of excitation light.

Emission with the lowest intensity is excited with a nitrogen laser with the photon energy 3.67 eV. The highest emission intensity is attained on excitation with LEDs with the photon energy in the emission peak 2.25 eV. This suggests that the band-to-band excitation of long-wavelength luminescence of the ZnTe:V crystals is inefficient. At the same time, under changes in the excitation photon energy, the position of emission peaks remains unchanged. It is also established that, as the excitation photon energy is lowered, the contribution of low-energy bands to the luminescence spectrum increases. This effect is typical of intracenter luminescence.

As the temperature is elevated from 77 to 300 K, the intensity of all emission lines decreases, while the positions of the peaks remain unchanged. Similar temperature behavior was observed for the corresponding absorption lines.

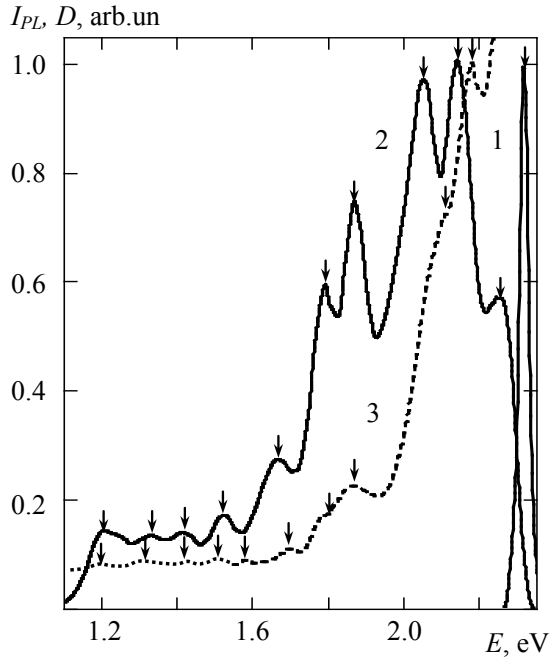

Fig. 2. (1, 2) Photoluminescence and (3) absorption spectra of (1) ZnTe and (2, 3) ZnTe:V crystals.

This suggests that the absorption and luminescence lines under study are due to intracenter optical transitions that occur within vanadium ions.

Conclusions

1. It is shown that the high-temperature long-wavelength photoconductivity of the ZnTe:V crystals is controlled by intracenter optical ransitions within the V^{2+} ions and by subsequent thermally induced transitions of electrons from the levels of the excited V^{3+} states into the conduction band.

2. It is established that doping with vanadium gives rise to a series of emission lines in the visible spectral region. The luminescence bands detected for the ZnTe:V crystals are attributed to intracenter transitions in the V^{2+} ions.

3. Efficient excitation in impurity-related luminescence of the ZnTe:V crystals is attained with light corresponding to the region of intrinsic absorption in the V^{2+} ions.

References

1. Kisiel V.E., Tolstik N.A., Scherbitsky V.G. et.al. Growth and spectroscopic characterization of Cr:ZnTe laser crystals //CLEO/Europe. 2005 Conference on Lasers and Electro-Optics Europe. – 12-17 June 2005.
2. Frolov M.P., Korostelin Yu.V., Kozlovskii V.I. et al. Laser radiation tunable within the range 4.35-5.45 μm in a ZnTe crystals doped with Fe^{2+} ions // Journal of Russian Laser Research. – 2011. V.11, N.6. – P.528-532.
3. Peka P, Lehr M.U, Schulz H., Pohl U.W. Vanadium centers in ZnTe crystals. I. Optical properties//Phys. rev. B. – V. 53(4). - P.1907-1916.
4. Arunas Kadys, Kestutis Jarasiunas, Markas Sudzius et. al. Photoelectric properties of highly excited ZnTe:V(Al, Sc) bulk crystals // Phys. Stat. Sol.(c). – 2005. - V. 2, P. 1389–1392.
5. Ваксман Ю.Ф., Ницук Ю.А., Яцун В.В., Влияние примеси железа на люминесценцию и фотопроводимость кристаллов ZnSe в видимой области спектра // ФТП. – 2011. – Т. 45, В. 9. – С. 1171-1174.
6. Ницук Ю.А., Ваксман Ю.Ф., Яцун В.В. Исследование примесной фотопроводимости и люминесценции в кристаллах ZnSe:Ni в видимой области спектра// ФТП. – 2012. – Т. 46, В. 10. – С. 1288-1292.
7. Ницук Ю.А. Оптическое поглощение ванадия в кристаллах ZnSe //ФТП. – 2014. – Т.48, №2. – С. 152-157.

This article has been received in April 2016

UDC 621.315.592

Yu. F. Vaksman, Yu. A. Nitsuk, A. V. Korenkova

STUDY OF THE IMPURITY PHOTOCONDUCTIVITY AND LUMINESCENCE IN ZnTe:V CRYSTALS

Abstract

The photoconductivity and photoluminescence spectra of ZnTe:V crystals in the visible spectral region are studied. It is established that the high-temperature impurity photoconductivity of ZnTe:V crystals is controlled by the optical transitions of electrons from the ground state $^4T_1(F)$ to high-energy excited states, with subsequent thermally activated transitions of electrons to the conduction band. A photoconductivity band associated with the photoionization of V impurities is revealed. The intracenter luminescence of ZnTe:V crystals is efficiently excited with light corresponding to the intrinsic absorption region of V^{2+} ion

Key words: zinc telluride, diffusion doping, vanadium impurity, photoconductivity, photoluminescence.

УДК 621.315.592

Ю. Ф. Ваксман, Ю. А. Ницук, А. В. Коренкова

ИССЛЕДОВАНИЕ ПРИМЕСНОЙ ФОТОПРОВОДИМОСТИ И ЛЮМИНЕСЦЕНЦИИ В КРИСТАЛЛАХ ZnTe:V

Резюме

Исследована фотопроводимость и фотолюминесценция кристаллов ZnTe:V в видимой области спектра. Установлено, что высокотемпературная фотопроводимость кристаллов ZnTe:V обусловлена оптическими переходами электронов из основного состояния $^4T_1(F)$ на более высокие возбужденные энергетические уровни иона V^{2+} с их последующей термической активацией в зону проводимости. Эффективное возбуждение внутрицентровой люминесценции кристаллов ZnTe:V осуществляется светом из области примесного поглощения ионов V^{2+}.

Ключевые слова: теллурид цинка, диффузионное легирование, примесь ванадия, фотопроводимость, фотолюминесценция.

УДК 621.315.592

Ю. Ф. Ваксман, Ю. А. Ніцук, А. В. Коренкова

ДОСЛІДЖЕННЯ ДОМІШКОВОЇ ФОТОПРОВІДНОСТІ ТА ЛЮМІНЕСЦЕНЦІЇ В КРИСТАЛАХ ZnTe:V

Резюме

Досліджено фотопровідність і фотолюмінесценцію кристалів ZnTe:V у видимій області спектру. Встановлено, що високотемпературна фотопровідність кристалів ZnTe:V обумовлена оптичними переходами електронів з основного стану $^4T_1(F)$ на більш високі збуджені енергетичні рівні іону V^{2+} з їх подальшою термічною активацією в зону провідності. Ефективне збудження внутришньоцентрової люмінесценції кристалів ZnTe:V відбувається світлом з області домішкового поглинання іонів V^{2+}.

Ключові слова: телурид цинку, дифузійне легування, домішка ванадію, фотопровідність, фотолюмінесценція.

UDC 539.182

A. V. Smirnov, V. V. Buyadzhi, A. V. Ignatenko, A. V. Glushkov, A. A. Svinarenko

Odessa State Environmental University, 15, Lvovskaya str., Odessa, Ukraine
Odessa National Polytechnical University, 1, Shevchenko av., Odessa, Ukraine
e-mail: quantsvi@mail.ru

SPECTROSCOPY OF THE COMPLEX AUTOIONIZATION RESONANCES IN SPECTRUM OF BERYLLIUM

We applied a generalized energy approach (Gell-Mann and Low S-matrix formalism) combined with the relativistic multi-quasiparticle (QP) perturbation theory (PT) with the Dirac-Kohn-Sham zeroth approximation and accounting for the exchange-correlation, relativistic corrections to studying autoionization resonances in the beryllium Be spectrum, in particular, we predicted the energies and widths of the number of the 2pns resonances. There are presented the results of comparison of our theory data for the autoionization resonances 2pnl with the available experimental data and those results of other theories, including, methods by Greene, by Tully-Seaton-Berrington and by Kim-Tayal-Zhou-Manson etc.

1. Introduction

Here we continue our investigations of studying the autoionization state and AR in spectra of a few electron complex atoms and ions. Let us note [1-5] that theoretical methods of calculation of the spectroscopic characteristics for heavy atoms and ions are usually divided into a few main groups [1-21]. Let us remind At first, one should mention the well known, classical multi-configuration Hartree-Fock method (as a rule, the relativistic effects are taken into account in the Pauli approximation or Breit hamiltonian etc.) allowed to get a great number of the useful spectral information about light and not heavy atomic systems, but in fact it provides only qualitative description of spectra of the heavy atoms and ions. Another more consistent method is given by the known multi-configuration Dirac-Fock (MCDF) approach. Besides, different methods such as various forms of the *R*-matrix method, the multiconfiguration Tamm-Dancoff approximation, the hyperspherical method, a hyperspherical close-coupling calculation, and a multiconfiguration relativistic random-phase approximation have been employed [3].

In this paper we applied a new relativistic approach [11-15] to relativistic studying the autoionization characteristics of the beryllium atom. The method wich has been used is in details presented in our prwvius papers (see, for example, [4]). LHere we remind that the new elements of the approach include the combined the generalized energy approach and the gauge-invariant QED many-QP PT with the Dirac-Kohn-Sham (DKS) "0" approximation (optimized 1QP representation) and an accurate accounting for relativistic, correlation and others effects. The generalized gauge-invariant version of the energy approach has been further developed in Refs. [12,13].

2. Relativistic approach in autoionization spectroscopy of beryllium atom

In refs. [11-15, 17-20] it has been in details presented, so here we give only the fundamental aspects. In relativistic case the Gell-Mann and Low formula expressed an energy shift ΔE through the QED scattering matrix including the interaction with as the photon vacuum field as the laser field. The first case is corresponding to definition of the traditional radiative and autoionization character-

istics of multielectron atom. The wave function zeroth basis is found from the Dirac equation with a potential, which includes the ab initio (the optimized model potential or DF potentials, electric and polarization potentials of a nucleus) [5]. Generally speaking, the majority of complex atomic systems possess a dense energy spectrum of interacting states with essentially relativistic properties. Further one should realize a field procedure for calculating the energy shifts ΔE of degenerate states, which is connected with the secular matrix *M* diagonalization [8-12]. The secular matrix elements are already complex in the second order of the PT. Their imaginary parts are connected with a decay possibility. A total energy shift of the state is presented in the standard form:

$$\Delta \mathrm{E} = \mathrm{Re}\,\Delta E + i\,\mathrm{Im}\,\Delta E \qquad \mathrm{Im}\,\Delta E = -\Gamma/2\,, \tag{1}$$

where Γ is interpreted as the level width, and the decay possibility $\mathrm{P} = \Gamma$. The whole calculation of the energies and decay probabilities of a non-degenerate excited state is reduced to the calculation and diagonalization of the *M*. The complex secular matrix *M* is represented in the form [9,10]:

$$M = M^{(0)} + M^{(1)} + M^{(2)} + M^{(3)}. \tag{2}$$

where $M^{(0)}$ is the contribution of the vacuum diagrams of all order of PT, and $M^{(1)}$, $M^{(2)}$, $M^{(3)}$ those of the one-, two- and three-QP diagrams respectively. The diagonal matrix $M^{(1)}$ can be presented as a sum of the independent 1QP contributions. For simple systems (such as alkali atoms and ions) the 1QP energies can be taken from the experiment. Substituting these quantities into (2) one could have summarized all the contributions of the 1QP diagrams of all orders of the formally exact QED PT. The optimized 1-QP representation is the best one to determine the zeroth approximation. In the second order, there is important kind of diagrams: the ladder ones. These contributions have been summarized by a modification of the central potential, which must now include the screening (anti-screening) effect of each particle by two others. The additional potential modifies the 1QP orbitals and energies. Let us remind that in the QED theory, the photon propagator D(12) plays the role of this interaction. Naturally, an analytical form of D depends on the gauge, in which the electrodynamic potentials are written. In general, the results of all approximate calculations depended on the gauge. Naturally the correct result must be gauge invariant. The gauge dependence of the amplitudes of the photoprocesses in the approximate calculations is a well known fact and is in details investigated by Grant, Armstrong, Aymar-Luc-Koenig, Glushkov-Ivanov [1,2,5,9]. Grant has studied the gauge connection with the limiting non-relativistic form of the transition operator and has formulated the conditions for approximate functions of the states, in which the amplitudes are gauge invariant (so called Grant's theorem). These results remain true in an energy approach as the final formulae for the probabilities coincide in both approaches. In ref. [16] it has been developed a new version of the approach to conserve gauge invariance. Here we applied it to get the gauge-invariant procedure for generating the relativistic DKS orbital bases (abbreviator of our method: GIRPT). A width of a state associated with the decay of the AR is determined by square of the matrix element of the interparticle interaction $\Gamma \infty |V(\beta_1\beta_2,\ \beta_3 k)|^2$. The total width is given by the expression:

$$\Gamma(n_1^0 j_1^0, n_2^0 j_2^0; J) = \frac{2\pi\varepsilon}{K_0} \sum_{\beta_1\beta_2} \sum_{\beta_1'\beta_2'} C^J(\beta_1\beta_2) \times$$
$$\times C^J(\beta_1'\beta_2') \sum_{\beta\ \beta_K} V_{\beta_1\beta_2;\beta\ \beta_K} V_{\beta_K\beta\ ;\beta_1'\beta_2'} \tag{3}$$

where the coefficients C are determined in [4].

The matrix element of the relativistic interparticle interaction

$$V(r_i r_j) = exp(i\omega_{ij} r_{ij}) \cdot (1 - \alpha_i \alpha)/r_{ij} \tag{4}$$

(here α_J –the Dirac matrices) in (3) is determined as follows:

$$V_{\beta_1\beta_2;\beta_4\beta_3} = \sqrt{(2j_1+1)(2j_2+1)(2j_3+1)(2j_4+1)} \times$$
$$\times (-1)^{j1+j2+j3+j4+m1+m2} \times$$
$$\times \sum_{a\mu} (-1)^{\mu} \begin{pmatrix} j_1 & j_3 & a \\ m_1 & -m_3 & \mu \end{pmatrix} \begin{pmatrix} j_2 & j_4 & a \\ m_2 & -m_4 & \mu \end{pmatrix} \times \tag{5}$$
$$\times Q_a(n_1 l_1 j_1 n_2 l_2 j_2; n_4 l_4 j_4 n_3 l_3 j_3),$$

$$Q_a = Q_a^{\mathrm{Qul}} + Q_a^{\mathrm{B}} \quad . \tag{6}$$

Here Q_a^{Qul} and Q_a^{B} is corresponding to the Coulomb and Breit parts of the interlparticle interaction (6). The Coulomb part Q_λ^{Qul} is expressed in the radial integrals R_λ, angular coefficients S_λ as follows:

$$\begin{aligned} Q_\lambda^{\mathrm{Qul}} \sim \{ & R_l(1243) S_\lambda(1243) + \\ & + R_\lambda(\tilde{1}24\tilde{3}) S_\lambda(\tilde{1}24\tilde{3}) + \\ & + R_\lambda(\tilde{1}\tilde{2}\tilde{4}3) S_\lambda(\tilde{1}\tilde{2}\tilde{4}3) + \\ & + R_\lambda(\tilde{1}\tilde{2}\tilde{4}\tilde{3}) S_\lambda(\tilde{1}\tilde{2}\tilde{4}\tilde{3}) \} \end{aligned} \tag{7}$$

The calculation of radial integrals $\mathbf{Re}R_\lambda(1243)$ is reduced to the solution of a system of differential equations:

$$\left.\begin{aligned} y_1' &= f_1 f_3 Z_\lambda^{(1)}(\alpha|\omega|r) r^{2+\lambda}, \\ y_2' &= f_2 f_4 Z_\lambda^{(1)}(\alpha|\omega|r) r^{2+\lambda}, \\ y_3' &= [y_1 f_2 f_4 + y_2 f_1 f_3] Z_\lambda^{(2)}(\alpha|\omega|r) r^{1-\lambda}. \end{aligned}\right\} \tag{8}$$

In addition, $y_3(\infty)=\mathbf{Re}R_\lambda(1243)$, $y_1(\infty)=X_\lambda(13)$. The system of differential equations includes also equations for functions $f/r^{|æ|-1}$, $g/r^{|æ|-1}$, $Z_\lambda^{(1)}$, $Z_\lambda^{(2)}$. The formulas for the autoionization (Auger) decay probability include the radial integrals $R_\alpha(\alpha k \gamma \beta)$, where one of the functions describes electron in the continuum state. When calculating this integral, the correct normalization of the function Ψ_k requires the attention. The correctly normalized function should have the following asymptotic at $r \to 0$:

$$\left.\begin{matrix} f \\ g \end{matrix}\right\} \to (\lambda\omega)^{-1/2} \begin{cases} \left[\omega + (\alpha Z)^{-2}\right]^{1/2} \sin(kr+\delta), \\ \left[\omega - (\alpha Z)^{-2}\right]^{1/2} \cos(kr+\delta). \end{cases} \tag{9}$$

When integrating the master system, the function is calculated simultaneously:

$$N(r) = \left\{ \pi\omega_k \left[f_k^2 \left[\omega_k + (\alpha Z)^{-2} \right] + g_k^2 \left[\omega_k + (\alpha Z^{-2}) \right] \right] \right\}^{1/2} \tag{10}$$

Other details can be found in refs.[10-13,16-20] as well as description of the "Superatom" and Cowan PC codes, used in all computing.

3. Results and conclusions

In figure 1 there are presented the Be+ ion-yield scan across the 2*pns* and 2*pnd* resonances (circles connected by a black line) and a least-squares fit curve of Fano profiles (gray curve) [3]. In Fig.2 there are presented The Be+ ion-yield scan across the 2*pns* and 2*pnd* resonances (solid line) together with calculated cross sections by Green (dash-dotted line), by Tully-Seaton-Berrington (gray solid line), and by Kim- Tayal-Zhou-Manson (dotted line). The experimental data [3] were scaled to match the theoretical cross section (from Ref.[3]).

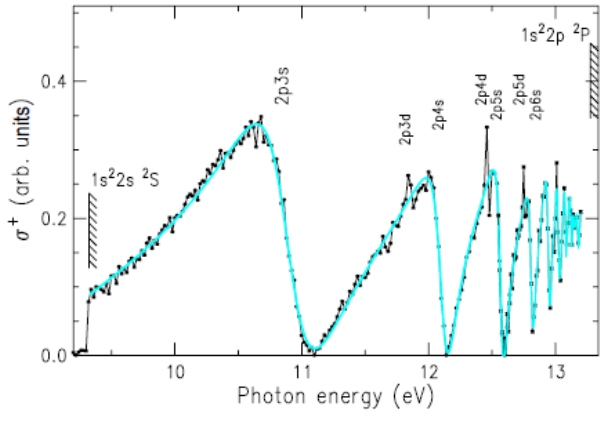

Figure 1. Be+ ion-yield scan across the 2pns and 2pnd resonances (circles connected by a black line) and a least-squares fit curve of Fano profiles (gray curve) [3]

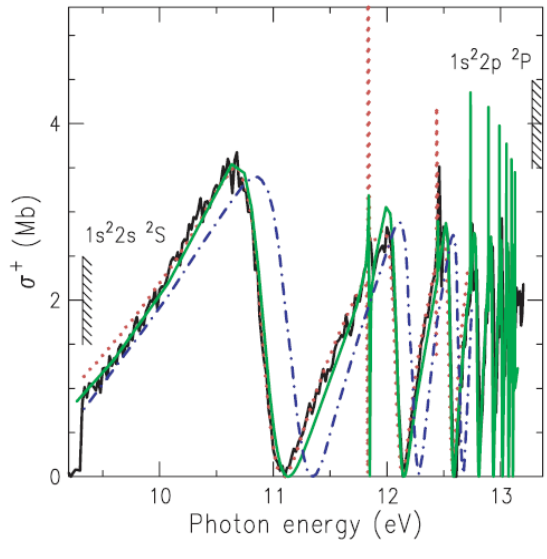

Figure 2. The Be+ ion-yield scan across the 2pns and 2pnd resonances (solid line) together with calculated cross sections by Green (dash-dotted line), by Tully-Seaton-Berrington (gray solid line), and by Kim- Tayal-Zhou-Manson (dotted line). The experimental data [3] were scaled to match the theoretical cross section.

In Tables 1 we present the resonance energies and widths for the 2pns resonances in the beryllium spectrum. The experimental (by Wehlitz-Lukic-Bluett, WLB; by Mehlman-Balloffet-Esteva, ME; by Esteva-Mehlman-Balloffet-Romand, EMR) and alternative theoretical data by Chi-Huang- Cheng (CHC), Tully-Seaton-Berrington (TSB) and by Kim- Tayal-Zhou-Manson (KTZM) are taken from Ref. [3].

Table 1a.

The energy position E, width Γof the Be 2pns resonances (see text)

The energy position E (eV)						
n	Exp, WLB	Exp, (EMR) (ME)	Th, (TSB)	Th, (CHC)	Th, KTZM	Our data
3	10.889	10.933 10.71	10.915	10.63	10.910	10.903
4	12.112	12.096 11.97	12.102	12.09	12.092	12.098
5	12.571	12.572 12.53	12.571	12.64	12.558	12.570
6	12.812	12.811 12.78	12.800	12.91	12.791	12.806
7	12.944	12.945 12.92	12.932	13.06	12.924	12.952
8	13.022	13.029 13.01	-	13.15	13.007	13.028
9	13.078	13.083	-	13.21	13.062	13.092
10	13.123	13.121	-	13.25	13.101	13.130
11	13.143	13.152	-	-	13.129	13.152
12	13.178	13.170	-	-	-	13.180
13	-	-	-	-	-	13.213
14	-	-	-	-	-	13.248

Table 1b.

The energy position E, width Γof the Be 2pns resonances (see text)

The width Γof the resonance (meV)					
n	Exp, WLB	Th, (TSB)	Th, Green	Th, KTZM	Our data
3	531. (10)	606	530	473	473
4	174. (10)	180	168	162	176
5	77.(10)	78	76	73	78
6	47.(3)	42	-	-	51
7	29.(3)	22	-	-	33
8	16.(3)	-	-	-	18
9	3(5)	-	-	-	5
10	3(5)	-	-	-	4
11		-	-	-	4
12		-	-	-	3

In the Table 2 we present the comparison of our data on the the resonance energies and widths for the AR 2pnd resonances in the beryllium spectrum.

Table 2.

Theoretical data for positions (eV) of the Be 2pnd resonances compared to previously published resonance positions (see text)

The energy position E (eV)						
n	Exp, WLB	Exp, (EMR) (ME)	Th, (TSB)	Th, (CHC)	Th, KTZM	Our data
3	11.840 (6)	11.855 11.862	11.840	12.03	12.831	11.848
4	12.460 (6)	12.503 12.466	12.448	12.61	12.437	12.458
5	12.742 (6)	12.789 12.757	12.735	12.89	12.727	12.746
6	-	12.952 12.919	12.893	13.05	12.886	12.908
7	-	-	-	-	-	13.092
8	-	-	-	-	-	13.262

On the one hand, there is sufficiently good accuracy of our theory, the secondly (bearing in mind that most of the listed methods are developed specifically for the study helium and can not be easily generalized to the case of the heavy multi-electron atoms) the definite advantage of the presented approach. Let us note that in ref. [14] (see also [5,12]) it had been predicted a new optics and spectroscopy effect of the giant changing of the AS width in a sufficiently weak electric field (for two pairs of the Tm, Gd AR). Naturally any two states of different parity can be mixed by the external electric field. The mixing leads to redistribution of the autoionization widths. In a case of the heavy elements such as lanthanide and actinide atoms the respective redistribution has a giant effect. In the case of degenerate or

near-degenerate resonances this effect becomes observable even at a moderately weak field. We have tried to discover the same new spectral effect in a case of the Be Rydberg autoionization states spectrum using the simplified version of the known strong-field operator PT formalism [5,14]. However, the preliminary estimates have indicated on the absence of the width giant broadening effect for the helium case, except for minor changes of the corresponding widths, which are well known in the standard atomic spectroscopy. In whole an detailed analysis shows quite physically reasonable agreement between the presented theoretical and experimental results. But some difference, in our opinion, can be explained by different accuracy of estimates of the radial integrals, using the different type basis's (gauge invariance conservation or a degree of accounting for the exchange-correlation effects) and some other additional computing approximations. In our theory there are used gauge-optimized basis's of the relativistic and such basis has advantage in comparison with the standard DF type basis's.

References

1. Grant I.P., Relativistic Quantum Theory of Atoms and Molecules.-Oxford, 2008.-650P.
2. Luc Koenig E., Aymar M., Van Leeuwen R., Ubachs W., Hogervorst W.//Phys. Rev.A.-1999.-Vol.52.-P.208-215.
3. Wehlitz R., Lukic D., Bluett J.B., Resonance parameters of autoionizing Be 2pnl states// Phys.Rev.A.-2003.-Vol.65.-P. 052708.
4. Glushkov A.V., Svinarenko A.A., Ternovsky V.V., Smirnov A.V. , Zaichko P.A., Spectroscopy of the complex autoionization resonances in spectrum of helium: Test and new spectral data//Photoelectronics ("Copernicus").-2015.-Vol.24.-P.94-102.
5. Glushkov A.V., Relativistic Quantum Theory. Quantum, mechanics of Atomic Systems.-Odessa: Astroprint, 2008.-700P.
6. Safronova U.I., Safronova M.S., Third-order relativistic many-body calculations of energies, transition rates, hyperfine constants, and blackbody radiation shift in $^{171}Yb^{+}$//Phys. Rev. A.-2009.-Vol.79.-P. 022512.
7. Bieron J, Froese-Fischer C., Fritzsche S., Pachucki K., Lifetime and hyperfine structure of $^{3}D_{2}$ state of radium// J.Phys.B:At.Mol.Opt.Phys.-2004.-Vol.37.-P.L305-311.
8. Ivanov L.N.,Ivanova E.P., Extrapolation of atomic ion energies by model potential method: Na-like spectra/ // Atom.Data Nucl .Data Tab.-1999.-Vol.24.-P.95-121.
9. Bekov G.I., Vidolova-Angelova E., Ivanov L.N.,Letokhov V.S., Mishin V.I., Laser spectroscopy of low excited autoionization states of the ytterbium atom// JETP.-1981.-Vol.80.-P.866-878.
10. Vidolova-Angelova E., Ivanov L.N., Autoionizing Rydberg states of thulium. Re-orientation decay due to monopole interaction// J.Phys.B:At.Mol.Opt. Phys.-1999.-Vol.24.-P.4147-4158
11. Ivanov L.N., Letokhov V.S. Spectroscopy of autoionization resonances in heavy elements atoms// Com.Mod. Phys.D.:At.Mol.Phys.-1995.-Vol.4.-P.169-184.
12. Glushkov A.V., Ivanov L.N., Ivanova E.P., Radiation decay of atomic states. Generalized energy approach// Autoioni-zation Phenomena in Atoms.- M.: Moscow State Univ.-1996. –P.58-160.
13. Glushkov A.V., Ivanov L.N. Radiation decay of atomic states: atomic residue and gauge non-invariant contributions // Phys. Lett.A.-1999.-Vol.170.-P.33-38.
14. Glushkov A.V., Ivanov L.N. DC Strong-field Stark-effect: consistent quantum-mechanical approach// J.Phys.B: At. Mol. Opt. Phys.-1993.-Vol.26.- P.L379-386.
15. Glushkov A.V., Khetselius O.Yu., Svinarenko A.A., Relativistic theory of cooperative muon-gamma-nuclear processes: Negative muon capture and metastable nucleus discharge//

Advances in the Theory of Quantum Systems in Chemistry and Physics (Springer).-2012.-Vol.22.-P.51-70.
16. Glushkov A.V., Khetselius O.Yu., Loboda A.V., Svinarenko A.A., QED approach to atoms in a laser field: Multiphoton resonances and above threshold ionization//Frontiers in Quantum Systems in Chemistry and Physics (Springer).-2008.-Vol.18.-P.541-558.
17. Glushkov A.V., Svinarenko A.A., Ignatenko A.V., Spectroscopy of autoionization resonances in spectra of the lanthanides atoms//Photoelectronics.-2011.-Vol.20.-P. 90-94**.**
18. Svinarenko A.A., Nikola L.V., Prepelitsa G.P., Tkach T., Mischenko E., The Auger (autoionization) decay of excited states in spectra of multicharged ions: Relativistic theory//Spectral Lines Shape.-2010.-Vol.16.-P.94-98
19. Svinarenko A.A., Spectroscopy of autoionization resonances in spectra of barium: New spectral data // Phototelectronics.-2014.-Vol.23.-P.85-90.
20. Malinovskaya S.V., Glushkov A.V., Khetselius O.Yu., Svinarenko A., Bakunina E.V., Florko T.A., The optimized perturbation theory scheme for calculating interatomic potentials and hyperfine lines shift for heavy atoms in buffer inert gas//Int. Journ.of Quantum Chemistry.-2009.-Vol.109.-P.3325-3329.
21. Khetselius O.Yu., Relativistic perturbation theory calculation of the hyperfine structure parameters for some heavy-element isotopes//Int. Journ. of Quantum Chemistry.-2009.-Vol.109,N14.-P.3330-3335.
22. Madden R., Codling K., New autoionization atomic energy levels in He, Ne, Ar// Phys.Rev.Lett. 1993-Vol.10.-P.516-520.
23. SakhoI., Konté K., Ndao A.S., Biaye M., Wagué A., Calculations of $(nl)^2$ and (3lnl') autoionizing states in two-electron systems/.// Physics Scripta.-2010.-Vol.82.-P. 035301 (8pp)
24. Ho Y.K., Autoionizing $^1P^0$ states of He between the N=2 and 3 threshold of He^+ //Phys.Rev.A.1999.-Vol.44.-P.4154-4161.

This article has been received in May 2016

UDC 539.183

A. V. Smirnov, V. V. Buyadzhi, A. V. Ignatenko, A. V. Glushkov, A. A. Svinarenko

SPECTROSCOPY OF THE COMPLEX AUTOIONIZATION RESONANCES IN SPECTRUM OF BERYLLIUM

Abstract

We applied a generalized energy approach (Gell-Mann and Low S-matrix formalism) combined with the relativistic multi-quasiparticle (QP) perturbation theory (PT) with the Dirac-Kohn-Sham zeroth approximation and accounting for the exchange-correlation, relativistic corrections to studying autoionization resonances in the beryllium Be spectrum, in particular, we predicted the energies and widths of the number of the Rydberg resonances. There are presented the results of comparison of our theory data for the autoionization resonance $3s3p\ ^1P_0$ with the available experimental data and those results of other theories, including, method Greene, by Tully-Seaton-Berrington and by Kim- Tayal-Zhou-Manson etc

Key words: spectroscopy of autoionization resonances, relativistic energy approach, beryllium

УДК 539.183

А. В. Смирнов, В. В. Буяджи, А. В. Игнатенко, А. В. Глушков, А. А. Свинаренко

СПЕКТРОСКОПИЯ СЛОЖНЫХ АВТОИОНИЗАЦИОННЫХ РЕЗОНАНСОВ В СПЕКТРЕ БЕРИЛЛИЯ

Резюме

Обобщенный энергетический подход (S-матричный формализм Гелл-Мана и Лоу) и релятивистская теория возмущений с дирак-кон-шэмовским нулевым приближением и учетом обменно-корреляционных и релятивистских поправок применены к изучению автоионизационных резонансов в атоме бериллия, в частности, предсказаны энергии и ширины ряда ридберговых резонансов. Представлены результаты сравнения данных нашей теории, в частности, для автоионизацийного резонанса 2pnl с имеющимися экспериментальными данными и результатами других теорий, в том числе, теорий Greene, Tully-Seaton-Berrington, Kim-Tayal-Zhou-Manson и т.д.

Ключевые слова: спектроскопия автоионизационных резонансов, релятивистский энергетический подход, бериллий

УДК 539.183

А. В. Смірнов, В. В. Буяджи, Г. В. Ігнатенко, О. В. Глушков, А. А. Свинаренко

СПЕКТРОСКОПІЯ СКЛАДНИХ АВТОІОНІЗАЦІЙНИХ РЕЗОНАНСІВ В СПЕКТРІ БЕРИЛІЮ

Резюме

Узагальнений енергетичний підхід (S-матричний формалізм Гелл-Мана та Лоу) и релятивістська теорія збурень з дірак-кон-шемівським нульовим наближенням та урахуванням обмінно-кореляційних і релятивістських поправок застосований до вивчення автоіонізаційних резонансів у атомі берилію, зокрема, передбачені енергії та ширини ряду рідбергових резонансів. Представлені результати порівняння даних нашої теорії, зокрема, для автоіонізаційного резонансу 2pnl з наявними експериментальними даними і результатами інших теорій, у тому числі, теорій Greene, Tully-Seaton-Berrington, Kim-Tayal-Zhou-Manson і т.д.

Ключові слова: спектроскопія автоіонізаційних резонансів, релятивістський енергетичний підхід, берилій

UDC 539.184

I. N. Serga, T. A. Kulakli, A. V. Smirnov, O. Yu. Khetselius, V. V. Buyadzhi

Odessa State Environmental University, 15, Lvovskaya str., Odessa, Ukraine
e-mail: nucserga@mail.ru

RELATIVISTIC THEORY OF SPECTRA OF USUAL AND EXOTIC ATOMS: NITROGEN HYPERFINE TRANSITIONS ENERGIES

A new theoretical approach to the description of spectral parameters pionic atoms in the excited states with precise accounting relativistic, radiation and nuclear effects is applied to the study of energy and spectral parameters of transitions between hyperfine structure components. As an example of the present approach presents new data on the energies of the hyperfine structure transitions 5g-4f, 5f-4d in the spectrum of pionic nitrogen are presented and it is performed comparison with the corresponding theoretical data by Trassinelli-Indelicato

1. Introduction

Our work is devoted to the further application of earlier developed new theoretical approach [1-3] to the description of spectra and different spectral parameters, in particular, radiative transitions probabilities for pionic atoms in the excited states with precise accouting relativistic, radiation. Here problem to be solved is estimate of the hyperfine structure components transition energies in the pionic atom of nitrogen. Earlier we have presented the corresponsing data on the radiation probabilities [1].

As it was indicated earlier [1-3] nowadays investigation of the pionic and at whole the exotic hadronic atomic systems represents a great interest as from the viewpoint of the further development of atomic and nuclear spectral theories as creating new tools for sensing the nuclear structure and fundamental pion-nucleus strong interactions [1-15]. It is, above all, the strong pion-nucleon interaction, new information about the properties of nuclei and hadrons themselves and their interactions with the nucleus of the measured energy X-rays emitted during the transition pion spectrum of the atom.

While determining the properties of pion atoms in theory is very simple as a series of H such models and more sophisticated methods such combination chiral perturbation theory (TC), adequate quantitative description of the spectral properties of atoms in the electromagnetic pion sector (not to mention even the strong interaction sector) requires the development of High-precision approaches, which allow you to accurately describe the role of relativistic, nuclear, radiation QED (primarily polarization electron-positron vacuum, etc.). pion effects in the spectroscopy of atoms. The most popular theoretical models are naturally based on the using the Klein-Gordon-Fock equation, but there are many important problems connected with accurate accounting for as pion-nuclear strong interaction effects as QED radiative corrections (firstly, the vacuum polarization effect etc.). This topic has been a subject of intensive theoretical and experimental interest (see [1-16]). The perturbation theory expansion on the physical; parameter aZ is usually used to take into account the radiative QED corrections, first of all, effect of the polarization of electron-positron vacuum etc. This approximation is sufficiently correct and comprehensive in a case of the light pionic atoms, however it becomes incorrect in a case of the heavy atoms with large charge of a nucleus Z.

The more correct accounting of the QED, finite nuclear size and electron-screening effects for pionic atoms is also very serious and actual problem to be solved more consistently in com-

parison with available theoretical models and schemes.

2. Theory

The basic topics of our theoretical approach have been earlier presented [1-3], so here we are limited only by the key elements. Naturally, the relativistic dynamic of a spinless boson (pion) particle is described by the Klein-Gordon-Fock (KGF) equation. As usually, an electromagnetic interaction between a negatively charged pion and the atomic nucleus can be taken into account introducing the nuclear potential A_ν in the KG equation via the minimal coupling $p_\nu \rightarrow p_\nu - qA_\nu$. The relativistic wave functions of the zeroth approximation for pionic atoms are determined from the KGF equation [1]:

$$m^2c^2\Psi(x) = \{\frac{1}{c^2}[i\hbar\partial_t + eV_0(r)]^2 + \hbar^2\nabla^2\}\Psi(x) \quad (1)$$

where *h* is the Planck constant, c the velocity of the light and the scalar wavefunction $\Psi_0(x)$ depends on the space-time coordinate x = (ct,r).

Here it is considered a case of a central Coulomb potential ($V_0(r)$,0). Then the standard stationary equation looks as:

$$\{\frac{1}{c^2}[E + eV_0(r)]^2 + \hbar^2\nabla^2 - m^2c^2\}\varphi(x) = 0 \quad (2)$$

where E is the total energy of the system (sum of the mass energy mc^2 and binding energy e_0). In principle, the central potential V_0 should include the central Coulomb potential, the radiative (in particular, vacuum-polarization) potential as well as the electron-screening potential in the atomic-optical (electromagnetic) sector. Surely, the full solution of the pionic atom energy especially for the low-excited state requires an inclusion the pion-nuclear strong interaction potential. However, the main problem considered here is computing the radiative transitions probabilities between components of the hyperfine structure for sufficiently high states, when the strong pion-nuclear interaction is not important from the quantitative viewpoint. However, if a pion is on the high orbit of the atom, the strong interaction effects can not be accounted because of the negligible value.

The next step is accounting the nuclear finite size effect or the Breit-Rosenthal-Crawford-Schawlow one. In order to do it we use the widespread Gaussian model for nuclear charge distribution. The advantages of this model in comparison with usually used models such as for example an uniformly charged sphere model and others had been analysed in Ref. [1-]. Usually the Gauss model is determined as follows:

$$\rho(r|R) = \left(4\gamma^{3/2}/\sqrt{\pi}\right)\exp\left(-\gamma r^2\right), \quad (3)$$

where $\gamma = 4\pi/R^2$, R is an effective radius of a nucleus.

In order to take into account very important radiation QED ceffects we use the radiative potential from the Flambaum-Ginges theory [15]. In includes the standard Ueling-Serber potential and electric and magnetic form-factors plus potentials for accounting of the high order QED corrections such as:

$$\Phi_{rad}(r) = \Phi_U(r) + \Phi_g(r) + \Phi_f(r) + . \\ + \Phi_l(r) + \frac{2}{3}\Phi_U^{high-order}(r) \quad (4)$$

where

$$\Phi_{rad}(r) = \Phi_U(r) + \Phi_g(r) + \Phi_f(r) + . \\ + \Phi_l(r) + \frac{2}{3}\Phi_U^{high-order}(r) \quad (5)$$

Here *e* – a proton charge and universal function *B*(*Z*) is defined by expression: *B*(*Z*)=0.074+0.35*Z*a.

At last to take into account the electron screening effect we use the standard procedure, based on addition of the total interaction potential SCF potential of the electrons, which can be determined within the Dirac-Fock method by solution of the standard relativistic Dirac equations. It should be noted however, that contribution of theses corrections is practically zeroth for the pionic nitrogen, however it can be very important in transition to many-electron as a rule heave pionic atoms.

Further in order to calculate the energies and probabilities of the radiative transitions between energy level of the pionic atoms we have used the well known relativistic energy approach (look [17-19] and Refs. in [16], which is used for computing probabilities.

The expression for the energy of the hyperfine splitting (magnetic part of) the energy levels of the atom in the pion:

$$E_1^{nlF} = \frac{\mu_I \mu_N e \mu_0 \hbar c^2}{4\pi\left(E_0^{nl} - \left\langle nl\left|V_0(r)\right|nl\right\rangle\right)} \times$$

$$\times\left[\frac{F(F+1) - I(I+1) - l(l+1)}{2I}\right]\left\langle nl\left|r^{-3}\right|nl\right\rangle \quad (6)$$

Here $m_N = e\hbar / 2m_p c$; other notations are standard. In a consistent precise theory it is important allowance for the contribution to the energy of the hyperfine splitting of the levels in the spectrum of the pion atom due to the interaction of the orbital momentum of the pion with the quadrupole moment of the atomic nucleus. The corresponding part can be presented as follows [3]:

$$< LIFM\left|W_Q\right|LIFM \geq \quad \Delta + B \quad (C+1) \quad (7)$$

where

$$C=F(F+1)-L(L+1)-I(I+1), \quad (8)$$

$$B = -\frac{3}{4}\frac{e^2 Q}{I(2I-1)}\frac{(\gamma \cdot L\|\eta_2\|\gamma \cdot L)}{\sqrt{L(L+1)(2L-1)(2L+1)(2L+3)}} \quad (9)$$

$$\Delta = \frac{e^2 Q(I+1)}{(2I-1)}\frac{(\gamma \cdot L\|\mu_2\|\gamma \cdot L)L(L+1)}{\sqrt{L(L+1)(2L-1)(2L+1)(2L+3)}} \quad (10)$$

Here L – is orbital moment of pion, F is a total moment of an atom.

3. Results and conclusions

As example of application of the presented approach, in tables 1, 2 we present the data on energies (in eV) of the hyperfine transitions 5g-4f in the spectrum of the pion nitrogen): Th1- data by Trassinelli-Indelicato; Th2- our data. In theory by Trassinelli-Indelicato (look, for example, [4]) it has been used the standard atomic spectroscopy amplitude scheme when the transitions energies and probabilities are calculated in the known degree separately. In table 2 we present our data for energies (in eV) of the hyperfine transitions 5f-4d in the spectrum of the pion nitrogen: our data

Table 1.

The energies (in eV) of the hyperfine transitions 5g-4f in the spectrum of the pion nitrogen: Th1- data by Trassinelli-Indelicato; Th2- our data

F-F’	T.I : P (5g-4f)	T.II : P (5g-4f)
5-4	4055.3779	4055.3728
4-3	4055.3821	4055.3777
4-4	4055.3762	4055.3715
3-2	4055.3852	4055.3804
3-3	4055.3807	4055.3765
3-4	4055.3747	4055.3710

Table 2.

The energies (in eV) of the hyperfine transitions 5f-4d in the spectrum of the pion nitrogen: our data

F-F’	Our data (5f-4d)
4-3	4057.6819
3-2	4057.6915
3-3	4057.6799
2-1	4057.6978
2-2	4057.6905
2-3	4057.6789

In whole, the computed values of energies for considered transitions between hyperfine structure components in the spectrum of the pion within theory by Trassinelli-Indelicato and ours demonstrate physically reasonable agreement. , however our values are a little different. This fact can be explained by difference in the computing schemes and different level of accounting for nuclear finite size, QED and other effects (look details [1-3,20,21]).

References

1. Serga I.N., Relativistic theory of spectra of pionic atoms: radiation transition probabilities// Photoelec-tronics ("Copernicus").-2015.-Vol.24.-P.44-49.
2. Serga I.N., Dubrovskaya Yu.V., Kvasikova A.S., Shakhman A.N., Sukharev D.E., Spectroscopy of hadronic atoms: Energy shifts// Journal of Physics: C Ser.-2012.- Vol.397.-P.012013.
3. Serga I.N., Relativistic theory of spectra of pionic atoms with account of the radiative corrections: hyperfine structure// Photoelectronics.-2014.-Vol.23.-P.171-175.
4. Deslattes R., Kessler E., Indelicato P., de Billy L., Lindroth E. , Anton J., Exotic atoms//Rev. Mod. Phys. -2003.-Vol.75.-P.35-70; Indelicato P., Trassinelli M., From heavy ions to exotic atoms// arXiv: physics.-2005.-V1-0510126v1.-16P.
5. Backenstoss G., Pionic atoms//Ann. Rev. Nucl.Sci.-1970.-Vol.20-P.467-510
6. Menshikov L I and Evseev M K, Some questions of physics of exotic atoms// Phys. Uspekhi.2001-Vol. 171.-P.150-184.
7. Mitroy J., Ivallov I.A., Quantum defect theory for the study of hadronic atoms// J. Phys. G: Nucl. Part. Phys.-2001.-Vol.**27.-P.**1421–1433
8. Lyubovitskij V., Rusetsky A., πp atom in ChPT: Strong energy-level shift// Phys. Lett.B.-2000.-Vol.494.-P.9-13.
9. Schlesser S., Le Bigot E.-O., Indelicato P., Pachucki K., Quantum-electro-dynamics corrections in pionic hydrogen // Phys.Rev.C.-2011.-Vol.84.-P.015211 (8p.).
10. Sigg D., Badertscher A., Bogdan M. et al, The strong interaction shift and width of the ground state of pionic hydrogen// Nucl. Phys. A.-1996.-Vol.609.-P.269-309.
11. Gotta D., Amaro F., Anagnostopoulos D., Conclusions from recent pionic–atom experiments//Cold Antimatter Plasmas and Application to Fundamental Physics, ed. Y.Kania and Y.Yamazaki (AIP).-2008.-Vol.CP1037.-P.162-177.
12. Gotta D., Amaro F., Anagnostopoulos D., Pionic Hydrogen//Precision Physics of Simple Atoms and Molecules, Ser. Lecture Notes in Physics (Springer, Berlin / Heidelberg).-2008.-Vol.745.-P.165-186
13. Deloff A., Fundamentals in Hadronic Atom Theory, Singapore: World Scientific, 2003.-352P.
14. Serga I.N., Dubrovskaya Yu.V., Kvasikova A.S., Shakhman A.N., Sukharev D.E., Spectroscopy of hadronic atoms: Energy shifts// Journal of Physics: C Ser.-2012.- Vol.397.-P.012013.
15. Flambaum V.V., Ginges J.S.M., Radiative potential and calculation of QED radiative corrections to energy levels and electromagnetic amplitudes in many-electron atoms //Phys.Rev.-2005.-Vol.72.-P.052115 (16p).
16. Glushkov A.V., Relativistic quantum theory. Quantum mechanics of atomic systems, Odessa: Astroprint, 2008.-700P.
17. Ivanov L.N.,Ivanova E.P., Extrapolation of atomic ion energies by model potential method: Na-like spectra/ // Atom. Data Nucl .Data Tab.-1999.-Vol.24.-P.95-121.
18. Glushkov A.V., Ivanov L.N., Ivanova E.P., Radiation decay of atomic states. Generalized energy approach// Autoionization Phenomena in Atoms.- M.: Moscow State Univ.-1986.
19. Glushkov A.V., Ivanov L.N. Radiation decay of atomic states: atomic residue and gauge non-invariant contributions // Phys. Lett.A.-1992.-Vol.170.-P.33-38.
20. Pavlovich V.N., Serga I.N., Zelentsova T.N., Tarasov V.A., Mudraya N.V., Interplay of the hyperfine, electroweak and strong interactions in heavy hadron-atomic systems and x-ray standards status// Sensor Electronics and Microsyst. Techn.-2010.-N2.-P.20-26.
21. Serga I.N., Relativistic theory of spectra of pionic atoms with account of the radiative and nuclear corrections// Photoelectronics.2013.-Vol.22.-P.84-92.

This article has been received in May 2016

UDC 539.184

I. N. Serga, T. A. Kulakli, A. V. Smirnov, O. Yu. Khetselius, V. V. Buyadzhi

RELATIVISTIC THEORY OF SPECTRA OF USUAL AND EXOTIC ATOMS WITH ACCOUNT OF THE NUCLEAR AND RADIATIVE CORRECTIONS: NITROGEN HYPERFINE TRANSITIONS ENERGIES

Abstract

A new theoretical approach to the description of spectral parameters pionic atoms in the excited states with precise accounting relativistic, radiation and nuclear effects is applied to the study of energy and spectral parameters of transitions between hyperfine structure components. As an example of the present approach presents new data on the energies of the hyperfine structure transitions 5g-4f, 5f-4d in the spectrum of pionic nitrogen are presented and it is performed comparison with the corresponding theoretical data by Trassinelli-Indelicato.

Keywords: relativistic theory, hyperfine structure, pionic atom

УДК 539.184

И. Н. Серга, Т. А. Кулакли, А. В. Смирнов, О. Ю. Хецелиус, В. В.Буяджи

РЕЛЯТИВИСТСКАЯ ТЕОРИЯ СПЕКТРОВ ОБЫЧНЫХ И ЭКЗОТИЧЕСКИХ АТОМОВ С УЧЕТОМ РАДИАЦИОННЫХ ПОПРАВОК: ЭНЕРГИИ ПЕРЕХОДОВ МЕЖДУ КОМПОНЕНТАМИ СВЕРХТОНКОЙ СТРУКТУРЫ АЗОТА

Резюме

Новый теоретический подход к описанию спектральных параметров пионных атомов в возбужденном состоянии с учетом релятивистских, радиационных эффектов применен к изучению энергетических параметров переходов между компонентами сверхтонкой структуры. В качестве примера применения представленного подхода, представлены новые данные по энергиям переходов между компонентами сверхтонкой структуры переходов 5g-4f, 5f-4d в спектре пионного азота и проведено сравнение с соответствующими теоретическими данными Trassinelli-Indelicato.

Ключевые слова: релятивистская теория, сверхтонкая структура, пионный атом

УДК 539.184

І. М. Сєрга, Т. О. Кулаклі, А. В. Смірнов, О. Ю. Хецеліус, В. В. Буяджи

РЕЛЯТИВІСТСЬКА ТЕОРІЯ СПЕКТРІВ ЗВИЧАЙНИХ ТА ЕКЗОТИЧНИХ АТОМІВ З УРАХУВАННЯМ РАДІАЦІЙНИХ ПОПРАВОК: ЕНЕРГІЇ ПЕРЕХОДІВ МІЖ КОМПОНЕНТАМИ НАДТОНКОЇ СТРУКТУРИ АЗОТУ

Резюме

Новий теоретичний підхід до опису спектральних параметрів піонних атомів у збудженому стані з урахуванням релятивістських, радіаційних ефектів на основі рівняння Клейна-Гордона-Фока застосовано до вивчення енергетичних параметрів переходів між компонентами надтонкої структури. Як приклад застосування представленого підходу, представлені нові дані про енергії переходів між компонентами надтонкої структури переходів 5g-4f, 5f-4d в спектрі піонного азоту і проведено порівняння з відповідними теоретичними даними Trassinelli-Indelicato.

Ключові слова: релятивістська теорія, надтонка структура, піоний атом

UDC 621.315.592

S. A. Gevelyuk[1], E. Rysiakiewicz-Pasek[2], I. K. Doycho[1]

DEPENDENCE OF PHOTOLUMINESCENCE OF NANOPARTICLE ENSEMBLES OF STANNUM (IV) COMPLEXES IN SILICA POROUS MATRIX ON CONCENTRATION OF SATURATING SOLUTION

[1]I. I. Mechnikov National University of Odessa, Dvoryanska St., 2, Odessa, 65026, Ukraine
[2] Institute of Physics, Wrocław University of Technology, W.Wyspianskiego 27, 50-370 Wrocław, Poland

Dependence of photoluminescence of high-molecular nanoformations of dyes on the basis of stannum (IV) complexes in porous glass on concentration of saturating solution has been researched. The results have been compared with photoluminescence of corresponding solutions, in which the effect of concentration quenching, was due to the Franck-Condon principle, was observed. It was found that intensity of luminescence for nanoparticle ensembles was always higher than in solution. At that, decrease of luminescence intensity alongside with concentration growth of saturating solution was observed as well. However, the observed dependence was more complicated than in solution. It can be explained by the fact that the pores with maximal sizes are filled at large concentrations of saturating solution of dye. The dye particles act almost the same as in solution, where photoluminescence is fainter, in such pores.

1. Introduction

It is known [1-2] that the dyes on base of the 4-valence stannum complexes are most sensitive to the gas composition of environment, therefore they can be used for construction of gas sensors, used for the ecological monitoring [3]. It is a big group of dyes, which are close structurally and differ with some details of their molecular composition only. Previous investigations show [4] that the luminescence centra in specified dyes are probable concentrated on the surface of molecules. So surface development of particles of this substance by creating of nanoparticles ensemble inside matrix of porous glass may result in increase of luminescence. We created such ensemble by soak glass with corresponding solution. At that concentration of the soaking solution is its most importable characteristic. Dependence of luminescence properties of nanoparticle ensemble on concentration of the soaking solution and also comparison of this result with luminscence of the solution itself are the subject of present paper. Such research will permit to elaborate ways of affecting their optic and photoluminescence features that will considerably widen the sphere of functional hybrid nanomaterials. An important factor, affecting the effectiveness of dye luminescence, is interaction of separate dye molecules when its concentration in solution grows [5-6]. In this case aggregating takes place, i.e. formation of molecular assemblies (clusters) [7]. As centers of dye luminescence are concentrated on surface of molecule [4], aggregating causes self-passivating of dye [8] that must considerably decrease luminescence. Use of porous glass minimizes interaction between molecules and aggregations and also among molecules of dye inside assemblies, weakening this effect and strengthening luminescence [9]. Quantity of nanoparticles, formed in pores, must depend on concentration of solution, saturating glass [10].

Two dyes on the basis of complexes of four-valent stannum [11]: 4-amic-benzoyl hydrazone of tetra-dimethyl aminobenzaldehyde (hereinaf-

ter – dye **(I)**) and 4-hydroxyl-benzoyl hydrazone of tetra-dimethyl aminobenzaldehyde (hereinafter – dye **(II)**) was studied in the present paper. Dependence of luminescence spectra of nanoparticle ensembles of specified dyes in porous glass on their concentration in dimethyl formamide (DMFA) solution, which was soaked glass, was researched. Results of research were compared with photoluminescence of solutions these dyes having correspondent concentration [12].

2. Materials and methods

Ensemble of nanoparticles of dye was formed by way of saturation of ***A***-type porous silica glass with corresponding solution in DMFA. The porous glass ***A*** is obtained from sodium boro-silicate glass. The glass is heated at the temperature of 763K at 165h in order to separate phases rich in silica and sodium-boron. Then it is immersed in 0.5N hydrochloric acid and deionized water. The porosity determined from the mass decrement after etching was: 38%. The texture parameters of investigated glasses were determined by adsorption poroscopy method. The average diameter of pores was 30 nm, total average pore volume was 292 mm^3/g and the average surface area was 54,7 m^2/g. The residual fine dispersed secondary silica gel presents in pores of glass after this chemical treatment.

Duration of saturation process was 10-12 hours and its end was fixed in accordance with visual changes in the system. After the end of saturation the sample was keeping by room temperature during a day (so called low temperature annealing) in order to secure uniform enough dimensional distribution of nanoparticles in the glass [1, 10].

For experimental research of influence of saturating solution concentration on photoluminescence of nanoparticle ensemble of dye in porous matrix, porous glass was saturated by two types of dye solutions on the basis of complexes of fourvalent stannum: dye **(I)** or dye **(II)**. Structural formulas of both types of dyes are shown in *Fig.1*. One can see, that both substances are very much similar as to their structure: they have the same tautomeric form «4», the same substituent type (benzoyl) and almost the same coodination set (there is "extra" hydrogen atom in dye **(II)**, securing electrical neutrality of the molecule). They differ in substituent: it is amic in dye **(I)** and hydroxyl in dye **(II)**.

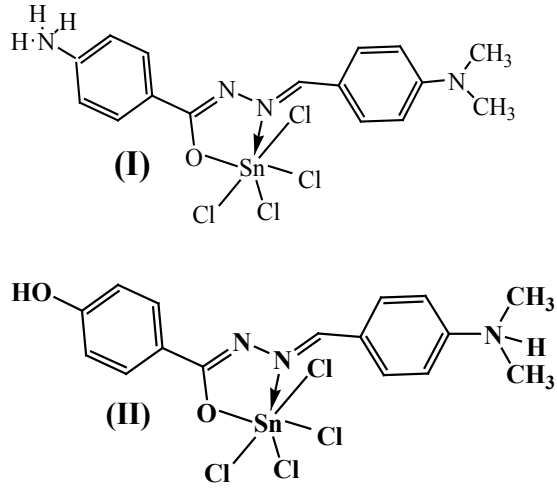

Fig.1. Structural formulas of dyes, for which dependence of luminescence on solution, saturating matrix, was researched: dye (I) – 4-amic-benzoyl hydrazone of tetra-dimethyl aminobenzaldehyde, dye (II) – 4-hydroxyl-benzoyl hydrazone of tetra-dimethyl aminobenzaldehyde

Saturating solutions were of five concentrations (10^{-5}, 5×10^{-5}, 10^{-4}, 5×10^{-4} and 10^{-3} *gMole/l*). The first one can be considered rather low, and the last one is close to limiting concentration of solution.

Photoluminescence spectra were excited with UV laser LCS-DTL-374QT (wavelength λ=355 nm, power 15 mW) and were recorded by standard set-up [13].

3. Experimental results

Fig.2 shows the groups of luminescence spectra for nanoparticle ensembles of dye **(I)** and dye **(II)**, obtained at different concentrations of corresponding saturation solutions. One can see, that the spectra have one maximum at all concentrations of saturating solution for both dyes. The glow intensity of dye **(II)** with hydroxyl substituent is more than for dye **(I)** with amic substituent at any concentration of saturating solution. Maxima of glow intensity of glow intensity are situated rather close to each other for all cases. However, whereas photoluminescence spectrum for dye **(II)** remains practically hyperchromic at

all concentrations of saturating solution, a small, but noticeable, bathochromic shift takes place for dye **(I)** if the concentration of saturating solution is maximal. Decrease of photoluminescence intensity corresponds to this shift.

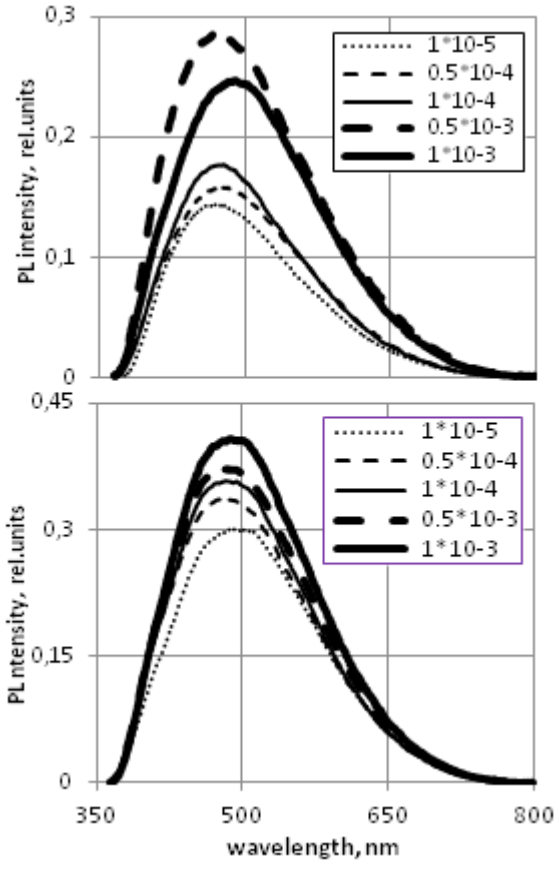

Fig. 2. Photoluminescence spectra of nanoparticle ensemble of dye (I) (on the top) and dye (II) (on the uppon) in porous matrix at different concentrations of saturating solution

Fig.3 shows the experimental concentration dependence of photoluminescence parameters of nanoparticle ensemble for dye **(I)** *(on the left)* and for dye **(II)** *(on the right)* in silica porous glass matrix. Upper part of the figure corresponds to dependence of glow intensity on concentration of saturating solution, and its lower part corresponds to its maximum position of concentration of saturating solution. One can see in *Fig.3* that the increase of photoluminescence intensity accords with "piecewise-linear" law, when concentrations of saturating solution are low. Photoluminescence intensity reduces for nanoparticles of dye ***(I)***, if the concentration of saturating solution is almost limiting one. At that, such reducing is not observed, if the concentration of saturating solution is high, for nanoparticles of dye ***(II)***.

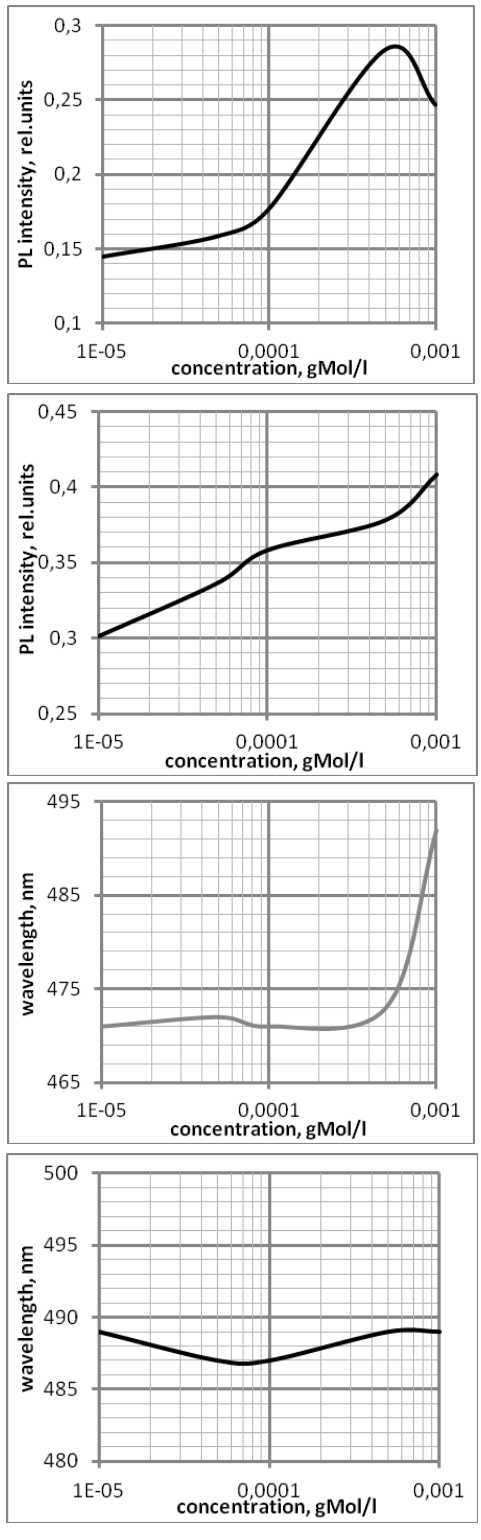

Fig. 3. Experimental concentration dependence of parameters of photoluminescence of nanoparticle ensemble of dye (I) (on the left) and dye (II) (on the right) in silica porous glass matrix

4. Discussion

«Piecewise-linear» law of increase of luminescence intensity of nanoparticle ensemble of dye **(I),** when concentration of saturating solution grows, is associated, evidently, with nonuniformity of filling different sizes of pores [13] when nanoparticles of dye are formed in porous glass. When concentrations of saturating solution are low not many molecules of dye penetrate into pores, and they either penetrate into the smallest pores one by one, or stay on surfaces of larger pores as a quantity of small dye particles (such as "dew"). The silica gel particles, which gather round these dye particles, will prevent merging of them [14]. Photoluminescence intensity at that slowly increases with concentration growth. Similar processes take place, when concentration of saturating solution reaches "middle" values. However, the surface of nanoparticles, appearing inside pores, turns out to be more developed due to increase of quantity of dye molecules. That leads to faster increase of glow intensity [15-16]. When concentration of saturating solution comes close to limiting one, luminescence intensity reduces.

It's interesting to compare these results with dependence of luminescence of dye **(I)** solution in DMFA on its concentration in solution (left part of *Fig.4*, see [12]). Intensity of glow increased linearly with concentration growth, when concentrations are low. When solution concentration comes close to limiting value, effect of concentration quenching was observed, and intensity of photoluminescence started decreasing almost parabolically. Concentration quenching of luminescence for dye **(I)** solution in DMFA is explained by presence of two competing processes in the system: light radiation and light absorption, which take place simultaneously [17] in according with the Franck-Condon principle. If concentration of solution is low, number of radiation transitions increases with its grow, and glow intensity increases too. When concentration of solution is rather high, the process of absorption of the light, which radiated by the solution, starts to prevail, obviously, that causes concentration quenching. This supposition is supported by concentration dependence of photoluminescence maximum position: when concentrations are low, spectrum is hyperchromic, and when they are high, bathochromic shift takes place. This shift indeed accords with supposition on prevalence of absorption process, as high energetic quanta of light are always absorbed first.

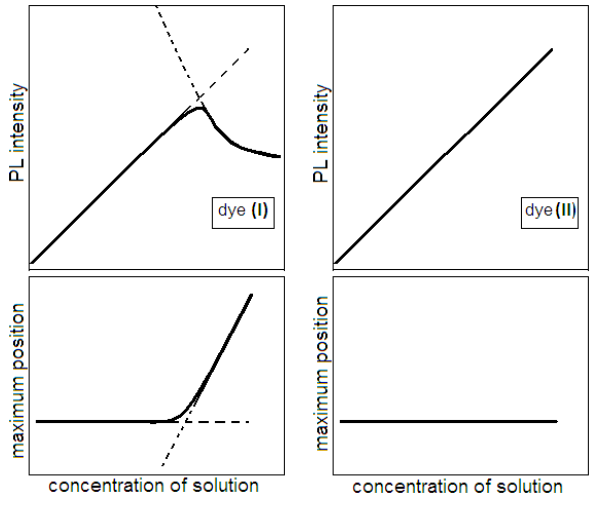

Fig. 4. Model concentration dependence of photoluminescence parameters of dye in solution [12]: when concentrations are low, both types of dye act similarly, but for dye (II) parabola, which corresponds to concentration quenching, is beyond the figure bounds

Our results for nanoparticles ensemble are in accord with this statement. However, reduce of luminescence intensity is not associated with concentration quenching, in contrast to solution, but with the fact that the largest pores (about hundreds of nanometers) turn out to be filled in this case. There would be so many small particles in the large pores, that they would merge in aggregation already at the stage of their formation and silica gel particles would passivate surface of dye molecules partially only wraping around already formed aggregations [7, 9, 14]. That is why the most part of dye, which penetrated into the large pores, acts as in solution, i.e. decrease of photoluminescence intensity, which has almost the same value as that for solution, is observed. This process is also followed by intensive absorption of high energy light quanta (as the lower part of *Fig.3* shows). That leads to additional decrease of dye glow intensity.

For DMFA solution of dye **(II)** when concentration of solution was high, glow intensity continued to increase linearly and no concentration

quenching took place (right part of *Fig.4*, see [12]). Apparently, limiting concentration for this dye is achieved before this effect appears. At that spectrum remained hyperchromic at all concentrations of the solution. These results reasonably accord with regularities, were found in our works [18-19]. Deviations of concentration dependence of photoluminescence intensity from linearity also take placefor ensemble of dye **(II)** nanoparticles, as in the case with dye **(I),** on comparing it with solution. They also are associated with non-uniformity of filling with dye molecules various sizes of pores. At that, decrease of glow intensity is not observed, when concentration of saturating solution is high, as there was no concentration quenching in solution, too. This assertion is supported by absence of bathochromic shift of spectra, is typical when absorption processes in the system prevail. Photoluminescence spectrum remains hyperchromic practically, when concentration of saturating solution grows, as the lower part of *Fig.3* shows.

5. Conclusions

Photoluminescence spectra of formed nanoparticle ensembles have one maximum and differ only in glow intensity and position of its peak for all concentrations of dye solutions on the basis of complexes of four-valent stannum, saturating porous matrix. At that, both in solution and for nanoparticle ensemble, first increase of photoluminescence intensity is observed, when concentration of solution grows, and when it comes to solubility limit, its decrease takes place, which is associated with prevalence of the process of photons' absorption over their radiation. This is supported by the fact that intensity increase is followed by hyperchromic spectrum, and its decrease is followed by bathochromic shift.

Acknowledgment

The authors express gratitude to associate professor of the Chair of General Chemistry and Polymers of I. I. Mechnikov National University of Odessa, Shmatkova N.V., for useful discussions during preparation of the present paper.

References

1. Zhu C., Zheng H., Li D., Liand S., Xu J. Fluorescence quenching method for the determination of sodium dodecyl sulphate with near-infrared hydrophobic dye in the presence of Triton X-100 // Spectrochim. Acta A. – 2004. – V.60. P.3173-3179.
2. Zhu Ch-Q., Wu Yu-Q., Zheng H., Chen J-L., LiD-H., Li Sh-H., Xu J-G. Determination of nucleic acids by near-infrared fluorescence quenching of hydrophobic thiacyanine dye in the presence of Triton X-100. // Anal. Sci. – 2004. – V. 20. P.945-949.
3. Бордовский В.А., Жаркой А.Б., Кастро Р.А., Марченко А.В. Свойства и структура полимерных материалов, включающих четырёхвалентное олово // Известия РГПУ им. А.И. Герцена. – 2007. – №38. С.41-50.
4. Qian L., Jin Zh-Sh., Yang Sh-Y., Du Z-L., and XuX-R. Bright Visible Photoluminescence from nanotube titania grown by soft chemical process // Chem. Mater. – 2005. – V.17. P.5334-5338.
5. Xiao M., Selvin P.R. Quantum yields of luminescent lanthanide chelates and far-red dyes measured by resonance energy transfer // J. Am. Chem. Soc. – 2001. – V.123, № 29. P.7067–7073.
6. Geddes C.D., Douglas P., Moore C.P., Wear T.J., Egerton P.L. New fluorescent indolium and quinolinium dyes for applications in aqueous halide sensing // Dyes Pigm. – 1999. – V.43. P.59–63.
7. Tyurin O.V., Bercov Y.M., Zhukov S.O., Levitskaya T.F., Gevelyuk S.A., Doycho I.K., Rysiakiewicz-Pasek E. Dye aggregation in porous glass // Optica Applicata. – 2010. – V.40, № 2. P. 311-321.
8. Kuznetsov K.A., Laptinska T.V., Mamayev Y.B. Triplen harmonics generation in *J*-aggeregated dyes in polymeric matrix // Quantum electronics. – 2004. – V.34, № 10. P.927-929.

9. Tyurin A.V., Churashov V.P., Zhukov S.A., Manchenko L.I., Levitskaya T.F., and Sviridova O.I.. Interaction of Molecular and Polymolecular Forms of a Dye // Optics and Spectroscopy. – 2008. – V.104, № 1. P.88-94.
10. Gevelyuk S.A., Doycho I.K., Prokopovich L.P., Rysiakiewicz-Pasek E., Marczuk K. The influence of anneal of incorporated carbon on the photoluminescence properties of porous glass and porous silicon // Polish Ceramic Bulletin 19, Ceramics 57 / Porous and Special Glasses (Proceedings of the 4-th International Seminar PGL'98) / edited by L.Stoch. – Polish Ceramic Society, Krakow: 1998. – P.59-64.
11. Шматкова Н.В., Сейфуллина И.И., Дойчо И.К., Гевелюк С.А., Витер Р.В. Фотолюминесценция наноразмерных частиц на основе комплексов Sn(IV) с гидразонами // X Всероссийская конференция с международным участием: «Спектроскопия координационных соединений». – Туапсе: 2013. С.140-142.
12. Shmatkova N.V., Seifullina I.I., Doycho I.K., Gevelyuk S.A., Smyntyna V.A., Viter R.V. Size effects on photoluminescence spectra of nanoparticles of tin(IV) complexes with hydrazones of 4-dimethylaminobenzaldehyde in silica porous matrix // II-nd International conference «Applied physical-inorganic chemistry» – "DIP", Simferopil: 2013. P.197-198.
13. Gevelyuk S.A., Doycho I.K., Lishchuk D.V., Prokopovich L.P., Safronsky E.D., Rysiakiewicz-Pasek E., Roizin Ya.O. Linear extension of porous glasses with modified internal surface in humid environment // Optica Applicata. – 2000. – V. 30, № 4. P.605-611.
14. Viter R.V., Geveluk S.A., Smyntyna V.A., Doycho I.K., Rysiakiewicz-Pasek E., Buk J., and KordásK. Optical properties of nanoporous glass filled with TiO_2 nanostructures // Optica Applicata. – 2012. – V.42, №2. P.307-313.
15. Gevelyuk S.A., Doycho I.K., Mak V.T., Zhukov S.A. Photoluminescence and structural properties of nanosize CdS inclusions in porous glasses // Photoelectronics. – 2007. – V.16. P.75-79.
16. Rysiakiewicz-Pasek E., Polańska J., Gevelyuk S.A., Doycho I.K., Mak V.T., Zhukov S.A. The photoluminescent properties of CdS clusters of different size in porous glasses // Optica Applicata. – 2008. – V.38, № 1. P.93-100.
17. Pertsin A.J., Kitaigorodsky A.I.. The atom-atom potential method. Application to organic molecular solids. – Springer-Verlag, Berlin-Heidelberg-NY: 1987. 397P.
18. Doycho I.K., Gevelyuk S.A., Rysiakiewicz-Pasek E. Photoluminescence of tautomeric forms of nanoparticle ensembles of dyes based on the 4-valence stannum complexes in porous silica glass // Photoelectronics. – 2015. – V.24. P.30-37.
19. Дойчо И.К. Исследование фотолюминесцен-тных свойств ансамблей наночастиц краси-телей // В кн. Неравновесные процессы в сенсорных наноструктурах / под ред. В.А.Смынтыны. – Одеса: ОНУ, 2015. – С.120-170.

This article has been received in April in 2016

UDC 621.315.592

S. A. Gevelyuk, E. Rysiakiewicz-Pasek, I. K. Doycho

DEPENDENCE OF PHOTOLUMINESCENCE OF NANOPARTICLE ENSEMBLES OF STANNUM (IV) COMPLEXES IN SILICA POROUS MATRIX ON CONCENTRATION OF SATURATING SOLUTION

Abstract

Dependence of photoluminescence of high-molecular nanoformations of dyes on the basis of stannum (IV) complexes in porous glass on concentration of saturating solution has been researched. The results have been compared with photoluminescence of corresponding solutions, in which the effect of concentration quenching, was due to the Franck-Condon principle, was observed. It was found that intensity of luminescence for nanoparticle ensembles was always higher than in solution. At that, decrease of luminescence intensity alongside with concentration growth of saturating solution was observed as well. However, the observed dependence was more complicated than in solution. It can be explained by the fact that the pores with maximal sizes are filled at large concentrations of saturating solution of dye. The dye particles act almost the same as in solution, where photoluminescence is fainter, in such pores.

Key words: photoluminescence, porous glass, dyes on base of stannum complexes, nanoparticle ensembles, concentration of saturating solution

UDC 621.315.592

С. А. Гевелюк, Е. Ришякевич-Пасек, І. К. Дойчо

ЗАЛЕЖНІСТЬ ФОТОЛЮМІНЕСЦЕНЦІЇ АНСАМБЛІВ НАНОЧАСТИНОК КОМПЛЕКСІВ 4-ВАЛЕНТНОГО СТАНУМУ ВСЕРЕДИНІ ШПАРИСТОЇ СИЛІКАТНОЇ МАТРИЦІ ВІД КОНЦЕНТРАЦІЇ НАСИЧУЮЧОГО РОЗЧИНУ

Резюме

Досліджено залежність фотолюмінесценції високомолекулярних формувань барвників на базі комплексів чотиривалентного стануму всередині шпаристого скла від концентрації насичуючого рохчину. Результати порівняно із фотолюмінесценцією відповідних розчинів, у яких спостерігається ефект концентраційного гасіння, зумовлений принципом Франка-Кондома. Виявлено, що інтенсивність люмінесценції ансамблю наночастинок завжди вища, аніж у розчині. При цьому, теж спостерігається зменшення інтенсивності люмінесценції при наближенні концентрації насичуючого розчину до границі розчинності. Проте, залежність, що спостерігається, є складнішою, аніж у розчині, і може пояснюватися заповнюванням шпарин максимальних розмірів у випадку великих концентрацій насичуючого розчину. Тож барвник поводить себе всередині таких шпарин майже, наче у розчині, де фотолюмінесценція слабша.

Ключові слова: фотолюмінесценція, шпаристе скло, барвники на базі комплексів стануму, ансамблі наночастинок, концентрація насичуючого розчину

UDC 621.315.592

С. А. Гевелюк, Е. Рысакевич-Пасек, И. К. Дойчо

ЗАВИСИМОСТЬ ФОТОЛЮМИНЕСЦЕНЦИИ АНСАМБЛЕЙ НАНОЧАСТИЦ КОМПЛЕКСОВ 4-ВАЛЕНТНОГО ОЛОВА В ПОРИСТОЙ СИЛИКАТНОЙ МАТРИЦЕ ОТ КОНЦЕНТРАЦИИ НАСЫЩАЮЩЕГО РАСТВОРА

Резюме

Исследована зависимость фотолюминесценции высокомолекулярных нанообразований красителей на основе комплексов четырёхвалентного олова в пористом стекле от концентрации насыщающего раствора. Результаты сравниваются с фотолюминесценцией соответствующих растворов, в которых наблюдается эффект концентрационного гашения, связанный с принципом Франка-Кондома. Обнаружено, что для ансамблей наночастиц интенсивность люминесценции всегда выше, чем в растворе. При этом так же наблюдается уменьшение интенсивности фотолюминесценции при приближении концентрации насыщающего раствора к пределу растворимости. Однако, наблюдаемая зависимость более сложная, чем в растворе, и может быть объяснена тем, что при больших концентрациях насыщающего раствора красителя оказываются заполненными поры максимальных размеров, в которых краситель ведёт себя почти, как в растворе, где фотолюминесценция слабее.

Ключевые слова: фотолюминесценция, пористое стекло, красители на основе комплексов олова, ансамбли наночастиц, концентрация насыщающего раствора

UDC 539.182

O. Yu. Khetselius, P. A. Zaichko, V. F. Mansarliysky, O. A. Antoshkina

Odessa State Environmental University, L'vovskaya str.15, Odessa-9, 65016, Ukraine
E-mail: okhetsel@gmail.com

THE HYPERFINE STRUCTURE AND OSCILLATOR STRENGTHS PARAMETERS FOR SOME HEAVY ELEMENTS ATOMS AND IONS: REVIEW OF DATA BY RELATIVISTIC MANY-BODY PERTURBATION THEORY CALCULATION

The energies and hyperfine structure constants for some heavy Li-like multicharged ions are calculated within the relativistic many-body perturbation theory formalism with a correct and effective taking into account the exchange-correlation, relativistic, nuclear and radiative corrections. The magnetic inter-electron interaction is accounted for in the lowest order on α^2 (α is the fine structure constant) parameter. The Lamb shift polarization part is taken into account in the modified Uehling-Serber approximation. The Lamb shift self-energy part is accounted for effectively within the generalized Ivanov-Ivanova non-perturbative procedure. The combined relativistic energy approach and relativistic many-body perturbation theory with the zeroth order optimized one-particle approximation are used for computing the Li-like ions (Z=11-42,69,70) and Cs energies and oscillator strengths, in particular, of radiative transitions from the ground state to the low-excited and Rydberg states $2s_{1/2}$ – $np_{1/2,3/2}$, $np_{1/2,3/2}$-$nd_{3/2,5/2}$ (n=2-12) in the Li-like ions. A comparison of the calculated oscillator strengths with available theoretical and experimental data is performed.

1. Introduction

The research on the spectroscopic and structural properties of the heavy neutral and highly ionized atoms has a fundamental importance in many fields of atomic physics (spectroscopy, spectral lines theory), astrophysics, plasma physics, laser physics and so on (see, for example, refs. [1-22]). One could also mention here the important astrophysical applications. The experiments on the definition of hyperfine splitting also enable to refine the deduction of nuclear magnetic moments of different isotopes and to check an accuracy of the various computational models employed for the theoretical description of the nuclear effects.

The multi-configuration relativistic Hartree-Fock (RHF) and Dirac-Fock (DF) approaches (see, for example, refs. [3-5, 8-18] are the most reliable versions of calculation for multi-electron systems with a large nuclear charge. Usually, in these calculations the one- and two-body relativistic effects are taken into account practically precisely. It should be given the special attention to three very general and important computer systems for relativistic and QED calculations of atomic and molecular properties developed in the Oxford and German-Russian groups etc ("GRASP", "Dirac"; "BERTHA", "QED", "Dirac") (see refs. [3-5, 8-18] and references there). The useful overview of the relativistic electronic structure theory is presented in refs. [12, 13,17-20] from the QED point of view.

In the present paper the combined relativistic energy approach and relativistic many-body perturbation theory with the zeroth order optimized one-particle approximation are used for computing the Li-like ions (Z=11-42,69,70) and Cs energies and oscillator strengths, in particular, of radiative transitions from the ground state to the low-excited and Rydberg states $2s_{1/2}$ – $np_{1/2,3/2}$, $np_{1/2,3/2}$-$nd_{3/2,5/2}$ (n=2-12) in the Li-like ions. Review of data and a comparison of the calculated oscillator strengths with different available theoretical and experimental data is presented.

2. Relativistic method to computing hyperfine structure parameters of atoms and multicharged ions

Let us describe the key moments of the approach (more details can be found in refs. [11, 14, 20-23]). The electron wave functions (the PT zeroth basis) are found from solution of the relativistic Dirac equation with potential, which includes ab initio mean-field potential, electric, polarization potentials of a nucleus. The charge distribution in the Li-like ion is modelled within the Gauss model. The nuclear model used for the Cs isotope is the independent particle model with the Woods-Saxon and spin-orbit potentials (see refs. [24]). Let us consider in details more simple case of the Li-like ion. We set the charge distribution in the Li-like ion nucleus *r(r)* by the Gaussian function:

$$\rho(r|R) = \left(4\gamma^{3/2}/\sqrt{\pi}\right)\exp\left(-\gamma r^2\right) \quad (1)$$

where $g=4/pR^2$ and R is the effective nucleus radius. The Coulomb potential for the spherically symmetric density $r(r)$ is:

$$V_{nucl}(r|R) = -\left((1/r)\int_0^r dr' r'^2 \rho\left(r'\middle|R\right) + \int_r^\infty dr' r' \rho\left(r'\middle|R\right)\right) \quad (2)$$

Consider the DF type equations for a three-electron system $1s^2nlj$. Formally they fall into one-electron Dirac equations for the orbitals 1s and *nlj* with the potential:

$$V(r) = 2V(r|1s) + V(r|nlj) + V_{ex}(r) + V(r|R) \quad (3)$$

$V(r|R)$ includes the electrical and the polarization potentials of the nucleus; the components of the Hartree potential (in the Coulomb units):

$$V(r|i) = \frac{1}{Z}\int d\vec{r}'\rho(r|i)/|\vec{r}-\vec{r}'| \quad (4)$$

Here $\rho(r|i)$ is the distribution of the electron density in the state $|i>$, V_{ex} is the exchange inter-electron interaction. The main exchange effect will be taken into account if in the equation for the valent electron orbital we assume $V(r) = V(r|core) + V(r|nlj)$ and in the equation for the *nlj* orbital $V(r) = 2V(b, r|core)$ (here b is the optimization parameter; see below). The rest of the exchange and correlation effects will be taken into account in the first two orders of the PT by the total inter-electron interaction [11, 12,15]. A procedure of taking into account the radiative QED corrections is in details given in the refs. [11,14,20-22]. Regarding the vacuum polarization effect let us note that this effect is usually taken into consideration in the first PT theory order by means of the Uehling-Serber potential. This potential is usually written as follows:

$$U(r) = -\frac{2\alpha}{3\pi r}\int_1^\infty dt \exp(-2rt/\alpha Z)\left(1+1/2t^2\right)\frac{\sqrt{t^2-1}}{t^2} \equiv -\frac{2\alpha}{3\pi r}C(g), \quad (5)$$

where $g=r/(aZ)$. In our calculation we use more exact approach [22]. The Uehling potential, determined as a quadrature (6), may be approximated with high precision by a simple analytical function. The use of new approximation of the Uehling potential permits one to decrease the calculation errors for this term down to 0.5 – 1%. A method for calculation of the self-energy part of the Lamb shift is based on an idea by Ivanov-Ivanova (see refs. [11]). It is supposed that for any ion with *nlj* electron over the core of closed shells the sought value may be presented in the form:

$$E_{SE}(Z, nlj) = 0.027148\frac{\xi^4}{n^3} f(\xi, nlj)\left(cm^{-1}\right), \quad (6)$$

The parameter $x=(E_R)^{1/4}$, E_R is the relativistic part of the bounding energy of the outer electron; the universal function $f(\xi, nlj)$ does not depend on the composition of the closed shells and the actual potential of the nucleus. The energies of electric quadruple and magnetic dipole interactions are defined by a standard way with the hyperfine structure constants, usually expressed through the standard radial integrals [27]:

$$A=\{[(4,32587)10^{-4}Z^2cg_I]/(4c^2-1)\}(RA)_{-2},$$

$$B=\{7.2878\ 10^{-7}\ Z^3Q/[(4c^2-1)I(I-1)\}\ (RA)_{-3}, \quad (7)$$

Here g_I is the Lande factor, Q is a quadruple momentum of nucleus (in Barn); $(RA)_{-2}$, $(RA)_{-3}$ are the radial integrals usually defined as follows:

$$(RA)_{-2,} = \int_0^\infty drr^2 F(r)G(r)U(1/r^2, R),$$

$$(RA)_{-3,} = \int_0^\infty drr^2[F^2(r) + G^2(r)U(1/r^2, R) \cdot \quad (8)$$

The radial parts *F* and *G* of the Dirac function two components for electron, which moves in the potential *V(r;R)+U(r;R),* are determined by solution of the Dirac equations. To define the hyperfine interaction potentials $U(1/r^n,R)$, we use the method by Ivanov et al [11]. The key elements of the optimized relativistic energy approach to computing oscillator strengths are presented in [1,15,29]. Let us remind that an initial general energy formalism combined with an empirical model potential method has been developed by Ivanov-Ivanova et al [11], further more general ab initio gauge-invariant relativistic approach has been presented in [12], where the calibration of the single model potential parameter b has been performed on the basis of the special *ab initio* procedure within relativistic energy approach [12] (see also [1529,30]). All calculations are performed on the basis of the numeral code Superatom-ISAN (version 93). The details of the used method can be found in the references [1,11,14,21-24].

4. Results and Conclusions

Firstly we present the results of computing the oscillator strengths of transitions in spectra of the Li-like ions (Z=11-42,69,70). There are considered the radiative transitions from ground state to the low-excited and Rydberg states, particularly, $2s_{1/2}$ – $np_{1/2,3/2}$, $np_{1/2,3/2}$-$nd_{3/2,5/2}$ (n=2-12). To test the obtained results, we compare our calculation results of the oscillator strengths values for some Li-like ions with the known theoretical and tabulated results [29,31]. As an example, in table 1 we present the computed oscillator strength values for the $2s_{1/2} - 2p_{1/2,3/2}$ transitions in Li-like ions S^{13+}, Ca^{17+}, Fe^{23+}, Zn^{27+}, Zr^{37+}, Mo^{39+}, Sn^{47+}, Tm^{66+}, Yb^{67+}. The DF calculation data by Zilitis [31b] and the "best" compillated (experimental) data [31a] for the low-Z Li-like ions are listed in table 1 for comparison too. Note that the experimental data on the oscillator strengths for many (especially, high-Z) Li-like ions are missing.

Overall, there is a physically reasonable agreement of the listed data. The important

features of the approach used are using the optimized one-particle representation and account for polarization effects. It should be noted that an estimate of the gauge-non-invariant contributions (the difference between the oscillator strengths values calculated with using the transition operator in the form of "length" and "velocity") is about 0.3%, i.e., the results obtained with different photon propagator gauges (Coulomb, Babushkon, Landau) are practically equal. In Table 2 we present our results (RMPT) of computing the reduced matrix elements (atomic units) of different radiative transitions in the ^{133}Cs spectrum [1,30b]. The experimental (Exp) and other theoretical (SD- the results of computing within the relativistic DF single-double approximation [4a]; DF, RHFc – the Dirac-Fock and relativistic

Table 1

Oscillator strengths of the $2s_{1/2} - 2p_{1/2,3/2}$ transitions in Li-like ions

Method	DF [31b]	DF [31b]	[31c]	[31c]	[30b]	[30b]
Ion	$2s_{1/2}$–$2p_{1/2}$	$2s_{1/2}$–$2p_{3/2}$	$2s_{1/2}$–$2p_{1/2}$	$2s_{1/2}$–$2p_{3/2}$	$2s_{1/2}$–$2p_{1/2}$	$2s_{1/2}$–$2p_{3/2}$
S^{13+}	0.0299	0.0643	0.030	0.064	0.0301	0.0641
Ca^{17+}	0.0234	0.0542	0.024	0.054	0.0236	0.0541
Fe^{23+}	0.0177	0.0482	0.018	0.048	0.0179	0.0481
Zn^{27+}	0.0153	0.0477	–	–	0.0156	0.0475
Zr^{37+}	0.0114	0.0543	–	–	0.0118	0.0540
Mo^{39+}	–	–	0.011	0.056	0.0107	0.0556
Sn^{47+}	0.0092	0.0686	–	–	0.0095	0.0684
Tm^{66+}	–	–	–	–	0.0071	01140
Yb^{67+}	0.0067	0.1170	–	–	0.0069	0.1167

Table 2

The reduced dipole matrix elements (a.u.) of some transitions in the Cs (see text)

Tran-Sition	SD [4a]	Scaled [4a]	DF [4b]	RHF [4c]	RHF[4d]	QDA [21c]	RMPT [1,30b]	Exp.
$6p_{1/2}$-6s	4.482	4.535	4.510	4.494	-	4.282	4.486	4.4890(7)
$6p_{3/2}$-6s	6.304	6.382	6.347	6.325	-	5.936	6.320	6.3238(7)
$7p_{1/2}$-6s	0.297	0.279	0.280	0.275	0.2825	0.272	0.283	0.284(2)
$7p_{3/2}$-6s	0.601	0.576	0.576	0.583	0.582	0.557	0.582	0.583(9)
$8p_{1/2}$-6s	0.091	0.081	0.078	-	-	0.077	0.087	-
$8p_{1/2}$-6s	0.232	0.218	0.214	-	-	0.212	0.225	-
$6p_{1/2}$-7s	4.196	4.243	4.236	4.253	4.237	4.062	4.231	4.233(22)
$6p_{3/2}$-7s	6.425	6.479	6.470	6.507	6.472	6.219	6.478	6.479(31)
$7p_{1/2}$-7s	10.254	10.310	10.289	10.288	10.285	9.906	10.308	10.308(15)
$7p_{3/2}$-7s	14.238	14.323	14.293	14.295	14.286	13.675	14.322	14.320(20)

Table 3

The hyperfine structure constants of some Li-like ions: $A=Z^3 g_I \overline{A}$ (cm^{-1}) and $B=\frac{Z^3 Q}{I(2I-1)}\overline{B}(mm^{-1})$

nlj	Z	20	69	79	92
3s	$\overline{A}$	26 –03	51 –03	63 –03	90 –03
4s	$\overline{A}$	15 –03	19 –03	24 –03	36 –03
$2p_{1/2}$	$\overline{A}$	25 –03	56 –03	71 –03	105 –02
$3p_{1/2}$	$\overline{A}$	81 –04	16 –03	20 –03	31 –03
$4p_{1/2}$	$\overline{A}$	32 –04	72 –04	91 –04	11 –03
$2p_{3/2}$	$\overline{A}$	50 –04	67 –04	71 –04	72 –04
	$\overline{B}$	9 –04	13 –04	15 –04	17 –04
$3p_{3/2}$	$\overline{A}$	13 –04	19 –04	21 –04	22 –04
	$\overline{B}$	31 –05	51 –05	55–05	62 –05
$4p_{3/2}$	$\overline{A}$	62 –05	89 –05	92 –05	8 –04
	$\overline{B}$	10 –05	20 –05	22 –05	26 –05
$3d_{3/2}$	$\overline{A}$	88 –05	10 –04	11 –04	12 –04
	$\overline{B}$	51 –06	9 –05	10 –05	11 –05
$4d_{3/2}$	$\overline{A}$	35 –05	51 –05	55 –05	58 –05
	$\overline{B}$	12 –06	44 –06	50 –06	56 –06
$3d_{5/2}$	$\overline{A}$	36 –05	48 –05	50 –05	52 –05
	$\overline{B}$	21 –06	38 –06	39 –06	40 –06
$4d_{5/2}$	$\overline{A}$	15 –05	19 –05	20 –05	21 –05
	$\overline{B}$	59 –07	15 –06	16 –06	17 –06
$4f_{5/2}$	$\overline{A}$	06–05	12 –05	13 –05	14 –05
	$\overline{B}$	16 –07	53 –07	58 –07	63 –07

Hartree —Fock method data with accounting for the second order correlation corrections; QDA-the data by the perturbation theory with the quantum defect approximation) [4,21,29,30] data are listed too.

In table 3 we present the calculated data of the hyperfine structure constants for some Li-like ions. There are presented results for the parameters: $A=Z^3 g_I \overline{A}$ and $B=\frac{Z^3 Q}{I(2I-1)}\overline{B}(mm^{-1})$.

In table 4 the experimental (A^{Exp}) and theoretical data of the magnetic dipole constant A (MHz) for the valent states of ^{133}Cs atom (I=7/2, g_i=0.7377208) are presented (from Ref. [1,5,29]). The theoretical results are obtained on the basis of the standard RHF (A^{RHF}) calculation, the RHF ($A^{RHF}+dA$) calculation with taking into account the PT second and higher corrections (look Refs. [5,15,29] and references therein) and the RMPT (A^{RMPT}) calculation (our data). The analysis shows

Table 4

The values (in MHZ) of the hyperfine structure constant A for valent states of the ^{133}Cs isotope: A^{Exp} - experiment; A^{RHF} - the RHF calculation data; $A^{RHF}+dA^{RHF}$ - the RHF calculation data with taking into account the PT second and higher orders contributions [5]; A^{RMPT} – the RMPT calculation data [29] (look details in Refs.[5,15,29])

State	A^{RHF} [5]	dA [5]	$A^{RHF}+dA$ [5]	dA^{RMPT} [29]	A^{RMPT} [29]	A^{Exp}
$6s_{1/2}$	1426,81	864,19	2291,00	870,96	2294,45	2298,16
$7s_{1/2}$	392,05	151,99	544,04	152,45	545,480	545,90(9)
$6p_{1/2}$	161,09	131,58	292,67	130,08	292,102	291,90(13)
$7p_{1/2}$	57,68	35,53	94,21	35,64	94,317	94,35(4)
$6p_{3/2}$	23,944	25,841	49,785	26,322	50,205	50,275(3)
$7p_{3/2}$	8,650	7,605	16,255	7,920	16,590	16,605(6)
$5d_{3/2}$	---	---	---	7,802	16,422	---

that taking into account the correlation and QED corrections is important to reach the physically reasonable agreement between theoretical and experimental data.

The fundamental reason of physically reasonable agreement between theory and experiment is connected with the correct taking into account the inter-electron correlation effects, nuclear (due to the finite size of a nucleus), relativistic and radiative corrections. The key difference between the results of the RHF, RMPT methods calculations is explained by using the different schemes of taking into account the inter-electron correlations. The contribution of the PT high order effects and nuclear contribution may reach the units and even dozens of MHz and should be correctly taken into account. So, it's necessary to take into account more correctly the spatial distribution of the magnetic moment inside a nucleus (the Bohr-Weisskopf effect), the nuclear-polarization corrections etc too.

References

1. O.Yu. Khetselius, Int. J. Quant.Chem. **109**, 3330 (2009); Phys. Scr.T. **135**, 014023 (2009).
2. P. Indelicato, S. Boucard, D.S. Covita, etal, Nucl. Instr. Methods Phys Res.A.**580,** 8 (2007); N. Nakamura, A.P. Kavanagh, H. Watanabe, etal, J. Phys. C Ser. **88**, 012066 (2007).
3. L.Labzowsky, W.Johnson, G. Soff, S. Schneider, Phys.Rev.A. **51**, 4597 (1995); V.Dzuba, V. Flambaum, M.S.Safranova, Phys. Rev A. **73**, 022112 (2006).
4. S.A. Blundell, J. Sapirstein, W.R. Johnson, Phys. Rev. D. **45**, 1602 (1992); V. Dzuba, V. Flambaum, O. Sushkov, Phys. Rev. A **56**, R4357 (1997).
5. K.Cheng, Y.Kim, J.Desclaux, Atom. Data Nucl. Data Tabl. **24**, 11 (1979); V. Yerokhin, A. Artemyev, V. Shabaev, Phys.Rev.A. **75**, 062501 (2007).
6. M.Tomaselli, T. Kuhl, W. Nortershauser, et al Phys.Rev.A. **65**, 022502 (2002);
7. M.Tomaselli, S. Schneider, E. Kankeleit, T. Kuhl, Phys.Rev.C. **51**, 2989-(1995).
8. J.Bieron, P.Pyykkő, P. Jonsson, Phys. Rev.A. 71, 012502 (2005).
9. P.J. Mohr, Phys. Rev. A. **26**, 2338 (1982); Phys. Scripta T. **46**, 44 (1993).
10. H. Persson, I. Lindgren, S. Salomonson, Phys. Rev. Lett. **76**, 204 (1996).
11. E.P. Ivanova, L.N. Ivanov, Atom. Dat. Nucl. Dat.Tab. **24,** 95 (1999); L.N. Ivanov, E.Ivanova, E.Aglitsky, Phys. Rep. **166**, 315 (1998); E.P. Ivanova, L.Ivanov, A.Glushkov, A.Kramida, Phys.Scr. **32**, 512 (1995).
12. A.V.Glushkov, L.N. Ivanov, Phys. Lett. A. **170,** 33 (1999); A.V. Glushkov,

in: Ser: Progr. Theor. Chem.& Phys., Vol.26, ed. by K.Nishikawa, J. Maruani, E.Brandas, G. Delgado-Barrio, P.Piecuch (Springer, 2012), pp. 231-254.
13. I.P. Grant, H.M.Quiney, Int. J. Quant. Chem. **80**, 283 (2000).
14. O. Yu. Khetselius, Hyperfine structure of atomic Spectra (Astroprint, Odessa, 2008), pp.1-290;
15. O.Yu. Khetselius, Spectral Line Shape. **15**, 363 (2009); **16**, 29 (2010).
16. A. Derevianko, S.G. Porsev, Phys. Rev.A. **71**, 032509 (2005); V.M. Shabaev, M. Tomaselli, T. Kuhl, V.A. Yerokhin, A.N. Artemyev, Phys.Rev.A. **56**, 252 (1997);
17. K.L. Bell, K.A. Berrington, D.S.F. Crothers, A. Hibbert, K.T. Taylor (eds.) Supercomputing, Collision Processes, and Application, Springer, New York, 1999, pp.1-296.
18. H.M. Quiney, in: New Trends in Quantum Systems in Chemistry and Physics, Series: Progr. Theor. Chem.& Phys., Vol. 6, ed. by J. Maruani, C. Minot, R. McWeeny, Y. Smeyers, S. Wilson (Springer, Berlin, 2002), pp.135-168.
19. A.Glushkov, S.Ambrosov, O.Khetselius, A.Loboda, Y.Chernyakova, A. Svinarenko, Nucl.Phys A. **734S,** 21 (2004) ;
20. A.V. Glushkov, Relativistic quantum theory. Quantum mechanics of atomic systems (Odessa: Astroprint, 2008).
21. A. Glushkov, S.Ambrosov, A. Loboda, E.Gurnitskaya, G. Prepelitsa, Int.J.Quant.Chem. **104**, 562 (2005) ; T.B. Tkach, Photoelectr. **21**, 14 (2012).
22. A.V. Glushkov, S.A. Ambrosov, A.V.Loboda, E.P. Gurnitskaya, O.Yu. Khetselius, in:, Ser: Progr. Theor. Chem.& Phys., Vol. 15, ed.by P.Julien, J.Maruani, D. Mayou, S. Wilson, G. Delgado-Barrio (Springer,2006), pp.285-300.
23. A.V. Glushkov, S.V. Malinovskaya, O.Yu. Khetselius, in: Progr. Theor. Chem.& Phys., Vol. 15, ed.by S. Wilson, P.J. Grout, J. Maruani, G. Delgado-Barrio, P. Piecuch, (Springer, 2008), pp. 505-558.
24. A. Glushkov, O. Khetselius, A. Loboda, E.P. Gurnitskaya,, Meson-Nucleon Physics and the Structure of Nucleon (IKP, Forschungzentrum Juelich, Germany), SLAC eConf C070910 (Menlo Park, CA, USA). **2**, 186 (2007).
25. B.D. Serot, J.D. Walecka, Advances in Nuclear Physics: The Relativistic Nuclear Many Body Problem (Plenum Press, N.-Y., 1996).
26. O.Yu. Khetselius, In Ser: Progr. Theor. Chem.& Phys., Vol. 26, ed. by K.Nishikawa, J. Maruani, E.Brandas, G. Delgado-Barrio, P.Piecuch (Springer, 2012), pp. 217-230;
27. A. Mitrushenkov, L.N. Labzowsky, I. Lindgren, etal, Phys. Lett. A. **200**, 51 (1995); D. Feili, Ph.Bosselmann, K.-H. Schartner, etal, Phys.Scr. T. **92,** 300 (2001).
28. I.I. Sobel'man, Introduction to theory of atomic spectra (Moscow, Nauka, 1977).
29. O.Yu. Khetselius, T.A. Florko, A.A. Svinarenko, T.Tkach, Phys. Scr. **T153**, 014037 (2013); A. Svinarenko, A. Ignatenko, V. Ternovsky, L.V. etal, J.Phys.: C Series. **548**, 012047 (2014).
30. A. Glushkov, O.Khetselius, A. Svinaren-ko A.A., Phys.Scripta. **T153**, 014029 (2013); A.Svinarenko, O. Khetselius, V.Buyadzhi, T. Florko etal, J.Phys: C Series. **548**, 012048 (2014);
31. G.Martin, W.Wiese, Phys.Rev.A. **13,** 699 (1976); V. Zilitis, Opt. Spectr. **55** 215 (1983); W. Schweizer, P. Faßbinder, R. Gonzalez-Ferez, Atom. Data. Nucl. Data. Tabl. **72,** 33 (1999).

This article has been received in May 2016

UDC 539.182

O. Yu. Khetselius, P. A. Zaichko, V. F. Mansarliysky, O. A. Antoshkina

THE HYPERFINE STRUCTURE AND OSCILLATOR STRENGTHS PARAMETERS FOR SOME HEAVY ELEMENTS ATOMS AND IONS: REVIEW OF DATA BY RELATIVISTIC MANY-BODY PERTURBATION THEORY CALCULATION

Abstract

The energies and hyperfine structure constants for some heavy Li-like multicharged ions are calculated within the relativistic many-body perturbation theory formalism with a correct and effective taking into account the exchange-correlation, relativistic, nuclear and radiative corrections. The magnetic inter-electron interaction is accounted for in the lowest order on a^2 (a is the fine structure constant) parameter. The Lamb shift polarization part is taken into account in the modified Uehling-Serber approximation, the Lamb shift self-energy part - within the generalized Ivanov-Ivanova procedure. The combined relativistic energy approach and many-body perturbation theory with the zeroth order optimized one-particle approximation are used for computing the Li-like ions (Z=11-42,69,70) and Cs energies and oscillator strengths, in particular, of radiative transitions from the ground state to the low-excited and Rydberg states $2s_{1/2} – np_{1/2,3/2}$, $np_{1/2,3/2}$-$nd_{3/2,5/2}$ (n=2-12) in the Li-like ions. A comparison of the calculated oscillator strengths with available theoretical and experimental data is performed.

Key words: Hyperfine structure – Oscillator strengths - Relativistic perturbation theory

УДК 539.184

О. Ю. Хецелиус, П. А. Заичко, В. Ф. Мансарлийский, О. А. Антошкина

СВЕРХТОНКАЯ СТРУКТУРА И СИЛЫ ОСЦИЛЛЯТОРОВ РАДИАЦИОННЫХ ПЕРЕХОДОВ ДЛЯ РЯДА АТОМОВ И ИОНОВ ТЯЖЕЛЫХ ЕЛЕМЕНТИВ: ОБЗОР ДАННЫХ ВЫЧИСЛЕНИЙ НА ОСНОВЕ РЕЛЯТИВИСТСКОЙ МНОГОЧАСТИЧНОЙ ТЕОРИИ ВОЗМУЩЕНИЙ

Резюме

Энергии и константы сверхтонкой структуры для некоторых тяжелых Li-подобных многозарядных ионов вычислены в рамках релятивистской многочастичной теории возмущений с эффективным с учетом обменно-корреляционных, релятивистских, ядерных и радиационных поправок. Магнитное межэлектронное взаимодействие учитывается в низшем порядке на a^2 (а постоянная тонкой структуры) параметру. Поляризационная часть сдвига Лэмба учитывается в модифицированном приближении Юлинга-Сербера, собственно-энергетическая часть сдвига Лэмба - эффективно в рамках обобщенной непертурбативной процедуры Иванова-Ивановой. Обобщенный релятивистский энергетический подход и многочастичная теории возмущений с оптимизированным нулевым приближением использованы для определения энергий, сил осцилляторов переходов в спектрах Cs, Li-подобных ионов (Z = 11-42,69,70) и, в частности, радиационных переходов из основного состояния в низшие возбужденные и ридберговские

$2s_{1/2}$ – $np_{1/2,3/2}$, $np_{1/2,3/2}$-$nd_{3/2,5/2}$ (n=2-12) состояния в Li-подобных ионах. Проведено сравнение экспериментальных данных и результатов расчетов на основе различных теоретических методов.

Ключевые слова: Сверхтонкая структура, Силы осцилляторов, Релятивистская теория возмущений

УДК 539.184

О. Ю. Хецелиус, П. О . Заічко, В. Ф. Мансарлійський, О. О. Антошкіна

НАДТОНКА СТРУКТУРА І СИЛИ ОСЦИЛЯТОРІВ РАПДІАЦІЙНИХ ПЕРЕХОДІВ ДЛЯ ДЕЯКИХ АТОМІВ ТА ІОНІВ ВАЖКИХ ЕЛЕМЕНТІВЖ ОГЛЯД ДАНИХ ОБЧИСЛЕНЬ НА ОСНОВІ РЕЛЯТИВІСТСЬКОЇ БАГАТОЧАСТИНКОВОЇ ТЕОРІЇ ЗБУРЕНЬ

Резюме

Енергії і константи надтонкої структури для деяких важких Li-подібних багатозарядних іонів обчислені в рамках релятивістської Багаточасткові теорії збурень з ефективним з урахуванням обмінно-кореляційних, релятивістських, ядерних і радіаційних поправок. Магнітна міжелектроннао взаємодія враховується в нижчому порядку на a^2 (a -стала тонкої структури) параметру. Поляризаційна частина зсуву Лемба враховується в модифікованому наближенні Юлінга-Сербера, власно-енергетична частина зсуву Лемба - ефективно в рамках узагальненої непертурбативної процедури Іванова-Іванової. Узагальнений релятивістський енергетичний підхід і багаточастинкова теорії збурень з оптимізованим “0” наближенням використані для визначення енергій і сил осциляторів переходів в спектрах Cs, Li-подібних іонів (Z = 11-42,69,70), зокрема, радіаційних переходів з основного стану в нижчі збуджені і ридберговскі $2s_{1/2}$ – $np_{1/2,3/2}$, $np_{1/2,3/2}$-$nd_{3/2,5/2}$ (n=2-12) стани у Li-подібних іонах. Проведено порівняння експериментальних даних і даних обчислень на основі різних теоретичних методів.

Ключові слова: Надтонка структура, Сили осциляторів, Релятивістська теорія збурень

UDC 539.182

A. N. Bystryantseva, O. Yu. Khetselius, Yu. V. Dubrovskaya, L. A. Vitavetskaya, A. G. Berestenko

Odessa National Polytechnical University, 1, Shevchenko pr., Ukraine
Odessa State Environmental University, 15, Lvovskaya str., Odessa, Ukraine
e-mail: quantsha@mail.ru

RELATIVISTIC THEORY OF SPECTRA OF HEAVY PIONIC ATOMIC SYSTEMS WITH ACCOUNT OF STRONG PION-NUCLEAR INTERACTION EFFECTS: 93Nb, 173Yb, 181Ta , 197Au

It is presented a consistent relativistic theory of spectra of the pionic atoms on the basis of the Klein-Gordon-Fock with a generalized radiation and strong pion-nuclear potentials. There are presented data of calculation of the energy and spectral parameters for pionic atoms of the 93Nb, 173Yb, 181Ta, 197Au, with accounting for the radiation (vacuum polarization), nuclear (finite size of a nucleus) and the strong pion-nuclear interaction corrections. The measured values of the Berkley, CERN and Virginia laboratories and alternative data based on other versions of the Klein-Gordon-Fock theories with taking into account for a finite size of the nucleus in the model uniformly charged sphere and the standard Uhling-Serber radiation correction and optical atomic theory are listed too.

1. Introduction

In papers [1-3] we have developed a new relativistic method of the Klein-Gordon-Fock equation with an generalized pion-nuclear potential to determine transition energies in spectroscopy of light, middle and heavy pionic atoms with accounting for the strong interaction effects. In this paper, which goes on our studying on spectroscopy of pionic atoms, we firstly applied method [1-3] to calculating calculation of the energy and spectral parameters for pioninc atoms of the ^{93}Nb, ^{173}Yb, ^{181}Ta , ^{197}Au, with accounting for the the radiation (vacuum polarization), nuclear (finite size of a nucleus) and the strong pion-nuclear interaction corrections..

Following [1-3], let us remind that spectroscopy of hadron atoms has been used as a tool for the study of particles and fundamental properties for a long time. Exotic atoms are also interesting objects as they enable to probe aspects of atomic and nuclear structure that are quantitatively different from what can be studied in electronic or "normal" atoms. At present time one of the most sensitive tests for the chiral symmetry breaking scenario in the modern hadron's physics is provided by studying the exotic hadron-atomic systems. Nowadays the transition energies in pionic (kaonic, muonic etc.) atoms are measured with an unprecedented precision and from studying spectra of the hadronic atoms it is possible to investigate the strong interaction at low energies measuring the energy and natural width of the ground level with a precision of few meV [1-10]. The strong interaction is the reason for a shift in the energies of the low-lying levels from the purely electromagnetic values and the finite lifetime of the state corresponds to an increase in the observed level width. For a long time the similar experimental investigations have been carried out in the laboratories of Berkley, Virginia (USA), CERN (Switzerland). The most known theoretical models to treating the hadronic (pionic, kaonic, muonic, antiprotonic etc.) atomic systems are presented in refs. [1-5,7,8]. The most difficult aspects of the theoretical modeling are reduced to the correct description of pion-nuclear strong interaction [1-3] as the electromagnetic part of the problem is reasonably accounted for.

2. Relativistic approach to pionic atoms spectra

As the basis's of a new method has been published, here we present only the key topics of an

approach [1-3]. All available theoretical models to treating the hadronic (kaonic, pionic) atoms are naturally based on the using the Klein-Gordon-Fock equation [2,5], which can be written as follows :

$$m^2c^2\Psi(x) = \{\frac{1}{c^2}[i\hbar\partial_t + eV_0(r)]^2 + \hbar^2\nabla^2\}\Psi(x) \quad (1)$$

where c is a speed of the light, *h* is the Planck constant, and Ψ_0(x) is the scalar wave function of the space-temporal coordinates. Usually one considers the central potential [V_0(r), 0] approximation with the stationary solution:

$$\Psi(\mathrm{x}) = \exp(-\mathrm{iE}t/\hbar)\varphi(x), \quad (2)$$

where $\varphi(x)$ is the solution of the stationary equation:

$$\{\frac{1}{c^2}[E + eV_0(r)]^2 + \hbar^2\nabla^2 - m^2c^2\}\varphi(x) = 0 \quad (3)$$

Here E is the total energy of the system (sum of the mass energy mc^2 and binding energy ε_0). In principle, the central potential V_0 naturally includes the central Coulomb potential, the vacuum-polarization potential, the strong interaction potential.

The most direct approach to treating the strong interaction is provided by the well known optical potential model (c.g. [2]). Practically in all papers the central potential V_0 is the sum of the following potentials. The nuclear potential for the spherically symmetric density $\rho(r|R)$ is [6,13]:

$$V_{nucl}(r|R) = -((1/r)\int_0^r dr'r'^2\rho\left(r'\middle|R\right) + \int_r^\infty dr'r'\rho\left(r'\middle|R\right) \quad (4)$$

The most popular Fermi-model approximation the charge distribution in the nucleus $\rho(r)$ (c.f.[11]) is as follows:

$$\rho(r) = \rho_0 / \{1 + \exp[(r-c)/a)]\}, \quad (5)$$

where the parameter *a=0.*523 fm, the parameter *c* is chosen by such a way that it is true the following condition for average-squared radius:

$$<r^2>^{1/2}=(0.836\times A^{1/3}+0.5700)\mathrm{fm}.$$

The effective algorithm for its definition is used in refs. [12] and reduced to solution of the following system of the differential equations:

$$V'nucl(r,R) = \left(1/r^2\right)\int_0^r dr'r'^2\rho\left(r',R\right) \equiv \left(1/r^2\right)y(r,R) \quad (6)$$

$$y'(r,R) = r^2\rho(r,R), \quad (7)$$

$$\rho'(r) = (\rho_0/a)\exp[(r-c)/a]\{1+\exp[(r-c)/a)]\}^2 \quad (8)$$

with the corresponding boundary conditions. Another, probably, more consistent approach is in using the relativistic mean-field (RMF) model, which been designed as a renormalizable meson-field theory for nuclear matter and finite nuclei [13].To take into account the radiation corrections, namely, the effect of the vacuum polarization we have used the generalized Ueling-Serber potential with modification to take into account the high-order radiative corrections [5,12].

The most difficult aspect is an adequate account for the strong interaction. On order to describe the strong π^-N interaction we have used the optical potential model in which the generalized Ericson-Ericson potential is as follows:

$$V_{\pi^-N} = V_{opt}(r) = -\frac{4\pi}{2m}\left\{q(r)\nabla\frac{\alpha(r)}{1+4/3\pi\xi\alpha(r)}\nabla\right\} \quad (9)$$

$$q(r) = \left(1+\frac{m_\pi}{m_N}\right)\{b_0\rho(r) + b_1[\rho_n(r)-\rho_p(r)]\} + \left(1+\frac{m_\pi}{2m_N}\right)\{B_0\rho^2(r) + B_1\rho(r)\delta\rho(r)\}, \quad (10)$$

$$\alpha(r) = \left(1+\frac{m_\pi}{m_N}\right)^{-1}\{c_0\rho(r) + c_1[\rho_n(r)-\rho_p(r)]\} + \left(1+\frac{m_\pi}{2m_N}\right)^{-1}\{C_0\rho^2(r) + C_1\rho(r)\delta\rho(r)\}. \quad (11)$$

Here $\rho_{p,n}(r)$ – distribution of a density of the protons and neutrons, respectively, ξ – parameter ($\xi = 0$ corresponds to case of "no correlation", $\xi = 1$, if anticorrelations between nucleons); respectively isoscalar and isovector parameters b_0, c_0, B_0, b_1,c_1, C_0 B_1, C_1 –are corresponding to the s-wave and p-wave (repulsive and attracting potential member) scattering length in the combined spin-isospin space with taking into account the absorption of pions (with different channels at p-p pair $B_{0(pp)}$ and *p-n* pair $B_{0(pn)}$), and isospin and spin dependence of an amplitude π^-N scattering

$$(b_0\rho(r) \to b_0\rho(r) + b_1\{\rho_p(r) - \rho_n(r)\},$$

the Lorentz-Lorentz effect in the p-wave interaction. For the pionic atom with remained electron shells the total wave-function is a product of the product Slater determinant of the electrons subsystem (Dirac equation) and the pionic wave function. In whole the energy of the hadronic atom is represented as the sum:

$$E \approx E_{KG} + E_{FS} + E_{VP} + E_N; \qquad (12)$$

Here E_{KG} -is the energy of a pion in a nucleus (Z, A) with the point-like charge (dominative contribution in (12)), E_{FS} is the contribution due to the nucleus finite size effect, E_{VP} is the radiation correction due to the vacuum-polarization effect, E_N is the energy shift due to the strong interaction V_N.

The strong pion-nucleus interaction contribution can be found from the solution of the Klein-Gordon-Fock equation with the corresponding pion-nucleon potential.

3. Results and conclusions

In table 1 our data on the *4f-3d, 5g-4f* transition energies for pionic atoms of the ^{93}Nb, ^{173}Yb, ^{181}Ta , ^{197}Au are presented. The measured values of the Berkley, CERN and Virginia laboratories and alternative data based on other versions of the Klein-Gordon-Fock theories with taking into account for a finite size of the nucleus in the model uniformly charged sphere and the standard Uhling-Serber radiation correction [5, 15] and optical atomic theory [17,18] are listed too.

The analysis of the presented data indicate on the importance of the correct accounting for the radiation (vacuum polarization) and the strong pion-nuclear interaction corrections. Obviously, it is clear that that the contributions provided by the finite size effect should be accounted in a precise theory. Besides, taking into account the increasing accuracy of the X-ray pionic atom spectroscopy experiments, it can be noted that knowledge of the exact electromagnetic theory data will make more clear the true values for parameters of the pion-nuclear potentials and correct the disadvantage of widely used parameterization of the potentials (9)-(11).

Table 1. **Transition energies (keV) in the spectra of some heavy pionic atoms (see text)**

π-A	Trans.	Berkley E_{EXP}	CERN E_{EXP}	E_{KGF+EM} [5, 15]	E_{KGF-EM} [16, 17]	E_N [5]	E_N [14, 18]	E_N, Our data
^{93}Nb	5g-4f	-	307.79 ± 0.02	-	-	-	-	307.85
^{173}Yb	5g-4f	-	-	-	-	-	-	412.26
^{181}Ta	5g-4f	453.1 ± 0.4	453.90 ± 0.20	453.06	453.78	-	453.52 453.62	453.71
^{197}Au	5g-4f	532.5 ± 0.5	533.16 ± 0.20	528.95	-	532.87	531.88	533.08
^{93}Nb	4f-3d	-	140.3 ± 0.1	-	-	-	-	140.81
^{173}Yb	4f-3d	-	-	-	-	-	-	838.67
^{181}Ta	4f-3d	-	1008.4 ± 1.3	-	-	-	992.75	1008.80
^{197}Au	4f-3d	-	1187.3 ± 1.9	-	-	-	1167.92	1186.35

References

1. Shakhman-Bystryantseva A.N., Strong π-nucleat interaction effects in spectroscopy of hadronic atoms //Photoelectronics.-2013.-Vol.22.-P.93-97
2. Serga I.N., Dubrovskaya Yu.V., Kvasikova A., Shakhman- Bystryantseva A.N., Sukharev D.E., Spectroscopy of hadronic atoms: Energy shifts// Journal of Physics: C Ser. (IOP).-2012.-Vol.397.-P.012013 (5p.).
3. Shakhman-Bystryantseva A.N., Relativis-tic theory of spectra of pionic atoms with account of strong pion-nuclear interaction effects// Photoelectronics.- 2015.-Vol.24.-P.109-115.
4. Deslattes R., Kessler E., Indelicato P., de Billy L., Lindroth E., Anton J., Exotic atoms// Rev. Mod. Phys. -2003.-Vol.75.-P.35-70.

5. Backenstoss G., Pionic atoms//Ann.Rev. Nucl.Sci.-1990.-Vol.20.-P.467-510.
6. Menshikov L I and Evseev M K, Some questions of physics of exotic atoms// Phys. Uspekhi.2001-Vol. 171.-P.150-184.
7. Scherer S, Introduction to chiral perturbation theory//Advances in Nuclear Physics, Eds. J.W. Negele and E.W. Vogt (Berlin, Springer).-2003.-Vol.27.-P.5-50.
8. Schroder H., Badertscher A., Goudsmit P., Janousch M., Leisi H., Matsinos E., Sigg D., Zhao Z., Chatellard D., Egger J., Gabathuler K., Hauser P., Simons L., Rusi El Hassani A., The pion-nucleon scattering lengths from pionic hydrogen and deuterium//Eur.Phys.J.-2001.-Vol. C21.-P.473
9. Lyubovitskij V., Rusetsky A., πp atom in ChPT: Strong energy-level shift/ // Phys. Lett.B.-2000.-Vol.494.-P.9-13.
10. Anagnostopoulos D., Biri S., Boisbourdain V., Demeter M., Borchert G. et al-PSI, Low-energy X-ray standards from pionic atoms/ //Nucl. Inst. Meth.B.-2003.-Vol.205.-P.9-18.
11. Batty C.J., Eckhause M., Gall K.P., et al, Strong interaction effects in high Z-K^- atoms//Phys. Rev. C.-1999.-Vol.40.-P.2154-2160.
12. Glushkov A.V., Gauge-invariant QED perturbation theory approach to calculating nuclear electric quadrupole moments, hyperfine structure constants for heavy atoms and ions/ Glushkov A.V., Khetselius O.Yu., Sukharev D.E., Gurnitskaya E.P., Loboda A.V., Florko T.A., Lovett L.// Frontiers in Quantum Systems in Chemistry and Physics (Berlin, Springer).-2008.-Vol.18.- P.505-522.
13. Serot B. D., Advances in Nuclear Physics Vol. 16: The Relativistic Nuclear Many Body Problem/ Serot B. D., Walecka J. D.-Plenum Press, New York, 1996.
14. Olaniyi B., Electric quadrupole moments and strong interaction effects in piomic atoms of ^{165}Ho, ^{175}Lu, ^{176}Lu,^{179}Hf, ^{181}Ta/Olaniyi B, Shor A, Cheng S., Dugan G., Wu C.S.//Nucl.Phys.A.-1982.-Vol.403.-P.572-588.
15. Indelicato P., Trassinelli M., From heavy ions to exotic atoms/ Indelicato P., Trassinelli M.// arXiv:physics.-2005.-V1-0510126v1.-16P;
16. Serga I., Relativistic theory of spectra of pionic atoms with account of the Radiative and nuclear corrections/ Serga I.N.//Photoelectronics.-2013.-Vol.22.-P.84-92.
17. Khetselius O.Yu., Hyperfine Structure, scalar-pseudoscalar interaction and parity non-conservation effect in some heavy atoms and ions/ Khetselius O.Yu., Florko T.A., Nikola L.V., Svinarenko A.A., Serga I.N., Tkach T.B., Mischenko E.V. // Quantum Theory: Reconsideration of Foundations (AIP).-2010.-Vol.1232.-P.243-250.
18. Kolomeitsev E.E., Chiral dynamics of deeply bound pionic atoms/ Kolomeitsev E.E., Kaiser N., Weise W.//Phys. Rev. Lett.-2003.-Vol.90.-P.092501.

This article has been received in April 2016

UDC 539.182

A. N. Bystryantseva, O. Yu. Khetselius, Yu. V. Dubrovskaya, L. A. Vitavetskaya, A. G. Berestenko

RELATIVISTIC THEORY OF SPECTRA OF THE PIONIC ATOMIC SYSTEMS WITH ACCOUNT OF STRONG PION-NUCLEAR INTERACTION EFFECTS: ^{93}Nb, ^{173}Yb, ^{181}Ta , ^{197}Au

Abstract

It is presented a consistent relativistic theory of spectra of the pionic atoms on the basis of the Klein-Gordon-Fock with a generalized radiation and strong pion-nuclear potentials. There are presented data of calculation of the energy and spectral parameters for pionic atoms of the ^{93}Nb, ^{173}Yb, ^{181}Ta , ^{197}Au, with accounting for the radiation (vacuum polarization), nuclear (finite size of a nucleus) and the strong pion-nuclear interaction corrections. The measured values of the Berkley, CERN and Virginia laboratories and alternative data based on other versions of the Klein-Gordon-Fock theories with taking into account for a finite size of the nucleus in the model uniformly charged sphere and the standard Uhling-Serber radiation correction and optical atomic theory are listed too

Key words: strong interaction, pionic atom, relativistic theory

УДК 539.182

А. Н. Быстрянцева, О. Ю. Хецелиус, Ю. В. Дубровская, Л. А. Витавецкая, А. Г. Берестенко

РЕЛЯТИВИСТСКАЯ ТЕОРИЯ СПЕКТРОВ ПИОННЫХ АТОМНЫХ СИСТЕМ С УЧЕТОМ ЭФФЕКТОВ СИЛЬНОГО ПИОН-ЯДЕРНОГО ВЗАИМОДЕЙСТВИЯ: ^{93}Nb, ^{173}Yb, ^{181}Ta , ^{197}Au

Резюме

Представлена последовательная релятивистская теория спектров пионных атомов на основе уравнения Клейна-Гордона-Фока с обобщенными радиационным и сильным пион-ядерным потенциалом. Выполнен расчет энергетических и спектральных параметров для пионных атомов ^{93}Nb, ^{173}Yb, ^{181}Ta , ^{197}Au, с учетом радиационных (поляризация вакуума), ядерных (конечный размер ядра) эффектов и поправки на сильное пион-нуклонное взаимодействие. Также для сравнения представлены данные измерений в лабораториях Berkley, ЦЕРН и Вирджиния и теоретические результаты, полученные на основе альтернативных теорий Клейна-Гордона-Фока с учетом конечного размера ядра в модели равномерно заряженной сферы и стандартной Юлинг-Сербер поправки.

Ключевые слова: сильное взаимодействие, пионный атом, релятивистская теория

УДК 539.182

А. М. Бистрянцева, О. Ю. Хецеліус, Ю. В. Дубровська, Л. А. Вітавецькаб А. Г. Берестенко

РЕЛЯТИВІСТСЬКА ТЕОРІЯ СПЕКТРІВ ПІОННИХ АТОМНИХ СИСТЕМ З УРАХУВАННЯМ ЕФЕКТІВ СИЛЬНОЇ ПІОН-ЯДЕРНОЇ ВЗАЄМОДІЇ: ^{93}Nb, ^{173}Yb, ^{181}Ta , ^{197}Au

Резюме

Представлена послідовна релятивістська теорія спектрів півоній атомів на основі рівняння Клейна-Гордона-Фока з узагальненими радіаційним і сильним півонія-ядерним потенціалом. Виконано розрахунок енергетичних і спектральних параметрів для піоних атомів ^{93}Nb, ^{173}Yb, ^{181}Ta , ^{197}Au, з урахуванням радіаційних (поляризація вакууму), ядерних (кінцевий розмір ядра) ефектів та поправки на сильну піон-нуклонну взаємодію. Також для порівняння представлені дані вимірювань в лабораторіях Berkley, ЦЕРН і Вірджинія і теоретичні результати, отримані на основі альтернативних теорій Клейна-Гордона-Фока з урахуванням кінцевого розміру ядра в моделі рівномірно зарядженої сфери і стандартної Юлінг-Сербер поправки..

Ключові слова: сильна взаємодія, піонний атом, релятивістська теорія

PACS 73.61.Le, 73.63.Bd

L. M. Filevska, A. P. Chebanenko, V. S. Grinevych, N. S. Simanovych

Odessa I. I. Mechnikov National University, Dvoryanska St.,2, Odessa, 65026,Ukraine,
e-mail: lfilevska@gmail.com

THE ELECTRICAL CHARACTERISTICS OF NANOSCALE SnO2 FILMS, STRUCTURED BY POLYMERS

The electrical characteristics of nanoscale tin dioxide layer were studied. They showed the significant differences in the conductivity values of films in vacuum and in air, which indicates a visible influence of adsorption interaction with oxygen in the air. The dark current temperature dependence activation character was established due to different donors type centers contribution to the conductivity which are “shallow” at low temperatures and are more "deep" at high temperatures. The values of the energy depth of these levels were calculated. The films’ conductivity changes at their heating at vacuum and at the subsequent cooling at vacuum till the initial temperature are reversible and repeatable many times, which testifies the stability of the electrical characteristics of the SnO2 films and is perspective for use of the layers as adsorptive-sensitive elements of gas sensors.

1. Introduction

A good combination of physical properties of tin dioxide (conductivity, its sensitivity to the external environment changes and electromagnetic radiation), stability of characteristics and low-cost production makes it to be one of the most popular and promising material for sensor [1, 2].

Tin dioxide plays its important role as a material for solid-state gas sensors whose operation is based on changing the conductivity of a sensitive layer at gas adsorption. Various kinds of nanostructured SnO_2 exhibit better properties compared to their bulk types both for gas analysis and for a wide range of other applications. Chemical and electrical properties of tin dioxide in nanocrystalline state depend strongly on particles’ size [1, 2]. The grain size decreasing influences both the defects role in surface layers on electronic processes in them and increases the contribution of grain boundaries to the transport processes of charge carriers.

Tin dioxide is a degenerative semiconductor with electronic conductivity due to a wide range of donor levels in the bandgap with activation energies of 0,21, 0,33, 0,52, 0,6, 0,72 eV [3, 4]. The SnO_2 film samples have donor levels which are typically shallow. Their activation energies are in thin interval of 0,15 eV and they decrease with the increase in charge carriers quantity.

Semiconductor metal oxides’ conductivity exists due to their composition deviation from stoichiometry. Defects (anion and cation) vacancies also play an important role in their conductivity. In the oxide semiconductor films deviations from stoichiometry, and hence the electrical properties, change reversible at their interaction with the gas environment. Their conductivity significantly depends on the structure of the layers, grain size and barrier effects on the grain boundaries, adsorption processes on surfaces, effect of temperature and external electric field. All these factors must be taken into account at the analysis of experimental results.

Since the main physical parameters (grain size, considerable surface area, the grains’ structure features etc.) are determined by technological peculiarities, then electrophysical properties also depend on technological factors. [5]

The present work is devoted to the investigation of current-voltage characteristics (I-V) and the dark current temperature dependences (DCTD) of nanoscale SnO_2, structured by poly-

mers, aiming the study their electrical conductivity mechanisms and the influence of adsorption processes on their electrical properties.

2. Sample preparation and experimental techniques

Nanostructured tin dioxide thin films were obtained using polymer materials by the sol-gel method [6]. Bis(acetylacetonato)dichlorotin (BADCT) was used as a tin dioxide precursor [7]. The polyvinyl acetate (PVA) was used as a polymer material for structured of nanofilms.

Experimental technique for SnO_2 nanofilms' electro-physical characteristics measurements was based on a standard method of current-voltage and current-temperature dependence registration.

The SnO_2 films were supplied with contacts of Indium thermally deposited in a high vacuum on the surface of the films shaped as two parallel strips. The distance between the electrodes was 2 mm.

3. Results and discussion

Fig. 1 shows current-voltage characteristics of SnO_2 films with different content of the precursor, measured on air at room temperature. They were independent on the polarity of the applied voltage and linear, which indicates the Ohmic type of indium contacts conductivity and negligible barrier effects influence.

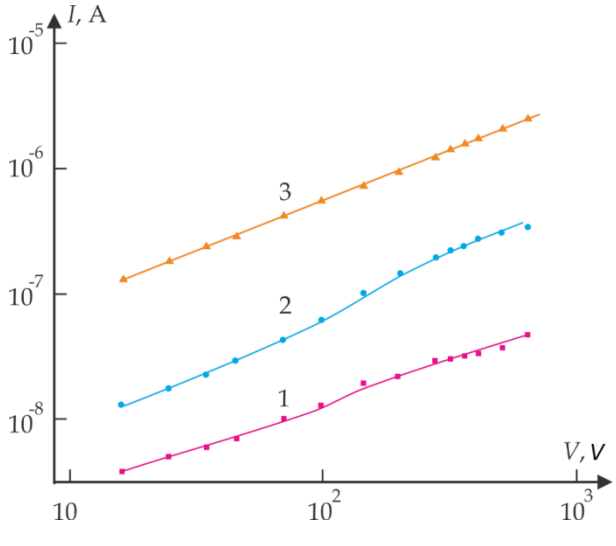

Fig. 1. I-V characteristics of SnO_2 with the content of precursor 1% (1), 5% (2) and 10% (3), measured in air (T = 290 K).

It may be seen the correlation between the precursor's concentration increasing in the initial solution and the films' resistance reduction. This may be connected with precursor's concentration increasing which resulted in the film's thickness growth, with the subsequent growth of charge carriers concentration and number of defects which contribute to the film conductivity increase too. Besides that, it is known that carrier mobility increases with film thickness increasing what also influences the conductivity.

Current–voltage characteristics of one of the samples measured in air (curve 1), and then in vacuum (curve 2) are shown in Fig.2. As it can be seen, the electrical conductivity of the films in vacuum increases significantly. The latter supposes that the value of the electrical conductivity of the investigated films greatly affect the processes of adsorption (desorption) of oxygen on their surface [8].

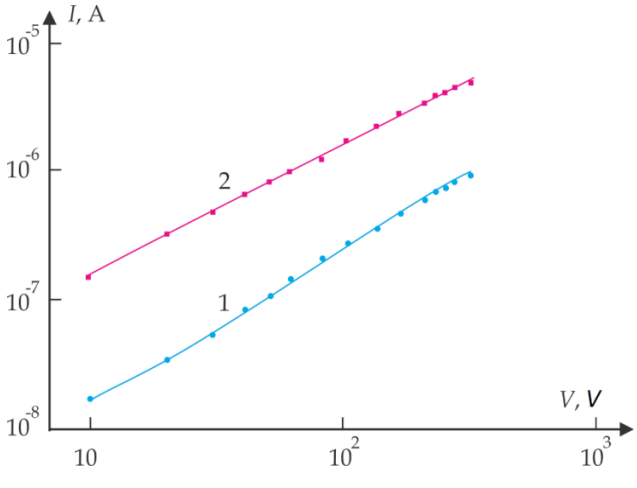

Fig. 2. I-V characteristics of sample with precursor content of 5% in air (1) and in vacuum (2). (T = 290 K).

The oxygen influence on the conductivity of the films is also confirmed by the results presented in Fig.3. Curve 1 (Fig.3) depicts the current–voltage characteristic of one of SnO_2 films measured in air at 290 K. Then, air was evacuated from the measuring chamber (to a pressure of about 10^{-3} mm Hg). The film was heated in vacuum to a temperature of 410 K and then again cooled to a room temperature. After that measuring of I-V curves (at 290 K) in vacuum was repeated (Fig. 3, curve

2). The significant increase in conductivity of the film (more than two orders of magnitude) is associated with desorption of oxygen and the formation of oxygen vacancies acting as donors [8] on the films' surfaces.

Curve 3 (Fig.3) was measured in 15 min after the atmospheric air was let into the chamber. It may be noticed a decrease in the electrical conductivity of the film due to atmospheric oxygen adsorption.

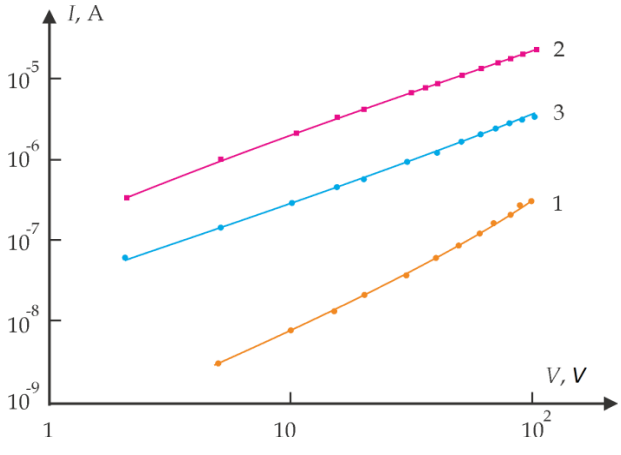

Fig. 3. I-V curves of the SnO_2 film with the precursor content of 10%(T = 290 K) (commentary in the text).

The decreasing current relaxation (Fig. 4) was observed in the process of air inlet into the chamber.

Straightening of the initial section of the current-time dependence in the coordinates $ln I \div t$ shows that in the initial time interval (0 to 30 seconds), the current decreases with time according to exponential law $I \sim exp\left(-\frac{t}{\tau}\right) I \sim exp\left(-\frac{t}{\tau}\right)$. Calculated from the graph the value for the relaxation time constant, τ was approximately 18 seconds. In later periods the rate of relaxation decreases monotonously. Thus, the processes of oxygen adsorption on the film surface at room temperature are characterized by definite inertia.

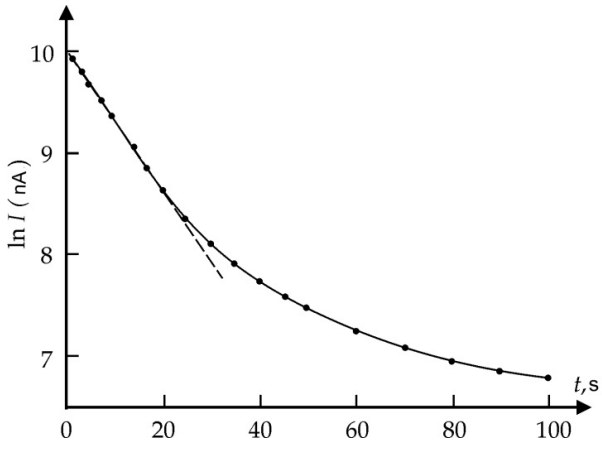

Fig. 4. Relaxation of current in the sample at letting air in the measurement chamber (V = 60 V).

The decreasing relaxation of current is associated with interaction of the film surface with oxygen at the inlet of atmospheric air. The initial section of the graph is associated both with a relatively rapid filling of the surface centers by oxygen ions, thus capturing electrons of conductivity and the disappearance of oxygen vacancies. In the future, the process of current relaxation slows down, because the near-surface layers of adsorbed oxygen limit the access to the surface for air oxygen.

The temperature dependences of dark current were fulfilled for the studied SnO_2 films. The results of these calculations for films with content of the precursor 1%, 5% and 10% are presented in Fig.5.

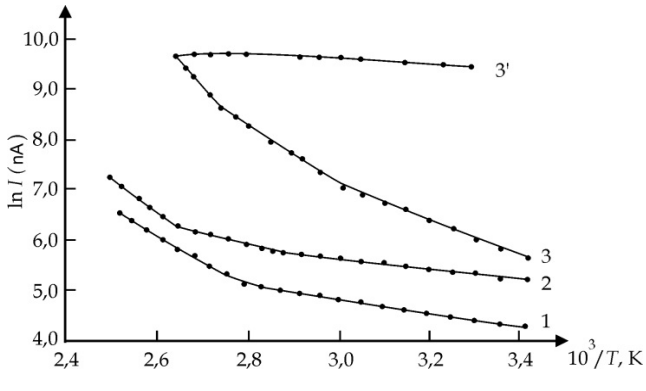

Fig. 5. The temperature dependence of dark current measured at U = 60 V for SnO_2 with the content of the precursor 1% (1), 5% (2) and 10% (3). Curve (3) measured at the sample cooling (U = 80 V).

The DCTD curves have the activation character at heating. The conductivity is contributed by different types of donor centers, "shallow" at low temperatures and "deeper" at high temperatures.

Depth values of the energy levels calculated from the slopes of the straight sections DCTD curves for different series of specimens are shown in the table.

Table

The content of precursor (%)	1	5	10
The ionization energy of donors (eV)	0,19 0.27	0,13 0,21 0,34	0,23 0,31 0,53

Obtained energies' values of 0.19 eV and 0.13 eV are close to literature value of donor level at 0.15 eV associated with double ionized oxygen vacancies formation [9]. The nature of donor centers, associated with other energy values in the table, remains unclear.

A large set of obtained values of the activation energy can be related to the fact that in the test films due to their nano structure the energy of known levels may change, for example, for those, which corresponds to oxygen vacancies. The additional levels associated with peculiarities of the films production and their storage may appear. There may be levels due to the presence in the films of tin monoxide SnO, etc.

Curve 3' (Fig.6) depicts DCTD of the samples measured at cooling. As can be seen, the current decreases at cooling enough slowly.

The conductivity of the film after its cooling to room temperature remains much higher than prior to the procedure of heating the film. This may be due to discharging of donor oxygen levels at high temperatures when the surface curve of energy bands decreases (the thickness of the surface potential barrier decreases correspondingly), thus resulting in the films conductivity increasing. It worth to note, that the above described features of DCTD behavior, measured at cooling, were observed for all series of the samples.

The process influencing the conductivity magnitude changes of the films by heating and subsequent cooling at vacuum till initial temperature is reversible and repeatable many times. For example, if at the end of the measurement the curve 3' (Fig. 6) the measuring chamber is filled with air, then after a certain period of time the current is reduced to levels (at the same temperature) corresponding the curve 3 (Fig.6).

The latter supposes that the electrical characteristics of the SnO_2 films is quite stable, which allows using them as adsorptive-sensitive elements for gas sensors.

4. Conclusions

The studies of electrical properties of nanolayers of tin dioxide revealed the following features:

The conductivity of the investigated films in vacuum and in air differs more than an order of magnitude, which indicates the considerable influence of adsorption interaction with oxygen in air.

Curves DCTD taken at heating the samples are of activation type due to different types of donor centers contribution to conductivity. Obtained values of the energies of 0.19 eV and 0.13 eV are close to the known from literature value of the ionization energy of the donor level at 0.15 eV associated with the formation of double ionized oxygen vacancies.

The change in conductivity of the films during heating and subsequent cooling at vacuum till the initial temperature is reversible and repeatable many times, which shows the stability of the electrical characteristics of the SnO_2 films and allows using them as adsorptive-sensitive elements for gas sensors.

References

1. M. Batzill, U. Diebold. The surface and materials science of tin oxide // Progress in Surface Science, 2005, 79, pp. 47-154.
2. В.В. Кривецкий Направленный синтез материалов на основе нанокристаллического SnO_2 для повышения селективности газовых сенсоров: Автореф. дисс… канд.хим.наук: Москва, 2010. – 26 с.
3. Синев И.В. Температурная зависи-

мость сопротивления тонкопленочных резисторов на основе диоксида олова. Дисс….канд. физ.-мат. наук. Саратов. 2014.- 209 с.
4. Мультисенсоры на основе пористых нано-структурированных материалов. Под ред. Аверина И. А. Пензенский государственный университет. Пенза. 2013, стр.302-305.
5. Jeong-Hoon Leea, Gun-Eik Janga, Dae-Ho Yoonb and Sang-Hee Sonc Effect of deposition temperature on electro-optical properties of SnO_2 thin films fabricated by a PECVD method // Journal of Ceramic Processing Research. 2007, 8(1), pp. 59-63.
6. Filevskaya LN, Smyntyna VA, Grinevich VS Morphology of nanostructured SnO_2 films prepared with polymers employment // Photoelectronics, 2006, 15, pp. 11-14.
7. B. Ulug, H.M. Türkdemir, A. Ulug, O. Büyükgüngör, M.B. Yücel, V.A. Smyntyna, V.S. Grinevich, L.N. Filevskaya. Structure, spectroscopic and thermal characterization of bis(acetylacetonato)dichlorotin(IV) synthesized in aqueous solution// Ukrainian chemical journal, 2010. 76 (7), pp. 12-17.
8. Давыдов С.Ю., Мошников В.А., Федотов А.А. Адсорбция молекул кислорода и окиси углерода на диоксиде олова.// Журнал технической физики, 2006. 79(1), pp. 141-142.
9. Домашевская Э.П., Рябцев С.В., Тутов Е.А., Юраков Ю.А., Чувенкова О.А., Лукин А.Н. Оптические свойства нанослоев SnO_{2-x}.// Письма в ЖТФ, 2006. 32(18), с.7-12.

This article has been received in April 2016

PACS 73.61.Le, 73.63.Bd

L. M. Filevska, A. P. Chebanenko, V. S. Grinevych, N. S. Simanovych

THE ELECTRICAL CHARACTERISTICS OF NANOSCALE SNO_2 FILMS, STRUCTURED BY POLYMERS

Abstract

The electrical characteristics of nanoscale tin dioxide layer were studied. They showed the significant differences in the conductivity values of films in vacuum and in air, which indicates a visible influence of adsorption interaction with oxygen in the air. The dark current temperature dependence activation character was established due to different donors type centers contribution to the conductivity which are “shallow” at low temperatures and are more “deep” at high temperatures. The values of the energy depth of these levels were calculated. The films’ conductivity changes at their heating at vacuum and at the subsequent cooling at vacuum till the initial temperature are reversible and repeatable many times, which testifies the stability of the electrical characteristics of the SnO_2 films and is perspective for use of the layers as adsorptive-sensitive elements of gas sensors**.**

PACS 73.61.Le, 73.63.Bd

Л. М. Філевська, А. П. Чебаненко, В. С. Гріневич, Н. С. Сіманович

ЕЛЕКТРИЧНІ ХАРАКТЕРИСТИКИ НАНОРОЗМІРНИХ ПЛІВОК SNO_2, СТРУКТУРОВАНИХ З ВИКОРИСТАННЯМ ПОЛІМЕРІВ

Резюме

Проведені в роботі дослідження електричних характеристик нанорозмірних шарів діоксиду олова дозволили виявити істотні відмінності в значеннях провідності плівок у вакуумі й на повітрі, що свідчить про помітний вплив адсорбційної взаємодії з киснем повітря. Встановлено активаційний характер кривих ТЗТТ зразків, що обумовлено внеском у провідність різних типів донорних центрів - більше «дрібних» при низьких температурах і більше «глибоких» при високих температурах. Розраховано значення глибини залягання цих енергетичних рівнів. Зміна величини провідності плівок при прогріві у вакуумі й наступному охолодженні у вакуумі до вихідної температури є оборотним і багаторазово відтворюваним, що свідчить про стабільність електричних характеристик досліджуваних плівок SnO_2 і перспективно для використання шарів в якості адсорбційно-чутливих елементів газових сенсорів.

Ключові слова: діоксид олова, нанорозмірні шари, електричні характеристики

PACS 73.61.Le, 73.63.Bd

Л. Н. Филевская, А. П. Чебаненко, В. С. Гриневич, Н. С. Симанович

ЭЛЕКТРИЧЕСКИЕ ХАРАКТЕРИСТИКИ НАНОРАЗМЕРНЫХ ПЛЕНОК SNO_2, СТРУКТУРИРОВАННЫХ С ИСПОЛЬЗОВАНИЕМ ПОЛИМЕРОВ

Резюме

Проведенные в работе исследования электрических характеристик наноразмерных слоев диоксида олова позволили выявить существенные отличия в значениях проводимости пленок в вакууме и на воздухе, что свидетельствует о заметном влиянии адсорбционного взаимодействия с кислородом воздуха. Установлен активационный характер кривых ТЗТТ образцов, что обусловлено вкладом в проводимость различных типов донорных центров – более «мелких» при низких температурах и более «глубоких» при высоких температурах. Рассчитаны значения глубины залегания этих энергетических уровней. Изменение величины проводимости пленок при прогреве в вакууме и последующем охлаждении в вакууме до исходной температуры является обратимым и многократно воспроизводимым, что свидетельствует о стабильности электрических характеристик исследуемых пленок SnO_2 и перспективно для использования слоев в качестве адсорбционно-чувствительных элементов газовых сенсоров.

Ключевые слова: диоксид олова, наноразмерные слои, электрические характеристики

UDC 530.182:510.42

Yu. Ya. Bunyakova, T. A. Florko, A. V. Glushkov, V. F. Mansarliysky, G. P. Prepelitsa, A. A. Svinarenko

Odessa State Environmental University, 15, Lvovskaya str., Odessa, Ukraine
Odessa National Polytechnical University, 1, Shevchenko av., Odessa, Ukraine
e-mail: yubunyak@mail.ru

STUDYING PHOTOKINETICS OF THE IR LASER RADIATION EFFECT ON MIXTURE OF THE CO2-N2-H20 GASES FOR DIFFERENT ATMOSPHERIC MODELS

A kinetics of energy exchange in the mixture of the atmosphere CO2-N2-H20 gases under passing the powerful CO2 laser radiation pulses within the three-mode model of kinetical processes is studied. More accurate data for the absorption coefficient are presented.

At present time the environmental physics has a great progress, provided by implementation of the modern quantum electronics and laser physics methods and technologies in order to study unusual features of the "laser radiation- substance (gases, solids etc.) interaction. A special interest attracts a problem of interaction of the powerful laser radiation with an aerosol ensemble and search of new non-linear optical effects. The latter is directly related with problems of modern aerosol laser physics (c.f.[1-13]). One could remind that there is a redistribution of molecules on the energy levels of internal degree of freedom in the resonant absorption of IR laser radiation by the atmospheric molecular gases. As a result of quite complicated processes one could define an essential changing of the gases absorption coefficient due to the saturation of absorption [1].

One interesting effect else to be mentioned is an effect of the kinetic cooling of environment (mixture of gases), as it was at first predicted in ref. [2,5]. Usually the effect of kinetical cooling (CO_2) in a process of absorption of the laser pulse energy by molecular gas is considered for the middle latitude atmosphere and for special form of a laser pulse. Besides, the approximate values for constants of collisional deactivation and resonant transfer in reaction CO_2-N_2 are usually used. In series of papers (see, for example, [11-13], computational modelling of the energy and heat exchange kinetics in the mixture of the CO_2-N_2-H_20 atmospheric gases interacting with IR laser radiation has been carried out within the general three-mode kinetical model. It is obvious that using more precise values for all model constants and generally speaking the more advanced atmospheric model parameters may lead to quantitative changing in the temporary dependence of the resonant absorption coefficient by CO_2.

Let us remind that the creation and accumulation of the excited molecules of nitrogen owing to the resonant transfer of excitation from the molecules CO_2 results in the change of environment polarizability. Perturbing the complex conductivity of environment, all these effects are able to transform significantly the impulse energetics of IR lasers in an atmosphere and significantly change realization of different non-linear laser-aerosol effects.

The aim of this paper is to present more accurate data for kinetics of energy and heat exchange in the mixture CO_2-N_2-H_20 gases in atmosphere under passing the powerful CO_2 laser radiation pulses on the basis of using the more advanced atmospheric model and more precise values for all kinetical model constants.

As usually, we start from the modified three-mode model of kinetic processes (see, for example, [1,11-13] in order to take into consideration the energy exchange and relaxation processes in the CO_2.– N_2 – H_2O mixture interacting with a laser radiation. As in ref. [11-13] we consider a kinetics of three levels: 10°0, 00°1 (CO_2) and v = 1 (N_2). Availability of atmospheric constituents O_2

and H_2O is allowed for the definition of the rate of vibrating-transitional relaxation of N_2. The system of balance equations for relative populations is written in a standard form as follows:

$$\frac{dx_2}{dt} = \omega x_1 - (\omega + Q + P_{20})x_2 + Qx_3 + P_{20}x_2^0,$$
$$\frac{dx_3}{dt} = \delta Q x_2 - (\delta Q + P_{30})x_3 + P_{30}x_3^0. \quad (1)$$

Here the following notations are used:

$$x_1 = N_{100}/N_{O_2},$$
$$x_2 = N_{001}/N_{O_2}, \quad (2)$$
$$x_3 = \delta N_{N_2}/N_{O_2},$$

where N_{100}, N_{001} are the level populations 10°0, 00°1 (CO_2); N_{N_2} is the level population v = 1 (N_2); N_{O_2} is the concentration of CO_2 molecules; δ is the ratio of the common concentrations of CO_2 and N_2 in the atmosphere ($\delta = 3.85\times10^{-4}$); x_1^0, x_2^0 and x_3^0 are the equilibrium relative values of populations under gas temperature T:

$$x_1^0 = \exp(-E_1/T),$$
$$x_2^0 = x_3^0 = \exp(E_2/T); \quad (3)$$

The values E_1 and E_2 in (1) are the energies (K) of levels 10°0, 00°1 (consider the energy of quantum N_2 equal to E_2); P_{10}, P_{20} and P_{30} are the probabilities (s^{-1}) of the collisional deactivation of levels 10°0, 00°1 (CO_2) and v = 1 (N_2), Q is the probability (s^{-1}) of resonant transfer in the reaction $CO_2 \rightarrow N_2$,ω is the probability (s^{-1}) of CO_2 light excitation, g = 3 is the statistical weight of level 02°0, $\beta = (1+g)^{-1} = 1/4$. As usually, the solution of the differential equations system (1) allows defining a coefficient of absorption of the radiation by the CO_2 molecules according to the formula:

$$\alpha_{O_2} = \sigma(x_1 - x_2)N_{O_2}. \quad (4)$$

The σ in (4) is dependent upon the thermodynamical medium parameters as follows [2]:

$$\sigma = \sigma_0 \frac{P}{P_0}\left(\frac{T}{T_0}\right)^{1/2}, \quad (5)$$

Here T and p are the air temperature and pressure, σ_0 is the cross-section of resonant absorption under $T = T_0$, $p = p_0$. One could remind that the absorption coefficient for carbon dioxide and water vapour is dependent upon the thermodynamical parameters of aerosol atmosphere. In particular, for radiation of CO_2-laser the coefficient of absorption by atmosphere defined as $\alpha_g = \alpha_{O_2} + \alpha_{H_2O}$ is equal in conditions, which are typical for summer mid-latitudes, $\alpha_g(H=0) = 2.4\cdot10^6$ cm^{-1}, from which $0.8\cdot10^6$ cm^{-1} accounts for CO_2 and the rest – for water vapour (data are from ref. [2]) . On the large heights the sharp decrease of air moisture occurs and absorption coefficient is mainly defined by the carbon dioxide.

The changing population of the low level 10°0 (CO_2), population of the level 00°1, the vibrating-transitional relaxation (VT-relaxation) and the inter modal vibrating-vibrating relaxation (VV'-relaxation) processes define the physics of resonant absorption processes. Moreover, the above indicated processes result in a redistribution of the energy between the vibrating and transitional freedom of the molecules. According to ref.[1], the threshold value, which corresponds to the decrease of absorption coefficient in two times, for the strength of saturation of absorption in vibrating-rotary conversion give $I_{sat} = (2 \div 5)\ 10^5$ W cm^{-2} for atmospheric CO_2. In this case the pulse duration t_i must satisfy the condition $t_R << t_i < t_{VT}$, where t_R and t_{VT} are the times of rotary and vibrating-transitional relaxation's. by The fast exchange of level 10°0 with basic state, and by the relatively slow relaxation of high level 00°1define a renewal process of thermodynamic equilibrium is characterized. The latter provides an energy outflow from the transitional degree of freedom onto vibrating ones and in the cooling of environment. It is easily understand that using more powerful laser radiation sources can lead to a strong non-linear interaction phenomena and, as result, significantly change a photo-kinetics of the corresponding processes.

In table 1 we present mode accurate our data (column C) for the relative coefficient of absorption $\overline{\alpha}_{O_2}$, which is normalized on the linear coefficient of absorption, calculated using (1) on corresponding height *H*. All data for $\overline{\alpha}_{O_2}$ are obtained for the height distribution of the pressure and temperature according to the advanced mid-latitude atmospheric model (all data are presented in series of refs. [14-20]). In table 1 there are presented also the analogous data from ref. [2] (column A) , from ref. [13] (column B).

Table 1.

Temporary dependence of resonant absorption relative coefficient $\overline{\alpha}_{O_2}$ (sm^{-1}) of laser radiation (λ=10,6μm) by CO_2 for rectangular (R) laser pulses (intensity $I=10^5$ W/sm^2) on the height (H, km) for the mid-latitude atmospheric model [1]: A- data of modelling [2]; B- data of modelling [13], C- data of modelling [14], D- this work

T μs	A [2] 10×I; R H=0	A[2] 10×I;R H=10	B [13] 10×I; G H=0	B [13] 10×I; G H=10
0	1,0	1,0	1,0	1,0
1	0,60	0,12	0,57	0,13
2	0,52	0,08	0,46	0,05
3	0,63	0,27	0.59	0,19
4	0,67	0,35	0,64	0,28
T μs	C [14] 10×I; G H=0	C [14] 10×I; G H=10	D, this 10×I; G H=0	D, this 10×I; G H=10
0	1,0	1,0	1,0	1,0
1	0,54	0,11	0,54	0,11
2	0,42	0,04	0,42	0,04
3	0.57	0,16	0.57	0,16
4	0,60	0,25	0,60	0,25

In Refs.[2 13,14] the analogous data for the relative coefficient of absorption $\overline{\alpha}_{O_2}$ and the height distribution of pressure and temperature are presented and obtained in a case of using the Odessa-latitude atmospheric conditions according to atmospheric model [7,8]. Here we use the world standard atmospheric model conditions [14-20]. Important moment is also connected with the more correct choice of probabilities P_{10}, P_{20} and P_{30} of the collisional deactivation of levels 10°0, 00°1 (CO_2) and v = 1 (N_2), probability *Q* of resonant transfer in the reaction $CO_2 \rightarrow N_2$, probability ω of CO_2 light excitation and other constants in comparison with refs. [2,13]. Let us in conclusion to note that obviously a quality of choice of the corresponding molecular constants and the corresponding atmospheric model parameters is of a great importance in modelling the effect of kinetic cooling of the CO_2 under propagation of the laser radiation in atmosphere. Naturally, principally another situation will occur in a case of the super intense laser pulses using for the atmosphere monitoring. Obviously, the modified model of photokinetical processes is to be developed in this case.

References

1. Zuev V.E., Zemlyanov A.A., Kopytin Y.D. Nonlinear Optics of Atmosphere.-L.:Hidrometeoizd., 1991.-256p.
2. Zuev V.E., Zemlyanov A.A., Kopytin Y.D., Kuzikovsky A.V. Powerful laser radiation in an atmospheric aerosol.-Novosybirsk, 1994.-224p.
3. Bagratashvili V.N., Letokhov V.S., Makarov A.A., Ryabov E.A. Multi-Photon Processes in Molecules in Infrared laser field.-M.: Nauka,1999-180p.
4. Bates N.R., Merlivat L. The influence of short-term wind variability on air-sea CO2 exchange // Geophysical Research Letters. – 2001. – Vol. 28. – No. 17. – P. 3281-3284.
5. Gordiets B.F., Osipov A.I., Khokhlov R.V. About cooling the gas under powerful CO_2 laser radiation passing in atmosphere// J.Techn.Phys.-1994.-Vol.14.-P.1063-1069.
6. Glushkov A., Malinovskaya S., Shpinareva I., Kozlovskaya V., Gura V., Quantum stochastic modelling energy transfer and effect of rotational and V-T relaxation on multiphoton excitation and dissociation for CF_3Br molecules//

Int. J.Quant.Chem.-2005,-Vol.104.-P.512-520.
7. Parkinson S., Young P. Uncertainty and sensitivity in global carbon cycle modeling // Climate Research. – 1998. – Vol. 9. – No. 3. – P. 157-174.
8. Stephens B.B., Keeling R.F., Heimann M., Six K.D., Murnane R., Caldeira K. Testing global ocean carbon cycle models using measurements of atmospheric O_2 and CO_2 concentration// Global Biogeochem. Cycles. –1998.–Vol.12.–P. 213-230.
9. Glushkov A.V., Ambrosov S.V., Malinovskaya S.V. etal, Spectroscopy of carbon dioxide: Oscillator strengths and energies of transitions in spectra of CO_2 // Opt.and Spectr.-1996.-Vol.80.-C.60-65.
10. Trenberth K.E., Stepaniak D.P., Caron J.M. Interannual variations in the atmospheric heat budget //J.Geophys. Res.–2002.–Vol.107.– P.4-1– 4-15.
11. Prepelitsa G.P., Shpinareva I.M., Bunyakova Yu.Ya., Photokinetics of interaction and energy exchange for ir laser radiation with mixture CO_2-N_2-H_20 of atmospheric gases// Photoelectronics.-2006.-Vol.16.-P.139-141.
12. Korban V., Prepelitsa G., Bunyakova Yu., Degtyareva L., Seredenko S., Karpenko A., Photokinetics of the IR laser radiation effect on mixture of CO_2-N_2-H_20 gases: advanced atmospheric model// Photoelectronics.-2009. -N18.-P.36-39.
13. Kistler R., Kalnay E., Collins W., Saha S., White G., Woollen J., Chelliah M., Ebisuzaki W., Kanamitsu M., Kousky V., van den Dool H., Jenne R., Fiorino M. The NCEP-NCAR 50-year reanalysis: monthly means CD-ROM and documentation // Bull. Amer. Meteor. Soc. – 2001. – Vol. 82. – P. 247-267.
14. Fyfe J., Boer G., Flato G., Predictable winter climate in the North Atlantic sector during the 1997–1999 ENSO cycle // Geophys. Res.Lett.-1999.-Vol.26.-P. 1601-1604.
15. Plattner G-K., Joos F., Stocker T.F., Marchal O. Feedback mechanisms and sensitivities of ocean carbon uptake under global warming // Tellus. – 2001. – Vol. 53B.-P. 564-592.
16. Jin X., Shi G. A simulation of CO_2 uptake in a three dimensional ocean carbon cycle model// Acta Meteorologica Sinica. – 2001. – Vol. 15. – No. 1. – P. 29-39.

This article has been received in May 2016

UDC 530.182:510.42

Yu. Bunyakova, T. Florko, A. Glushkov, V. Mansarliysky, G. Prepelitsa, A. Svinarenko

STUDYING PHOTOKINETICS OF THE IR LASER RADIATION EFFECT ON MIXTURE OF THE CO_2-N_2-H_20 GASES FOR DIFFERENT ATMOSPHERIC MODELS

Abstract. A kinetics of energy exchange in the mixture of the atmosphere CO_2-N_2-H_20 gases under passing the powerful CO_2 laser radiation pulses within the three-mode model of kinetical processes is studied. More accurate data for the absorption coefficient are presented.

Key words: photokinetics, laser field, mixture of gases, atmospheric model

УДК 530.182:510.42

Ю. Бунякова, Т. Флорко, А. Глушков, В. Мансарлийский, Г. Препелица, А. Свинаренко

ИЗУЧЕНИЕ ФОТОКИНЕТИКИ ВЗАИМОДЕЙСТВИЯ ИК ЛАЗЕРНОГО ИЗЛУЧЕНИЯ СО СМЕСЬЮ CO_2-N_2-H_20 ГАЗОВ ДЛЯ РАЗНЫХ АТМОСФЕРНЫХ МОДЕЛЕЙ

Резюме. Рассмотрена фотокинетика энергообмена в смеси CO_2-N_2-H_20 атмосферных газов при прохождении через атмосферу мощного излучения CO_2 лазера в рамках уточненной 3-модовой модели кинетических процессов. Получены более точные значения коэффициента поглощения.

Ключевые слова: фотокинетика, лазерное поле, смесь газов, атмосферная модель

УДК 530.182:510.42

Ю. Бунякова, Т. Флорко, О. Глушков, В. Мансарлійський, Г. Препелиця, А. Свинаренко

ДОСЛІДЖЕННЯ ФОТОКІНЕТИКИ ВЗАЄМОДІЇ ІЧ ЛАЗЕРНОГО ВИПРОМІНЮВАННЯ ІЗ СУМІШЕЙ CO_2-N_2-H_20 ГАЗІВ ДЛЯ РІЗНИХ АТМОСФЕРНИХ МОДЕЛЕЙ

Резюме. Розглянуто фотокінетику енергообміну у сумішу CO_2-N_2-H_20 атмосферних газів при проходженні скрізь атмосферу міцного випромінювання CO_2 лазера у межах уточненої 3-модової моделі кінетичних процесів. Отримані більш точні оцінки для коефіцієнта поглинання.

Ключові слова: фотокінетика, лазерне поле, суміш газів, атмосферна модель

UDC 539.184

V. F. Mansarliysky

Odessa State Environmental University, 15, Lvovskaya str., Odessa, Ukraine
e-mail: mansmet@mail.ru

NEW RELATIVISTIC APPROACH TO CALCULATING THE HYPERFINE LINE SHIFT AND BROADENING FOR HEAVY ATOMS IN THE BUFFER GaS

It is presented a new consistent relativistic approach, based on the atomic gauge-invariant relativistic perturbation theory and the optimal construction of the interatomic potential function within exchange perturbation theory . As illustration it is applied to calculating the interatomic potentials, hyperfine structure line collision shift and broadening for heavy atoms in an atmosphere of the buffer inert gas. The accurate account for the relativistic and exchange-correlation and continuum pressure effects is necessary for an adequate description of the energetic and spectral properties of the heavy atoms in an atmosphere of the heavy inert gases.

The broadening and shift of atomic spectral lines by collisions with neutral atoms has been studied extensively since the very beginning of atomic physics, physics of collisions etc [1–16]. High precision data on the collisional shift and broadening of the hyperfine structure lines of heavy elements (alkali, alkali-earth, lanthanides, actinides and others) in an atmosphere of the buffer (for example, inert) gases are of a great interest for modern quantum chemistry, atomic and molecular spectroscopy, astrophysics and metrology as well as for studying a role of weak interactions in atomic optics and heavy-elements chemistry [1-14]. As a rule (see [15]), the cited spectral lines shift and broadening due to a collision of the emitting atoms with the buffer atoms are very sensitive to a kind of the intermolecular interaction. It means that these studies provide insight into the nature of interatomic forces and, hence, they provide an excellent test of theory. Besides, calculation of the hyperfine structure line shift and broadening allows to check a quality of the wave functions (orbitals) and study a contribution of the relativistic and correlation effects to the energetic and spectral characteristics of the two-center (multi-center) atomic systems.

The detailed non-relativistic theory of collisional shift and broadening the hyperfine structure lines for simple elements (such as light alkali elements etc.) was developed by many authors (see, for example, Refs. [1-3,15]). However, until now an accuracy of the corresponding available data has not been fully adequate to predict or identify transitions within accuracy as required for many applications. It is obvious that correct taking into account the relativistic and correlation effects is absolutely necessary in order to obtain sufficiently adequate description of spectroscopy of the heavy atoms in an atmosphere of the buffer gases. This stimulated our current investigation whose goals were to propose a new precise relativistic approach perturbation theory approach to calculating the interatomic potentials and hyperfine structure line collision shifts and broadening for the alkali and lanthanide atoms in an atmosphere of the inert gases. The basic expressions for the collision shift and broadening hyperfine structure spectral lines are taken from the kinetic theory of spectral lines [6,7,11,12].

In order to calculate a collision shift of the hyperfine structure spectral lines one can use the following expression known in the kinetic theory

of spectral lines shape (see Refs. [11,12,15]):

$$f_p = \frac{D}{p} = \frac{4\pi w_0}{kT}\int_0^{\infty}[1+g(R)]\,dw\,(R)\exp\left(-U(R)/kT\right)R^2 dR \quad (1a)$$

$$g(R) = \begin{cases} \dfrac{2}{3\sqrt{\pi}}\left(-\dfrac{U(R)}{kT}\right)^{3/2}, & U<0, \\ 0, & U>0, \end{cases} \quad (1b)$$

Here *U(R)* is an effective potential of interatomic interaction, which has the central symmetry in a case of the systems *A—B (*in our case, for example, *A*=Rb,Cs*; B*=He*)*; *T* is a temperature, w_0 is a frequency of the hyperfine structure transition in an isolated active atom; *dw(R)=Dw(R)/*w_0 is a relative local shift of the hyperfine structure line; $(1+g(R))$ is a temperature form-factor.

The local shift is caused due to the disposition of the active atoms (say, the alkali atom and helium He) at the distance *R*. In order to calculate an effective potential of the interatomic interaction further we use the exchange perturbation theory formalism (the modified version EL-HAV) [1]).

Since we are interested by the alkali (this atom can be treated as a one-quasiparticle systems, i.e. an atomic system with a single valence electron above a core of the closed shells) and the rare-earth atoms (here speech is about an one-, two- or even three-quasiparticle system), we use the classical model for their consideration. The interaction of alkali (A) atoms with a buffer (B) gas atom is treated in the adiabatic approximation and the approximation of the rigid cores. Here it is worth to remind very successful model potential simulations of the studied systems (see, for example, Refs. [32-41]).

In the hyperfine interaction Hamiltonian one should formally consider as a magnetic dipole interaction of moments of the electron and the nucleus of an active atom as an electric quadrupole interaction (however, let us remind that, as a rule, the moments of nuclei of the most (buffer) inert gas isotopes equal to zero) [6].

The necessity of the strict treating relativistic effects causes using the following expression for a hyperfine interaction operator H_{HF} (see, eg., [1,5]):

$$H_{\mathrm{HF}} = a\sum_{i=1}^{N} I\frac{\alpha_i \times r_i}{r_i^3}d = -2\mu\frac{e^2 h}{2m_p c}, \quad (2)$$

where I – the operator of the nuclear spin active atom, a_i – Dirac matrices, m_p – proton mass, μ - moment of the nucleus of the active atom, expressed in the nuclear Bohr magnetons. Of course, the summation in (2) is over all states of the electrons of the system, not belonging to the cores. The introduced model of consideration of the active atoms is important to describe an effective interatomic interaction potential (an active atom – an passive atom), which is centrally symmetric (J_A=$^1/_2$) in our case (the interaction of an alkali atom with an inert gas atom).

Let us underline that such an approximation is also acceptable in the case system "thallium atom – an inert gas atom" and some rare-earth atoms, in spite of the presence of p-electrons in the thallium (in the case of rare-earth atoms, the situation is more complicated).

As it is well known (see also Refs. [1, 2]), the non-relativistic Hartree-Fock method is mostly used for calculating the corresponding wave functions. More sophisticated approach is based on using the relativistic Dirac-Fock wave functions (first variant) [12]. Another variant is using the relativistic wave functions as the solutions of the Dirac equations with the corresponding density functional, i.e within the Dirac-Kohn-Sham theory [8,15]. It is obvious that more sophisticated relativistic many-body methods should be used for correct treating relativistic, exchange-correlation and even nuclear effects in heavy atoms. (including the many-body correlation effects, intershell correlations, possibly the continuum pressure etc]). In our calculation we have used the relativistic functions, which are generated by the Dirac Hamiltonian [8]. The potential of the inter-electron interaction with accounting the retarding effect and magnetic interaction in the lowest order on parameter a^2 (the fine structure constant) is as follows:

$$U(r_i r_j) = \exp(i\,\omega_{ij} r_{ij})\cdot\frac{(1 - \alpha_i \alpha_j)}{r_{ij}}, \quad (3)$$

where w_{ij} is the transition frequency; a_i ,a_j are the Dirac matrices. The Dirac equation potential includes the electric potential of a nucleus and electron shells and the exchange-correlation potentials in the Kohn-Sham approximation. Besides,

we introduce into the zeroth order Hamiltonian the corresponding correlation functional [5]

$$V_C[\rho(r),r] = -0.0333 \cdot b \cdot \ln[1+18.3768 \cdot \rho(r)^{1/3}], \quad (4)$$

where b is the optimization parameter (for details see Refs. [5,8,15]). The optimization is reduced to minimization of the gauge dependent multi-electron contribution $ImdE_{ninv}$ of the lowest relativistic perturbation theory corrections to the radiation widths of atomic levels. The minimization of the functional $ImdE_{ninv}$ leads to the Dirac-Kohn Sham-like equations for the electron density that are numerically solved. The further elaboration of the method can be reached by means of using the Dirac-Sturm approach [5]. To calculate an effective potential of the interatomic interaction we use a method of the exchange perturbation theory (in the modified version EL-HAV [1]). Within exactness to second order terms on potential of Coulomb interaction of the valent electrons and atomic cores a local shift can be written as:

$$\delta(R) = \frac{S_0}{1-S_0} + \Omega_1 + \Omega_2 - \sum_n \frac{C_n}{R^n}, \quad (5)$$

where values W_1, W_2 are the non-exchange and exchange non-perturbation sums of the first order correspondingly, which express through the matrix elements of the hyperfine interaction operator. The other details are in Refs.[1,8,15].

Further we present some test results of our studying hyperfine line collisional shift for alkali atoms (rubidium and caesium) in the atmosphere of the helium gas. In Table 1 and 2 we present our theoretical results for the hyperfine line observed shift f_p (1/Torr) in a case of the Rb-He and Cs-He pairs. The experimental and alternative theoretical results by Batygin et al [11] for f_p are listed too. At present time there are no precise experimental data for a wide interval of temperatures in the literature. The theoretical data from Refs. [11] are obtained on the basis of calculation within the exchange perturbation theory with using the He wave functions in the Clementi-Rothaane approximation [42] (column: Theory[a]), and in the Z-approximation (column: Theory[b]), and in the Löwdin approximation (column: Theory[c]).

Table 1.

The observed f_r (10^{-9} 1/Torr) shifts for the systems of Rb-He and corresponding theoretical data (see text).

T, K	Exp.	[13]	[11] a	[11] b	[11]c	This
223	-	113	79	67	81	116
323	105	101	73	56	75	103
423	-	89	62	48	64	91
523	-	80	55	43	56	83
623	-	73	50	38	50	75
723	-	-	-	-	-	73
823	-	-	-	-	-	71

Note:[a] –calculation with using the He wave functions in the Clementi-Rothaane approximation; [b] – calculation with using the He wave functions in the Z-approximation;

[c] –calculation with using the He wave functions in the Löwdin approximation;

Table 2.

The observed f_r (10^{-9} 1/Torr) shifts for the systems of the Cs-He and corresponding theoretical data (see text).

T, K	Exp	[11] a	[11] b	[11]c	This
223	-	164	142	169	175
323	135	126	109	129	136
423	-	111	96	114	122
523	-	100	85	103	110
623	-	94	78	96	103
723	-	-	-	-	96
823	-	-	-	-	91

Note:[a] –calculation with using the He wave functions in the Clementi-Rothaane approximation; [b] – the Z-approximation; [c] –the Löwdin approximation;

The important feature of the developed optimized perturbation theory approach is using the optimized relativistic orbitals basis, an accurate accounting for the exchange-correlation and continuum pressure effects with using the effective functionals [18,34].

The difference between the obtained theoretical data and other alternative calculation results can be explained by using different perturbation theory schemes and different approximations for calculating the electron wave functions of heavy atoms. It is obvious that the correct account for the relativistic and exchange-correlation and continuum pressure effects will be necessary for an adequate description of the energetic and spectral properties of the heavy atoms in an atmosphere of the heavy inert gases (for example, such as Xe).

References

1. Kaplan I.G., Theory of intermolecular interactions (Nauka, Moscow, 1995), p.1-380.
2. Nikitin E.E., Semiempirical methods of calculation of interatomic interaction potentials. Series: Structure of molecules and chemical bond, vol. **4**, ed. by E.E.Nikitin and S.Ya. Umansky (VINITI, Moscow, 1990).
3. I.M. Torrens, Interatomic potentials (Academic Press, , N-Y., 1992), p.1-390.
4. A.J. Freeman and R.H. Frankel, Hyperfine interactions (Plenum, N.-Y., 1997).
5. Glushkov A.V., Relativistic and correlation effects in spectra of atomic systems.-Odessa: Astroprint, 2006.
6. Khetselius O.Yu., Relativistic many-body perturbation theory calculation of the hyperfine structure and oscillator strengths parameters for some heavy elements atoms and ions/ Quantum Systems in Physics, Chemistry, and Biology. Series: Progress in Theoretical Chemistry and Physics, Eds. A.Tadjer, R.Pavlov, J.Maruani, E.Brändas, G.Delgado-Barrio (Springer).-2016-Vol.B30.-P.131-140.
7. Khetselius O.Yu., Florko T.A., Svinarenko A.A., Tkach T.B., Radiative and collisional spectroscopy of hyperfine lines of the Li-like heavy ions and Tl atom in atmosphere of inert gas//Phys.Scripta (IOP).-2013.-Vol.T153-P.014037.
8. Glushkov A.V., Khetselius O.Yu., Lopatkin Yu.M., Florko T.A., Kovalenko O.A., Mansarliysky V.F., Collisional shift of hyperfine line for rubidium in an atmosphere of the buffer inert gas// Journal of Physics: C Series (IOP, London, UK).-2014.-Vol.548.-P. 012026
9. Chi X., Dalgarno A., Groenenborn G.C., Dynamic polarizabilities of rare-earth-metal atoms and dispersion coefficients for their interaction with helium atoms// Phys.Rev.A.-2007.-Vol.75.-P.032723.
10. Svinarenko A.A., Glushkov A.V. , Mansarliysky V.F>, Mischenko E.V. Relativistic theory of shift and broadening spectral lines of the hyperfine transitions for heavy atoms in atmosphere of buffer inert gases/ -Odessa: OSENU.-2008.-120P.
11. Batygin V.V., Gorny M.B., Gurevich B.M., The interatomic potentials shifts lines HF structure and diffusion coefficients of rubidium and cesium atoms in a helium buffer//J. Tech.Fiz.-1998-Vol.48.-P.1097-1105.
12. Batygin V. V., Sokolov I. M., Collisional shift and adiabatic broadening of line of the hyperfine transition in the ground state of thallium in an atmosphere of the buffer helium, krypton and xenon//Opt. Spectr.-1993.-Vol.55.-P.30-38.
13. Mischenko E., Loboda A., Svinarenko A., Dubrovskaya Yu.V., Quantum measure of frequency and sensing collisional shift of the ytterbium hyperfine lines in medium of helium gas// Sensor Electr. and Microsyst. Techn.-2009.-N1.-P.25-29.
14. Khetselius O.Yu., Optimized perturbation theory to calculating the hyperfine line shift and broadening for heavy atoms in the buffer gas// Frontiers in Quantum Methods and Applications in Chemistry and Physics, (Springer).-2015-Vol.29.-Ch.4.-P.54-76.
15. Buchachenko A.A., Szczesniak M.M., Chalasinski G., Calculation of Van der Waals coefficients for interaction of rare-earth metal atoms with helium atoms// J.Chem. Phys.-2006.-Vol.124.-P.114301.
16. Sobel'man I.I. Introduction to theory of atomic spectra.-Moscow: Nauka.-1997.

This article has been received in April 2016.

UDC 539.184

V. F. Mansarliysky

NEW RELATIVISTIC APPROACH TO CALCULATING THE HYPERFINE LINE SHIFT AND BROADENING FOR HEAVY ATOMS IN THE BUFFER GaS

Abstract

It is presented a new consistent relativistic approach to hyperfine structure line collision shift and broadening for heavy atoms in an atmosphere of the buffer inert gas, based on the atomic gauge-invariant relativistic perturbation theory and the optimal construction of the interatomic potential function within exchange perturbation theory . As illustration it is applied to calculating the interatomic potentials, hyperfine structure line collision shift for heavy atoms in an atmosphere of the buffer inert gas. The accurate account for the relativistic and exchange-correlation and continuum pressure effects is necessary for an adequate description of the energetic and spectral properties of the heavy atoms in an atmosphere of the heavy inert gases.

Keywords: Relativistic many-body perturbation theory, hyperfine line collision shift

УДК 539.184

В. Ф. Мансарлийский

НОВЫЙ РЕЛЯТИВИСТСКИЙ ПОДХОД К ОПРЕДЕЛЕНИЮ СДВИГА И УШИРЕНИЯ ЛИНИЙ СВЕРХТОНКОЙ СТРУКТУРЫ В ТЯЖЕЛЫХ АТОМАХ В БУФЕРНЫХ ГАЗАХ

Резюме

Представлен новый релятивистский подход к определению сдвига и уширения линии сверхтонкой структуры тяжелых атомов в атмосфере буферных газов. Метод основан на атомной калибровочно-инвариантной теории возмущений и оптимальной конструкции межатомного потенциала в обменной теории возмущений. В качестве иллюстрация приведены результаты расчета сдвига сверхтонких линий ряда тяжелых атомов, в частности, щелочных атомов в атмосфере буферных инертных газов. Аккуратный учет релятивистских, обменно-корреляционных и эффектов давления континуума необходим для адекватного описания энергетических и спектральных свойств тяжелых атомов в атмосфере тяжелых инертных газов.

Ключевые слова: релятивистская теория возмущений, столкновительный сдвиг линий сверхтонкой структуры

УДК 539.184

В. Ф. Мансарлійський

НОВИЙ РЕЛЯТИВІСТСЬКИЙ ПІДХІД ДО ВИЗНАЧЕННЯ ЗСУВУ ТА УШИРЕННЯ ЛІНІЙ НАДТОНКОЇ СТРУКТУРИ У ВАЖКИХ АТОМАХ В БУФЕРНИХ ГАЗАХ

Резюме

Представлено новий релятивістський підхід до визначення зсуву та уширення лінії надтонкої структури важких атомів в атмосфері буферних газів. Метод базується на атомній калібрувально-інваріантній теорії збурень та оптимальній конструкції міжатомного потенціалу в обмінній теорії збурень. Як ілюстрація наведені результати розрахунку зсуву надтонких ліній ряду важких атомів, зокрема, лужних атомів в атмосфері буферних інертних газів. Акуратний облік релятивістських, обмінно-кореляційних і ефектів тиску континууму необхідний для адекватного опису енергетичних і спектральних властивостей важких атомів в атмосфері важких інертних газів.

Ключові слова: релятивістська теорія збурень, зсув за рахунок зіткнень ліній надтонкої структури

UDC 539.184, 539.186

A. V. Ignatenko, A. A. Kuznetsova, A. S. Kvasikova, A. V. Glushkov, M. Yu. Gurskaya

Odessa State Environmental University, 15, Lvovskaya str., Odessa, Ukraine
Odessa National Maritime Academy, Odessa, 4, Didrikhsona str., Odessa, Ukraine
Odessa National Polytechnical University, 1, Shevchenko av., Odessa, Ukraine
e-mail: quantign@mail.ru

NONLINEAR CHAOTIC DYNAMICS OF ATOMIC AND MOLECULAR SYSTEMS IN AN ELECTROMAGNETIC FIELD

It has been numerically studied a chaotic dynamics of diatomic molecules (on example of the GeO molecule in an infrared field) and some laser systems. An advanced generalized techniques such as the wavelet analysis, multi-fractal formalism, mutual information approach, correlation integral analysis, false nearest neighbour algorithm, the Lyapunov exponent's (LE) analysis, and surrogate data method, prediction models etc is used. It has been shown that systems exhibit a nonlinear behaviour with elements of a low-or high-dimensional chaos. There are firstly presented the numerical data on topological and dynamical invariants of chaotic systems, in particular, the correlation, embedding, Kaplan-York dimensions, LE, Kolmogorov's entropy etc for GeO molecule in an electromagnetic infrared field in the chaotic regime..

In last years the phenomena of dynamical chaos and dynamical stabilization attract a great interest as a manifestation of this effect in photo-optical systems may in a significant degree change a functional regime (e.g.[1-15]). Cited effect is usually observed in the physical systems and related to a type of non-linear effects. As a rule, dynamical chaos is manifested in the quantum systems, which are not linear in a classic limit. Above especially effective manifestations of this effect in the quantum systems one could mention systems which interact with external, time dependent, for example laser, field. It has been discovered that dynamics of atomic and molecular, cluster and nano-optical systems in a laser field has features of the random, stochastic kind and its realization does not require the specific conditions. The importance of studying a phenomenon of stochasticity or quantum chaos in dynamical systems in laser field is provided by a whole number of technical applications, including a necessity of understanding chaotic features in a work of different electronic devices and systems. The important topic of the laser-atomic dynamics and hierarchy systems physics is connected with governing and control of quantum chaotic diffusion and stabilisation effects in atomic systems in the intense laser field (especially important case is atoms in electromagnetic traps and heat bath) [2,15,16]. The principal aim of coherent control is to steer a quantum system towards a desired final state through interaction with light while simultaneously inhibiting paths leading to undesirable outcomes. Controlling mechanisms have been proposed and demonstrated for atomic and solid-state systems. Gibson performs calculations for three-level systems and 1D model of a two-electron molecule (see refs in [3]). Transitions to excited state occur via a 12-photon interaction for an 800 nm intense pulse of length 244 au, or just over 2 cycles. The stabilization dynamics of model He beyond the dipole approximation and with two active electrons was is investigated [6] in the presence of a high-intensity and high-frequency laser pulse. There may exist a laser frequency and intensity regime in which the total ionization yield decreases with increasing laser amplitude. In the near future, free electron lasers will further deliver laser pulses of such high frequencies and intensities to meet the conditions needed for the stabilization of atomic systems more easily. Along with those technological de-

velopments, a wide range of theoretical methods including analytical model calculations, Monte Carlo simulations and numerical calculations have been applied to the ionization of hydrogen-like atoms. Further progress was achieved concerning the ionization and stabilization of atoms with two active electrons. In ref.[11,12] an effective approach to adequate treating and sensing a spectral hierarchy and dynamical stabilisation in atomic systems in the intense laser field is considered and based on non-relativistic and relativistic time-dependent complex rotation method (for atomic systems) and non-Hermitian Floquet formalism (for molecular systems). The stabilization of helium (study of the 2D two-electron atom) in intense high-frequency laser pulses is modelled within the relativistic scheme. It has been carried out modeling generation of the atto-second VUV and X-ray pulses under ionization of atomic (molecular) system by femto-second optical pulse.

In this paper we present the results of analysis of the chaotic dynamics for diatomic molecules in an electromagnetic (infrared) field. In this paper we numerically studied a chaotic dynamics of diatomic molecules (on example of the GeO molecule in an infrared field) and some laser systems.

An advanced generalized techniques such as the wavelet analysis, multi-fractal formalism, mutual information approach, correlation integral analysis, false nearest neighbour algorithm, the Lyapunov exponent's (LE) analysis, and surrogate data method, prediction models etc (look details in Refs.[3-19]) is used. It has been shown that systems exhibit a nonlinear behaviour with elements of a low-or high-dimensional chaos. There are firstly presented the numerical data on topological and dynamical invariants of chaotic systems, in particular, the correlation, embedding, Kaplan-York dimensions, LE, Kolmogorov's entropy etc for GeO molecule in an electromagnetic infrared field in the chaotic regime.

The analysis is based on the numerical solution of the time-dependent Schrödinger equation and realistic Simons-Parr-Finlan model for the potential of diatomic molecule $U(x)$ (the quantum unit). Secondly, it is based on using an universal approach to analysis of nonlinear chaotic dynamics (chaos-geometric unit). The Simons-Parr-Finlan formulae [20] for the molecular potential is:

$$U(r) = B_0[r - r_e)/r]^2\{1 + \sum_n b_n[r - r_e)/r]^n\} \quad (1a)$$

or introducing $x = r - r_0$:

$$U(r) = B_0[x(x + r_0]^2\{1 + \sum_n b_n[x(x + r_0]^n\} \quad (1b)$$

where the coefficients b_i are linked with corresponding molecular constants [20].

The problem of dynamics of diatomic molecules in an infrared field is reduced to solving the Schrödinger equation:

$$i\partial\Psi/\partial t = [H_0 + U(x) - d(x)E_M\varepsilon(t)\cos(\omega_L t)]\Psi$$

where E_M - the maximum field strength, $e(t)=E_0 cos(nt)$ corresponds the pulse envelope (chosen equal to one at the maximum value of electric field). A molecule in the field gets the induced polarization and its high-frequency component can be defined as:

$$P_x(t) = p_c^{(x)}(t)cos\omega t + p_s^{(x)}(t)sin\omega t,$$
$$P_y(t) = p_c^{(y)}(t)cos\omega t + p_s^{(y)}(t)sin\omega t,$$
$$p_c^{(x,y)}(t) = \left(\frac{1}{T}\right)\oint\langle\psi(t)|\hat{d}_{x,y}|\psi(t)\rangle cos\omega t dt, \quad (3)$$

where T – period of the external field, d –dipole moment. The power spectrum can be further determined as $S(\omega) = |F[p(t)]|^2$. To avoid the numerical noise during the Fourier transformation, the attenuation technique used,i.e. at $t > t_p$, p (t) is replaced by

$$p(t)cos^2\{\pi(t - t_p)/[2(T - t_p)]\}, \quad (t_p < t < T)$$
with $T=1.6t_p$. (4)

It is understood that in the regular case of molecular dynamics, a spectrum will consist of a small number of the well resolved lines. In the case of chaotic dynamics of molecule in a field situation changes essentially. The corresponding energy of interaction with the field is much higher than anharmonicity constant $W > x\hbar\Omega$. It is obvious that a spectrum in this case become more complicated [17,18].

We have carried out the numerical computing dynamics of the diatomic molecule GeO in the electromagnetic field (the molecule and field parameters are as follows : $\hbar\Omega$=985.8 cm^{-1}, $y\hbar\Omega$

=4.2cm^{-1}, B = 0.48 cm^{-1}, d_0 = 3.28 D, M=13.1 a.e.м.; the field intensity is 2.5-25 GW/cm^2, respectively: W = 3.39-10.72cm^{-1}). The corresponding Chirikov parameter in this case is as: $\delta n = 2(Ed/B)^{\frac{1}{2}} \gg 1$.

According to classical-dynamical treating [41], these parameters correspond to chaotic regime. The principle of quantum mechanics enter, of course, into the mixed interpretation in terms of classical trajectories [42]. From one side, the final answers are at least understandable intuitively, from other one they are result of numerical analysis of complex molecular dynamics, which involve a superposition of high-order energy transitions, intensive interaction of non-linear resonances and chaotic motion of a molecule [41,42,44,46]. In fig.1 we list the computed theoretical time dependence of polarization for GeO molecule in an electromagnetic field in a chaotic regime. In order to perform numerical analysis of the systems dynamics we used an advanced generalized techniques such as the wavelet analysis, multi-fractal formalism, mutual information approach, correlation integral analysis, false nearest neighbour algorithm, the Lyapunov exponent's (LE) analysis, and surrogate data method, prediction models etc [4-16]. The further step is an analysis of the corresponding time series (with the time step Dt=4×10^{-14}s). In Table 1 we list the computed values of the correlation dimension d_2, embedding dimension d_N , which are computed on the basis of the of false nearest neighbouring points algorithm with noting (%) of false points for different values of the lag time t. Accordingly in Table 2 we list the computed values of the Kaplan-York attractor dimension (d_L), LE (l_i, i=1-3) and the Kolmogorov entropy (K_{entr}).

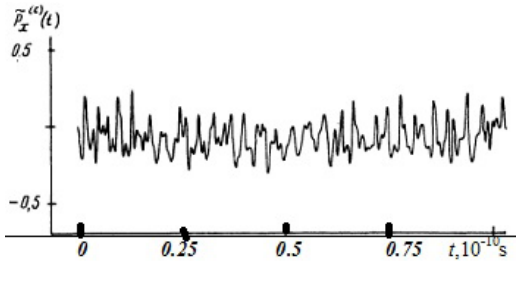

Figure 1. The computed characteristic time dependence of polarization of the GeO molecule in a field in a chaotic regime (see parameters in text).

Table 1.

The correlation dimension d_2, embedding dimension d_N, which are computed on the basis of the of false nearest neighbouring points algorithm with noting (%) of false points for different values of the lag time t

τ	d_2	(d_N)
42	3.04	5 (4.2)
4	2.73	3 (1.1)
6	2.73	3 (1.1)

Table 2.

The Kaplan-York attractor dimension (d_L), LE (l_i, i=1-3) and the Kolmogorov entropy (K_{entr})

λ_1	λ_2	λ_3	d_L	K_{entr}
0.146	0.0179	-0.321	2.51	0.16

Analysis of the received data on the LE, correlation, Kaplan York dimensions, Kolmogorov entropy etc shows that the dynamics of the Geo molecules in an electric field has the elements of a deterministic chaos (low-D strange attractor) and this conclusion is entirely agreed with the results of the classical-dynamical treating [18]. It is important to note that the Kaplan-York dimension is less than the embedding one confirming the correctness of the choice of the latter.

References

1. Staudt A Gutzwiller M.,Chaos in Classical and Quantum Mechanics.-N.-Y.:Springer-Verlag, 1990.-720p.
2. Kleppner D., Chun-Ho I., Welch G.R., Irregular Atomic Systems and Quantum Chaos, Ed. J.C.Gay, N-Y.: Kluwer, 1999.-P.21-48.
3. Glushkov A.V., Fedchuk A.P., Khetselius O.Yu., First predicting the generation of ultra-short VUV and X-ray pulses in sodium cluster system in a strong laser field//Photoelectronics.-2007.-N16.-P.150-155.
4. Gallager R.G., Information theory and reliable communication, Wiley, New York.-1986.

5. Kennel M., Brown R., Abarbanel H., Determining embedding dimension for phase-space reconstruction using geometrical construction//Phys. Rev.A.-1992.-Vol.45.-P.3403–3411.
6. Packard N., Crutchfield J., Farmer J., Shaw R., Geometry from time series// Phys.Rev.Lett-1998.-Vol.45.-P.712–716.
7. Grassberger P., Procaccia I., Measuring the strangeness of strange attractors// Physica D.-1993.-Vol.9.-P.189–208.
8. Fraser A., Swinney H., Independent coordinates for strange attractors from mutual information// Phys Rev A.-1986.-Vol.33.-P.1134–1140.
9. Takens F., Detecting strange attractors in turbulence. In: Dynamical systems and turbulence, ed. Rand D., Young L.-(Springer).-1981.-P.366–381.
10. Glushkov A.V., Khokhlov V.N., Tsenenko I., Atmospheric teleconnection patterns and eddy kinetic energy content: wavelet analysis// Nonlinear Proc.in Geophys.-2004.-Vol.11.-P.285-293.
11. Glushkov A.V. Sensing the stochastic laser pulse structure and chaotic, photon-correlation effects in the non-linear multi-photon atomic dynamics in laser and DC electric field/ Glushkov A.V., Prepelitsa G.P., Svinarenko A.A.// Sensor Electr. and Microsyst. Techn.-2004.-№2.-P.8-14.
12. Prepelitsa G.P., Glushkov A.V., Lepikh Ya.I., Buyadzhi V.V., Ternovsky V.B., Zaichko P.A., Chaotic dynamics of non-linear processes in atomic and molecular systems in electromagnetic field and semiconductor and fiber laser devices: new approaches, uniformity and charm of chaos// Sensor Electronics and Microsyst. Techn.-2014.-Vol.11,N4.-P.43-57.
13. Glushkov A.V., Ivanov L.N., DC Strong-Field Stark-Effect: consistent quantum-mechanical approach // J.Phys.B: At.Mol. Opt.Phys.-1993.-V.26.-P.L379-388.
14. Shevchuk V.G., Prepelitsa G.P., Shumlyansky I.I., Ignatenko V.M., Atom of hydrogen in electric field: Modefied Operator Perturbation theory // Uzhgorod Univ.Scientific Herald.Ser.Phys.-Math.-2001.-Vol.8.-P.331-335.
15. Prepelitsa G.P., Nonlinear dynamics of quantum and laser systems with elements of a chaos// Photoelectronics.-2014.-Vol.23.-P.73-78
16. Glushkov A.V., Prepelitsa G.P., Svinarenko A.A., Zaichko P.A. Studying interaction dynamics of the non-linear vibrational systems within non-linear prediction method (application to quantum autogenerators)// Dynamical Systems. Theory, Eds. J. Awrejcewicz, M. Kazmierczak, P. Olejnik, J, Mrozowski (WSEAS, Lodz).-2013.-Vol.T1.-P.467-477.
17. Zhang C., Katsouleas T., Joshi C., Harmonic frequency generation and chaos in laser driven molecular vibrations/// Proc. of Shortwavelength Physics with Intense Laser Pulses.-San-Diego (USA).-1993.-P.21-28.
18. Berman G. P., Kolovskii A., Quantum chaos in a diatomic molecule interacting with a resonant field//JETP.-1989.-Vol.95.-P.1552-1561.
19. Jaron-Becker A., Becker A., Faisal F.H.M., Ionization of N2, O2 and linear carbon clusters in a strong laser pulse// Phys.Rev.A.-2004.-Vol.69.-P.023410.
20. Simons G., Parr R.G., Finlan J.M., New alternative to the Dunham potential for diatomic molecules//J.Chem. Phys.-1993.-Vol.59.-P.3229-3242.

This article has been received in May 2016.

UDC 539.184, 539.186

A. V. Ignatenko, A. A. Kuznetsova, A. S. Kvasikova, A. V. Glushkov, M. Yu. Gurskaya

NONLINEAR CHAOTIC DYNAMICS OF ATOMIC AND MOLECULAR SYSTEMS IN AN ELECTROMAGNETIC FIELD

Abstract

It has been numerically studied a chaotic dynamics of diatomic molecules (on example of the GeO molecule in an infrared field) and some laser systems. An advanced generalized techniques such as the wavelet analysis, multi-fractal formalism, mutual information approach, correlation integral analysis, false nearest neighbour algorithm, the Lyapunov exponent's (LE) analysis, and surrogate data method, prediction models etc is used. It has been shown that systems exhibit a nonlinear behaviour with elements of a low-or high-dimensional chaos. There are firstly presented the numerical data on topological and dynamical invariants of chaotic systems, in particular, the correlation, embedding, Kaplan-York dimensions, LE, Kolmogorov's entropy etc for GeO molecule in an electromagnetic infrared field in the chaotic regime.

Key words: molecular system, electromagnetic field, chaotic dynamics

УДК 539.184, 539.186

А. В. Игнатенко, А. А. Кузнецова, А. С. Квасикова, А. В. Глушков, М. Ю. Гурская

НЕЛИНЕЙНАЯ ХАОТИЧЕСКАЯ ДИНАМИКА АТОМНЫХ И МОЛЕКУЛЯРНЫХ СИСТЕМ В ЭЛЕКТРОМАГНИТНОМ ПОЛЕ

Резюме

Представлены результаты численного анализа и моделирования хаотической динамики двухатомных молекул (на примере молекулы GeO) во внешнем электромагнитном (инфракрасном) поле. В анализе использованы эффективные версии таких методов анализа как мультифрактальный и вейвлет-анализ, метод корреляционного интеграла, алгоритмы средней взаимной информации, ложных ближайших соседей, суррогатных данных анализ показателей Ляпунова, энтропии Колмогорова,

спектральные методы и т.д. Показано, что двухатомная система в электромагнитном поле демонстрируют нелинейное поведение с элементами динамического хаоса. Представлены численные данные о топологических и динамических инвариантов системы в хаотическом режиме, в частности, корреляционной размерности, размерностей вложения, Каплана-Йорка, показателей Ляпунова, энтропии Колмогорова энтропия и т.д. для молекулы GeO в электромагнитном инфракрасном поле в хаотическом режиме.

Ключевые слова: молекулярная система, электромагнитное поле, хаотическая динамика,

УДК 539.184, 539.186

Г. В. Ігнатенко, А. О. Кузнецова, А. С. Квасикова, О. В. Глушков, М. Ю. Гурська

НЕЛІНІЙНИХ ХАОТИЧНА ДИНАМІКА АТОМНИХ ТА МОЛЕКУЛЯРНИХ СИСТЕМ В ЕЛЕКТРОМАГНІТНОМУ ПОЛІ

Резюме

Представлені результати чисельного аналізу і моделювання хаотичної динаміки двоатомних молекул (на прикладі молекули GeO) в зовнішньому електромагнітному (інфрачервоному) поле. В аналізі використані ефективні версії таких методів аналізу як мультіфрактальний і вейвлет-аналіз, метод кореляційного інтеграла, алгоритми середньої взаємної інформації, помилкових найближчих сусідів, сурогатних даних аналіз показників Ляпунова, ентропії Колмогорова, спектральні методи і т.і. Показано, що двоатомна система в електромагнітному полі демонструє нелінійне поведінку з елементами динамічного хаосу. Представлені чисельні дані по топологічним і динамічним інваріантам системи в хаотичному режимі, зокрема, кореляційної розмірності, розмірності вкладення, Каплана-Йорка, показників Ляпунова, ентропії Колмогорова тощо для молекули GeO в електромагнітному інфрачервоному поле в хаотичному режимі.

Ключові слова: молекулярна система, електромагнітне поле, хаотична динаміка

UDC 541.13

G. P. Prepelitsa, S. V. Brusentseva, A. V. Duborez, O. Yu. Khetselius, P. G. Bashkaryov

Odessa State Environmental University, 15, Lvovskaya str., Odessa, Ukraine
Odessa National Polytechnical University, 1, Shevchenko av., Odessa, Ukraine
e-mail: quantpre@mail.ru

NEW NONLINEAR ANALYSIS, CHAOS THEORY AND INFORMATION TECHNOLOGY APPROACH TO STUDYING DYNAMICS OF CHAIN OF QUANTUM AUTOGENERATORS

A chaos-geometric approach [7-11] that consistently includes a number of new or improved known methods of analysis (the correlation integral, the fractal analysis, algorithms of the average mutual information, and false nearest neighbors, the Lyapunov exponents analysis, the Kolmogorov entropy, the method of surrogate data, a set of the spectral methods, a neural network algorithms, etc. .) is used to solve the problem of quantitative modeling and analysis of chaotic dynamics of a chain of two quantum autogenerators. There are theoretically studied a chaos scenario generation and obtained quantitative data on the dynamic and topological invariants of the system in the chaotic regime.

1 Introduction

In many papers (see, for example, [1-18]) it has been noted that a chaos is alternative of randomness and occurs as in very simple deterministic systems as quite complex ones. Although chaos theory places fundamental limitations for long-rage prediction (see e.g. [1-9]), it can be used for short-range prediction since ex facte random data can contain simple deterministic relationships with only a few degrees of freedom. Chaos theory establishes that apparently complex irregular behaviour could be the outcome of a simple deterministic system with a few dominant nonlinear interdependent variables. The past decade has witnessed a large number of studies employing the ideas gained from the science of chaos to characterize, model, and predict the dynamics of various systems phenomena (see e.g. [1-13]). The outcomes of such studies are very encouraging, as they not only revealed that the dynamics of the apparently irregular phenomena could be understood from a chaotic deterministic point of view but also reported very good predictions using such an approach for different systems.

In a modern quantum electronics and laser physics etc there are many systems and devices (such as multi-element semiconductors and gas lasers etc), dynamics of which can exhibit chaotic behaviour. These systems can be considered in the first approximation as a grid of autogenerators (quantum generators), coupled by different way [2,14,15].

In this paper a chaos-geometric approach [7-11] that consistently includes a number of new or improved known methods of analysis (the correlation integral, the fractal analysis, algorithms of the average mutual information, and false nearest neighbors, the Lyapunov exponents analysis, the Kolmogorov entropy, the method of surrogate data, a set of the spectral methods, a neural network algorithms, etc.; see details in Refs. [1-34]) is used to solve the problem of quantitative modeling and analysis of chaotic dynamics of a chain of two quantum autogenerators. There are theoretically studied a chaos scenario generation and obtained quantitative data on the dynamic and topological invariants of the system in the chaotic regime

2. Methods of studying dynamics of the laser systems

As used non-linear analysis, chaos theory and information technology methods to studying non-linear dynamics of the laser systems have been earlier in details presented [1-20] here we are limited only by the key ideas. As usually, we formally consider scalar measurements $s(n) = s(t_0 + n\mathrm{D}t) = s(n)$, where t_0 is the start

time, Dt is the time step, and is n the number of the measurements. Packard et al. [18] introduced the method of using time-delay coordinates to reconstruct the phase space of an observed dynamical system. The direct use of the lagged variables $s(n + t)$, where t is some integer to be determined, results in a coordinate system in which the structure of orbits in phase space can be captured. First approach to compute t is based on the linear autocorrelation function. The second method is an approach with a nonlinear concept of independence, e.g. the average mutual information. Briefly, the concept of mutual information can be described as follows [5,7,13]. One could remind that the autocorrelation function and average mutual information can be considered as analogues of the linear redundancy and general redundancy, respectively, which was applied in the test for nonlinearity. If a time series under consideration have an n-dimensional Gaussian distribution, these statistics are theoretically equivalent as it is shown in Ref. [22].

The goal of the embedding dimension determination is to reconstruct a Euclidean space R^d large enough so that the set of points d_A can be unfolded without ambiguity. There are several standard approaches to reconstruct the attractor dimension (see, e.g., [1,7,23]), but let us consider in this study two methods only. The correlation integral analysis is one of the widely used techniques to investigate the signatures of chaos in a time series. The analysis uses the correlation integral, $C(r)$, to distinguish between chaotic and stochastic systems. To compute the correlation integral, the algorithm of Grassberger and Procaccia [23] is the most commonly used approach. According to this algorithm, the correlation integral is

$$C(r) = \lim_{N\to\infty} \frac{2}{N(n-1)} \sum_{\substack{i,j \\ (1\le i<j\le N)}} H\left(r - |\, \mathbf{y}_i - \mathbf{y}_j \,|\right) \tag{1}$$

where H is the Heaviside step function with $H(u) = 1$ for $u > 0$ and $H(u) = 0$ for $u \le 0$, r is the radius of sphere centered on $\mathbf{y}_i$ or $\mathbf{y}_j$, and N is the number of data measurements. If the time series is characterized by an attractor, then the integral $C(r)$ is related to the radius r given by

$$d = \lim_{\substack{r\to 0 \\ N\to\infty}} \frac{\log C(r)}{\log r}, \tag{2}$$

where d is correlation exponent that can be determined as the slop of line in the coordinates log $C(r)$ versus log r by a least-squares fit of a straight line over a certain range of r, called the scaling region.

There are certain important limitations in the use of the correlation integral analysis in the search for chaos. To verify the results obtained by the correlation integral analysis, we use surrogate data method. The method of surrogate data [1,7,19] is an approach that makes use of the substitute data generated in accordance to the probabilistic structure underlying the original data. Advanced version is presented in [7-9].

The next step is computing the Lyapunov's exponents (LE). The LE are the dynamical invariants of the nonlinear system. A negative exponent indicates a local average rate of contraction while a positive value indicates a local average rate of expansion. In the chaos theory, the spectrum of LE is considered a measure of the effect of perturbing the initial conditions of a dynamical system. Note that both positive and negative LE can coexist in a dissipative system, which is then chaotic. Since the LE are defined as asymptotic average rates, they are independent of the initial conditions, and therefore they do comprise an invariant measure of attractor. In fact, if one manages to derive the whole spectrum of the LE, other invariants of the system, i.e. Kolmogorov entropy and attractor's dimension can be found. The Kolmogorov entropy, K, measures the average rate at which information about the state is lost with time. An estimate of this measure is the sum of the positive LE. The inverse of the Kolmogorov entropy is equal to an average predictability.

Estimate of dimension of the attractor is provided by the Kaplan and Yorke conjecture. There are a few approaches to computing the LE. One of them computes the whole spectrum and is based on the Jacobi matrix of system [27]. In the case where only observations are given and the system function is unknown, the matrix has to be estimated from the data. In this case, all the suggested methods approximate the matrix by fitting a local map to a sufficient number of nearby points.

In our work we use the method with the linear fitted map proposed by Sano and Sawada [27] added by the neural networks algorithm [7-10].

3. Chaotic elements in dynamics of the grid of two autogenerators and conclusions

Here we present results of non-linear analysis of the chaotic oscillations in a grid of two autogenerators. Dynamics of this systems has intensively studied from the viewpoint of the corresponding differential equations solutions (e.g. [2,14,15]). In Refs.[2,14,15] the time series for the characteristic vibration amplitude are presented in a case of two semiconductors lasers connected through general resonator. We have studied the time series in a regime of the hyper chaos (input data contain 4096 points). Firstly we have computed the variations of the autocorrelation coefficient for the amplitude level. Autocorrelation function exhibits some kind of exponential decay up to a lag time of about 100 time units. Such an exponential decay can be an indication of the presence of chaotic dynamics in the process of the level variations. On the other hand, the autocorrelation coefficient failed to achieve zero, i.e. the autocorrelation function analysis not provides us with any value of t. Such an analysis can be certainly extended to values exceeding 1000, but it is known that an attractor cannot be adequately reconstructed for very large values of t. The correlation dimension is computed on the basis of the correlation integral scheme.

To verify the results obtained by the correlation integral analysis, we use surrogate data method. The method of surrogate data is an approach that makes use of the substitute data generated in accordance to the probabilistic structure underlying the original data. This means that the surrogate data possess some of the properties, such as the mean, the standard deviation, the cumulative distribution function, the power spectrum, etc., but are otherwise postulated as random, generated according to a specific null hypothesis. We have evaluated the percentage of false nearest neighbours that was determined for the amplitude level series, for phase-spaces reconstructed with embedding dimensions from 1 to 20. In Table 1 we list the computed values of the correlation dimension d_2, embedding dimension d_N, which are computed on the basis of the false nearest neighbouring points algorithm with noting (%) of false points for different values of the lag time t. Accordingly in Table 2 we list the computed values of the Kaplan-York attractor dimension (d_L), LE (l_i, i=1-3) and the Kolmogorov entropy (K_{entr}).

Table 1

The correlation dimension d_2 , embedding dimension d_N , which are computed on the basis of the false nearest neighbouring points algorithm with noting (%) of false points for different values of the lag time t

τ	d_2	(d_N)
64	7.9	10 (12)
10	7.1	8 (1.2)
12	7.1	8 (1.2)

Table 2

The Kaplan-York attractor dimension (d_L), LE (l_i, i=1-3) and the Kolmogorov entropy (K_{entr}) for the system of two semiconductors lasers connected through general resonator (the hyperchaos regime)

λ_1	λ_2	λ_3	d_L	K_{entr}
0.515	0.198	-0.146	6.9	0.745

References

1. H.Abarbanel, R.Brown, J.Sidorowich and L.Tsimring, Rev.Mod.Phys. (1999) 5, 1331.
2. A.Vedenov, A.Ezhov and E. Levchenko, in Non-linear waves. Structure and bifurcations, ed. by A. Gaponov-Grekhov and M. Rabinovich, (Nauka, Moscow, 1997), pp.53-69.
3. M. Gutzwiller, Chaos in Classical and Quantum Mechanics (N.-Y., Springer, 1999), 720 p.
4. E. Ott, Chaos in dynamical systems, (Cambridge: Cambridge Univ.Press, 2002), 490p.
5. R. Gallager, Information theory and reliable communication (N.-Y.,Wiley, 1996).
6. D. Ullmo, Rep. Prog. Phys. 71, 026001 (2008).

7. A.V. Glushkov, Modern theory of a chaos, (Odessa, Astroprint, 2008), 450p.
8. G.P. Prepelitsa, Nonlinear dynamics of quantum and laser systems with elements of a chaos// Photoelectronics.-2014.-Vol.23.-P.96-106.
9. A. Glushkov, O. Khetselius, S. Brusentseva, P. Zaichko and V. Ternovsky, in Adv. in Neural Networks, Fuzzy Systems and Artificial Intelligence, Series: Recent Adv. in Computer Engineering, vol. 21, ed. by J.Balicki (WSEAS, Gdansk, 2014), pp.69-75.
10. A. Glushkov, A. Svinarenko, V. Buyadzhi, P. Zaichko and V. Ternovsky, in: Adv.in Neural Networks, Fuzzy Systems and Artificial Intelligence, Series: Recent Adv. in Computer Engineering, vol.21, ed. by J.Balicki (WSEAS, Gdansk, 2014), pp.143-150.
11. A.V. Glushkov, O.Yu. Khetselius, A.A. Svinarenko, G.P. Prepelitsa, Energy approach to atoms in a Laser Field and Quantum Dynamics with Laser Pulses of Different Shape, In: Coherence and Ultrashort Pulsed Emission, ed. by F.J. Duarte (Intech, Vienna, 2011), 101-130.
12. G.P.Prepelitsa, Chaotic dynamics of the semiconductor GaAs / GaAlAs laser within nonlinear chaos-geometric information analysis// Sensor Electr. and Microsyst. Techn.-2015.-Vol.13,N1.-P.24-32A.V.
13. Prepelitsa G.P., New nonlinear analysis, chaos theory and information technology approach to studying dynamics of the the erbium one-ring fibre laser// Photoelectronics ("Copernicus").-2015.-Vol.24.-P.38-43.
14. Prepelitsa G.P., Modeling of interaction of the non-linear vibrational systems on the basis of temporal series analyses (application to semiconductor quantum generators)/ Prepelitsa G.P., Glushkov A.V., Khetselius O.Yu., Kuzakon V.M., Solyanikova E.P., Svinarenko A.A.// Dynamical Systems - Theory and Applications.-2011.-Vol.2.-P.31-38.-BIF110 (8p.)
15. A.V.Glushkov, G. Prepelitsa, A. Svinarenko and P. Zaichko, in: Dynamical Systems Theory, vol.T1, ed by J. Awrejcewicz, M. Kazmierczak, P. Olejnik, and J. Mrozowski (Lodz, Polland, 2013), pp.P.467-487.
16. A. Glushkov, Y. Bunyakova, A. Fedchuk, N. Serbov, A. Svinarenko and I. Tsenenko, Sensor Electr. and Microsyst. Techn. 3(1), 14 (2007).
17. A.V. Glushkov, V. Kuzakon, V. Ternovsky and V. Buyadzhi, in: Dynamical Systems Theory, vol.T1, ed by J. Awrejcewicz, M. Kazmierczak, P. Olejnik, and J. Mrozowski (Lodz, Polland, 2013), P.461-466.
18. A.V.Glushkov, O.Yu.Khetselius, S.V. Brusentseva, P.Zaichko, V.B. Ternovsky, In: Advances in Neural Networks, Fuzzy Systems and Artificial Intelligence, Series: Recent Advances in Computer Engineering, Ed. J.Balicki.(Gdansk, World Sci.Pub.).-2014.-Vol.21.-P.69-75.
19. E. N. Lorenz, Journ. Atm. Sci. 20, 130 (1963).
20. N. Packard, J. Crutchfield, J. Farmer and R. Shaw, Phys.Rev.Lett. 45, 712 (1988).
21. M. Kennel, R. Brown and H. Abarbanel, Phys.Rev.A. 45, 3403 (1992).
22. F. Takens in: Dynamical systems and turbulence, ed by D. Rand and L. Young (Springer, Berlin, 1981), pp.366–381
23. R. Mañé, in: Dynamical systems and turbulence, ed by D. Rand and L. Young (Springer, Berlin, 1981), pp.230–242.
24. M. Paluš, E.Pelikán, K. Eben, P. Krejčíř and P. Juruš, in: Artificial Neural Nets and Genetic Algorithms, ed. V. Kurkova (Springer, Wien, 2001), pp. 473-476.
25. P. Grassberger and I. Procaccia, Physica D. 9, 189 (1993).
26. J. Theiler, S. Eubank, A. Longtin, B. Galdrikian, J. Farmer, Phys.D. 58, 77 (1992).
27. A. Fraser and H. Swinney, Phys Rev A. 33, 1134 (1996).
28. J. Havstad and C. Ehlers, Phys.Rev.A. 39, 845 (1999).
29. M. Sano and Y. Sawada, Phys Rev.Lett., 55, 1082 (1995).
30. T. Schreiber, Phys.Rep. 308, 1 (1999).

31. H. Schuste, Deterministic Chaos: An Introduction (Wiley, N.-Y., 2005), 312 p.
32. A. Glushkov, G. Prepelitsa, S. Dan'kov, V. Polischuk and A. Efimov, Journ. Tech. Phys. 38, 219 (1997).
33. A.G. Vladimirov and E.E. Fradkin, Optics and Spectr. 67, 219 (1999).
34. S.P. Kuznetsov and D.I. Trubetskov, Izv. Vuzov. Ser. Radiophys. 48, 1 (2004).
35. C. Feng, F. Yu-Ling, Y. Zhi-Hai, F.Jian, S.Yuan-Chao, Z. Yu-Zhu Chin. Phys. B. 21, 100504 (2013).

This article has been received in May 2016.

UDC 541.13

G. P. Prepelitsa, S. V. Brusentseva, A. V. Duborez, O. Yu. Khetselius, P. G.Bashkaryov

NEW NONLINEAR ANALYSIS, CHAOS THEORY AND INFORMATION TECHNOLOGY APPROACH TO STUDYING DYNAMICS OF CHAIN OF QUANTUM AUTOGENERATORS

Abstract

Chaos-geometric approach that consistently includes a number of new or improved known methods of analysis (the correlation integral, the fractal analysis, algorithms of the average mutual information, and false nearest neighbors, the Lyapunov exponents analysis, the Kolmogorov entropy, the method of surrogate data, a set of the spectral methods, a neural network algorithms, etc. .) is used to solve the problem of quantitative modeling and analysis of chaotic dynamics of a chain of two quantum autogenerators. There are theoretically studied a chaos scenario generation and obtained quantitative data on the dynamic and topological invariants of the system in the chaotic regime.

Keywords: chain of quantum autogenerators, dynamics, chaos, nonlinear analysis

УДК 541.13

Г. П. Препелиця, С. В. Брусенцева, А. В. Дуборез, О. Ю. Хецелиус, П. Г. Башкарьов

НОВЫЙ ПОДХОД НА ОСНОВЕ НЕЛИНЕЙНОГО АНАЛИЗА, ТЕОРИИ ХАОСА И ИНФОРМАЦИОННЫХ ТЕХНОЛОГИЙ К ИЗУЧЕНИЮ ДИНАМИКИ КВАНТОВЫХ ГЕНЕРАТОРОВ И ЛАЗЕРНЫХ СИСТЕМ

Резюме

Хаос-геометрический подход, который единообразно включает ряд новых или усовершенствованных известных методов анализа (корреляционный интеграл, фрактальный анализ, алгоритмы средней взаимной информации, ложных ближайших соседей, показатели Ляпунова, энтропия Колмогорова, метод суррогатных данных, спектральные методы, нейросетевые алгоритмы и т.д.) использован для решения задачи количественного моделирования и анализа хаотической динамики цепочки двух квантовых автогенераторов. Теоретически изучен сценарий генерации хаоса и получены количественные данные по динамическим и топологическим инвариантам системы в хаотическом режиме.

Ключевые слова: цепочка квантовых автогенераторов, динамика, хаос, нелинейный анализ

УДК 541.13

Г. П. Препелиця, С. В. Брусенцева, А. В. Дуборез, О. Ю. Хецелиус, П. Г. Башкарьов

НОВИЙ ПІДХІД НА ОСНОВІ НЕЛІНІЙНОГО АНАЛІЗУ, ТЕОРІЇ ХАОСУ ТА ІНФОРМАЦІЙНИХ ТЕХНОЛОГІЙ ДО ВИВЧЕННЯ ДИНАМІКИ ЛАНЦЮЖКА КВАНТОВИХ АВТОГЕНЕРАТОРІВ

Резюме

Хаос-геометричний підхід, що одноманітно включає низку нових або удосконалених відомих методів аналізу (кореляційний інтеграл, фрактальний аналіз, алгоритми середньої взаємної інформації, хибних найближчих сусідів, показники Ляпунова, ентропія Колмогорова, сурогатних даних, нелінійний прогноз, спектральні методи, нейромережеві алгоритми тощо) використаний для вирішення задач кількісно моделювання та аналізу хаотичної динаміки ланцюжка квантових автогенераторів. Теоретично вивчений сценарій генерації хаосу, отримані кількісні дані по динамічним та топологічним інваріантам системи у хаотичному режимі.

Ключові слова: ланцюжок квантових автогенераторів, динаміка, хаос, нелінійний аналіз

UDC 539.182

P. A. Zaichko

Odessa National Maritime Academy, Odessa, 4, Didrikhsona str., Odessa, Ukraine
e-mail: pgbash@mail.ru

RELATIVISTIC THEORY OF EXCITATION AND IONIZATION OF HEAVY ALKALI RYDBERG ATOMS IN A BLACK-BODY RADIATION FIELD: NEW DATA

The combined relativistic energy approach and relativistic many-body perturbation theory with the zeroth Dirac-Fock potential approximation are used for computing the thermal Blackbody radiation ionization characteristics of the alkali Rydberg atoms, in particular, the rubidium and caesium in Rydberg states with principal quantum number n=20-100. Preliminary application of theory to computing ionization rate for the Rydberg sodium atom in the have demonstrated physically reasonable agreement between the theoretical and experimental data. The accuracy of the theoretical data is provided by a correctness of the corresponding relativistic wave functions and accounting for the exchange-correlation effects.

In Refs. [1,2] it has been proposed a combined relativistic energy approach and relativistic many-body perturbation theory with the zeroth model potential approximation for determination the thermal Blackbody radiation ionization characteristics of the Rydberg atoms. As example, there have been computed the ionization parameters of the sodium in Rydberg states with n=17,18,40-70.

A great progress in experimental laser physics and appearance of the so called tunable lasers allow to get the highly excited Rydberg states of atoms. In fact this is a beginning of a new epoch in the atomic physics with external electromagnetic field. It has stimulated a great number of papers on the ad and dc Stark effect [1-12].

From the other side, the experiments with Rydberg atoms had very soon resulted in the discovery of an important ionization mechanism, provided by unique features of the Rydberg atoms. Relatively new topic of the modern theory is connected with consistent treating the Rydberg atoms in a field of the Blackbody radiation (BBR). It should be noted that the BBR is one of the essential factors affecting the Rydberg states in atoms [1].

The account for the ac Stark shift, fast redistribution of the levels' population and photoionization provided by the environmental BBR became of a great importance for successfully handling atoms in their Rydberg states.

The most popular theoretical approaches to computing ionization parameters of the Rydberg atom in the BBR are based on the different versions of the model potential (MP) method, quasiclassical models. It should be mentioned a simple approximation for the rate of thermal ionization of Rydberg atoms, based on the results of our systematic calculations in the Simons-Fues MP [1]. In fact, using the MP approach is very close to the quantum defect method and other semi-empirical methods, which were also widely used in the past few years for calculating atom–field interaction amplitudes in the lowest orders of the perturbation theory. The significant advantage of the Simons-Fues MP method in comparison with other models is the possibility of presenting analytically (in terms of the hypergeometric functions) the quantitative characteristics for arbitrarily high orders, related to both bound–bound and bound–free transitions. Naturally, the standard methods of the theoretical atomic physics, including the Hartree-Fock and Dirac-Fock approximations should be used in order to determine the thermal ionization characteristics of neutral and Rydberg atoms [2]. One could note that the correct treating of the heavy Rydberg atoms parameters in an external electromagnetic field, including the BBR field, requires using strictly relativistic models. In a case of multielectron atomic systems it is neces-

sary to account for thee exchange-correlation corrections.

Here we apply an energy approach [11-16] and relativistic perturbation theory (PT) with the Dirac-Fock zeroth approximation [16-20] to computing the thermal BBR ionization characteristics of the heavy alkali Rydberg atoms, in particular, the rubidium, caesium. It is self-understood that the other alkali elements are also of a great actuality and importance.

Qualitative picture of the BBR Rydberg atoms ionization is in principle easily understandable. Even for temperatures of order $T=10^4$ K, the frequency of a greater part of the BBR photons ω does not exceed 0.1 a.u. One could use a single- electron approximation for calculating the ionization cross section $\sigma_{nl}(\omega)$. The latter appears in a product with the Planck's distribution for the thermal photon number density:

$$\rho(w,T)=\frac{\omega^2}{\pi^2 c^3[\exp(\omega/kT)-1]}, \qquad (1)$$

where k=3.1668×10^{-6} a.u., K^{-1} is the Boltzmann constant, c = 137.036 a.u. is the speed of light.

Ionization rate of a bound state *nl* results in the integral over the Blackbody radiation frequencies:

$$P_{nl}(T)=c\int_{|E_{nl}|}^{\infty}\sigma_{nl}(\omega)\rho(\omega,T)d\omega. \qquad (2)$$

The ionization cross-section from a bound state with a principal quantum number n and orbital quantum number l by photons with frequency ω is as follows:

$$\sigma_{nl}(\omega)=\frac{4\pi^2\omega}{3c(2l+1)}[M^2_{nl\to E,l-1}+ \\ +(l+1)M^2_{nl\to E,l+1}], \qquad (3)$$

where the radial matrix element of the ionization transition from the bound state with the radial wave function $R_{nl}(r)$ to continuum state with the wave function $R_{El}(r)$ normalized to the delta function of energy. The corresponding radial matrix element looks as:

$$M_{nl\to E,l'}=\int_0^{\infty}R_{E,l'}(r)r^3R_{nl}(r)dr. \qquad (4)$$

We apply a generalized energy approach [11-15] and relativistic perturbation theory with the MP zeroth approximation [16-20] to computing the Rydberg atoms ionization parameters. In relativistic theory radiation decay probability (ionization cross-section etc) is connected with the imaginary part of electron energy shift. The total energy shift of the state is usually presented in the form: DE = ReDE + i G/2, where G is interpreted as the level width, and a decay probability P = G. The imaginary part of electron energy shift is defined in the PT lowest order as:

$$\mathrm{Im}\,\Delta E(B)=-\frac{e^2}{4\pi}\sum_{\substack{\alpha>n>f\\[\alpha<n\le f]}}V^{|\omega_{\alpha n}|}_{\alpha n\alpha n}, \qquad (6)$$

where (a>n>f) for electron and (a<n<f) for vacancy. The matrix element is determined as follows:

$$V^{|\omega|}_{ijkl}=\int dr_1dr_2\varphi^*_i(r_1)\varphi^*_j(r_2)\frac{\sin|\omega|r_{12}}{r_{12}}(1-\alpha_1\alpha_2)\varphi^*_k(r_2)\varphi^*_l(r_1)$$

$$V^{|\omega|}_{ijkl}=\int dr_1dr_2\varphi^*_i(r_1)\varphi^*_j(r_2)\frac{\sin|\omega|r_{12}}{r_{12}}(1-\alpha_1\alpha_2)\varphi^*_k(r_2)\varphi^*_l(r_1) \qquad (7)$$

Their detailed description of the matrix elements and procedure for their computing is presented in Refs. [12,13,15]. The relativistic wave functions are calculated by solution of the Dirac equation with the potential, which includes the Dirac-Fock consistent field potential and additionally polarization potential [20]. All calculations are performed on the basis of the numeral code Superatom-ISAN (version 93).

In Ref.[1] there were presented the results of computing the ionization rate calculation for the Rydberg sodium atom in the states (17,18D, 18P) at temperatures of 300 K and 500 K and obtained physically reasonable agreement between the theoretical and experimental (by Kleppner etal and Burkhardt etal [4,5]) data. Besides, there are listed new results for for the Rydberg sodium atom ionization rate (s^{-1}) with n=20-70 induced by BBR radiation (T = 300 K) . Here (Table 1)

we present new data on the ionization rate (s^{-1}) for different alkali atoms Rydberg states (with n=20-70) induced by BBR radiation (T = 300 K) .

Table 1.

Ionization rate (s^{-1}) for the heavy alkali atoms in the Rydberg states (with n = 20-100), induced by BBR radiation (T = 300 K; our data).

Atom	20	30	40
K S	80.5	103	84.5
K P	201	210	159
K D	736	584	391
Rb S	118	170	130
Rb P	159	172	125
Rb D	718	621	432
Cs S	108	181	150
Cs P	471	597	451
Cs D	465	495	368
Atom	50	70	100
K S	66.4	37	17
K P	113	61	27
K D	264	128	57
Rb S	105	60	28
Rb P	89	45	18
Rb D	298	151	68
Cs S	114	66	29
Cs P	329	1671	78
Cs D	261	140	67

Obviously, the accuracy of the theoretical data is provided by a correctness of the corresponding relativistic wave functions and accounting for the exchange-correlation effects.

References

1. Svinarenko A.A., Khetselius O.Yu., Buyadzhi V.V., Florko T.A., Zaichko P.A., Ponomarenko E.L., Spectroscopy of Rydberg atoms in a Black-body radiation field: Relativistic theory of excitation and ionization// Journal of Physics: C Series (IOP, London, UK).-2014.-Vol.548.-P. 012048 (6p.).
2. Svinarenko A.A., Khetselius O.Yu., Buyadzhi V.V., Kvasikova A.S., Zaichko P.A., Spectroscopy of Rydberg atoms in a Black-body radiation field: Relativistic theory of excitation and ionization// Photoelectronics.-2014.-Vol.23.-P.147-151.Beterov I.I., Ionization of Rydberg atoms by blackbody radiation/ Beterov I.I., TretyakovD.V., Ryabtsev I.I., Entin V.M., Ekers A., Bezuglov N.N.//New J. Phys.-2009.-Vol.11.-P.013052.
3. Burkhardt C.E., Ionization of Rydberg atoms/ Burkhardt C.E., Corey R.L., Garver W.P., Leventhal J.J., Allergini M., Moi L. //Phys. Rev. A.-1996.-Vol.34.-P.80–86.
4. Spencer W.P., Photoionization by blackbody radiation / Spencer W.P., Vaidyanathan A., Kleppner D., Ducas T.//Phys. Rev.A.-1992.-Vol.26.-P.1490–1493
5. Safronova U.I., Third-order relativistic many-body calculations of energies, transition rates, hyperfine constants, and blackbody radiation shift in $^{171}Yb^{+}$/ Safronova U.I., Safronova M.S. //Phys. Rev. A.-2009.-Vol.79.-P.022512.
6. Gallagher T.F., Interactions of Blackbody Radiation with Atoms/ Gallagher T.F., Cooke W.E.//Phys. Rev. Lett.-1999.-Vol.42.-P.835–839.
7. Lehman G. W., Rate of ionization of H and Na Rydberg atoms by black-body radiation /Lehman G. W.// J. Phys. B: At. Mol. Phys.-1993.-Vol.16.-P.2145-2156.
8. Glukhov I., Thermal photoionization of Rydberg states in He and alkali-metal atoms/Glukhov I.,Ovsiannikov V.//J. Phys.B:At.Mol.Phys.-2009.-Vol.42.-P.075001
9. D'yachkov L.G., Pankratov P.M., On the use of the semiclassical approximation for the calculation of oscillator strengths and photoionization cross

sections/ D'yachkov L.G., Pankratov P.M.//J. Phys. B: At. Mol. Opt. Phys.-1994.-Vol. 27.-P.461-468
10. Killian T.C., Creation of an ultracold neutral plasma/Killian T.C., Kulin S., Bergeson S.D., Orozco L.A., Orzel C., Rolston S.L.//Phys. Rev. Lett.-1999.-Vol. 83.-P.4776–4779
11. Li W., Evolution dynamics of a dense frozen Rydberg gas to plasma/ Li W., Noel M.W., Robinson M.P., Tanner P.J., Gallagher T.F.//Phys. Rev. A.-2004.-Vol.70.-P.042713 (10pp.).
12. Ivanov L.N., Energy approach to consistent QED theory for calculation of electron-collision strengths/ Ivanov L.N., Ivanova E.P., Knight L.//Phys. Rev.A.-1993.-Vol. 48.-P.4365-4374.
13. Ivanov L.N., Autoionization states of multielectron atoms/ Ivanov L.N., Letokhov V.S.//Com. Of Modern Phys. D. Atom. and Mol.Phys.-1995.-Vol.4.-P.169-184.
14. Ivanova E.P. Modern Trends in Spectroscopy of multi-charged Ions/ Ivanova E.P., Ivanov L.N., Aglitsky E.V. // Physics Rep.-1988.-Vol.166,N6.-P.315-390.
15. Glushkov A.V., Radiation Decay of Atomic States: atomic residue and gauge non-invariant contributions/ Glushkov A.V., Ivanov L.N.//Phys. Lett.A.-1992.-Vol.170.-P.33-38
16. Glushkov A.V.,Ternovsky V.B., Buyadzhi V.V., Zaichko P.A., Nikola L.V., Advanced relativistic energy approach to radiation decay processes in atomic systems//Photoelectronics.-2015.-Vol.24.-P.11-22.
17. Glushkov A.V., Malinovskaya S.V., Khetselius O.Yu., Svinarenko A.A., Mischenko E.V., Florko T.A., Optimized perturbation theory scheme for calculating the interatomic potentials and hyperfine lines shift for heavy atoms in the buffer inert gas//Int. J. Quant. Chem.-2009.-Vol.109,N14.-P.3325-3329
18. Glushkov A.V. // J. of Phys.: Conf. Ser. – 2012. – Vol. 397. – P. 012011 (6p.).
19. Glushkov A.V., Khetselius O.Yu., Loboda A.V., Svinarenko A.A. Frontiers in Quantum Systems in Chem. and Phys. // Ser. Progress in Theoretical Chemistry and Physics, (Berlin: Springer) ed. S. Wilson, P.J. Grout, J. Maruani, G. Delgado-Barrio, P. Piecuch. – 2008. Vol. 18. – P. 543
20. Glushkov A.V., Svinarenko A.A., Ternovsky V.V., Smirnov A.V. , Zaichko P.A., Spectroscopy of the complex autoionization resonances in spectrum of helium: Test and new spectral data//Photoelectronics ("Copernicus").-2015.-Vol.24.-P.94-102.

This article has been received in May 2016.

UDC 539.182

P. A. Zaichko

RELATIVISTIC THEORY OF EXCITATION AND IONIZATION OF HEAVY ALKALI RYDBERG ATOMS IN A BLACK-BODY RADIATION FIELD: NEW DATA

Abstract

The combined relativistic energy approach and relativistic many-body perturbation theory with the zeroth Dirac-Fock potential approximation are used for computing the thermal Blackbody radiation ionization characteristics of the alkali Rydberg atoms, in particular, the rubidium and caesium in Rydberg states with principal quantum number n=20-100. Preliminary application of theory to computing ionization rate for the Rydberg sodium atom in the have demonstrated physically reasonable agreement between the theoretical and experimental data. The accuracy of the theoretical data is provided by a correctness of the corresponding relativistic wave functions and accounting for the exchange-correlation effects.

Key words: Rydberg alkali atoms, relativistic theory, radiation field.

УДК 539.182

П. А. Заичко

РЕЛЯТИВИСТСКАЯ ТЕОРИЯ ВОЗБУЖДЕНИЯ И ИОНИЗАЦИИ ТЯЖЕЛЫХ ЩЕЛОЧНЫХ РИДБЕРГОВСКИХ АТОМОВ В ПОЛЕ ИЗЛУЧЕНИЯ ЧЕРНОГО ТЕЛА: НОВЫЕ ДАННЫЕ

Резюме

Комбинированный релятивистский энергитический подход и релятивистская теория возмущений многих тел с оптимизированныи дирак-фоковским нулевым приближением используются для вычисления ионизационных характеристик щелочных ридберговских атомов в поле теплового излучения черного тела, в частности, атомов рубидия и цезия в ридберговских состояниях с главным квантовым числом n=20-100. Предварительное применение теории к вычислению скорости ионизации атома натрия ридберговских состояниях продемонстрировало физически разумное согласие между теоретическими и экспериментальными данными. Точность теоретических данных обеспечивается корректностью вычисления соответствующих релятивистских волновых функций и полнотой учета обменно-корреляционных эффектов.

Ключевые слова: ридберговские щелочные атомы, релятивистская теория, тепловое излучение.

УДК 539.182

П. О. Заічко

РЕЛЯТИВІСТСЬКА ТЕОРІЯ ЗБУРЕННЯ ТА ІОНІЗАЦІЇ ВАЖКИХ ЛУЖНИХ РІДБЕРГІВСЬКИХ АТОМІВ У ПОЛІ ВИПРОМІНЮВАННЯ ЧОРНОГО ТІЛА: НОВІ ДАНІ

Резюме

Комбінований релятивістський енергетичний підхід і релятивістська теорія збурень багатьох тіл з з оптимізованим дірак-фоківським нульовим наближенням використовуються для обчислення іонізаційних характеристик лужних рідбергівських атомів в полі теплового випромінювання абсолютно чорного тіла, зокрема, атомів рубідію і цезію в рідбергівських станах з головним квантовим числом n = 20-100. Попереднє застосування теорії до обчислення швидкості іонізації атома натрію ридберговских станах продемонструвало фізично розумну згоду між теоретичними і експериментальними даними. Точність теоретичних даних забезпечується коректністю обчислення відповідних релятивістських хвильових функцій і повнотою урахування обмінно-кореляційних ефектів.

Ключові слова: рідбергівські лужні атоми, релятивістська теорія, теплове випромінювання.

UDC 530.182:510.42

Yu. Ya. Bunyakova, T. A. Florko, A. V. Glushkov, V. F. Mansarliysky, G. P. Prepelitsa, A. A. Svinarenko

Odessa State Environmental University, 15, Lvovskaya str., Odessa, Ukraine
Odessa National Polytechnical University, 1, Shevchenko av., Odessa, Ukraine
e-mail: yubunyak@mail.ru

STUDYING PHOTOKINETICS OF THE IR LASER RADIATION EFFECT ON MIXTURE OF THE CO2-N2-H20 GASES FOR DIFFERENT ATMOSPHERIC MODELS

A kinetics of energy exchange in the mixture of the atmosphere CO_2-N_2-H_20 gases under passing the powerful CO_2 laser radiation pulses within the three-mode model of kinetical processes is studied. More accurate data for the absorption coefficient are presented.

At present time the environmental physics has a great progress, provided by implementation of the modern quantum electronics and laser physics methods and technologies in order to study unusual features of the "laser radiation- substance (gases, solids etc.) interaction. A special interest attracts a problem of interaction of the powerful laser radiation with an aerosol ensemble and search of new non-linear optical effects. The latter is directly related with problems of modern aerosol laser physics (c.f.[1-13]). One could remind that there is a redistribution of molecules on the energy levels of internal degree of freedom in the resonant absorption of IR laser radiation by the atmospheric molecular gases. As a result of quite complicated processes one could define an essential changing of the gases absorption coefficient due to the saturation of absorption [1].

One interesting effect else to be mentioned is an effect of the kinetic cooling of environment (mixture of gases), as it was at first predicted in ref. [2,5]. Usually the effect of kinetical cooling (CO_2) in a process of absorption of the laser pulse energy by molecular gas is considered for the middle latitude atmosphere and for special form of a laser pulse. Besides, the approximate values for constants of collisional deactivation and resonant transfer in reaction CO_2-N_2 are usually used. In series of papers (see, for example, [11-13], computational modelling of the energy and heat exchange kinetics in the mixture of the CO_2-N_2-H_20 atmospheric gases interacting with IR laser radiation has been carried out within the general three-mode kinetical model. It is obvious that using more precise values for all model constants and generally speaking the more advanced atmospheric model parameters may lead to quantitative changing in the temporary dependence of the resonant absorption coefficient by CO_2.

Let us remind that the creation and accumulation of the excited molecules of nitrogen owing to the resonant transfer of excitation from the molecules CO_2 results in the change of environment polarizability. Perturbing the complex conductivity of environment, all these effects are able to transform significantly the impulse energetics of IR lasers in an atmosphere and significantly change realization of different non-linear laser-aerosol effects.

The aim of this paper is to present more accurate data for kinetics of energy and heat exchange in the mixture CO_2-N_2-H_20 gases in atmosphere under passing the powerful CO_2 laser radiation pulses on the basis of using the more advanced atmospheric model and more precise values for all kinetical model constants.

As usually, we start from the modified three-mode model of kinetic processes (see, for exam-

ple, [1,11-13] in order to take into consideration the energy exchange and relaxation processes in the CO_2.– N_2 – H_2O mixture interacting with a laser radiation. As in ref. [11-13] we consider a kinetics of three levels: 10°0, 00°1 (CO_2) and v = 1 (N_2). Availability of atmospheric constituents O_2 and H_2O is allowed for the definition of the rate of vibrating-transitional relaxation of N_2. The system of balance equations for relative populations is written in a standard form as follows:

$$\frac{dx_1}{dt} = -\beta(\omega + 2gP_{10})x_1 + \beta(\omega + 2gP_{10})x_1^0,$$

$$\frac{dx_2}{dt} = \omega x_1 - (\omega + Q + P_{20})x_2 + (Q + P_{20})x_2^0,$$

$$\frac{dx_3}{dt} = \delta Q x_2 - (\delta Q + P_{30})x_3 + P_{30}x_3^0. \qquad (1)$$

Here the following notations are used:

$$x_1 = N_{100}/N_{O_2},$$
$$x_2 = N_{001}/N_{O_2}, \qquad (2)$$
$$x_3 = \delta N_{N_2}/N_{O_2},$$

where N_{100}, N_{001} are the level populations 10°0, 00°1 (CO_2); N_{N_2} is the level population v = 1 (N_2); N_{O_2} is the concentration of CO_2 molecules; δ is the ratio of the common concentrations of CO_2 and N_2 in the atmosphere ($\delta = 3.85\times10^{-4}$); x_1^0, x_2^0 and x_3^0 are the equilibrium relative values of populations under gas temperature T:

$$x_1^0 = \exp(-E_1/T),$$
$$x_2^0 = x_3^0 = \exp(E_2/T); \qquad (3)$$

The values E_1 and E_2 in (1) are the energies (K) of levels 10°0, 00°1 (consider the energy of quantum N_2 equal to E_2); P_{10}, P_{20} and P_{30} are the probabilities (s^{-1}) of the collisional deactivation of levels 10°0, 00°1 (CO_2) and v = 1 (N_2), Q is the probability (s^{-1}) of resonant transfer in the reaction $CO_2 \rightarrow N_2$,ω is the probability (s^{-1}) of CO_2 light excitation, g = 3 is the statistical weight of level 02°0, $\beta = (1+g)^{-1} = 1/4$. As usually, the solution of the differential equations system (1) allows defining a coefficient of absorption of the radiation by the CO_2 molecules according to the formula:

$$\alpha_{O_2} = \sigma(x_1 - x_2)N_{O_2}. \qquad (4)$$

The σ in (4) is dependent upon the thermodynamical medium parameters as follows [2]:

$$\sigma = \sigma_0 \frac{P}{P_0}\left(\frac{T}{T_0}\right)^{1/2}, \qquad (5)$$

Here T and p are the air temperature and pressure, σ_0 is the cross-section of resonant absorption under $T = T_0$, $p = p_0$. One could remind that the absorption coefficient for carbon dioxide and water vapour is dependent upon the thermodynamical parameters of aerosol atmosphere. In particular, for radiation of CO_2-laser the coefficient of absorption by atmosphere defined as $\alpha_g = \alpha_{O_2} + \alpha_{H_2O}$ is equal in conditions, which are typical for summer mid-latitudes, $\alpha_g(H=0) = 2.4\cdot10^6$ cm^{-1}, from which $0.8\cdot10^6$ cm^{-1} accounts for CO_2 and the rest – for water vapour (data are from ref. [2]) . On the large heights the sharp decrease of air moisture occurs and absorption coefficient is mainly defined by the carbon dioxide.

The changing population of the low level 10°0 (CO_2), population of the level 00°1, the vibrating-transitional relaxation (VT-relaxation) and the inter modal vibrating-vibrating relaxation (VV'-relaxation) processes define the physics of resonant absorption processes. Moreover, the above indicated processes result in a redistribution of the energy between the vibrating and transitional freedom of the molecules. According to ref.[1], the threshold value, which corresponds to the decrease of absorption coefficient in two times, for the strength of saturation of absorption in vibrating-rotary conversion give I_{sat} = (2 ÷ 5) 10^5 W cm^{-2} for atmospheric CO_2. In this case the pulse duration t_i must satisfy the condition $t_R \ll t_i < t_{VT}$, where t_R and t_{VT} are the times of rotary and vibrating-transitional relaxation's. by The fast exchange of level 10°0 with basic state, and by the relatively slow relaxation of high level 00°1define a renewal process of thermodynamic equilibrium is characterized. The latter provides an energy outflow from the transitional degree of freedom onto vibrating ones and in the cooling

of environment. It is easily understand that using more powerful laser radiation sources can lead to a strong non-linear interaction phenomena and, as result, significantly change a photo-kinetics of the corresponding processes.

In table 1 we present mode accurate our data (column C) for the relative coefficient of absorption $\overline{\alpha}_{O_2}$, which is normalized on the linear coefficient of absorption, calculated using (1) on corresponding height H. All data for $\overline{\alpha}_{O_2}$ are obtained for the height distribution of the pressure and temperature according to the advanced mid-latitude atmospheric model (all data are presented in series of refs. [14-20]). In table 1 there are presented also the analogous data from ref. [2] (column A) , from ref. [13] (column B).

Table 1.

Temporary dependence of resonant absorption relative coefficient $\overline{\alpha}_{O_2}$ (sm^{-1}) of laser radiation (λ=10,6μm) by CO_2 for rectangular (R) laser pulses (intensity I=10^5 W/sm^2) on the height (H, km) for the mid-latitude atmospheric model [1]: A- data of modelling [2]; B- data of modelling [13], C- data of modelling [14], D- this work

T μs	A [2] 10×I; R H=0	A[2] 10×I;R H=10	B [13] 10×I; G H=0	B [13] 10×I; G H=10
0	1,0	1,0	1,0	1,0
1	0,60	0,12	0,57	0,13
2	0,52	0,08	0,46	0,05
3	0,63	0,27	0.59	0,19
4	0,67	0,35	0,64	0,28
T μs	C [14] 10×I; G H=0	C [14] 10×I; G H=10	D, this 10×I; G H=0	D, this 10×I; G H=10
0	1,0	1,0	1,0	1,0
1	0,54	0,11	0,54	0,11
2	0,42	0,04	0,42	0,04
3	0.57	0,16	0.57	0,16
4	0,60	0,25	0,60	0,25

In Refs.[2 13,14] the analogous data for the relative coefficient of absorption $\overline{\alpha}_{O_2}$ and the height distribution of pressure and temperature are presented and obtained in a case of using the Odessa-latitude atmospheric conditions according to atmospheric model [7,8]. Here we use the world standard atmospheric model conditions [14-20]. Important moment is also connected with the more correct choice of probabilities P_{10}, P_{20} and P_{30} of the collisional deactivation of levels 10°0, 00°1 (CO_2) and v = 1 (N_2), probability Q of resonant transfer in the reaction $CO_2 \rightarrow N_2$, probability ω of CO_2 light excitation and other constants in comparison with refs. [2,13]. Let us in conclusion to note that obviously a quality of choice of the corresponding molecular constants and the corresponding atmospheric model parameters is of a great importance in modelling the effect of kinetic cooling of the CO_2 under propagation of the laser radiation in atmosphere. Naturally, principally another situation will occur in a case of the super intense laser pulses using for the atmosphere monitoring. Obviously, the modified model of photokinetical processes is to be developed in this case.

References

1. Zuev V.E., Zemlyanov A.A., Kopytin Y.D. Nonlinear Optics of Atmosphere.-L.:Hidrometeoizd., 1991.-256p.
2. Zuev V.E., Zemlyanov A.A., Kopytin Y.D., Kuzikovsky A.V. Powerful laser radiation in an atmospheric aerosol.-Novosybirsk, 1994.-224p.
3. Bagratashvili V.N., Letokhov V.S., Makarov A.A., Ryabov E.A. Multi-Photon Processes in Molecules in Infrared laser field.-M.: Nauka,1999-180p.
4. Bates N.R., Merlivat L. The influence of short-term wind variability on air-sea CO2 exchange // Geophysical Research Letters. – 2001. – Vol. 28. – No. 17. – P. 3281-3284.
5. Gordiets B.F., Osipov A.I., Khokhlov R.V. About cooling the gas under powerful CO_2 laser radiation passing in atmosphere// J.Techn.Phys.-1994.-Vol.14.-P.1063-1069.
6. Glushkov A., Malinovskaya S., Shpinareva I., Kozlovskaya V., Gura V.,

Quantum stochastic modelling energy transfer and effect of rotational and V-T relaxation on multiphoton excitation and dissociation for CF_3Br molecules// Int. J.Quant.Chem.-2005,-Vol.104.-P.512-520.
7. Parkinson S., Young P. Uncertainty and sensitivity in global carbon cycle modeling // Climate Research. – 1998. – Vol. 9. – No. 3. – P. 157-174.
8. Stephens B.B., Keeling R.F., Heimann M., Six K.D., Murnane R., Caldeira K. Testing global ocean carbon cycle models using measurements of atmospheric O_2 and CO_2 concentration// Global Biogeochem. Cycles. –1998.–Vol.12.–P. 213-230.
9. Glushkov A.V., Ambrosov S.V., Malinovskaya S.V. etal, Spectroscopy of carbon dioxide: Oscillator strengths and energies of transitions in spectra of CO_2 // Opt.and Spectr.-1996.-Vol.80.-C.60-65.
10. Trenberth K.E., Stepaniak D.P., Caron J.M. Interannual variations in the atmospheric heat budget //J.Geophys. Res.–2002.–Vol.107.– P.4-1– 4-15.
11. Prepelitsa G.P., Shpinareva I.M., Bunyakova Yu.Ya., Photokinetics of interaction and energy exchange for ir laser radiation with mixture CO_2-N_2-H_20 of atmospheric gases// Photoelectronics.-2006.-Vol.16.-P.139-141.
12. Korban V., Prepelitsa G., Bunyakova Yu., Degtyareva L., Seredenko S., Karpenko A., Photokinetics of the IR laser radiation effect on mixture of CO_2-N_2-H_20 gases: advanced atmospheric model// Photoelectronics.-2009. -N18.-P.36-39.
13. Kistler R., Kalnay E., Collins W., Saha S., White G., Woollen J., Chelliah M., Ebisuzaki W., Kanamitsu M., Kousky V., van den Dool H., Jenne R., Fiorino M. The NCEP-NCAR 50-year reanalysis: monthly means CD-ROM and documentation // Bull. Amer. Meteor. Soc. – 2001. – Vol. 82. – P. 247-267.
14. Fyfe J., Boer G., Flato G., Predictable winter climate in the North Atlantic sector during the 1997–1999 ENSO cycle // Geophys. Res.Lett.-1999.-Vol.26.-P. 1601-1604.
15. Plattner G-K., Joos F., Stocker T.F., Marchal O. Feedback mechanisms and sensitivities of ocean carbon uptake under global warming // Tellus. – 2001. – Vol. 53B.-P. 564-592.
16. Jin X., Shi G. A simulation of CO_2 uptake in a three dimensional ocean carbon cycle model// Acta Meteorologica Sinica. – 2001. – Vol. 15. – No. 1. – P. 29-39.

UDC 530.182:510.42

Yu. Bunyakova, T. Florko, A. Glushkov, V. Mansarliysky, G. Prepelitsa, A. Svinarenko

STUDYING PHOTOKINETICS OF THE IR LASER RADIATION EFFECT ON MIXTURE OF THE CO_2-N_2-H_20 GASES FOR DIFFERENT ATMOSPHERIC MODELS

Abstract. A kinetics of energy exchange in the mixture of the atmosphere CO_2-N_2-H_20 gases under passing the powerful CO_2 laser radiation pulses within the three-mode model of kinetical processes is studied. More accurate data for the absorption coefficient are presented.

Key words: photokinetics, laser field, mixture of gases, atmospheric model

УДК 530.182:510.42

Ю. Бунякова, Т. Флорко, А. Глушков, В. Мансарлийский, Г. Препелиця, А. Свинаренко

ИЗУЧЕНИЕ ФОТОКИНЕТИКИ ВЗАИМОДЕЙСТВИЯ ИК ЛАЗЕРНОГО ИЗЛУЧЕНИЯ СО СМЕСЬЮ CO_2-N_2-H_20 ГАЗОВ ДЛЯ РАЗНЫХ АТМОСФЕРНЫХ МОДЕЛЕЙ

Резюме. Рассмотрена фотокинетика энергообмена в смеси CO_2-N_2-H_20 атмосферных газов при прохождении через атмосферу мощного излучения CO_2 лазера в рамках уточненной 3-модовой модели кинетических процессов. Получены более точные значения коэффициента поглощения.

Ключевые слова: фотокинетика, лазерное поле, смесь газов, атмосферная модель

УДК 530.182:510.42

Ю. Бунякова, Т. Флорко, О. Глушков, В. Мансарлійський, Г. Препелиця, А. Свинаренко

ДОСЛІДЖЕННЯ ФОТОКІНЕТИКИ ВЗАЄМОДІЇ ІЧ ЛАЗЕРНОГО ВИПРОМІНЮВАННЯ ІЗ СУМІШЕЙ CO_2-N_2-H_20 ГАЗІВ ДЛЯ РІЗНИХ АТМОСФЕРНИХ МОДЕЛЕЙ

Резюме. Розглянуто фотокінетику енергообміну у сумішу CO_2-N_2-H_20 атмосферних газів при проходженні скрізь атмосферу міцного випромінювання CO_2 лазера у межах уточненої 3-модової моделі кінетичних процесів. Отримані більш точні оцінки для коефіцієнта поглинання.

Ключові слова: фотокінетика, лазерне поле, суміш газів, атмосферна модель

UDC 539.182

S. V. Brusentseva, A. V. Glushkov, Ya. I. Lepikh, V. B. Ternovsky

Odessa State Environmental University, L'vovskaya str.15, Odessa-16, 65016, Ukraine
Odessa National Maritime Academy, Odessa, 4, Didrikhsona str., Odessa, Ukraine
E-mail: quantbru@mail.ru

NONLINEAR DYNAMICS OF RELATIVISTIC BACKWARD-WAVE TUBE IN AUTOMODULATION AND CHAOTIC REGIME WITH ACCOUNTING THE EFFECTS WAVES REFLECTION, SPACE CHARGE FIELD AND DISSIPATION

It has been performed quantitative modelling, analysis, forecasting dynamics relativistic backward-wave tube (RBWT) with accounting relativistic effects, dissipation, a presence of space charge etc. There are computed the temporal dependences of the normalized field amplitudes (power) in a wide range of variation of the controlling parameters which are characteristic for distributed relativistic electron-waved self-vibrational systems: electric length of an interaction space N, bifurcation parameter L and relativistic factor γ0. The computed temporal dependence of the field amplitude (power) are very well correlated with the results by Ryskin-Titov, who give the detailed studying the RBWT dynamics with accounting the reflection effect, but without accounting dissipation effect and space charge field influence etc. The analysis techniques including multi-fractal approach, methods of correlation integral, false nearest neighbour, Lyapunov exponent's, surrogate data, is applied analysis of numerical parameters of chaotic dynamics of RBWT. There are computed the dynamic and topological invariants of the RBWT dynamics in auto-modulation(AUM)/chaotic regimes, correlation dimensions values), embedding, Kaplan-York dimensions, Lyapunov's exponents (LE: +,+) Kolmogorov entropy.

1. Introduction

The backward-wave tube is an electronic device for generating electromagnetic vibrations of the superhigh frequencies range. In refs.[1-14] there have been presented the temporal dependences of the output signal amplitude, phase portraits, statistical quantifiers for a weak chaos arising via period-doubling cascade of self-modulation and for developed chaos at large values of the dimensionless length parameter. The authors of [1-14] solved the different versions of system of equations of nonstationary nonlinear theory for the O type backward-wave tubes with and without account of the spatial charge, without energy losses etc. It has been shown that the finite-dimension strange attractor is responsible for chaotic regimes in the backward-wave tube.

In our work it has been performed quantitative modelling, analysis, forecasting dynamics relativistic backward-wave tube (RBWT) with accounting relativistic effects (g_0>1), dissipation, a presence of a space charge field etc. There are computed the temporal dependences of the normalized field amplitudes (power) in a wide range of variation of the controlling parameters which are characteristic for distributed relativistic electron-waved self-vibrational systems: electric length of an interaction space N, bifurcation parameter L one and relativistic factor g_0. The computed temporal dependence of the field amplitude (power) are very well correlated with the results by Ryskin-Titov [7], who give the detailed studying the RBWT dynamics with accounting the reflection effect, but without accounting dissipation effect and space charge field influence etc.

2. Method and Results

As the key ideas of our technique for nonlinear analysis of chaotic systems have been in details presented in refs. [13-28], here we are limited only

by brief representation. The first important step is a choice of the model of the RBWT dynamics. We use the standard non-stationary theory [3-7], however, despite the cited papers we take into account a number of effects, namely, influence of space charge, dissipation, the waves reflections at the ends of the system and others [12,13]. Usually relativistic dynamics is described system of equations for unidimensional relativistic electron phase $\grave{e}(æ,\hat{o},\grave{e}_0)$ (which moves in the interaction space with phase q_0 ($q_0\hat{I}[0; 2p]$) and has a coordinate z at time moment t) and field unidimensional complex amplitude $F(æ,\hat{o}) = \tilde{E} / (2\hat{a}_0 UC^2)$ as [240, 249]:

$$\partial^2\theta/\partial\zeta^2 = -L^2\gamma_0^3[\,1+\frac{1}{2\pi N}\partial\theta/\partial\zeta)^2 - \beta_0^2\,]^{3/2}$$

$$\mathrm{Re}[F\exp(i\theta) + \frac{4Q}{k}\sum_{k=1}^{M} I_k \exp(k\,\theta)]$$

$$\partial F/\partial\tau - \partial F/\partial\zeta + \text{đF} = -L\tilde{I}\,,$$

$$I_k = -\frac{1}{\eth}\int_0^{\eth} e^{-ik\grave{e}} d\grave{e}_0 \qquad (1)$$

with the corresponding boundary and initial conditions. In is important to note that the system studied has a few controlling parameters which are characteristic for distributed relativistic electron-waved self-vibrational systems: electric length of an interaction space N, bifurcation parameter $L = 2\pi N / \gamma_0$ (here C- is the known Piers parameter) and relativistic factor $\gamma_0 = (1-\beta_0^2)^{-1./2}$. As input parameters there were taken following initial values: relativistic factor g_0=1.5 (further we will increase g_0 in 2 and 4 times), electrical length of the interaction space $N = k_0 l\,(2\pi)$=10, electrons speed v_0=0.75c, v_{rp}=0.25c, dissipation parameter D = 5Db, starting reflection parameters: s = 0.5, r=0.7, $0<\phi<2p$. A choice of j due to the fact that the dependence upon it is periodic. The influence of reflections leads to the fact that bifurcational parameter L begins to be dependent on the phase j of the reflection parameter (see discussion regarding it in [7,8]).

Since processes resulting in the chaotic behaviour are fundamentally multivariate, it is necessary to reconstruct phase space using as well as possible information contained in the dynamical parameter $s(n)$, where n the number of the measurements. Such a reconstruction results in a certain set of d-dimensional vectors y(n) replacing the scalar measurements. Packard et al. [19] introduced the method of using time-delay coordinates to reconstruct the phase space of an observed dynamical system. The direct use of the lagged variables $s(n + t)$, where t is some integer to be determined, results in a coordinate system in which the structure of orbits in phase space can be captured. Then using a collection of time lags to create a vector in d dimensions, y(n) = [$s(n)$, $s(n + t)$, $s(n + 2t)$,…,$s(n + (d\text{-}1)t)$], the required coordinates are provided. In a nonlinear system, the $s(n + jt)$ are some unknown nonlinear combination of the actual physical variables that comprise the source of the measurements. The dimension d is called the embedding dimension, d_E. According to Mañé and Takens [24,25], any time lag will be acceptable is not terribly useful for extracting physics from data. The autocorrelation function and average mutual information can be applied here. The first approach is to compute the linear autocorrelation function C_L(d) and to look for that time lag where C_L(d) first passes through zero (see [18]). This gives a good hint of choice for t at that $s(n + jt)$ and $s(n + (j + 1)t)$ are linearly independent. a time series under consideration have an n-dimensional Gaussian distribution, these statistics are theoretically equivalent (see [15]). The goal of the embedding dimension determination is to reconstruct a Euclidean space R^d large enough so that the set of points d_A can be unfolded without ambiguity. In accordance with the embedding theorem, the embedding dimension, d_E, must be greater, or at least equal, than a dimension of attractor, d_A, i.e. $d_E > d_A$. In other words, we can choose a fortiori large dimension d_E, e.g. 10 or 15, since the previous analysis provides us prospects that the dynamics of our system is probably chaotic. However, two problems arise with working in dimensions larger than really required by the data and time-delay embedding [5,6,18]. First, many of computations for extracting interesting properties from the data require searches and other operations in R^d whose com-

putational cost rises exponentially with *d*. Second, but more significant from the physical point of view, in the presence of noise or other high-D contamination of the observations, the extra dimensions are not populated by dynamics, already captured by a smaller dimension, but entirely by the contaminating signal. There are several standard approaches to reconstruct the attractor dimension (see, e.g., [3-6,15]). The correlation integral analysis is one of the widely used techniques to investigate the signatures of chaos in a time series. The analysis uses the correlation integral, $C(r)$, to distinguish between chaotic and stochastic systems. To compute the correlation integral, the algorithm of Grassberger and Procaccia [10] is the most commonly used approach. If the time series is characterized by an attractor, then the integral $C(r)$ is related to the radius r as

$$d = \lim_{\substack{r\to 0 \\ N\to\infty}} \frac{\log C(r)}{\log r}, \qquad (2)$$

where d is correlation exponent.The saturation value of correlation exponent is defined as the correlation dimension (d_2) of attractor. The Lyapunov exponents are the dynamical invariants of the nonlinear system. In a general case, the orbits of chaotic attractors are unpredictable, but there is the limited predictability of chaotic physical system, which is defined by the global and local Lyapunov exponents. Since the Lyapunov exponents are defined as asymptotic average rates, they are independent of the initial conditions, and therefore they do comprise an invariant measure of attractor. In fact, if one manages to derive the whole spectrum of Lyapunov exponents, other invariants of the system, i.e. Kolmogorov entropy and attractor's dimension can be found. The Kolmogorov entropy, K, measures the average rate at which information about the state is lost with time. An estimate of this measure is the sum of the positive Lyapunov exponents. There are several approaches to computing the Lyapunov exponents (see, e.g., [5,6,15-18]).

In figure 1 we list the data on the time dependence of normalized field amplitude $F(æ,ô) = \tilde{E} / (2â_0 UC^2)$ (our data subject dissipation, the influence of space charge, the effect of reflections waves) at the values of the bifurcation parameter L:(a) – 3.5, (b) – 3.9 (other parameters: g_0=1.5, N = 10, s=0.5, r=0.7, ϕ =1.3p).

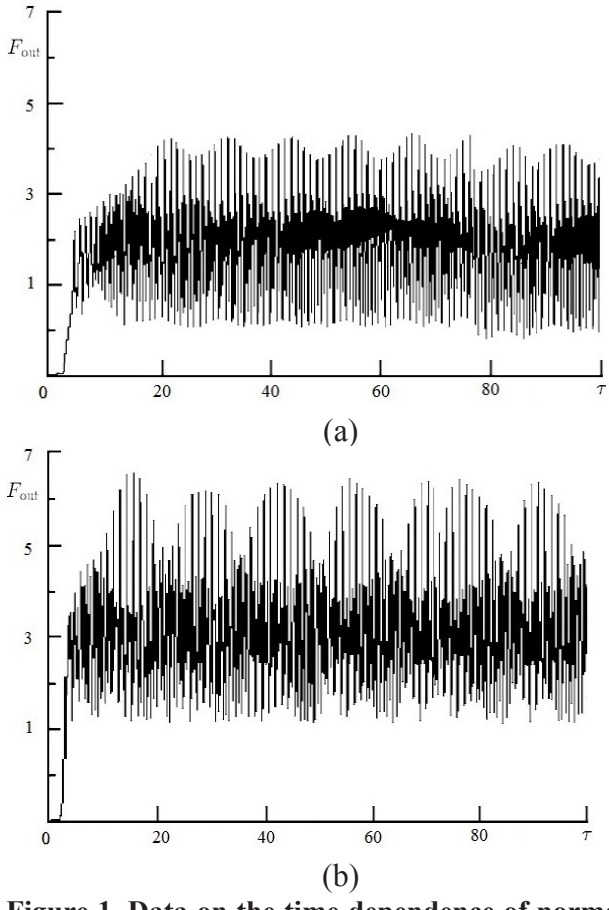

Figure 1. Data on the time dependence of normalized field amplitude F(z,t)(our data with accounting dissipation, the influence of space charge and an effect of wave reflections) at the values of the bifurcation parameter L: (a) – 3.5, (b) – 3.9 (other parameters: g_0=1.5, N = 10, s=0.5, r=0.7, ϕ =1.3p).

Figures 1a,b are corresponding to the regimes of quasi-periodical automodulation (a) and essentially chaotic regime (b). Importantly, our results obtained are very well correlated with the results by Ryskin-Titov in Ref. [7], where it has been in details studied the RBWT dynamics with accounting the reflection effect, but without accounting dissipation effect and space charge field influence etc. In table 1 we list our data on the correlation dimension d_2, embedding dimension, determined on the basis of false nearest neighbours algorithm (d_N) with percentage of false neighbours (%). calculated for different values of lag t (data on fig1b, regime of a chaos).

Table 1.

Correlation dimension d_2, embedding dimension, determined on the basis of false nearest neighbours algorithm (d_N) with percentage of false neighbours (%) calculated for different values of lag t

τ	τ	d_2	(d_N)
60	68	8.1	10 (12)
6	9	6.4	8 (2.1)
8	12	6.4	8 (2.1)

In Table 2 we list our computing data on the Lyapunov exponents (LE), the dimension of the Kaplan-York attractor, the Kolmogorov entropy K_{entr}.

Table 2.

The Lyapunov exponents (LE), the dimension of the Kaplan-York attractor, the Kolmogorov entropy K_{entr}. (our data)

λ_1	λ_2	λ_3	λ_4	*K*
0.507	0.198	-0.0001	–0.0003	0.71

For studied series there are the positive and negative LE values. he resulting dimension Kaplan York in both cases are very similar to the correlation dimension (calculated by the algorithm by Grassberger-Procachia). More important is the analysis of the RBWT nonlinear dynamics in the plane "relativistic factor – bifurcation parameter." Actually in this context a three-parametric relativistic nonlinear dynamics is fundamentally different from processes in non-relativistic BWT dynamics.

Conclusions

In this work we have performed quantitative modelling, analysis, forecasting dynamics relativistic backward-wave tube (RBWT) with accounting relativistic effects (g_0>1), dissipation, a presence of space charge, reflection of waves at the end of deceleration system etc. There are computed the temporal dependences of the normalized field amplitudes (power) in a wide range of variation of the controlling parameters which are characteristic for distributed relativistic electron-waved self-vibrational systems: electric length of an interaction space N, bifurcation parameter L (the automodulation and chaotic regimes) relativistic factor g_0=1.5-6.0). There are computed the dynamic and topological invariants of the RBWT dynamics in auto-modulation/chaotic regimes, correlation dimensions values, embedding, Kaplan-York dimensions, LE(LE:+,+) Kolmogorov entropy. In the further work we will try to present the bifurcation diagrams with definition of the dynamics self-modulation/chaotic areas in planes: «L-g_0», «D-L», predict emergence of highly-d chaotic attractor, which evolves at a much complicated scenario.

References

1. Glushkov A.V., Prepelitsa G.P., Khetselius O.Yu., Kuzakon V.M., Solyanikova E.P., Svinarenko A.A., Modeling of interaction of non-linear vibrational systems on basis of temporal series analyses (application to semiconductor quantum generators)// Dynamical Systems - Theory and Applications.-2011.-P.BIF-110 (8p.).
2. Trubetskov D.I., Anfinogentov V.G., Ryskin N.M., Titov V.N., Khramov A.E., Complex dynamics of electron microwave devices (nonlinear non-stationary theory from nonlinear dynamics)// Radioeng. -1999. – Vol.63. -P.61-68.
3. Ginsburg H. S., Kuznetsov S.P., Fedoseyev T.N. etal, Theory of transients in relativistic BWO// Izv. Vuzov. Ser. Radiophys.-1998.-T.21.- C.1037-1052.
4. Ginzburg N.S., Zaitsev N.A., Ilyakov E., Kulagin V.I., Novozhilov Yu., Rosenthal P., Sergeev V., Chaotic generation in backward wave tube of the megawatt power level// Journ. Of Techn.Phys.--2001-Vol.71.-P.73-80.
5. Kuznetsov S.P., Trubetskov D.I., Chaos and hyper-chaos in the backward wave tube// Izv. Vuzov. Ser. Radiophys.-2004.-Vol.XLVII.-P.383-399.
6. Levush B., Theory of relativistic backward wave oscillator with end reflections/ Levush B., Antonsen T.M.,

Bromborsky A., Lou W.R., Carmel Y.// IEEE Trans, on Plasma Sci.-1992.-V.20.-N3.-P.263-280.
7. Ryskin N.M., Self-modulation and chaotic regimes of generation in a relativistic backward-wave oscillator with end reflections/Ryskin N.M., Titov V.N.// Radiophysics and Quant.Electr.-2001.-Vol. 44,N10.-P.793-806.
8. Chang T., Chen S., Bamett L., Chu K., Characterization of stationary and non-stationary behavior in gyrotron oscillators//Phys.Rev.Lett.-2001.-Vol. 87.-P.321-325.
9. Levush B., Antonsen T.,Bromborsky A., Lou W., Relativistic backward wave oscillator: theory and experiment/ // Phys.Fluid-1992.-V.B4-P. 2293-2299.
10. Glushkov A., Khetselius O., Ternovsky V., Brusentseva S., Zaichko P., Studying interaction dynamics of chaotic systems within a non-linear prediction method: application to neurophysiology// Adv. in Neural Networks, Fuzzy Systems and Artificial Intelligence, Series: Recent Advances in Computer Eng., Ed. J.Balicki (World Sci. Pub.).-2014.-Vol.21.-P.69-75.
11. Glushkov A., Svinarenko A., Buyadzhi V., Ternovsky V., Zaichko P., Chaos-geometric attractor and quantum neural networks approach to simulation chaotic evolutionary dynamics during perception process // Ibid.-P.143-150.
12. Sivakumar B., Chaos theory in geophysics: past, present and future//Chaos, Solitons & Fractals.-2004.-Vol.19.-P.441–462.
13. Glushkov A.V., Khokhlov V.N., Tsenenko I.A. Atmospheric teleconnection patterns: wavelet analysis// Nonlin. Proc. in Geophys.-2004.-V.11.-P.285-293.
14. Glushkov A.V., Khokhlov V.N., Svinarenko A.A., Bunyakova Yu.Ya., Prepelitsa G.P., Wavelet analysis and sensing the total ozone content in the Earth atmosphere: MST “Geomath”// Sensor Electr. and Microsyst.Techn.-2005.-N3.-P.43-48.
15. Ott E. Chaos in dynamical systems. Cambridge: Cambridge Univ.Press, 2002.-490p.
16. Abarbanel H., Brown R., Sidorowich J., Tsimring L., The analysis of observed chaotic data in physical systems// Rev Modern Phys.-1993.-Vol.65.-P.1331–1392.
17. Kennel M., Brown R., Abarbanel H., Determining embedding dimension for phase-space reconstruction using geometrical construction//Phys. Rev.A.-1992.-Vol.45.-P.3403–3411.
18. Havstad J., Ehlers C., Attractor dimension of nonstationary dynamical systems from small data sets//Phys Rev A.-1989.-Vol.39.-P.845–853.
19. Packard N., Crutchfield J., Farmer J., Shaw R., Geometry from a time series//Phys Rev Lett.-1998.-Vol.45.-P.712–716.
20. Gallager R.G., Information theory and reliable communication, Wiley, New York.-1996.
21. Grassberger P., Procaccia I., Measuring the strangeness of strange attractors// Physica D.-1993.-Vol.9.-P.189–208.
22. Fraser A., Swinney H., Independent coordinates for strange attractors from mutual information// Phys Rev A.-1996.-Vol.33.-P.1134–1140.
23. Takens F., Detecting strange attractors in turbulence//Lecture notes in mathematics (Springer).-1981.-N.898.-P.366–381
24. Mañé R., On dimensions of the compact invariant sets of certain non-linear maps// Lecture notes in mathematics (Springer).-1991.-N898.-P.230–242
25. Sano M., Sawada Y., Measurement of Lyapunov spectrum from a chaotic time series//Phys.Rev.Lett.-1995.-Vol.55.-P.1082–1085
26. Rusov V.D., Glushkov A.V., Prepelitsa G.P., et al, On possible genesis of fractal dimensions in turbulent pulsations of cosmic plasma- galactic-origin rays-turbulent pulsation in planetary atmosphere system//Adv. Space Res.-2008.-Vol42.-P.1614-1617.

This article has been received in May 2016.

UDC 517.9

S. V. Brusentseva, A. V. Glushkov, Ya. I. Lepikh, V. B. Ternovsky

NON-LINEAR DYNAMICS OF RELATIVISTIC BACKWARD-WAVE TUBE IN SELF-MODULATION AND CHAOTIC REGIME WITH ACCOUNTING THE WAVES REFLECTION, SPACE CHARGE FIELD AND DISSIPATION EFFECTS

Abstract

It has been performed quantitative modelling, analysis of dynamics relativistic backward-wave tube (RBWT) with accounting relativistic effects, dissipation, a presence of space charge etc. There are computed the temporal dependences of the normalized field amplitudes in a wide range of variation of the controlling parameters which are characteristic for distributed relativistic electron-waved self-vibrational systems: electric length of an interaction space N, bifurcation parameter L and relativistic factor $\gamma 0$. The computed temporal dependence of the field amplitude is in a good agreement with theoretical data by Ryskin-Titov regarding the RBWT dynamics with accounting the reflection effect, but without accounting dissipation effect and space charge field influence etc. The analysis techniques including multi-fractal approach, methods of correlation integral, false nearest neighbour, Lyapunov exponent's, surrogate data, is applied analysis of numerical parameters of chaotic dynamics of RBWT. There are computed the dynamic and topological invariants of the RBWT dynamics in auto-modulation, chaotic regimes, correlation dimensions values), embedding, Kaplan-York dimensions, LE(+,+) Kolmogorov entropy.

Key words: relativistic backward-wave tube, chaos, non-linear methods

УДК 517.9

С. В. Брусенцева, А. В. Глушков, Я. И. Лепих, В. Б. Терновский

НЕЛИНЕЙНАЯ ДИНАМИКА РЕЛЯТИВИСТСКОЙ ЛАМПЫ ОБРАТНОЙ ВОЛНЫ В АВТОМОДУЛЯЦИОННОМ И ХАОТИЧЕСКОМ РЕЖИМАХ С УЧЕТОМ ЭФФЕКТОВ ОТРАЖЕНИЯ ВОЛН, ВЛИЯНИЯ ПОЛЯ ПРОСТРАНСТВЕННОГО ЗАРЯДА И ДИССИПАЦИИ

Резюме

Приведены результаты моделирования, анализа динамики процессов в релятивистской лампе обратной волны (РЛОВ) с учета релятивистских эффектов, диссипации, наличия пространственного заряда и т.д. Вычислены временные зависимости нормированной амплитуды поля в широком диапазоне изменения управляющих параметров: электрическая длина пространства взаимодействия N, бифуркационный параметр L и релятивистский фактор $\gamma 0$. Вычисленная зависимость амплитуды поля находится в хорошем согласии с теоретическими данными Рыскина-Титова о динамике РЛОВ с учетом эффекта отражения волн, но без учета эффектов диссипации и влияния поля пространственного заряда, т.д. Техника нелинейного

анализа, которая включает методы корреляционных интегралов, ложных ближайших соседей, экспонент Ляпунова, суррогатных данных, использована для анализа численных параметров хаотического режима в РЛОВ. Рассчитаны динамические и топологические инварианты динамики РЛОВ в автомодуляционном и хаотическом режимах, корреляционная размерность, размерности вложения, Каплан-Йорка, показатели Ляпунова (+, +), энтропия Колмогорова.

Ключевые слова: релятивистская лампы обратной волны, хаос, нелинейные методы

УДК 517.9

С. В. Брусенцева, О. В. Глушков, Я. І. Лепіх, В. Б. Терновський

НЕЛІНІЙНА ДИНАМІКА РЕЛЯТИВІСТСЬКОЇ ЛАМПИ ЗВЕРНЕНОЇ ХВИЛІ В АВТОМОДУЛЯЦІЙНОМУ ТА ХАОТИЧНОМУ РЕЖИМАХ З УРАХУВАННЯМ ЕФЕКТІВ ВІДДЗЕРКАЛЕННЯ ХВИЛЬ, ВПЛИВУ ПОЛЯ ПРОСТОРОВОГО ЗАРЯДУ І ДИСИПАЦІЇ

Резюме

Наведені результати моделювання, аналізу динаміки процесів в релятивістської лампі зворотної хвилі (РЛЗХ) з урахуванням релятивістських ефектів, дисипації, наявності просторового заряду і т.і. Обчислені часові залежності нормованої амплітуди поля в широкому діапазоні зміни керуючих параметрів: електрична довжина простору взаємодії N, біфуркаційний параметр L, і релятивістський фактор $\gamma 0$. Обчислена залежність амплітуди поля знаходиться в хорошій згоді з теоретичними даними Рискіна-Титова щодо динаміки РЛЗХ з урахуванням ефекту віддзеркалення хвиль, але без урахування ефектів дисипації і впливу поля просторового заряду, тощо. Техніка нелінійного аналізу, яка включає методи кореляційних інтегралів, хибних найближчих сусідів, експонент Ляпунова, сурогатних даних, використана для аналізу чисельних параметрів хаотичних режимів у РЛЗХ. Розраховані динамічні та топологічні інваріанти динаміки РЛЗХ в автомодуляціоному і хаотичному режимах, кореляційна розмірність, розмірності вкладення, Каплан-Йорка, показники Ляпунова (+, +), ентропія Колмогорова.

Ключові слова: релятивістська лампи зворотної хвилі, хаос, нелінійні методи

UDC 525.315.592

V. A. Borschak, M. I. Kutalova, N. P. Zatovskaya, L. N. Vilinskaya, A. O. Karpenko

FEATURES of VOLT - FARAD DEPENDENCE of NONIDEAL HETEROJUNCTIONS BARRIER CAPACITY

Abstract.

Abnormal dependence of volt-farad characteristics of «nonideal» heterojunction barrier capacity is investigated. It is shown that in heterojunctions with the big concentration and non-uniform distribution of defects tunnel currents essentially influence on the barrier capacity size.

The model for an explanation of abnormal barrier capacity dependence on the voltage, using tunneling-recombination mechanism of carriers carry through the area of a spatial charge is offered. The put forward assumptions put in a model basis, are confirmed experimentally.

Key words: nonideal heterojunctin, volt-farad characteristic

УДК 525.315.592

В. А. Борщак, М. І. Куталова, Н. П. Затовська, Л. М. Вілінська, А. О. Карпенко

ОСОБЛИВОСТІ ВОЛЬТ-ФАРАДНОЇ ЗАЛЕЖНОСТІ БАР'ЄРНОЇ ЄМНОСТІ НЕІДЕАЛЬНИХ ГЕТЕРОПЕРЕХОДІВ

Резюме

Досліджено аномальну залежність вольт-фарадної характеристики бар'єрної ємності «неідеальних» гетеропереходів. Показано що в гетеропереходах з великою концентрацією і неоднорідним розподілом дефектів тунельні струми істотно впливають на величину бар'єрної ємності.

Запропоновано модель для пояснення аномальної залежності бар'єрної ємності від напруги, що використовує тунельно-рекомбінаційний механізм переносу носіїв через область просторового заряду. Висунуті припущення, покладені в основу моделі, підтверджені експериментально.

Ключеві слова: неідеальний гетероперехід, вольт-фарадна характеристика, стрибкова провідність

УДК 525.315.592

В. А. Борщак, М. И. Куталова, Н. П. Затовская, Л. Н. Вилинская, А. А. Карпенко

ОСОБЕННОСТИ ВОЛЬТ-ФАРАДНОЙ ЗАВИСИМОСТИ БАРЬЕРНОЙ ЕМКОСТИ НЕИДЕАЛЬНЫХ ГЕТЕРОПЕРЕХОДОВ

Резюме

Исследована аномальная зависимость вольт-фарадной характеристики барьерной емкости «неидеальных» гетеропереходов. Показано что в гетеропереходах с большой концентрацией и

неоднородным распределением дефектов туннельные токи существенно влияют на величину барьерной емкости.

Предложена модель для объяснения аномальной зависимости барьерной емкости от напряжения, использующая туннельно-рекомбинационный механизм переноса носителей через область пространственного заряда. Выдвинутые предположения, положенные в основу модели, подтверждены экспериментально.

Ключевые слова: неидеальный гетеропереход, вольт-фарадная характеристика, прыжковая проводимость

At selection of semiconductor substances for heterojunction (HJ) creation the semiconductor "ideal" pairs are considered those which crystal lattices constants differ on the tenth part of percent. However at the majority of the semiconductor compounds suitable to manufacturing HJ with necessary properties, crystal lattices constants differ in some percents. Such lattices discrepancy creates on the interface high density of states (~ 10^{14} sm^2) [15], being the centres through which recombination and tunneling can be carried out. These phenomena usually degrade the HJ work, nevertheless some "nonideal" heteropairs are perspective. Classical type of "nonideal" HJ is pair CdS - Cu_2S, used as a photo cell with efficiency of 7... 9 %.

In the present work cadmium sulfide – cupper sulfide HJ, received in a aninted vacuum cycle on a glass substrate with the transparent SnO_2 conducting layer were investigated. The technology of HJ obtaining is based on consecutive thermal evaporation of cadmium sulfide and copper chloride in vacuum.

Formation of heterojunction CdS-Cu_2S occurs as a result of solid-state substitution reaction by ions Cu^+ ions Cd^{2+} on a surface of cadmium sulfide at heating of the CdS-CuCl structure in vacuum [2].

Crystal lattices constants of CdS and Cu_2S differ on 4 % [3] that is the reason of occurrence of the big concentration of mismatch dislocation which can serve as centres of recombination, and also centres of capture for holes and electrons. These centres play the important role in processes of current transport and charges separation and are located in the spatial charge region (SCR), completely laying in volume of cadmium sulfide, because of heterojunction asymmetry.

Data on these centre parameters and on donor concentration distribution in SCR can be received, by investigating the barrier capacity dependences on voltage. Measurement of volt-farad characteristics of "nonideal" HJ usually gives in coordinates C^{-2}...U a straight line with one or several breaks (fig. 1, curve α). These sections testify the presence of areas with various charge concentration amounts in SCR [1].

For CdS-Cu_2S heterojunctions, received on the described technology, volt-farad characteristic had more complex character shown in abnormal behaviour of curve C^{-2}...U dependence at small negative and positive voltages (fig. 1, curve *b*).

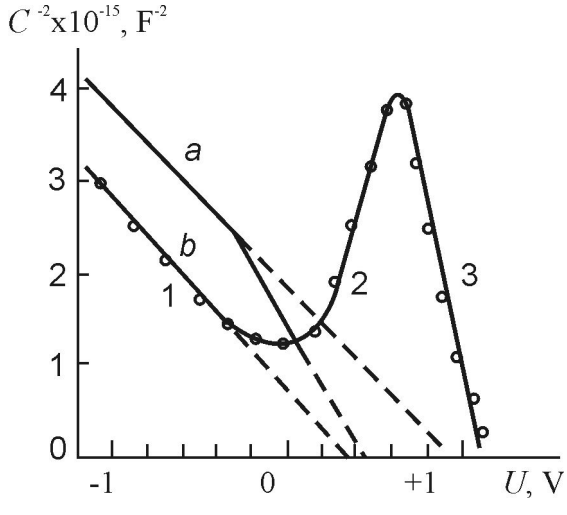

Fig. 1. Dependence of C^{-2} amount on a voltage for heterojunction with the step distribution of charge concentration in base: a - theoretical dependence; b - experimental curve

Presence of two linear sections 1 and 3 on the experimental curve is connected to existence of two layers with various charge carrier concentrations. These layer extents L_1 and L_2 were calculated under the formula:

$$L_{1,2} = \left[\frac{2\varepsilon\varepsilon_0 (\varphi - eU)}{e^2 N_{1,2}} \right]^{\frac{1}{2}}$$

Where ε_0 - absolute dielectric permeability; ε - relative dielectric permeability of of cadmium sulfide; e - electron charge; U - the voltage biased to heterojunction; φ - the barrier height determined on a cut-off voltage: φ_1 = 0,27 eV, φ_2 = 1,05 eV. Concentration of a charge in layers is determined by expression

$$N_{1,2} = \frac{2}{\varepsilon\varepsilon_0 e S^2}\left[\frac{d\left(C^{-2}\right)}{dU}\right]^{-1}$$

where S – HJ area.

For layer L_1 = 0,51 microns, $N_1 = 4{,}1\cdot10^{15}$ cm^{-3}. For layer L_2 = 0,12 microns, $N_2=2{,}2\cdot10^{16}$cm^{-3}. Smaller values of concentration N_1 of boundary layer L_1 are connected to copper diffusion into cadmium sulfide volume at heterojunction formation. Copper atoms are acceptors in cadmium sulfide and, lower the charge density by compensating donor centres.

On fig. 2 the band diagram constructed on calculated values N_1, N_2 and L_1, L_2 is given. However, such model allows to explain only volt-farad dependence submitted by the curve *a* on fig. 1.

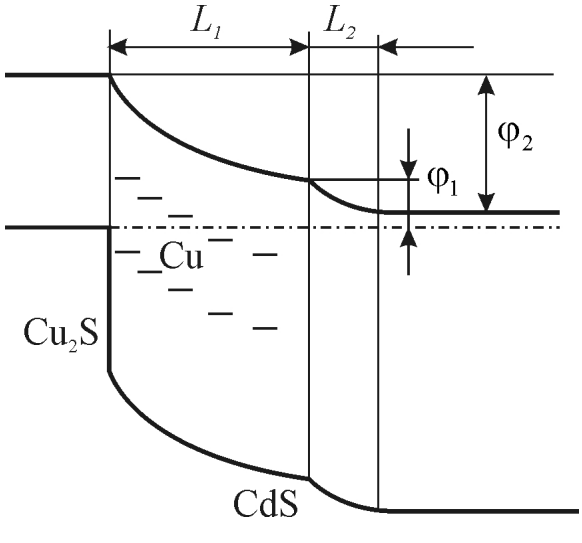

Fig. 2. The band diagram of heterojunction, constructed on the data of the experimental volt-farad dependence

As it is obvious from fig. 1 (curve *b*), the experimental curve has an abnormal section on which the capacity grows with reduction of a direct voltage. The behaviour of the volt-farad dependence curve on a section 2 does not find an explanation within the framework of model [1].

The observable trend of curve can be the consequence of a field devastation of the electronic capture levels located in volume of cadmium sulfide near to HJ border. Intensity of an electric field necessary for this process is realized in SCR at negative and small positive biases. The competition of the deep electronic traps filling processes and their full devastation results in increase or reduction of SCR width. Change of the barrier capacity amount in this case should be accompanied by a current relaxation at change of bias polarity. However the experiment which has been carried out in a wide range of frequencies, has not found out current relaxation that does not allow using the described mechanism.

For interpretation of abnormal course experimental volt-farad characteristics the assumption that conductivity G_1 of layer L_1 is much more than conductivity G_2 of layer L_2 is made. The assumption is made contrary to inequalities: $L_1 > L_2$, $n_1 < n_2$, however is justified as conductivity in barrier areas of nonideal HJ can be connected to the tunnel mechanism.

For more information on the current transport mechanism temperature dependences of heterojunction conductivity were investigated. Temperature dependence of samples conductivity at positive bias on junction in an interval of temperatures from nitrogen up to room is badly straightened in $lnG...T^{-1}$ coordinates. The average amount of activation energy, determined on the specified dependence, is equal 0,012 eV. However the measured temperature dependence is well straightened in $G...T^{-1/4}$ coordinates. According to Mott-Devis theory [6] such dependence observing in homogeneously - disorderly semiconductor substance what the area of heterojunction CdS-Cu_2S spatial charge is, and also the abnormal low energy of thermal activation of conductivity, specify on jumping mechanism of current transport on local states. This is specified with observing frequency dependence of active component of conductivity $G...\omega^{0,8}$ in a range of frequencies $5 < \omega\cdot < 200$ kHz.

Conductivity of barrier areas of researched samples in the greater degree is determined by a tunnel transparency, than the carrier concentration. At cupper diffusion into CdS boundary layer

arise a plenty of failures of a crystal lattice that provides multistage process of tunneling through rather extended area L_1 [7].

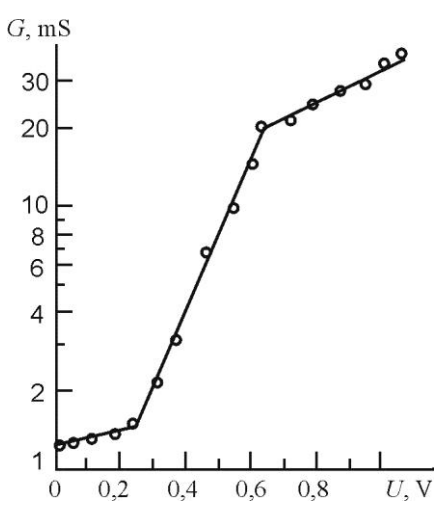

Fig. 3. Dependence of dark conductivity on positive bias on heterojunction (frequency of a measuring signal is equal 10 kHz)

HJ capacity, measured experimentally, is connected to a layer of the lowest electroconductivity. At negative bias on junction when SCR has the big extent, and at performance of inequality $G_1 >> G_2$, the capacity of only layer L_2 is measured, and layer L_1 is perceived by the measuring device as series connection resistance.

At the apply on HJ positive bias thickness of L_2 layer decreases and it should result in increase of measured capacity. Simultaneously there is a redistribution of measuring signal voltage: it grows on L_1 and decreases on L_2.

Under these conditions, the capacity of both layers is measured and the abnormal behavior of volt-farad dependence is observed. Reduction of capacity proceeds until SCR does not become equal to layer L_1 thickness. At the further increase of positive bias capacity SCR, laying only in layer L_1 is measured, as now this area has the lowest conduction. In these conditions, the normal section of volt-farad characteristic is again observed.

The confirmation of the offered model is the measured dependence *G=f(U)* submitted in fig. 3. Really, at the voltages appropriate to an abnormal section of a curve $C^{-2} = f(U)$ and to redistribution of decline in potential between areas L_2 and L_1. sharp increase of heterojunction electroconductivity is observed.

It is typical for the given band diagram, that he position of L_1 border has "biographic" character while the width of L_2 layer depends on the bias voltage or other influences. At excitation of heterojunction by light the space charge region has smaller extent as a result of the capture level filling by photoexcited holes [4]. In such conditions at zero bias on heterojunction the space charge region is placed only in the compensated layer, characterized, as it was shown above, by tunnel-recombination mechanism of conductivity.

Thus, on the example of classical nonideal structure on the basis of semiconductor compounds cadmium sulfide – cupper sulfide it is shown, that in heterojunctions with the big concentration and nonuniform distribution of defects in boundary region tunnel currents essentially change dependence of barrier capacity on a voltage.

This article has been received in April 2016.

UDC 525.315.592

V. A. Borschak, M. I. Kutalova, N. P. Zatovskaya, L. N. Vilinskaya, A. O. Karpenko

FEATURES of VOLT - FARAD DEPENDENCE of NONIDEAL HETEROJUNCTIONS BARRIER CAPACITY

Abstract

Abnormal dependence of volt-farad characteristics of «nonideal» heterojunction barrier capacity is investigated. It is shown that in heterojunctions with the big concentration and non-uniform distribution of defects tunnel currents essentially influence on the barrier capacity size.

The model for an explanation of abnormal barrier capacity dependence on the voltage, using tunneling-recombination mechanism of carriers carry through the area of a spatial charge is offered. The put forward assumptions put in a model basis, are confirmed experimentally.

Key words: nonideal heterojunctin, volt-farad characteristic

УДК 525.315.592

В. А. Борщак, М. І. Куталова, Н. П. Затовська, Л. М. Вілінська, А. О. Карпенко

ОСОБЛИВОСТІ ВОЛЬТ-ФАРАДНОЇ ЗАЛЕЖНОСТІ БАР'ЄРНОЇ ЄМНОСТІ НЕІДЕАЛЬНИХ ГЕТЕРОПЕРЕХОДІВ

Резюме

Досліджено аномальну залежність вольт-фарадної характеристики бар'єрної ємності «неідеальних» гетеропереходів. Показано що в гетеропереходах з великою концентрацією і неоднорідним розподілом дефектів тунельні струми істотно впливають на величину бар'єрної ємності.

Запропоновано модель для пояснення аномальної залежності бар'єрної ємності від напруги, що використовує тунельно-рекомбінаційний механізм переносу носіїв через область просторового заряду. Висунуті припущення, покладені в основу моделі, підтверджені експериментально.

Ключеві слова: неідеальний гетероперехід, вольт-фарадна характеристика, стрибкова провідність

УДК 525.315.592

В. А. Борщак, М. И. Куталова, Н. П. Затовская, Л. Н. Вилинская, А. А. Карпенко

ОСОБЕННОСТИ ВОЛЬТ-ФАРАДНОЙ ЗАВИСИМОСТИ БАРЬЕРНОЙ ЕМКОСТИ НЕИДЕАЛЬНЫХ ГЕТЕРОПЕРЕХОДОВ

Резюме

Исследована аномальная зависимость вольт-фарадной характеристики барьерной емкости «неидеальных» гетеропереходов. Показано что в гетеропереходах с большой концентрацией и неоднородным распределением дефектов туннельные токи существенно влияют на величину барьерной емкости.

Предложена модель для объяснения аномальной зависимости барьерной емкости от напряжения, использующая туннельно-рекомбинационный механизм переноса носителей через область пространственного заряда. Выдвинутые предположения, положенные в основу модели, подтверждены экспериментально.

Ключевые слова: неидеальный гетеропереход, вольт-фарадная характеристика, прыжковая проводимость

UDC 539.142 : 539.184

E. L. Ponomarenko, A. A. Kuznetsova, Yu. V. Dubrovskaya, E. V. Bakunina (Mischenko)

Odessa State Environmental University, L'vovskaya str.15, Odessa-16, 65016, Ukraine
Odessa National Maritime Academy, Odessa, 4, Didrikhsona str., Odessa, Ukraine
E-mail: quantmis@mail.ru

ENERGY AND SPECTROSCOPIC PARAMETERS OF DIATOMICS WITHIN GENERALIZED EQUATION OF MOTION METHOD

The spectral data on energies of transitions in spectrum of the nitrogen diatomics e are presented on the basis of calculation by modified motion equations method (MEM) with effective account for important correlation effects within a density functional approach. It differs from the standard version of the MEM by method by effective accounting for interelectron correlation effects, namely, effects of the "two holes- two particles". As a result an inaccuracy of calculation of the molecular excited states energies decreases significantly in comparison with the standard 1p-1h MEM approximation, namely, from 1.5-2 eV to decimal parts of eV, if you take into account the 2p-2h effects.

In last several decades quantum chemistry methods has been refined with a sophisticated and comprehensive approaches of the correct interelectron correlations and electron-nuclear dynamics treatments [1]. Information about excitation energies, probabilities and oscillator strengths of electron transitions in molecules is very important for a whole number of applications including different fields of a photo-chemistry and photophysics. Different calculation methods, namely, ab initio method of multi-configuration interaction (MCI), perturbation theory with Hartree-Fock zeroth approximation (Möller-Plesset theory), density functional theory (DF) etc [1] are used in calculations of atoms and molecules. As alternative in this situation one may consider method of equations of motion (MEM), which has been initially carried out by McKoy and co-workers with account for correlation effects within random phase approximation (RPA) (c.f.[2,3]). In series of papers [4-7] new approach in the MEM, based on account of correlation effects within DF approximation and essentially improving the standard version of the MEM, has been developed. Such an approach allows direct calculating amplitudes of different quantum processes, including absorption and emission of photons etc., and avoiding problems, connected with calculation of the wave functions and entire energies of molecules. Though it does not provide exact results, as for example, known limited variants of variation solving problem, however, it is sufficiently effective in calculations of the excitation energies and oscillator strengths of the electron transitions. In this paper new advanced method, which generalizes the MEM one is presented and applied to determination calculation of the transition energies and oscillator strengths for the nitrogen molecule. It differs from the standard version of the MEM by method to effective accounting for interelectron correlation effects, namely, effects of the "two holes- two particles" (2h-2p) polarization interaction). As it is shown, for example, in ref. [4,5], on order to reach an acceptable accuracy of calculation one may use sufficiently limited (on volume) basis's of orbitals. However, an account of such important correlation effects (effects, connected with 2*p*-2*h* interactions, a pressure of continuum, energy dependence of the self-consistent field potential, etc.) is obligatorily needed. It is well known that an account of majority of these effects based on standard methodic (for example, within perturbation theory) results in significant complication of calculation procedure (c.f. [1-4]).

According to ref. [2,], operator Q_λ^+, which generates an excited state $|\lambda\rangle$ of the atom from the ground state $|0\rangle$, i.e. $|\lambda\rangle = Q_\lambda^+ |0\rangle$, is an exact solution of equation of motion:

$$\langle 0 \| \left[\delta Q_\lambda , H, Q_\lambda^+ \right] \| 0 \rangle = \omega_\lambda \left[\delta Q_\lambda , Q_\lambda^+ \right], \qquad (1)$$

Here w_l is the transition frequency, amplitudes Q_λ^+ are elements of matrix of the transition $|0\rangle$ ® $|\lambda\rangle$. Equation (1) can be reduced to matrix equation for amplitudes $\{Y_{mg}\}$ и $\{Z_{mg}\}$ with account for the 1p-1h excitations as:

$$\begin{vmatrix} A & B \\ -B^* & -A^* \end{vmatrix} \begin{Vmatrix} Y(\lambda) \\ Z(\lambda) \end{Vmatrix} = \omega_\lambda \begin{vmatrix} D & 0 \\ 0 & D \end{vmatrix} \begin{Vmatrix} Y(\lambda) \\ Z(\lambda) \end{Vmatrix}, \quad (2)$$

the matrix elements A, B, D are as follows:

$$\begin{aligned} A_{m\gamma n\delta} &= \left\langle \left\| \left[C_{m\gamma} , H, C_{n\delta}^+ \right] \right\| \right\rangle, \\ B_{m\gamma n\delta} &= \left\langle \left\| \left[C_{m\gamma} , H, C_{n\delta}^+ \right] \right\| \right\rangle, \\ D_{m\gamma n\delta} &= \left\langle \left\| \left[C_{m\gamma} , H, C_{n\delta}^+ \right] \right\| \right\rangle, \end{aligned} \qquad (3)$$

Here C^+ is the particle-hole creation operator (C – destroying), indexes m, n denote the particles states; indexes d, g – the holes states; H is a Hamiltonian of quantum system in the representation of second quantization. The wave function of the ground state can be chosen in the following form:

$$|0\rangle \cong N_0 (1+U) |HF\rangle, \qquad (4)$$

where $U = (1/2) \sum C_{m\gamma n\delta} C_{m\gamma}^+ C_{n\delta}^+, |HF\rangle$ is the Hartree-Fock function. With account for equation (4) the matrix elements A, B, D have the following form:

$$\begin{aligned} A_{m\gamma n\delta} &= A^0_{m\gamma n\delta} + \delta_{\gamma\delta} \left[T_{mn} - (1/2)(\varepsilon_m + \varepsilon_n - 2\varepsilon_\gamma) \rho^{(2)}_{mn} \right] \\ &- \delta_{mn} \left[T_{\gamma\delta} - (1/2)(\varepsilon_m - \varepsilon_\gamma - \varepsilon_\delta) \rho^{(2)}_{\gamma\delta} \right], \\ B_{m\gamma n\delta} &= B^0_{m\gamma n\delta} + (-1)^\lambda S_{m\gamma n\delta}, \\ D_{m\gamma n\delta} &= \delta_{mn} \delta_{\gamma\delta} + \delta_{mn} \rho^{(2)}_{\gamma\delta} - \delta_{\gamma\delta} \rho^{(2)}_{\gamma\delta}. \end{aligned} \qquad (5)$$

The matrices A^0, B^0 etc are in details described in ref. [15]. Variables e in eq. (5) define the Hartree-Fock orbital energies; $\rho^{(2)}_{mn}$ and $\rho^{(2)}_{\gamma\delta}$ are the corrections to matrix of density of the second order and dependent upon correlation coefficients. If the corrected coefficients are omitted, then matrix elements will be reduced to the corresponding matrix elements of the RPA [2]. In this approximation, the equations of motion for definition of the 1*p*-1*h*-amplitudes $\{Y\}$, $\{Z\}$ and corresponding excitation energies w can be solved by standard methods of linear algebra. Acceptable accuracy of calculation is reached even using the limited basis's of orbitals due to the correct accounting for most important PI effects, connected with excitations of the 2p-2h type. From physical point of view, its inclusion is corresponding to an account for self-consistent reconstruction of the holes orbitals in a process of the virtual excitations in the ground configuration. An account of the 2*p*-2*h*-components in Q_λ^+ is equivalent to renor-malization of matrices in Eq.(3). It leads to dependence on the frequency w and reduces to appearance of the weight multiplier in the matrix elements [14- 18]:

$$a(r) = \left[1 - \Sigma_2(r) \right]^{-1}. \qquad (6)$$

In approximation of the quasiparticle DF a variable S expresses through the corresponding correlation functional [13]. In the simplified form of applying out methodic a variable $a(r)$ can be exchanged by (0) without essential loss of accuracy and according to well known procedure in theory of atomic photo-effect, which is based on the RPA with exchange (c.f.[11]). Indeed, the parameter a is corresponding to the known in spectroscopy one, which is a spectroscopic factor $F_{\gamma\delta}$. Its standard definition for atomic or molecular system (it is usually defined from the ionization cross-sections) [6]:

$$F_{\gamma\delta} = \left\{ 1 - \frac{\partial}{\partial \in} \sum_k \left[-(V.I.P.)_k \right] \right\} \qquad (7)$$

The terms $\partial \sum / \partial \varepsilon$ and $\sum_2$ is directly linked [6]. In the terms of the Green function method expression (7) is in fact corresponding to the pole strength of the Green's function [6]. Calculation

is carried out with using the correlation functional of the Lee-Yang-Parr (LYP) (look details in ref. [8-12]).Note further that amplitudes $\{Y_{mg}\}$ and $\{Z_{mg}\}$ define the moment of transition M_{0l}.

$$M_{0\lambda} = (2)^{1/2} \sum_{m\gamma} \left\{ Y^{*}_{m\gamma}(\lambda) M_{m\gamma} + Z^{*}_{m\gamma}(\lambda) M_{m\gamma} \right\} \qquad (8)$$

and oscillator strength:

$$f_{0\lambda} = (2/3) G \omega_{\lambda} \left| M_{0\lambda} \right|^2 \qquad (9)$$

Here G is the degeneration factor, M_{0l} is the particle-hole matrix element. Besides the procedure of account for the 2p-2h effects, other details of our calculation procedure are fully similar to scheme of the standard MEM approach (c.f.[10,14]). In tables 1 and 2 we present the results of our calculation (d) for the excited states energies and oscillator strengths of some states in N_2.

Table 1.

Excited state energies (eV) for N_2 (see text).

	$B^3\Pi_g$	$a^1\Pi_g$	$A^3\sum_u^+$	$B'^3\sum_g^-$	$W^3\Delta_u$
a	9,6	11,5	8,4	11,3	10,1
b	7,5	8,8	7,8	10,2	9,4
c	8,06	9,66	7,14	9,5	8,59
d	8,12	9,71	7,14	9,6	8,73
E	8,1	9,3	7,8	9,7	8,9
	$a'^1\sum_u^-$	$\omega^1\Delta_u$	$b'^1\sum_u^+$	$c^3\Pi_u$	$b^1\Pi_u$
a	11,3	12,0	16,8	13,3	17,4
b	10,6	11,0	15,0	10,8	14,0
c	9,61	10,2	14,28	11,3	13,92
d	9,74	10,31	14,38	11,39	13,92
E	9,9	10,3	14,4	11,1	12,8

The chosen geometry of the molecule is corresponding to generally accepted one for N_2 [1]. There are also presented the analogous data by McKoy et al in the 1p-1h (a) and 2p2-h (b), Glushkov (c) and experimental data (E) for comparison too. As one can wait for, an account of the 2p-2h effects is very important An inaccuracy of calculation of the transitions energies to low lying excited states in the 1p-1h MEM approximation decreases significantly, namely, from 1.5-2 eV to decimal parts of eV, if you take into account the 2p-2h effects.

Table 2.

Oscillator strengths for some electron transitions in the N_2

State	a	c	d	Exp	
$c'^1\sum_u^+$	0,11	0,10	0,13	0,14 ± 0,04	0,16
$b^1\Pi_u$	0,32	0,26	0,28	<0,3	
$b'^1\sum_u^+$	0,49	0,39	0,41	0,83	0,40

References

1. Ph.Duranrd, J.P.Malriew, Ab initio methods of Quantum Chemistry. Ed. Lawley K.P.,Chichester B.etc., N.-Y.: Academic Press,204.-550p.
2. Rose J., Shibua T., McKoy V., Equations of motion method including renormalization and double excited mixing: Random phase approximation// J.Chem.Phys.-1993.-Vol.58.-P.500-507.
3. Rose J., Shibua T., McKoy V. The equations of motion method in molecular calculations I //J.Chem.Phys.-1993.-Vol.58.- P.74-86.
4. Glushkov A.V., The Green's functions and density functional approach to vibrational structure in the photoelectron spectra of molecules: Review of method// Photoelectronics.-2014.-Vol.23.-P.54-72.
5. Glushkov A.., Koltzova N., Effective account of polarization effects in calculation of oscillator strengths and energies for atoms and molecules by method of equations of motion// Opt. Spectr. -1994.- Vol. 76,№6.-P.885-890.
6. Glushkov A.V., New approach in theoretical determination of molecules ionization potentials on the basis of the Green's functions method // J. of Phys. Chem.-1992.– Vol.66.-P.2671-2677.
7. Glushkov A.V., Quasiparticle approach

in the density functional theory under finte temperatures and dynamics of effective Bose -condensate // Ukr. Phys. Journ..- 1993.-Vol. 38,№8.-P.152-157.
8. Mischenko E.V., An effective account of correlation in calculation of excited states energies for molecules by equation of motion method: O_3//Photoelectronics.-2007.-N16.-P.123-125.
9. Zangwill A.,Soven P.J. Density-functional approach to local field effects in finite systems. Photo-absorption in rare gases // Phys.Rev.A.-1980.-Vol.21,N5-P.1561-1572.
10. Kobayashi K., Kurita N., Kumahora H., Kuzatami T. Bond-energy calculations of Cu , Ag, CuAg with the generalized gradient approximation// Phys. Rev.A.-1991.-Vol.43.-P.5810-5813.
11. Lagowscki J.B., Vosko S.H. Analysis of local and gradient- correction correlation energy functionals using electron removal energies// J. Phys.B: At. Mol. Opt. Phys.-1998.-Vol.21,N1-P.203-208.
12. Guo Y., Whitehead M.A. Effect of the correlation correction on the ionization potential and electron affinity in atoms// Phys.Rev.A-1999.-Vol.39,N1.-P.28-34.

This article has been received in May 2016.

UDC 539.142 : 539.184

E. L. Ponomarenko, A. A. Kuznetsova, Yu. V. Dubrovskaya, E. V. Bakunina (Mischenko)

ENERGY AND SPECTROSCOPIC PARAMETERS OF DIATOMICS WITHIN GENERALIZED EQUATION OF MOTION METHOD

Abstract

The spectral data on energies of transitions in spectrum of the nitrogen diatomics e are presented on the basis of calculation by modified motion equations method (MEM) with effective account for important correlation effects within a density functional approach. It differs from the standard version of the MEM by method by effective accounting for interelectron correlation effects, namely, effects of the “two holes- two particles”. As a result an inaccuracy of calculation of the molecular excited states energies decreases significantly in comparison with the standard 1p-1h MEM approximation, namely, from 1.5-2 eV to decimal parts of eV, if you take into account the 2p-2h effects.

Key words: molecule, inter electron correlation, motion equations method, density functional

УДК 539.142 : 539.184

Е. Л. Пономаренко, А. А. Кузнецова, Ю. В. Дубровская, Е. В. Бакунина (Мищенко)

ЭНЕРГЕТИЧЕСКИЕ И СПЕКТРОСКОПИЧЕСКИЕ ПАРАМЕТРЫ ДВУХАТОМНЫХ МОЛЕКУЛ НА ОСНОВЕ РАСЧЕТА ОБОБЩЕННЫМ МЕТОДОМ УРАВНЕНИЙ ДВИЖЕНИЯ

Резюме. На основе расчета обобщенным методом уравнений движения (МУД) с эффективным учетом важнейших корреляционных эффектов в приближении корреляционного функ-

ционала плотности получены энергетические и спектроскопические данные по энергиям возбужденных состояний и силам осцилляторов ряда переходов в молекуле азота. Новая версия отличается от стандартной версии МУД методикой эффективного учета межэлектронного эффектов корреляции, а именно, эффектов типа «двух частицы – две дырки». В результате неточность расчета энергий молекулярных возбужденных состояний значительно уменьшается по сравнению со стандартным 1p-1h МУД приближением, а именно, от 1.5-2 эВ до десятых долей эВ при учета 2p-2h эффектов.

Ключевые слова: молекула, под электронной корреляции, метод уравнений движения, функционал плотности

УДК 539.142 : 539.184

О. Л. Пономаренко, А. А. Кузнецова, Ю. В. Дубровська, О. В. Бакуніна (Міщенко)

ЕНЕРГЕТИЧНІ І СПЕКТРОСКОПІЧНІ ПАРАМЕТРИ ДВОАТОМНИХ МОЛЕКУЛ НА ОСНОВІ РОЗРАХУНКУ УЗАГАЛЬНЕНИМ МЕТОДОМ РІВНЯНЬ РУХУ

Резюме. На основі розрахунку узагальненим методом рівнянь руху (МУР) з ефективним урахуванням найважливіших кореляційних ефектів в наближенні кореляційного функціонала густини отримані енергетичні і спектроскопічні дані по енергіях збуджених станів і силам осциляторів ряду переходів в молекулі азоту. Нова версія відрізняється від стандартної версії МУД методикою ефективного обліку межелектронних ефектів кореляції, а саме, ефектів типу «дві частинки - дві дірки». В результаті неточність розрахунку енергій молекулярних збуджених станів значно зменшується в порівнянні зі стандартним 1p-1h МУД наближенням, а саме, від 1.5-2 еВ до десятих часток еВ при урахування 2p-2h ефектів.

Ключові слова: молекула, міжелектронні кореляції, метод рівнянь руху, функціонал густини

UDC 539.182

T. A. Florko, A. V. Glushkov, A. V. Ignatenko, O. Yu. Khetselius, A. A. Svinarenko, V. B. Ternovsky

Odessa State Environmental University, 15, Lvovskaya str., Odessa, Ukraine
Odessa National Polytechnical University, 1, Shevchenko av., Odessa, Ukraine
Odessa National Maritime Academy, Odessa, 4, Didrikhsona str., Odessa, Ukraine
e-mail: quantsvi@mail.ru

ADVANCED LASER PHOTOIONIZATION SEPARATION SCHEME AND TECHNOLOGY FOR HEAVY RADIOACTIVE ISOTOPES AND NUCLEAR ISOMERS

We present new optimal scheme of the separating highly radioactive isotopes and products of atomics energetics such as 210-214Fr, 133,135,137Cs and others, which is based on the selective laser excitation of the isotopes atoms into excited Rydberg states and further autoionization or DC electric field pulse ionization. As result, requirements to energetic of the ionized pulse are decreased at several orders. And an effectiveness of a scheme increases. There are theoretically calculated values of the characteristics of heavy Rydberg atoms in an external electromagnetic field (DC Stark effect) In particular, data on the energy level, the energy widths of Stark resonances for Rydberg Cs, Fr (n <45).

In series of our papers we considered the different schemes of a laser photoionization isotopes and nuclear isomers schemes. In this work, which goes on this studying, we present an advanced scheme of the separating highly radioactive isotopes and products of atomics energetics such as $^{210\text{-}214}$Fr and ^{133,135,137}Cs, which is based on the selective laser excitation of the isotopes atoms into excited Rydberg states and further autoionization or DC electric field pulse ionization. Following to [1,4], let us remind that related a search of the effective methods for isotopes and nuclear isomers separation and obtaining especially pure substances at atomic level is related to number of the very actual problem of modern nuclear technology, quantum and photoelectronics.The basis for its successful realization is, at first, carrying out the optimal multi stepped photo-ionization schemes for different elements and, at second, availability of enough effective UV and visible range lasers with high average power (Letokhov, 1977, 1979, 1983; etc) [9]. The standard laser photo-ionization scheme may be realized with using processes of the two-step excitation and ionization of atoms by laser pulse. The scheme of selective ionization of atoms, based on the selective resonance excitation of atoms by laser radiation into states near ionization boundary and further photo-ionization of the excited states by additional laser radiation, has been at first proposed and realized by Letokhov et al (Letokhov, 1969, 1977) [1]. It represents a great interest for laser separation of isotopes and nuclear isomers. The known disadvantage of two-step laser photoionization scheme a great difference between cross-sections of resonant excitation s_{exc} and photo-ionization s_{ion}. It requires using very intensive laser radiation for excited atom ionization. The same is arisen in a task of sorting the excited atoms and atoms with excited nuclei in problem of creation of g -laser on quickly decayed nuclear isomers. Originally, Goldansky and Letokhov (1974) [17] have considered a possibility of creating a g -laser, based on a recoilless transition between lower nuclear levels and shown that a g -laser of this type in the 20-60 keV region is feasible. But, it is obvious that here there is a problem of significant disadvantage of the two-step selective ionization of atoms by laser radiation method. The situation is more simplified for autoionization and Stark resonance's in the atomic spectra, but detailed data about characteristics of these levels are often

absent [1-16]. Several new optimal schemes for the laser photo-ionization sensors of separating heavy isotopes and nuclear isomers are proposed [1,4]. It is based on the selective laser excitation of the isotope atoms into excited Rydberg states and further autoionization and DC electric field ionization mechanisms.

Let us remind that in a classic scheme the laser excitation of the isotopes and nuclear isomers separation is usually realized at several steps: atoms are resonantly excited by laser radiation and then it is realized photo ionization of excited atoms. In this case photo ionization process is characterized by relatively low cross section $s_{ion}=10^{-17}$-10^{-18}cm^2 and one could use the powerful laser radiation on the ionization step. This is not acceptable from the energetics point of view [1-8]. The alternative mechanism is a transition of atoms into Rydberg states and further ionization by electric field or electromagnetic pulse. As result, requirements to energetic of the ionized pulse are decreased at several orders. The main feature and innovation of the presented scheme is connected with using the DC electric field (laser pulse) autoionization on the last ionization step of the laser photoionization technology. There is a principal difference of the simple ionization by DC electric filed. The laser pulse ionization through the auto ionized states decay channel has the advantages (more high accuracy, the better energetics, universality) especially for heavy elements and isotopes, where the DC electric field ionization from the low excited states has not to be high effective. This idea is a key one in the realization of sorting the definite excited atoms with necessary excited nuclei of the A^+ kind, obtained by optimal method of selective photo-ionization of the A kind atoms at the first steps. The suitable objects for modeling laser photoionization separation technology are the isotopes of alkali element Cs, long-lived transuranium elements etc.

We considered the isotopes of $^{210\text{-}214}$Fr and ^{133,135,137}Cs,. For example, the resonant excitation of the Cs atoms can be realized with using dye lasers with lamp pumping (two transitions wavelengths are: $6^2S_{1/2}$®$7\ ^2P_{3/2}$ 4555A and $6^2S_{1/2}$®$7\ ^2P_{1/2}$ 4593A). The next step is in the further excitation to the Rydberg S,P,D states with main quantum number n=35-50. The final step is the autoionization of the Rydberg excited atoms by a laser pulse or DC electric field pulse ionization and output of the created ions. The scheme will be optimal if an atom is excited by laser radiation to state, which has the decay probability due to the autoionization (pulse ionization) higher than the radiation decay probability. So, one could guess that the accurate data on the autoionization states energies and widths and the same parameters for the DC Stark resonances are needed. The consistent and accurate theoretical approach to calculation of these characteristics is based on the operator perturbation theory formalism [18] and corresponding advances relativistic version with model potential approximation [22, 23]. In Fig.1a we present the energy dependence (note that the level energy in the absence of field is taken as zero) of Stark components $(j,|m_j|)$ of the caesium state 39D Cs field strength: Experiment - squares, circles, triangles, diamonds [33]; Theory 1 - semi-empirical perturbation theory on the field by Zhao et al [25]; 2 – our data; In Fig.1b we list the Stark shift (in MHz) for the state 46D Cs in dependence on the square of the field: the experiment - squares, circles, triangles [25]; Theory – continuous.

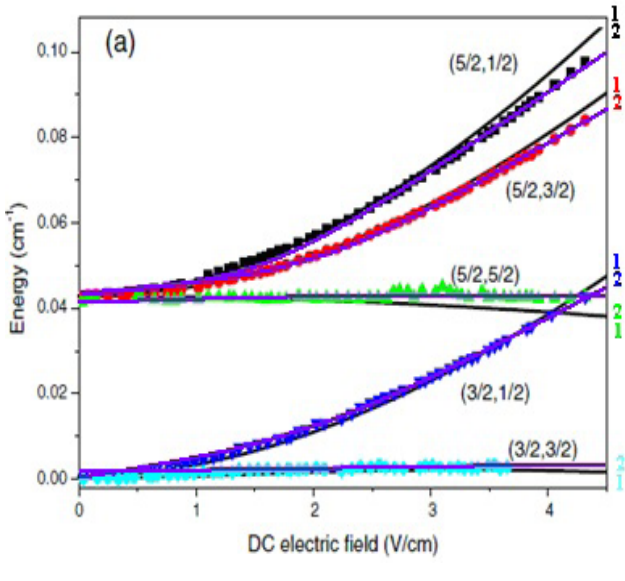

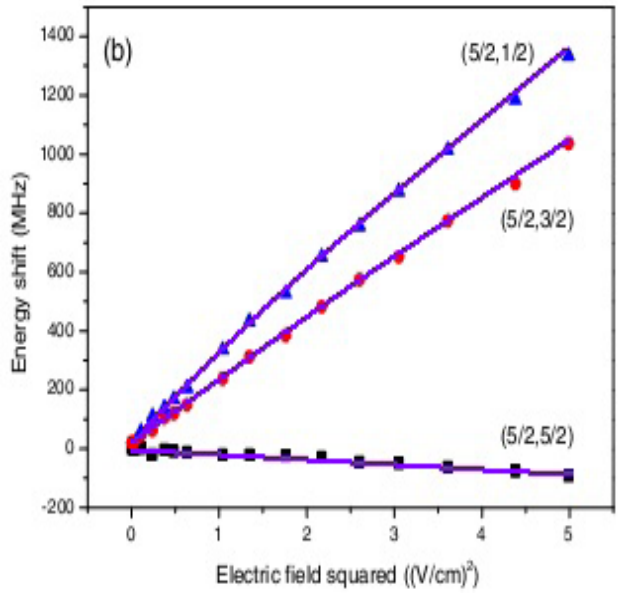

Fig.1 a – The energy dependence (note that the level energy in the absence of field is taken as zero) of Stark components (j,|m$_j$|) of the caesium state 39D Cs field strength: Experiment - squares, circles, triangles, diamonds [25]; Theory 1 – semi-empirical perturbation theory on the field by Zhao et al [25]; 2 – our data; b – Stark shift (in MHz) for the state 46D Cs in dependence on the square of the field: the experiment - squares, circles, triangles [25]; Theory – continuous

In Fig.2 we present a dependence of the Stark component (j,|m_j|) energies (MHz) of the state 44D for the francium atom of the square of the electric field (the first data).

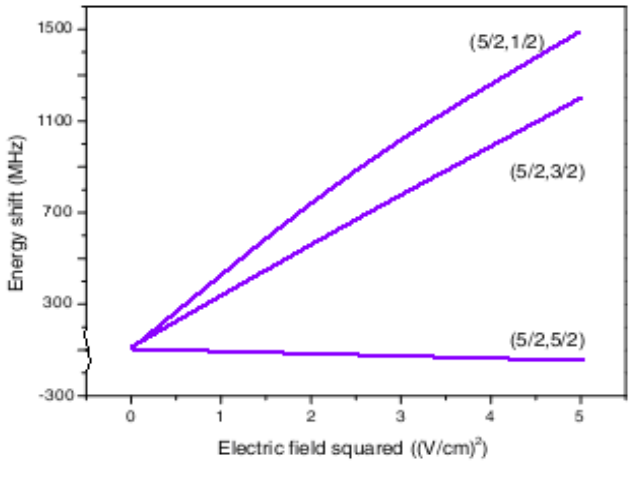

Fig.2. Dependence of the Stark component (j,|m$_j$|) energies (MHz) of the state 44D for the francium atom of the square of the electric field (our data)

In figure 3 we present the numerical modeling results of the excited and ground states populations in the photoionization scheme of the ^{133,137}Cs isotopes separation process with auto- and electric field ionization by solving the corresponding differential equations system [4].

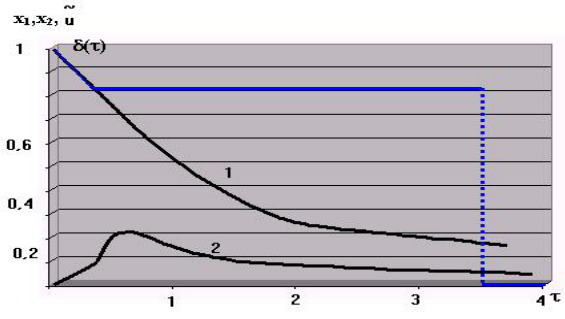

Fig.3. Results of modelling ^{133,137}Cs isotopes separation process by the laser photo-ionization method (d+dashed – laser pulse optimal form; see text)

The following definitions are used: d+dashed line is corresponding to optimal form of laser pulse, curves 1 and 2 are corresponding to populations of the ground and excited states of Cs. The d -pulse provides maximum possible level of excitation (the excitation degree is about ~0,25; in experiment (Letokhov, 1983) with rectangular pulse this degree was ~ 0,1). It is worth to turn attention on some analogy between modeling results for diferent alkali isotopes. Indeed, the relative populations for indicated atoms in the highly excited states are very closed to each other, however the absolute values of the radiation parameters for different isotopes naturally differ. Let us remember data regarding the Cs excitation and the ionization cross sections: the excitation cross section at the first step of the scheme is ~10^{-11}cm^2; the ionization cross-section from excited 7^2P_2 state: s_2=10^{-16}cm^2, from ground state s_2=10^{-18}cm^2 [2]. One can see that the relation of these cross sections is 10^5 and 10^7 correspondingly. This fact provides the obvious non-efficiency of standard photoionization scheme. Using d-pulse indeed provides a quick ionization, but the ionization yield will be less than 100% because of the stick-

ing on intermediate levels. So, from energetic point of view, this type of ionization can be very perspective alternative to earlier proposed classical two-step and more complicated photoionization schemes (Letokhov, 1983) [1]. The similar situation and analogous conclusions are obtained for the Sr and I isotope separation with the corresponding difference in the energetic and radiative characteristics data. So, one can say here about sufficiently optimal scheme of the separating highly radioactive isotopes and products of atomics energetics such as Cs and others. The key features of the corresponding scheme (technology) are based on the selective laser excitation of the isotopes atoms to the excited Rydberg states and further autoionization (or DC electric pulse ionization). One could remember here that a step of laser isotope separation has to be very important one in solving the modern actual problems of the transmutation of radioactive elements and decreasing the energy loses in the modern atomic energetics cycles [20,21].

References

1. Glushkov A.V., Lepikh Ya.I., Prepelitsa G.P., Ambrosov S.V., Bakunina E.V., Svinarenko A.A., Loboda A.V., Physics of the laser-photoionization atomic processes in the isotopes and gases separator devices: new optimal schemes// Sensors Electronics and Microsystems Technologies.-2011.-Vol.2(8),N1.-P.27-35.
2. Glushkov A.V., Khetselius O.Yu., Svinarenko A.A., Prepelitsa G.P., Energy Approach to Atoms in a Laser Field and Quantum Dynamics with Laser Pulses of Different Shape//In: Coherence and Ultrashort Pulsed Emission, Ed. Duarte F. J. (Intech, Vienna).-2010.-P.159-186.
3. Glushkov A.V. , Lepikh Ya.I. , Ambrosov S.V., Khetselius O.Yu., New optimal schemes of the laser photoionization technologies for cleaning the semiconductor materials and preparing the films of pure composition at atomic level// Ukrainian Journal of Physics.-2008.-Vol.53,N10.-P.1017-1022.
4. Glushkov A.V., Prepelitsa G.P., Svinarenko A.A., Pogosov A.Yu., Shevchuk V.G., Ignatenko A.V., Bakunina E.V., New laser photoionization isotope separation scheme with autoionization sorting of highly excited atoms for highly radioactive isotopes and products of atomic energetics//Sensors Electr. and Microsyst.Tech.-2011.-Vol.2(8),N2.-P.81-86
5. Glushkov A.V., Ambrosov S.V., Loboda A.V., Gurnitskaya E.P., Prepelitsa G.P., Consistent QED approach to calculation of electron-collision excitation cross-sections and strengths: Ne-like ions // Int. Journ.Quant.Chem.-2005.-Vol.104, N4 .-P. **562-569.**
6. Glushkov A.V., Lepikh Ya.I., Fedchuk A.P., Ignatenko A.V., Khetselius O.Yu., Ambrosov S.V , Wannier-Mott excitons and atoms in a DC electric field: photoionization, Stark effect, resonances in the ionization continuum// Sensor Electr. and Microsyst. Techn. (Ukraine).-2008.-N4.-P.5-11.
7. Glushkov A.V.,Ambrosov S.V., Kozlovskaya V.P., Prepelitsa G.P., Auger effect in atoms and solids: Calculation of characteristics of Auger decay in atoms, quasi-molecules and solids with application to surface composition analysis// Functional Materials.-2003.-V.10, N2.-P.206-210.
8. Khetselius O.Yu., Relativistic perturbation theory of the hyperfine structure for some heavy-element isotopes//Int. Journal of Quantum Chem.-2009.-Vol.109.-P. 3330-3335.
9. Letokhov V.S., Laser isotope separation// Nature.-1999.-N277.-P.605-610.
10. Velikhov E.P., Baranov V.S., Letokhov V.S., Rybov E.A., Starostin A.N., Pulsed CO2-lasers and their application for isotope separation.-Moscow: Nauka, 1993.
11. Basov N.G., Letokhov V.S., Optical frequency standards//Sov. Physics Uspekhi-1999.-Vol.11.-P.855-880 (UFN.-

1998.-Vol.96,N12).
12. Bokhan P.A., Buchanov V.V., Fateev N.V., Kalugin M.M., Kazaryan M.A., Prokhorov A.M., Zakrevskỳ D., Laser Isotope Separation in Atomic Vapor-WILEY-VCH Verlag, 2006.
13. Duarte, F. J. , Tunable lasers for atomic vapor laser isotope separation: the Australian contribution. Australian Physics.-2010.-Vol..47,N2.-P.38-48.
14. Glushkov A.V., Atom in an electromagnetic field.-Kiev: KNT, 2005.-450P.
15. Baldwin G.G., Salem J.C., Goldansky V.I., Approaches to the development of gamma ray lasers // Rev.Mod. Phys.-1991.-Vol.53.-P.687-742
16. Ivanov L.N., Letokhov V.S. Spectroscopy of autoionization resonances in heavy elements atoms// Com.Mod. Phys.D.:At.Mol.Phys.-1995.-Vol.4.-P.169-184.
17. Goldansky V.I., Letokhov V.S. Effect of laser radiation on nuclear decay processes// Sov. Phys. JETP.-1994.-Vol.67.-P.513-516.
18. Glushkov A.V., Ivanov L.N. DC Strong-Field Stark-Effect: consistent quantum-mechanical approach// J.Phys. B: At. Mol. Opt. Phys.-1993.-Vol.26,N16.-P.L379-386.
19. Glushkov A.V., Ivanov L.N., Letokhov V.S., Nuclear quantum optics// Preprint of Institute for Spectroscopy of the USSR AS, ISAN-N4, 1991.-16P.
20. Solatz R.W., May C.A., Carlson L.R. et al, Detection of Rydberg states in atomic uranium using time-resolved stepwise laser photoionization//Phys. Rev.A.-1996.-Vol.14.-P.1129-1148.
21. Ivanov L.N., Ivanova E.P., Knight L. Energy Approach to consistent QED theory for calculation of electron-collision strengths// Phys.Rev.A.-1993.-Vol.48.-P.4365-4374.
22. Ternovsky V., Svinarenko A., Ignatenko A., Nikola V., Seredenko S., Tkach T.B., Advanced relativistic model potential approach to calculation of radiation transition parameters in spectra of multicharged ions// Journal of Physics: C Series (IOP, London, UK).-2014.-Vol.548.-P. 012047 (6p.).
23. Ternovsky V., Glushkov A.V., Zaichko P., Khetselius O.., Florko T.A., New relativistic model potential approach to sensing radiative transitions probabilities in spectra of heavy Rydberg atomic systems/ // Sensor Electr. and Microsyst. Techn.-2015.-Vol.12, N4.-P.19-26.
24. Zhi-Gang Feng, Lin-Jie Zhang, Jian-Ming Zhao, Chang-Yong Liand Suo-Tang Jia, Lifetime measurement of ultracold caesium Rydberg states/ // J. Phys. B: At. Mol. Opt. Phys.-2009.-Vol.42.-P.145303 (5P.);
25. J.Zhao, H.Zhang, Z. Feng, X.Zhu, L.Zhang, C.Li, S.Jia , Measurement of Polarizability of Cesium *n*D State in Magneto-Optical Trap/ //J. Phys. Soc. Jpn. 80 (2011) 034303 (7P.).
26. van Wijngaarden W.A., Xia J., Lifetimes and polarizabilities of low lying S,P, D states of francium/ Journ. Quant. Spectr. Rad.Transfer.-1999.-Vol.61, N4.-P.557-561.
27. Huang S., Sun Q., Calculation of the Rydberg Energy Levels for Francium Atom// Phys.Res.Internat.-2010.-Vol.33.-P. 203497 (5P.).

This article has been received in May 2016.

UDC 539.183

T. A. Florko, A. V. Glushkov, A. V. Ignatenko, O. Yu. Khetselius, A. A. Svinarenko, V. B. Ternovsky

ADVANCED LASER PHOTOIONIZATION SEPARATION SCHEME AND TECHNOLOGY FOR HEAVY RADIOACTIVE ISOTOPES AND NUCLEAR ISOMERS

Abstract

We present new optimal scheme of the separating highly radioactive isotopes and products of atomics energetics such as $^{210\text{-}214}$Fr, ^{133,135,137}Cs and others, which is based on the selective laser excitation of the isotopes atoms into excited Rydberg states and further autoionization or DC electric field pulse ionization. As result, requirements to energetic of the ionized pulse are decreased at several orders. And an effectiveness of a scheme increases. There are theoretically calculated values of the characteristics of heavy Rydberg atoms in an external electromagnetic field (DC Stark effect) In particular, data on the energy level, the energy widths of Stark resonances for Rydberg Cs, Fr (n <50).

Key words: laser photoionization method, highly radioactive isotopes, new scheme

УДК 539.183

Т. О. Флорко, А. В. Глушков, А. В. Игнатенко, О. Ю. Хецелиус, А. А. Свинаренко, В. Б. Терновский

УЛУЧШЕННАЯ ЛАЗЕРНО-ФОТОИОНИЗАЦИОННЫЕ СХЕМА РАЗДЕЛЕНИЯ ИЗОТОПОВ ДЛЯ ТЯЖЕЛЫХ РАДИОАКТИВНЫХ ИЗОТОПОВ И ЯДЕРНЫХ ИЗОМЕРОВ

Резюме

Представлена новая оптимальная схема лазерного разделения высоко радиоактивных изотопов, продуктов атомной энергетики таких как $^{210\text{-}214}$Fr, ^{133,135,137}Cs и других, базирующаяся на лазерном возбуждении атомов изотопов в ридберговские состояния и дальнейшей автоионизации или ионизации импульсом электрического поля. Теоретически вычислены значения характеристик тяжелых ридберговских атомов во внешнем электромагнитном поле (DC эффект Штарка), в частности, данные по энергиям уровней, энергиям, ширинам штарковских резонансов для ридберговских Cs, Fr (n <50).

Ключевые слова: лазерный фотоионизационный метод, высоко радиоактивные изотопы, новая схема

УДК 539.183

Т. О Флорко, О. В. Глушков, Г. В. Ігнатенко, О. Ю. Хецеліус, А. А.Свинаренко, В. Б. Терновский

ПОКРАЩЕНА ЛАЗЕРНО-ФОТОІОНІЗАЦІЙНА СХЕМА ПОДІЛЕННЯ ІЗОТОПІВ ДЛЯ ВАЖКИХ РАДІОАКТИВНИХ ІЗОТОПІВ ТА ЯДЕРНИХ ІЗОМЕРІВ

Резюме

Представлена нова оптимальна схема лазерного поділення високо радіоактивних ізотопів, продуктів атомної енергетики, зокрема, таких як $^{210\text{-}214}$Fr, ^{133,135,137}Cs та інші, яка базуються на лазерному збудженні атомів ізотопів у ридбергові стани та подальшій автоіонізації або іонізації імпульсом електричного поля. Теоретично обчислені значення характеристик важких ридберговских атомів у зовнішньому електромагнітному полі (DC ефект Штарка), зокрема, дані по енергіях рівнів, енергіям, ширинам штарківських резонансів для рідбергових Cs, Fr (n <40).

Ключові слова: лазерний фотоіонізаційний метод, високо радіоактивні ізотопи, нова схема

PACS: 73.20.Hb, 73.25.+I; UDC 621.315.592

O. O. Ptashchenko[1], F. O. Ptashchenko[2], V, R.Gilmutdinova[1]

EFFECT OF WATER VAPORS ON THE TIME-RESOLVED SURFACE CURRENT INDUCED BY AMMONIA MOLECULES ADSORPTION IN GaAs P-N JUNCTIONS

[1]I. I. Mechnikov National University of Odessa, Dvoryanska St., 2, Odessa, 65026, Ukraine
[2]National University "Odessa Maritime Academy", Odessa, Didrikhsona St., 8, Odessa, 65029, Ukraine

The time-resolved surface current in an n-conducting channel, due to ammonia and water molecules adsorption in GaAs p-n structures was studied. It is shown that the presence of water vapors in the ambient atmosphere strongly affects the current decay curves after the ammonia vapors removal. The current decay curve in this case has three exponential components with different characteristic times: , and , as well as a component with . The results are explained in terms of a simple model taking into account a dynamic equilibrium between the free electrons in the conducting channel and electrons on slow surface centers. Each decay curve exponential component is due to the emptying of corresponding centers. The characteristic time of a current decay curve exponential component is determined by the depth and density of the corresponding surface levels, as well as the conducting channel thickness.

Key words: p-n structure, ammonia vapors, water vapors, adsorption, conducting channel, current decay, surface centers.

1. Introduction

Barrier structures on Si and GaAs, such as *p-n* junctions [1–4], porous membranes [5, 6], and nanowires [7], are promising materials for the gas sensors development. The Si *p-n* junctions can be combined in a transistor, which has much higher gas sensitivity than a single junction [8]. They can be easy integrated into microelectronic circuits. And the GaAs *p-n* junctions have a very high gas sensitivity, as well as a threshold ammonia vapors partial pressure of 0,1 Pa [4].

The sensitivity of the mentioned barrier structures, as well of GaP [9] and InGaN [10] *p-n* junctions, to ammonia vapors was observed only in presence of water vapors.

The aim of this work is a study of the influence of water vapors on the time resolved surface current in GaAs *p-n* structures, due to ammonia molecules adsorption.

2. Experiment

The measurements were carried out on GaAs *p-n* structures, described in the previous paper [10]. *I-V* characteristics of the forward and reverse currents were measured in air with various concentrations of ammonia vapors and saturated water vapors at T=290 K. The chemical composition of the ambient atmosphere was changed in 2 s by placing the sample in an appropriate container.

The curve 1 in Fig.1 represents the time dependence of the forward current, measured at V=0,3 Volts in a *p-n* structure, which was first placed in dry air; at t_1=200 s – in air with wet ammonia vapors (NH_3 partial pressure P=200 Pa); at t_2=3800 s – in dry air. After changing the ambient atmosphere from wet ammonia vapors to dry air (at $t>t_2$) the current drops from I_{max}=122 nA to 0,1 I_{max} in a time of 71 s. In the case of the curve 2, at t_2=3800 s the sample was placed in the atmosphere, containing air and saturated water vapors. And after 3 hours, at t_3=14600 s the sample was placed in dry air.

It is seen that the current decay curve 2 has three different sections: a “fast” section; a “slow” section; and a drop after the atmosphere changing from wet air to dry air.

Fig. 2 shows the time dependence of the current in the same sample for a following atmosphere change: dry air → (t_1) air + water vapors→(t_2) dry air. It is seen from Fig. 2, that maximum current in wet air is of 8,2 nA, which is considerably lower than in the "slow" component of the curve 2 in Fig. 1. This indicates that the slow decrease in the current after the atmosphere change from wet ammonia vapors to wet air can be explained only taking into account the presence of some electrically active centers on the crystal surface.

3. Discussion

The experimental results can be explained with the model, depicted in fig. 3 [11]. Ionized ammonia molecules 2 are located on the natural oxide surface

Their electric field bends the depletion layer 3 and forms a *n*-conducting channel 4. The forward current consists of two components. Arrow *a* corresponds to the through component I_t of the current in the channel

And arrow *b* represents the current component I_i due to electron injection from the channel into the p^+ layer at the contact.

The adsorbed water molecules (without ammonia molecules) also form such an *n*-conducting channel and remarkably enhance the current in the *p-n* junction, which is evident in Fig. 2.

In the uniform section of the channel, the following equation can be written

$$N_{ns} = N_i - N_{sf}^- - N_{ss}^- + N_{sD}^+ - N_{sA}^- , \qquad (1)$$

where N_{ns} is the free electrons number in the channel per 1cm^2 of the surface; N_i is the adsorbed ions surface density; N_{sf}^- and N_{ss}^- are the densities of filled fast and slow acceptor surface centers, respectively; N_{sD}^+ is the ionized donor surface centers density; N_{sA}^- is the number of ionized acceptor centers in the surface depletion layer per 1cm^2 of the surface:

$$N_{sA}^- = N_A^- w_s ; \qquad (2)$$

N_A^- is the ionized acceptor concentration in *p*- region; w_s is the surface depletion layer thickness [10].region; w_s is the surface depletion layer thickness [10].

The section of the curve 2 in Fig. 1 at $t > t_2$ can be decomposited in three exponential components, presented in Fig. 4. The characteristic times for the fast component, presented in Fig. 4a is $\tau_1 = 30$ s.

For two "slow" components, showed in Fig. 4b, $\tau_2 = 1900$ s and $\tau_3 = 9400$ s, respectively, are obtained.

The mentioned decomposition includes also a "constant" component with a characteristic time $\tau_4 \gg \tau_3$ with the amplitude $I_4^0 = 30$ nA. The fast decay component of the curve 2 in Fig. 1 can be ascribed to the desorption of ammonia ions. An analogous component has curve 1 in Fig. 1.

The components 2, 3 and 4 of the curve 2 in Fig. 1 can be explained taking into account presence of some slow centers on the naturally oxidized GaAs surface [4, 12, 13]. These centers are responsible for the peculiarities of the stationary characteristics [4] and the response time [13] of GaAs p-n structures as gas sensors.

The gradual descent in the curve 2 in Fig. 1 at $t > t_2$ is due to gradual decrease in the density of filled slow acceptor surface centers N_{ss}^- in (1). After an atmosphere ammonia → water vapors changing, the ions surface density drops. Therefore the electrons number N_{ns} in the conducting channel strongly falls down, which corresponds to the «fast» exponential component of the current decay curve, presented in Fig. 4A. And the electrons number N_{ss}^- on slow acceptor surface centers gradually decreases due to their thermal transitions to the conduction band. These transitions generate free electrons in the channel, slowing the decrease of the current. This effect can be described with a differential equation

$$\frac{d(N_{ns} + N_{ss}^-)}{dt} = G - N_{ns} / \tau , \qquad (3)$$

where G is the electrons generation rate in the cannel due to donors (water molecules) adsorption; τ is the electrons life time in the channel. In the case of a dynamic equilibrium between the free and captured electrons, a relation is valid

$$N_{ss}^- = N_{ns} N_{ss} /(N_c d) \exp[(E_c - E_{ss}) /(kT)], \qquad (4)$$

where N_{ss} is the full density of slow acceptor surface centers; N_c denotes the effective states density in the c-band; *d* is the channel thickness; $E_c - E_{ss}$ is the slow surface acceptor level depth; kT is the Boltzmann factor.

The initial condition for equation (3) is

$$N_{ns}(0) = N_{ns}^{0} > G\tau\,, \qquad (5)$$

because at t=0 the ambient atmosphere is changed from wet ammonia to water vapors.

Equation (3) under this initial condition has a solution

$$N_{ns}(t) = G\tau + (N_{ns}^{0} - G\tau)\exp(-t/\tau_{eff})\,, \qquad (6)$$

where

$$\tau_{eff} = (1+\nu)\tau\,, \qquad (7)$$

and

$$\nu = N_{ss}/(N_c d)\exp[(E_c - E_{ss})/(kT)]\,. \qquad (8)$$

It is seen from (7) and (8) that the channel current decay time after an ammonia → water vapors atmosphere change depends from the depth and density of slow surface levels, as well from the channel thickness. Two exponential components of the current decay curve, presented in Fig. 4b, are due to the presence of two slow surface centers on the GaAs natural oxide.

4. Conclusions

A change from wet ammonia vapors to water vapors in the ambient atmosphere results in a decrease of the surface current in GaAs *p-n* junctions. The current decay curve has a fast exponential component with a characteristic time τ_1<100 s and three slow components with $\tau_4 \gg \tau_3 \gg \tau_2 \gg \tau_1$.

The complicated shape of the current decay curve can be explained in terms of a simple model taking into account a dynamic equilibrium between the free electrons in the conducting channel and electrons on slow surface centers. Each decay curve exponential component is due to the emptying of corresponding centers.

The characteristic time of a current decay curve exponential component is determined by the depth and density of the corresponding surface levels, as well as the conducting channel thickness.

References

1. Ptashchenko F. O. Vplyv pariv amiaku na poverkhnevyi strum u kremniyevykh *p-n* perekhodakh // Visnyk ONU, ser. Fizyka.– 2006. – V. 11, No. 7. – P. 116 – 119.
2. Ptashchenko O. O., Ptashchenko F. O., Dovganyuk G. V. Vplyv struktury kremniyevykh *p-n* perekhodiv na yikh kharakterystyky yak gazovykh sensoriv // Sensorna Electronika i mikrosystemni tekhnologii. . – 2011 – V. 2 (8), № 4. – P. 13 – 19.
3. Ptashchenko O. O., Artemenko O. S., Ptashchenko F. O. Vplyv pariv amiaku na poverkhnevyi strum v *p-n* perekhodakh na osnovi napivprovidnykiv A^3B^5 // Journal of physical studies. – 2003. – V. 7, №4. – P. 419 – 425.
4. Ptashchenko O. O., Ptashchenko F. O., Gilmutdinova V. R. Vplyv poverkhnevogo leguvannya na charakterystyky *p-n* perekhodiv na osnovi GaAs yak gazovykh sensoriv // Sensorna elektronika i mikrosystemni tekhnologiyi– 2013. – V. 10, № 1. – P. 114 – 123.
5. Konstantinova E., Pavlikov A., Vorontsov A. et al. IR and EPR study of ammonia adsorption effect on silicon nanocrystals // Phys. Status Solidi A. – 2009. – V. 206, №6. – P. 1330-1332.
6. Boarino L., Borini S., Amato G. Electrical properties of mesoporous silicon: from a surface effect to coulomb blockade and more // J. Electrochem. Soc. – 2009. – V. 156, No. 12. – P. K223–K226.
7. Yuan G. D., Zhou Y. B., Guo C. S. et al. Tunable electrical properties of silicon nanowires via surface-ambient chemistry // ACS Nano. – 2010.– V. 4, No. 6. – P. 3045–3052.
8. Ptashchenko F. O. Characteristics of silicon transistors as gas sensors. // Photoelectronics. – 2010. – No. 19. – P. 18 – 21.
9. Ptashchenko O. O., Artemenko O. S., Dmytruk M. L. et al. Effect of ammonia vapors on the surface morphology and surface current in *p-n* junctions on GaP. // Photoelectronics. – 2005. – No. 14. – P. 97 – 100.
10. Ptashchenko F. O. Effect of ammonia vapors on surface currents in InGaN *p-n* junctions. // Photoelectronics. – 2007. – No. 17. – P. 113 – 116.

11. Ptashchenko O. O., Ptashchenko F. O., Gilmutdinova V. R. Tunnel surface current in GaAs *p-n* junctions induced by ammonia molecules adsorption // Photoelectronics. – 2013. – No. 22. – P. 38 – 42.
12. Fedorov Yu.Yu., Kharlamova T.S., Chikun V.V. Zavisimost' koncentracii glubokikh urovnei ot sposoba okisleniya poverkhnosti arsenida galliya // Elektronnaya tekhnika. Ser. SVCH-tekhnika. – 1993, No 2 (456). – P. 33-35.
13. Ptashchenko O. O., Ptashchenko F. O., Gilmutdinova V. R. Effect of deep centers on the time-resolved surface current induced by ammonia molecules adsorp-

PACS: 73.20.Hb, 73.25.+I; UDC 621.315.592

O. O. Ptashchenko, F. O. Ptashchenko, V. R. Gilmutdinova

EFFECT OF WATER VAPORS ON THE TIME-RESOLVED SURFACE CURRENT INDUCED BY AMMONIA MOLECULES ADSORPTION IN GaAs P-N JUNCTIONS

Summary

The time-resolved surface current in an *n*-conducting channel, due to ammonia and water molecules adsorption in GaAs *p-n* structures was studied. It is shown that the presence of water vapors in the ambient atmosphere strongly affects the current decay curves after the ammonia vapors removal. The current decay curve in this case has three exponential components with different characteristic times: $\tau_1 = 30$ s, $\tau_2 = 1900$ s and $\tau_3 = 9400$ s, as well as a component with $\tau_4 \gg \tau_3$. The results are explained in terms of a simple model taking into account a dynamic equilibrium between the free electrons in the conducting channel and electrons on slow surface centers. Each decay curve exponential component is due to the emptying of corresponding centers. The characteristic time of a current decay curve exponential component is determined by the depth and density of the corresponding surface levels, as well as the conducting channel thickness.

Key words: *p-n* structure, ammonia vapors, water vapors, adsorption, conducting channel, current decay, surface centers

PACS: 73.20.Hb, 73.25.+I; UDC 621.315.592

О. О. Птащенко, Ф. О. Птащенко, , В. Р. Гільмутдінова

ВПЛИВ ПАРІВ ВОДИ НА КІНЕТИКУ ПОВЕРХНЕВОГО СТРУМУ, ІНДУКОВАНОГО АДСОРБЦІЄЮ МОЛЕКУЛ АМІАКУ В P-N ПЕРЕХОДАХ НА ОСНОВІ GaAs

Резюме

Досліджено кінетику поверхневого струму в *n*-провідному каналі, обумовленому адсорбцією молекул аміаку і води, в *p-n* переходах н основі GaAs. Показано, що наявність парів води у навколишньому середовищі сильно впливає на криві спадання струму після видалення парів аміаку. Крива спадання струму в цьому випадку має три експоненціальні компоненти з різними значеннями характеристичного часу: $\tau_1 = 30$ с, $\tau_2 = 1900$ с і $\tau_3 = 9400$ с, а також компоненту з $\tau_4 \gg \tau_3$. Результати пояснюються в рамках простої моделі, яка враховує динамічну рівновагу між вільними електронами у провідному каналі та електронами на повільних поверхневих

центрах. Кожна експоненціальна компонента обумовлена спустошенням відповідних центрів. Характеристичний час кожної експоненціальної компоненти кривої спадання струму визначається глибиною і щільністю відповідних поверхневих рівнів, а також товщиною провідного каналу.

Ключові слова: *p-n* структура, пари аміаку, водяні пари, адсорбція, провідний канал, спадання струму, поверхневі центри.

PACS: 73.20.Hb, 73.25.+I; UDC 621.315.592

А. А. Птащенко, Ф. А. Птащенко, В. Р. Гильмутдинова

ВЛИЯНИЕ ПАРОВ ВОДЫ НА КИНЕТИКУ ПОВЕРХНОСТНОГО ТОКА, ИНДУЦИРОВАННОГО АДСОРБЦИЕЙ МОЛЕКУЛ АММИАКА В P-N ПЕРЕХОДАХ НА ОСНОВЕ GaAs

Резюме

Исследована кинетика поверхностного тока в *n*-проводящем канале, обусловленном адсорбцией молекул аммиака и воды, в *p-n* переходах н основе GaAs. Показано, что наличие паров воды в окружающей среде сильно влияет на кривые спадания тока после удаления паров аммиака. Кривая спадания тока в этом случае имеет три экспоненциальные компоненты с различными значениями характеристического времени: $\tau_1 = 30$ с , $\tau_2 = 1900$ с и $\tau_3 = 9400$ с , а также компоненту с $\tau_4 \gg \tau_3$. Результаты объясняются в рамках простой модели, которая учитывает динамическое равновесие между свободными электронами в проводящем канале и электронами на медленных поверхностных центрах. Характеристическое время каждой экспоненциальной компоненты кривой спадания тока определяется глубиной и плотностью соответствующих поверхностных уровней, а также толщиной проводящего канала.

Ключевые слова: *p-n* структура, пары аммиака, водные пары, адсорбция, проводящий канал, спадание тока, поверхностные центры.

UDC 621.315.592

O. P. Minaeva, N. S. Simanovych, N. P. Zatovskaya, Y. N. Karakis, M. I. Kutalova, G. G. Chemeresiuk

FEATURES OF LUMINOUS CONDUCTIVITY IN THE CRYSTALS TREATED IN A CORONA DISCHARGE

Odessa national university, 42, Pastera Str., 723-34-61
e-mail:photoelectronics@onu.edu.ua

The technology of semiconductor crystal processing in the corona discharge has been developed. It was established that as a result of this exposure, the samples acquire alternating spectral sensitivity.

The observed phenomenon is explained by the emergence of a saddle of the potential barrier in the element surface region the unusual properties which can allow the creation of a new type device.

It is known that the properties of semiconductor crystals can vary within wide limits depending on the quantity and quality of the formed defects. It must have an effect on the contact of the semiconductor sample.

In the present work we consider the problem about the behavior of the originally ohmic contact to the semiconductor at the appearance in its space charge region of charged unevenly distributed electron traps. Despite the urgency of this problem, in the literature it is almost not lit.

The introduction of the trapping centers in the crystal contact layer can dramatically change this region energy structure. In particular, in the case of electronic traps, the formation of the locking barrier is possible. This significantly changed the conditions of current transfer and hasspecific effects, similar in nature to the negative photoconductivity.

To analyze this situation it is necessary to eliminate the dependencies that describes the kind of arising barrier in the conduction band, as in the dark and in the light. As well as depending of the parameters of this barrier, its width, height, the maximum coordinate, the wall slopes – on the properties of trap – theirs energy depth, initial concentration and distribution in the sample depth.

The aim of this work is to show that the charged unevenly distributed of electron traps are able to form a locking barrier in ohmic contact space charge region. Its parameters are associated uniquely with the parameters of the traps and thus can manage technologically. In this case thank to the resulting barrier the sensor based on semiconductor crystal acquires new properties, including anomalous.

The change of photoconductivity, caused by the processing of cadmium chalcogenides monocrystal samples in the gas discharge was studied by authors [1-3]. The technology of this treatment is as follows. The element was placed in a vacuum

1. The effect of traps on the barrier structure

If the contact is formed for high-resistance semiconductor, due to the considerable differences of transmissibility prectically all the space charge region (SCR) is in its contact layer.

Let's in such a semiconductor were introduced electron traps N_t, which concentration decreases from the surface deep into the volume according to the law

$$N_t = N_{t0} e^{-\frac{x}{\ell_0}} \qquad (3)$$

where N_{t0} - the concentration on a geometric surface, and l_0 - a characteristic length that indicates how far the number of traps decreases in e times.

The activation energy of the traps (E_C–E_t). Then, just at the contact (region I Fig.1), traps are below the Fermi level. Such traps are filled with electrons regardless of the free charge concentration . On the surface their distance from the Fermi energy and, consequently, the filling will be at its maximum. Therefore, at point x=0 the appearance of such trap concentration of free electrons and the energy distribution do not change. Still they are described by formulas (1) and (2).

As can be seen from Fig.1, the greater is the depth of the traps (E_C–E_t), the wider is the region 1, enriched by electrons, as for large coordinate x traps are below the Fermi level and in the region of the Fermi level.

And, as will be further shown, the greater the initial concentration of traps N_{t0}, the steeper the dependence $\frac{dE}{dx}$ goes up. Both of these factors, acting together, should provide greater height of the formed barrier.

On the contrary, in the depth of the volume at $x > L_1$ the aquarance of electronic trap conditions will change significantly. The traps are partially filled and are able to capture an additional charge. The concentration of free charge, initially account n_0 (curve 1 Fig.1a) should decrease, which is accompanied by increase in the distance from the bottom of the conduction band up to the Fermi level.

Let's consider the impurities N_t edge of the front of spreading (region III of Fig.1a). The concentration of traps in the region $x = L_1$ is small, so in general it remains electroneutral. The part of free charge goes to the traps. The equation of electroneutrality in this case looks like:

$$N_d^+ = n_0 e^{-\frac{E(x)}{kT}} + N_{t0} e^{-\frac{x}{\ell_0}} \qquad (4)$$

Given the fact that numerically the of ionized donors concentration N_d^+ is equal to n_0 and using the decay exponent in the range from (4) obtain

$$n_0 \frac{E(x)}{kT} = N_{t0} e^{-\frac{x}{\ell_0}} .$$

From which

$$E_3(x)\Big|_{x \to L_2} = \frac{N_{t0}}{n_0} kT e^{-\frac{x}{\ell_0}} \qquad (5)$$

Decreasing of the x coordinate to the surface side, the value of the energy of the conduction band edge increases, although only slightly. If all the free charge n_0 will move to traps, then $(E–E_c) \sim kT$ (on the border of areas II and III).

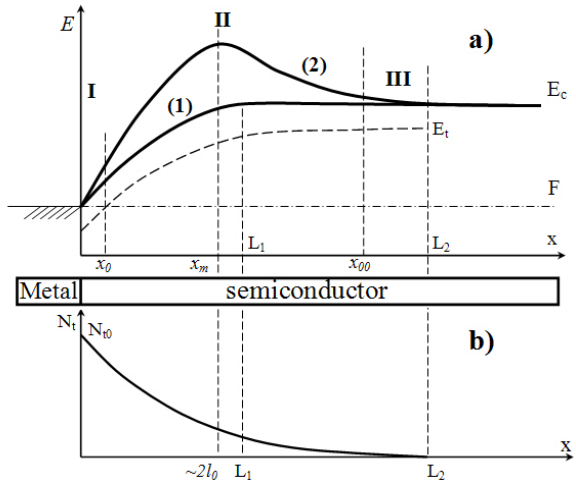

Fig. 1. (a) - structure of the SCR of ohmic contact to the high resistance semiconductor: (1) - the initial state; (2) – after the introduction of the traps; (b) - the distribution of the electron traps concentration in depth of the sample

The studied processes on the edges of the SCR are sufficient for predicting the energy distribution changes. If in the volume depth the energy curve $E_c(x)$ is directed upward, and on contact with the metal comes to the same point where it was without taking into account the traps, the overall profile of the SCR should be bell-shaped (curve 2 Fig.1a). And its width is controlled only by these traps penetration depth determined by technological factors in the crystal processing.

1. **The energy distribution in the crystal near-contact layers with traps for electrons**

The profile of the barrier in region I of Fig.1a can be determined by using the Poisson equation

$$\frac{d^2 E_1}{dx^2} = \frac{4\pi e^2}{\varepsilon} \rho(x) = \frac{4\pi e^2}{\varepsilon} \left[N_d^+ - N_t(x) - n(x) \right] \qquad (6)$$

where E – the energy, a $N_d^+ = n_0 << n_k$. Using expressions (2) and (3) formula (6) takes the form

$$\frac{d^2E_1}{dx^2} = \frac{4\pi e^2}{\varepsilon}\left[-N_{t0}e^{-\frac{x}{\ell_0}} - n_k\left(\frac{a}{a+x}\right)^2\right]. \quad (7)$$

Note that negative values of the second derivative indicate the convexity of the function E_1 in the region I.

After integrating

$$E_1(x) = \frac{4\pi e^2}{\varepsilon}\left[-\ell_0^2 N_{t0}e^{-\frac{x}{\ell_0}} + n_k a^2 \ln|a+x| + C_1 x + C_2\right]. \quad (8)$$

The values of the constants C_1 and C_2 can be determined from comparison with the distribution (1) for a pure semiconductor.

When using for contact of metals with possibly small work function the value of the jump at the boundary of $\Delta E(0)\to 0$. In this case, when x=0 $(E_C–F)$=0 and $n_k \approx N_c = 10^{19}$cm^{-3}. According to [4] value of cadmium concentration on the surface ~ 10^{21}cm^{-3}. Taking this quantity for 0.1÷1% of the total values we obtain that on the surface $N_{t0} \le n_k$.

Considering also the calculations described in paragraph 1, regarding the filling of the traps without the free charge concentration changing, would be fair:

$$\left.\frac{dE}{dx}\right|_{x=0} = \left.\frac{dE_1}{dx}\right|_{x=0} \quad \text{or from (7) and (1)}$$

$$\frac{2kT}{a+x} = \frac{4\pi e^2}{\varepsilon}\left[\ell_0 N_{t0}e^{-\frac{x}{\ell_0}} + \frac{n_k a^2}{a+x} + C_1\right], \text{where as}$$

x=0 is obtained $C_1 = \frac{2kT}{a}\frac{\varepsilon}{4\pi e^2} - \ell_0 N_{t0} - n_k a$. (9)

The value of the constant C_2 in (8) can be found from the condition $E_1(0) = 0$. From this it follows

$$C_2 = \ell_0^2 N_{t0} - n_k a^2 \ln a . \quad (10)$$

Finally (8) with (9) and (10) becomes:

$$E_1(x) = \frac{4\pi e^2}{\varepsilon}\left[\ell_0^2 N_{t0}\left(1-e^{-\frac{x}{\ell_0}}\right) + n_k a^2 \ln\frac{a+x}{a} + \left(\frac{2kT}{a}\frac{\varepsilon}{4\pi e^2} - \ell_0 N_{t0} - n_k a\right)x\right]. \quad (11)$$

The resulting expression is too cumbersome for further analysis. Therefore, we believe that the value l_0 in the traps distribution is large enough, and the point of linkage with the function E_2 *(x)* (i.e. the width of region I) lies in the coordinate that is smaller than the screening radius a. Then expanding in a number of the exponent and the logarithm of (11) will obtain the expression:

$$E_1(x) = \frac{2kT}{a}x \quad (12)$$

which, as expected, not influenced by the parameters l_0 and traps N_{t0}. In the surface layer the distribution of the energy barrier represented by almost a straight line with a slope *2kT/a*. In this graph $E_1(x)$ lies above the curve 1 Fig. 1a. This means that from the beginning with the coordinate increasing the concentration of free charge decreases faster than the concentration of traps.

2. The barrier structure in depleted layer

In the central part of the barrier (region II Fig. 1) free charge virtually absent and the concentration of electrons on traps significantly exceeds the number of ionized donors, since for these distances x number of traps is still quite large. Then $n_t(x) > N_d^+$; $n(x)$. In this case, the charge density

$$\rho(x) = -en_t(x) = -eN_t(x)f(x),$$

where $f(x)$ - the probability of filling traps Fermi – Dirac

$$f(x) = e^{-\frac{(E-E_t)-(E-F)}{kT}} = e^{-\frac{E-E_t}{kT}}\cdot e^{-\frac{E-F}{kT}}$$

In this expression, the first exponent associated with the activation energy of the traps, with the coordinate does not change, and the rate of the second exponent depends on x.

Finally, the Poisson equation has a view

$$\frac{d^2E_2(x)}{dx^2} = -Ae^{-\frac{x}{\ell_0}}e^{\frac{E_2}{kT}} \quad (13)$$

where

$$A = \frac{4\pi e^2}{\varepsilon}N_{t0}e^{\frac{E_c-E_t}{kT}}. \quad (14)$$

It is seen that in this region the second derivative is negative. The curve is concave. Using the substitution

$$Z = -\left(\frac{x}{\ell_0} + \frac{E_2}{kT}\right) \qquad (15)$$

have

$$\frac{d^2 z}{d\,x^2} = \frac{A}{kT} e^Z \,. \qquad (16)$$

Or

$$\frac{1}{2} d\left(\frac{dz}{dx}\right)^2 = \frac{A}{kT} e^Z dz \,.$$

Where after integration

$$\left(\frac{dz}{dx}\right)^2 = 2\frac{A}{kT} e^Z + C_1 \qquad (17)$$

The value of C_1 can be obtained at the position of the maximum, where $\frac{dE}{dx} = 0$. Then

$$\tilde{N}_1 = \left(\frac{1}{\ell_0}\right)^2 - 2\frac{\grave{A}}{kT} \mathring{a}^{-\frac{x_{\max}}{\ell_0}} \cdot \mathring{a}^{-\frac{E_{\max}}{kT}} \qquad (18)$$

On the rising curve where x<x max and E< E max is true (see 15)

$$C_1 << 2\frac{A}{kT} e^Z$$

For strong enough barriers on the drop-down of the value of x and x_{max} that have the same order, and $E < E_{max}$. Therefore, this condition remains valid here. In general formula (17) takes the form $\left(\frac{dz}{dx}\right)^2 = 2\frac{A}{kT} e^Z$.

From where

$$\frac{dz}{dx} = \pm\sqrt{\frac{2A}{kT}} e^{\frac{Z}{2}} \,. \qquad (19)$$

In accordance with (11) on the ascending part of the curve the derivative is negative. On falling apart for all $\frac{dE}{dx} < \frac{kT}{\ell_0}$ (i.e. slow decay), it also remains in force. Then in (19) should leave the sign «–». Where after integration is determined

$$-2e^{-\frac{Z}{2}} = -\sqrt{\frac{2A}{kT}} x - C_2 \,. \qquad (20)$$

Substituting (10) into (16) and simplifying the expression, it turns out

$$E_2(x) = -kT\frac{x}{\ell_0} + 2kT\ln\left(\sqrt{\frac{A}{2kT}} x + C_2\right). \qquad (21)$$

2. **Detalization of the explicit form of the energy distribution function**

From the equality of the derivatives at the point of stitching x_0 is obtained

$$\frac{2kT}{a} = -\frac{kT}{\ell_0} + \frac{2kT\sqrt{\frac{A}{2kT}}}{x_0\sqrt{\frac{A}{2kT}} + C_2} \,,$$

From where for large l_0, when $\frac{1}{2\ell_0} < \frac{1}{a}$

$$x_0\sqrt{\frac{A}{2kT}} + C_2 = a\sqrt{\frac{A}{2kT}} \qquad (22)$$

Then the value

$$x_0 = a - \frac{C_2}{\sqrt{\frac{A}{2kT}}} \,. \qquad (23)$$

After substitution into the expression $E_1(x_0) = E_2(x_0)$ we can find:

$$\frac{2kT}{a}\left(a - \frac{C_2}{\sqrt{\frac{A}{2kT}}}\right) = -\frac{kT}{\ell_0}\left(a - \frac{C_2}{\sqrt{\frac{A}{2kT}}}\right) + 2kT\ln\left(a\sqrt{\frac{A}{2kT}}\right) \qquad (24)$$

In the second term on the right in (24) takes into account the dependence (22). Reducing *2kT* and bringing like, it turns to $2\ell_0 > a$

$$\left[1 - \ln\left(a\sqrt{\frac{A}{2kT}}\right)\right] \cdot a \cdot \sqrt{\frac{A}{2kT}} = C_2 \,. \qquad (25)$$

If the growing part of the barrier sufficiently sharp, then the value x_0 in (23) is not large compared to a. In this case, from a comparison of (23) and (25) follows $\ln\left(a\sqrt{\frac{A}{2kT}}\right) < 1$, and finally

$$C_2 = a\sqrt{\frac{A}{2kT}}$$

$$E_2(x) = -\frac{kT}{\ell_0} x + 2kT\ln\left[\sqrt{\frac{A}{2kT}}(x + a)\right] \qquad (26)$$

As can be seen from (26) in the maximum when

$$\frac{dE_2}{dx} = -\frac{kT}{\ell_0} + \frac{2kT}{x_m +} = 0$$

$$x_m = 2\ell_0 - a \approx 2\ell_0 . \qquad (27)$$

The width of increasing side of the barrier and, consequently, the field strength is controlled by the parameters of the distribution of traps $2l_0$. Substituting (27) in (26) is determined by the value of the function E_2 in maximum:

$$E_{2\max} \cong -2kT + 2kT \ln \sqrt{\frac{A}{2kT}} (2\ell_0) . \qquad (28)$$

The more the $2l_0$, the higher the barrier.

The dependence on the initial concentration of traps N_{t0} and their activation energy (E_C–E_t) is dened by the value $A = \frac{4\pi e^2}{\varepsilon} N_{t0} e^{\frac{E_c - E_t}{kT}}$. From (28) it follows that with increasing of these parameters, the barrier height also increases linearly in proportion to (E_C – E_t) and logarithmically proportional to N_{t0}.

The total width of the SCR can be determined when $E_2(x)$=0:

$$\frac{L_2}{2\ell_0} = \ln\left(\sqrt{\frac{A}{2kT}} L_2 \right). \qquad (29)$$

It is considered that for this task the traps diffuse on L_1 and already at the maximum coordinate is $x_{max} > a$. Equation (29) does not allow to explicitly obtain the dependence of $L_2(l_0, A)$, but allows to reveal tendencies of this dependence by using methods borrowed from the theory of numbers.

Consider (29) in the form

$$\frac{L_2}{2\ell_0} - \ln L_2 = \ln \sqrt{\frac{A}{2kT}} . \qquad (30)$$

The type of traps is not changed (i.e., fixed A), but at the expense of technological methods increasing l_0. In this case, since the right part does not change, and the denominator of the first term increases, the value of L_2 should increase, although not proportionally. If L_2 is not changed, the left side of (30) is also decreased. This follows from

$$\frac{d\left(\frac{L_2}{2\ell_0} - \ln L_2 \right)}{dL_2} = \frac{1}{2\ell_0} \downarrow - \frac{1}{L_2} \uparrow < 0$$

Conversely, l_0=const, and the value of A increases. Then the left side in (30) should increase. Since the logarithmic function $y = \ln L_2$ slower linear change $y = \frac{L_2}{2\ell_0}$, in general, L_2 increases. With increasing concentration of the traps on the surface of the N_{t0} and their activation energy (E_C–E_t) of the SCR width increases.

Note that for this conclusion it is important simultaneous increase in both parameters. Fundamentally, it is possible when there are few deeper traps [$\exp\left(\frac{E_c - E_t}{kT}\right)$ more] on the geometric surface (less N_{t0}). Since the value of N_{t0} is controlled technologically, this competition can be avoided.

3. Energy profile of the barrier in the bulk of semiconductor

After stitching at point x_0 the function $E_2(x)$ in the depth of the volume has also been found associated with the surface condition (see 6).

The standard procedure for suturing in the depth of the scope of functions $E_2(x)$ and $E(x)$ leads to a too complicated system of equations that can be solved only by numerical methods.

Therefore, it was applied workaround [5]. The value of the function at the maximum at $x=x_m$ is equal to

$$\frac{dE_2(x_m)}{dx} = -\frac{kT}{\ell_0} + \frac{2kT\sqrt{\frac{A}{2kT}}}{\sqrt{\frac{A}{2kT}} x_{00} + C_2} = 0$$

From that

$$\sqrt{\frac{A}{2kT}} x_m + C_2 = 2\ell_0 \sqrt{\frac{A}{2kT}}$$

and $C_2 = \sqrt{\frac{A}{2kT}} (2\ell_0 - x_m)$.

This is after substitution in $E_2(x)$ gives

$$E_2(x) = -\frac{kT}{\ell_0} x + 2kT \ln\left[\sqrt{\frac{A}{2kT}} (x + 2\ell_0 - x_m) \right]$$

and in maximum ($x=x_m$) (31)

It is seen that the closer to the boundary the barrier forms (x_m decreases), the higher it is. With increasing concentration of traps N_{t0} and their depth ($E_C - E_t$) (i.e., increases) the barrier also increases. This coincides with the previously obtained.

At the point of stitching the barrier function $E_2(x)$ with the function in the quasi-neutral region $E \approx kT$. Therefore, we can assume that x_{00} determines the overall width of the SCR: $x_{00} = L_2$. It turns out:

$$2\ln\left[\sqrt{\frac{A}{2kT}}\left(L_2 + 2\ell_0 - x_m\right)\right] = \frac{L_2}{\ell_0} + 1,$$

and $L_2 >> l_0$ and therefore $\frac{L_2}{\ell_0} >> 1$. (32)

Then

$$L_2 + 2\ell_0 - x_m = \frac{e^{\frac{L_2}{2\ell_0}}}{\sqrt{\frac{A}{kT}}}$$

or

$$L_2 \approx 2\ell_0 \ln\left(2\ell_0\sqrt{\tfrac{A}{2kT}}\right).$$

The width of the space charge region increases with increasing $2l_0$, which also coincides with the previously obtained.

The technology of sample doping

In [2], a method of creating electron traps on the semiconductor surface due to the processing gas discharge is described. The advantages of this technique are associated with the presence of an electric field during technological operations. By varying the magnitude and direction of this field it is possible to control the process of introduction of defects and profile of their distribution.

In [6] indicates significant migration of the impurity ions in wide band gap semiconductors in the fields of order 10^5 V/m.

In addition to creating electronic traps and managed process of introducing them into the volume of semiconductor sensor, the proposed method of treatment in a corona discharge contributes to the formation of donor on the surface of the sample [3]. The same electric field which promotes the outflow of these traps, accumulates donors in the surface layers, increasing their conductivity. Thus, it becomes possible to make processing of crystals with pre-applied contacts and in the same cycle to make measurements without the presence of air in the chamber.

The sample was a rectangular plate of monocrystal cadmium sulfide with a thickness of ~ The width of the space charge region increases with increasing 2l0, which also coincides with the previously obtained.

The technology of sample doping

In [2], a method of creating electron traps on the semiconductor surface due to the processing gas discharge is described. The advantages of this technique are associated with the presence of an electric field during technological operations. By varying the magnitude and direction of this field it is possible to control the process of introduction of defects and profile of their distribution.

In [6] indicates significant migration of the impurity ions in wide band gap semiconductors in the fields of order 105 V/m.

In addition to creating electronic traps and managed process of introducing them into the volume of semiconductor sensor, the proposed method of treatment in a corona discharge contributes to the formation of donor on the surface of the sample [3]. The same electric field which promotes the outflow of these traps, accumulates donors in the surface layers, increasing their conductivity. Thus, it becomes possible to make processing of crystals with pre-applied contacts and in the same cycle to make measurements without the presence of air in the chamber.

The sample was a rectangular plate of monocrystal cadmium sulfide with a thickness of ~ 1,5 mm and an area of the front surface of about one square centimeter. The crystal was placed in a vacuum chamber, which created a vacuum of the order of 10-2÷10-3 mm. Hg.

Stable symmetric discharge (Fig. 2.b) managed to create [7] when the cathode end was attached to the conical form. When an insufficient degree of vacuum in a chamber, the discharge passed into the avalanche and was twisting, and in the working field of high voltage the twisting moment was almost independent of the field. All the following results are obtained after processing in the mode of glow discharge.

The best results are obtained when the gap width is 8-12 mm. We attribute this to the fact that with the insufficient value of the period expiring on the electron has not gained enough energy to create defects in the structure of the investigated crystal.

The high voltage of the order of 4-5 kV was created by high-voltage rectifier. In this case, the contrast described earlier (see [1-3]) is to use DC voltage for processing.

For processing in a gas discharge were selected samples, which have symmetrical linear graphs like the VAC in the dark and in the light. Has been used quite photosensitive crystals. In both cases – and in the dark and when illuminated – after the manufacturing process, the overall resistance of the crystal increased. After the appearance of these traps initially low resistivity space-charge region of the ohmic contact due to formation of the barrier significantly increases its resistance. The base resistance in the dark was ~ $5 \cdot 10^4$ Ohm, in the light - $(2 \div 3)10^4$ Ohm. Insignificant difference of the obtained values leads to the conclusion that the resulting width of the barrier is determined only by the penetration depth of the traps. Far from the surface of the crystal layers of the traps is very small and therefore they are already filled in in the dark. The light does not change their fill and, therefore, the width of the SCR, and with it the resistance.

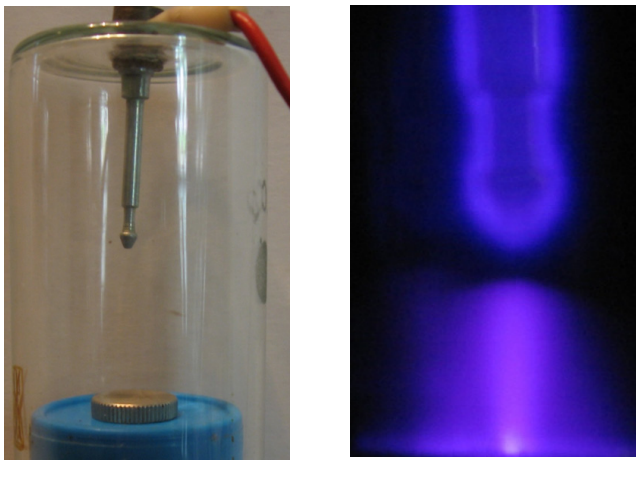

a) b)

Fig. 2. The design of the arrester (a) and processing of the samples the vacuum in the gas discharge (b)

When illumination by strongly absorbed light carriers are generated in the surface layers of the sensor and must move along the surface by the applied field. Processing in a gas discharge contributes, according to [1,2], the formation on the surface additional donor centers. In this case the surface conductivity increases, and the impact of recombination is weakened.

In the spectral range 540-600 nm by the impact of a gas discharge, we observed a slight increase of the photocurrent. This indicates the predicted occurrence as a result of processing of crystals of deep trap levels.

Conditions of formation barrier in our structures are also seen in the dependence of the curve shape of the spectral distribution of the photocurrent polarity from the applied voltage. For conventional barriers with increasing applied forward bias, the barrier height and width decrease. The field strength in the SCR barrier, as the ratio of these quantities varies little. When changing the polarity of the applied field on the opposite of both these parameters – the height and width are simultaneously increased, but their ratio is again significant changes does not undergo.

In our case it is not. The resulting width of the barrier is determined only by the penetration depth of the traps and does not depend on the applied voltage. An external electric field in this case reduces the height of the barrier and distorts its symmetry (see Fig.1). The side of the potential barrier, the field strength at which is opposite to external, is reduced to a greater extent. Because it is one-sided coverage, short-wave and long-wave part of the curve the spect

Experimentally proved to be correct to investigate the spectral distribution of the emerging photo – EMF. Such an approach allows not to take into account the nuances of the formation of the photocurrent – recombination in the inner regions of the crystal, the influence of the resistances of its parts, etc. But instead to identify the main – effect of the emerging traps in the surface layers of the sample due to the processing in a gas discharge and donor levels on its geometric surface.

Without the participation of the external field on the samples processed in a gas discharge, for the longitudinal conductivity, we observed the

unusual origin and distribution of EMF in the excitation light of different wavelengths. A curve is represented in Fig. 3

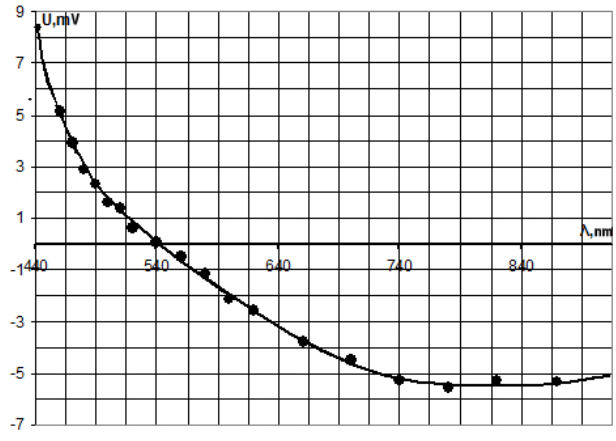

Fig. 3.The spectral distribution of the photo EMF for crystals, processed in a gas discharge

In our case, we found that the magnitude of photo-EMF under white light of 100 Lux was less than that in monochromatic light. This is due to the unusual form of a graph Fig.3. Shortwave and longwave contributions do not add up as usual in the white light, and subtracted.

This happens due to the unusual kind of barrier. Typically, SCR is either a growing part from the surface deep into the crystal (ohmic contact) or falling (gate contact). In our case presented both of the slope of the barrier (Fig.1). It shifted in the whole volume of the crystal from the surface. In this regard, when illuminated from the side of a contact on the surface of the sample, first, the absorption occurs in the increasing part of the barrier to short wavelength light with strong absorption. Photoexcited electrons by the field barrier are returned to the contact on the illuminated surface, where they increase the negative potential relatively to the lower contact to the sample. In Fig.3 we adopted this value for the positive part of the curve (area 440-540 nm).

As can be seen from the figure, with increasing the excitation wavelength, the contribution of this component decreases. This is because of that for larger wavelength the absorption coefficient decreases, and part of the photons reaches the deeper layers of the crystal, where the falling part of the barrier is. In this case, the field strength causes the non-equilibrium electrons move in the opposite direction. It is obvious that for a wave length of 540 nm, when in Fig.3, there is a curve crossing the x-axis, both processes balance each other and the resulting potential difference is equal to zero.

With further increase in wavelength, more photons are absorbed by the falling part of the barrier (Fig.1). Field barrier primarily directs the electrons into the sample, a negative potential of lower contact increases.

For sufficiently large wavelengths ~ 800 nm or more, the signal Fig.3 stabilizes, remaining negative. This indicates the predominant light absorption in the right side of the barrier (Fig.1). In addition, the photons can penetrate deep enough into the crystal and be absorbed outside the SCR contact without making any contribution to the signal formation Fig. 3.

The limit of the change curve Fig.3 is a conventional spectral distribution of photo reply.

Used processing methods cause changes in this schedule with some ratio of temperature, light, tension, the used field and the duration of the treatment. In our case the best results we have obtained with 15 min treatment with 8 mm distance to the needle on which it was 4000 V. Then the schedule gets abnormal appearance with maximally large negative values.

If too large saturation of the traps during processing in a gas discharge, their concentration gradient is insignificant, and the spectral distribution returns to its original state. This is the same crystal, which just increased the resistance due to the presence of traps.

Thus, the proposed technology of sensors, in full accordance with the developed model allows to obtain sensors with abnormal spectral sensitivity. The view according to Fig. 3 makes it possible to use them as receptors in a certain, prescribed in the course of technological processing, the wavelength of the radiation. Moreover, since at this point the value of the signal is zero, this sensor will be completely insensitive to any noise and interference, including artificially supplied.

In addition, since the light from different spectral regions the sign of the EMF and therefore the current is reversed, this property can be used to create optical devices of new generation.

References

1. Чемересюк Г.Г., Сердюк В.В. Явления, обусловленные захватом носителей, инжектированных в освещенные монокристаллы селенида кадмия.// Известия высших учебных заведений. Физика.– 1998.– №12.– С.7-12.
2. Чемересюк Г.Г. Отрицательная фотопроводимость в селениде кадмия, обусловленная уменьшением подвижности свободных носителей.// Studia Universitatis babes-bolyai: Series Physica Fasciculus 1.–1992.–21с.
3. Чемересюк Г.Г., Сердюк В.В. Коротковолновое гашение продольной фотопроводимости монокристаллов селенида кадмия.// Физика и техника полупроводников.-1999.-Т.3, в.3.-С. 396-399.
4. Физика и химия соединений AIIBVI.// Под ред. проф. С.А. Медведева.- М.: Мир, 1999.-С.103-104.
5. Драгоев А.А., Каракис Ю.Н., Балабан А.П., Чемересюк Г.Г. Расчёт профиля ОПЗ датчиков со знакопеременной спектральной чувствительностью // 4 nd International Scientific and Technical Conference "Sensors Electronics and Microsystems Technology" (CEMCT-4). Book of abstracts s. 192. Секция II Проектування та математичне моделювання сенсорів". Україна, Одеса, 28 червня – 2 липня 2010 р. "Астропринт". 2010
6. A.A. Dragoev, A.V. Muntjanu, Yu. N. Karakis, M. I. Kutalova Calculation for migration-dependent changes in near-contact space-charge regions of sensitized crystals// "Photoelectronics", n. 19. Odessa "Astroprint" 2010. s. 74 – 78.
6. Минаева О.П. Влияние газового разряда на формирование энергетического барьера в приповерхностной области кристаллов сульфида кадмия.// Материалы 63-й отчетной студенческой научной конференции. Секция физики полупроводников и диэлектриков. – Одесса, 2007. – С. 3-4.

This article has been received in May 2016.

UDC 621.315.592

O. P. Minaeva, N. S. Simanovych, N. P. Zatovskaya, Y. N. Karakis, M. I. Kutalova, G. G. Chemeresiuk

FEATURES LUMINOUS CONDUCTIVITY IN THE CRYSTALS TREATED IN A CORONA DISCHARGE

Abstract

The technology of processing of semiconductor crystals is developed in the corona discharge. It is established that as a result of this exposure, the samples acquire alternating spectral sensitivity.

The observed phenomenon is explained by the emergence of a saddle of the potential barrier in the surface region of the element, the unusual properties which can allow the creation of a new type of device.

Key words: LUMINOUS CONDUCTIVITY, THE CRYSTALS, CORONA DISCHARGE

УДК 621.315.592

О. П. Минаева, А. С. Симанович, Н. П. Затовская, Ю. Н. Каракис, М. И. Куталова, Г. Г.Чемересюк

ОСОБЕННОСТИ СВЕТОВОЙ ПРОВОДИМОСТИ В КРИСТАЛЛАХ, ОБРАБОТАННЫХ В КОРОННОМ РАЗРЯДЕ

Резюме

Разработана технология обработки полупроводниковых кристаллов в коронном разряде. Установлено, что в результате этого воздействия образцы приобретают знакопеременную спектральную чувствительность. Наблюдаемые явления объяснены возникновением двухскатного потенциального барьера в приповерхностной области элемента, необычные свойства которого могут позволить создание прибора нового типа.

Ключевые слова: Кристаллы, коронный разряд , световая проводимость,

УДК 621.315.592

О. П. Мінаєва, А. С. Симанович, Н. П. Затовська, Ю. М. Каракіс, М. І. Куталова, Г. Г. Чемересюк

ОСОБЛИВОСТІ СВІТЛОВОЇ ПРОВІДНОСТІ В КРИСТАЛАХ, ОБРОБЛЕНИХ У КОРОННОМУ РОЗРЯДІ

Резюме

Розроблено технологію обробки напівпровідникових кристалів у коронному розряді. Встановлено, що в результаті цього впливу зразки набувають знакоперемінну спектральну чутливість. Явища, що спостерігаються, пояснені виникненням двосхилого потенційного бар'єра в приповерхній області елемента, незвичайні властивості якого можуть дозволити створення приладу нового типу.

Ключові слова: кристали, коронний розряд, світлова провідність

UDC 539.183

A. S. Kvasikova, V. F. Mansarliysky, A. A. Kuznetsova, Yu. V. Dubrovskaya, E. L. Ponomarenko

[1]Odessa State Academy of Technical Regulation and Quality, 15, Kovalskaya str., Odessa, 65020, Ukraine
Odessa State Environmental University, 15, Lvovskaya str., Odessa, Ukraine
Odessa National Maritime Academy, Odessa, 4, Didrikhsona str., Odessa, Ukraine
e-mail: quantkva@mail.ru

NEW QUANTUM APPROACH TO DETERMINATION OF THE MOLECULAR SPECTRAL CONSTANTS AND PROBABILITIES FOR COOPERATIVE VIBRATION-ROTATION-NUCLEAR TRANSITIONS IN SPECTRA OF DIATOMICS AND THE HADRONIC MOLECULES

It is proposed a new approach to construction of the potential function of diatomic molecules as a sum of the known perturbed Morse oscillator function, the Simons-Parr-Finlan molecular potential in the middle of the potential curve, function of the -Cn/R^n type at the large internuclear distances. Within this approach it is presented a precise scheme for computing the molecular spectral parameters, namely, vibrational, rotational, centrifugal constants for the electronic states of diatomics. As application it was carried out calculation of the of molecular constants (cm-1) for the $X^1\Sigma^+$ $B^1\Pi$ states of the KRb dimer and rubidium dimer and performed further comparison with experimental data. Within consistent approach to calculation of the electron-nuclear γ transition spectra (set of vibration-rotational satellites in molecule) of molecule there are obtained the estimates for vibration-rotation-nuclear transition probabilities in a case of the emission and absorption spectrum of nucleus ^{127}I ($E^{(0)\gamma}$= 203 keV) in the molecule of H127I for different approximations of the for potential curves: the harmonic oscillator, the Dunham model and presented approach.

From physical viewpint it is obvious that any alteration of the molecular state must be manifested in the quantum transitions, for example, in a spectrum of the *g*-radiation of a nucleus (see for example [1-9]). In result of the gamma nuclear transition in a nucleus of a molecule there is arised a set of the electron-vibration-rotation satellites, which are due to an alteration of the state of the molecular system interacting with photon. The known example is the Szilard-Chalmers effect which results to molecular dissociation because of the recoil during radiating gamma quantum with large energy.

In series of works [3-9] it has been carried out detailed studying the co-operative dynamical phenomena due the interaction between atoms, ions, molecule electron shells and nuclei nucleons. There have been developed a few advanced approaches to description of a new class of dynamical laser-electron-nuclear effects in molecular spectroscopy, in particular, a nuclear gamma-emission or absorption spectrum of a molecule. A consistent quantum- mechanical approach to calculation of the electron-nuclear g transition spectra (set of vibration-rotational satellites in molecule) of a nucleus in the multiatomic molecules has been earlier proposed [5,7] and generalizes the well known approach by Letokhov-Minogin [4]. Earlier there were have been obtained estimates and calculations of the vibration-nuclear transition probabilities in a case of the emission and absorption spectrum of nucleus ^{191}Ir ($E^{(0)}$ = 82 keV) in the molecule of IrO_4, ^{188}Os ($E^{(0)}_g$ = 155 keV in OsO_4 and other molecules were listed. In Ref [8] there are firstly presented theoretical data on the vibration-nuclear transition

probabilities in a case of the emission and absorption spectrum of the nucleus of rhenium ^{186}Re ($E^{(0)}_g$ = 186.7 keV) in the molecule of ReO_4, estimated on the basis of the simplified version [5,7] of the consistent quantum-mechanical approach to cooperative electron-g-nuclear spectra (a set of the vibration-rotational satellites in a spectrum of molecule) of multiatomic molecules.

In this paper we present a genetralization of the cited theory of cooparative electron-gamma-nuclear (vibrational, rotational) transitions in a case of the diatomic moleules using new principle of construction of the potential curves for diatomic, which is in some degree analogous to the Smirnov approach [10,11]. Moreover the proposed method allow to determine the molecular spectral parameters, that ic checked on the example of the some alkali dimers. Besides, we will give a short generalization of the theory on a case of the exotic hadronic (pionic) molecules.

It should be noted that the diatomics potential function can be obtained on the decision of the electronic Schrödinger equation, however, due to significant computational difficulties in the present, this problem is reliably solving only for the case of the simplest diatomics having a small number of electrons [10-15]. In this regard, the first promising more used semi-empirical methodsy, where the potential curves are determined in the adiabatic approach using experimental vibrational and rotational spectroscopic constants. Some authors have studied solutions of the Schrodinger (or Klein-Gordon) equation with some known physical potential models, such as the Morse potential, Rosen-Morse potential, Manning-Rosen potential, Poschl-Teller potential, Deng-Fan potential, ring-shaped potential, and hyperbolic Scarf potential etc (look details for example in Ref. [10,16-18]).

Ler us remind shortly a scheme for computing the cooperative on the vibration-nuclear transition probabilities in a case of the emission and absorption spectrum of the nucleus of diatomics as the corresponding method is earlier presented in details (look [5-8]). The aim is to compute parameters of the gamma transitions (a probability of transition) or spectrum of the gamma satellites because of changing the electron-vibration-rotational states of the molecule under gamma quantum radiation (absorption).

Our purpose is calculation of a structure of the gamma transitions (probability of transition) or spectrum of the gamma satellites because of the changing the electron-vibration-rotational states of diatomic molecules under the gamma quantum radiation (absorption). In adiabatic approximation a wave function of molecule is multiplying the electronic wave function and wave function of nuclei: $y(r_e)y(R_1,R_2)$. Hamiltonian of interaction of the gamma radiation with system of nucleons for the first nucleus can be expressed through the co-ordinates of nucleons r_n' in a system of the mass centre of the first nucleus [4,7]:

$$H(r_n) = H(r_n')\exp(-ik_\gamma R_1) \qquad (1)$$

where k_g is a wave vector of the gamma quantum. The matrix element for transition from initial state "a" to final state "b" is presented as usually:

$$< \Psi^*_b(r_n) \mid H(r_n) \mid \Psi_a(r_n) > \bullet$$

$$\bullet < \Psi^*_b(r_e)\Psi^*_b(R_1,R_2) \mid e^{-ik_\gamma R_1} \mid \Psi_a(r_e)\Psi_a(R_1,R_2) > \qquad (2)$$

The first multiplier in (1) is defined by the gamma transition of nucleus and is not dependent upon an internal structure of molecule in a good approximation. The second multiplier is a matrix element of transition of the molecule from initial state "a" to final state "b":

$$M_{ba} = < \Psi^*_b(r_e) \mid \Psi_a(r_e) > \bullet$$
$$\bullet < \Psi^*_b(R_1,R_2) \mid e^{-ik_\gamma R_1} \mid \Psi_a(R_1,R_2) > \qquad (3)$$

The expression (7) gives a general formula for calculation of the probability of changing internal state of molecule under absorption or emitting gamma quantum by nucleus of the molecule and defines an amplitude of the corresponding gamma satellites. Their positions are fully determined by the energy and pulse conserving laws as follows [2]:

$$\pm E_\gamma + E_a + (1/2)Mv_0^2 = \pm E^{(0)}_\gamma + E_b + (1/2)Mv^2 \qquad (4)$$
$$Mv_0 \pm \hbar k_\gamma = Mv$$

Here M is the molecule mass, v_0 and v are velocities of molecule before and after interaction of

nucleus with g quantum, E_a and E_b are the energies of molecule before and after interaction, E_g is an energy of nuclear transition. Then an energy of the g satellite is as follows):

$$E_\gamma = E_\gamma^{(0)} + \hbar k_\gamma v_0 \pm R_{om} \pm (E_b - E_a) \qquad (5)$$

Here R_{om} is an energy of recoil: $R_{om} = [(E_g^{(o)}]^2/2Mc^2$. It is well known (c.f.[4,7]) that the practical interest are presented only transitions between vibration-rotational levels of the ground electron state, including transitions into continuum with further molecular dissociation. The matrix element of transition for these transitions is

$$M_{ba} = < \Psi_b^*(R_1, R_2) | e^{-ik_\gamma R_1} | \Psi_a(R_1, R_2) > \qquad (6)$$

The values of energy, accepted by vibration and rotational degrees of freedom of the molecule are as follows:

$$\varepsilon_{vib} \approx v\hbar\omega = R_{om}(m_2/m_1),$$
$$\varepsilon_{rot} \approx BJ^2 = R_{om}(m_2/m_1). \qquad (7)$$

The simple adequate model for definition of the rotational motion is the rigid rotator approximation. In this approximation the wave functions with definite values of quantum numbers J,K are the eigen functions of the angle momentum operator, i.e.:

$$\psi(R_1,R_2) = Y_{J,K}(\theta, \varphi). \qquad (8)$$

In a case of the vibration motion the wave functions with definite value of the vibration quantum number are numerically found by

solving the corresponding Schrödinger equation with potential function, choice of which was discussed above. The simple approximation is surely the harmonic oscillator onee. The harmonic oscillator wave functions were used for estimating matrix elements of the vibration-nuclear transitions in ref. [4]. In general the matrix element of the vibration-rotation-nuclear transition can be written as follows:

$$M^{v_b,v_a}_{J_b,K_b;J_a,K_a} = (4\pi)^{1/2}[(2J_a+1)(2J_b+1)]^{1/2}(-1)^{K_b}$$
$$\sum_{l=|J_b-J_a|}^{J_a+J_b} i^l \{2l+1\}^{1/2} < \Psi_{v_b} | (\pi/2a)^{1/2} J_{l+1/2}(a) | \Psi_{v_a} >$$
$$\begin{pmatrix} J_a & J_b & l \\ 0 & 0 & 0 \end{pmatrix} \sum_{m=-l}^{+l} Y^*_{lm} \begin{pmatrix} J_a & J_b & l \\ k_a & -k_b & m \end{pmatrix}$$

$$a = (E_\gamma^{(o)}/\hbar c)(m_2/M)R^*(1 + Q/[(m)^{1/2}R^*] \qquad (9)$$

Here $Q=(R-R_o)(m)^{1/2}$, $m=m_1m_2/M$ is the reduced mass of the molecule, m_1 and m_2 are the masses of nuclei. The co-ordinate of mass centre of the first nucleus relatively the molecule mass centre is defined by expression:

$$R_1 = -(m_2/M)R = -(m_2/M)[R_o + Q/(m)^{1/2}] =$$
$$-(m_2/M)R_o - (m_2/m_1M)^{1/2}Q$$

The corresponding probability can be written in the following form:

$$P^{v_b v_a}_{J_b J_a} = (2J_b+1)$$
$$\sum_{l=|J_b-J_a|}^{J_a+J_b} \{2l+1\} | < \Psi_{v_b} | (\pi/2a)^{1/2} J_{l+1/2}(a) | \Psi_{v_a} > |^2 \cdot$$
$$\begin{pmatrix} J_a & J_b & l \\ 0 & 0 & 0 \end{pmatrix}^2 \qquad (10)$$

Our new approach in in construction of the final potential function as a sum of a few potentyial curves. Each diatomic potential curve dimer is approximated by three functions corresponding to different portions of it. As in Ref. [10], the first portion is approximated by the known perturbed Morse oscillator function:

$$U(R) = V_e\left(y^2 + \sum_{n=4}^{\infty} b_n y^n\right),$$
$$y = 1 - \exp[-\rho(R - R_e)], \qquad (11)$$

where R, R_e- and equilibrium internuclear internuclear distance; V_e, ρ, b_n - the parameters of the Morse oscillator function.

tion VM.

Often in the middle of the potential curve (it is experimentally investigated range of vibrational quantum numbers) it is usuaaly used the potential of the Rydberg-Klein-Rees (look for example [10-15,18]). This potential curve has not the analytical form, and it is built as a set of R_{min} and R_{max} classical turning points for experimental study of vibrational energy levels. Insit of it in our new scheme we apply the Simons-Parr-Finlan molecular potential which looks as follows [15]:

$$U(r) = B_0[(r - r_e)/r]^2\{1 + \sum_n b_n[(r - r_e)/r]^n\} \qquad (12a)$$

or introducing $x = r - r_0$:

$$U(r) = B_0[x/(x + r_0]^2\{1 + \sum_n b_n[x/(x + r_0]^n\} \qquad (12b)$$

where the coefficients b_i are linked with corresponding molecular constants [14].

Finally, the plot of the potential curve for large values of the internuclear distance is approximated by the standard function:

$$U(R) = D_e - \sum \frac{C_n}{R^n} - \Delta U_{\text{обм}}(R), \qquad (13)$$

where D_e - experimental value of dissociation energy; C_n – the function parameters (6); n = 3-8. Let us note that the model (11)-(13) is obviously more exact and consistent in comparison with a simple harmonic oscillator one. As an application it was carried out computing the rubidium dimers (Rb2, KRb) diatomics spectral parameters. The results of calculation of molecular constants (cm^{-1}) for the $X^1\Sigma^+$ state of the KRb dimer are presented in table 1 tohether with experimental data [10,19,20] and theoretical data [10,11] obtained with using the Morse- Rydberg - Klein - Rees (M-RKR) method.

Table 1

The molecular constants (cm^{-1}) for the $X^1\Sigma^+$ state of the KRb dimer: Experimantal data – Exp; Theory: a- [10]; b- our data

KRb	$X^1\Sigma^+$		
	Th: a	Th: b	Exp
ω_e	75,846	75,844	75,842
$\omega_e x_e$	0,230	0,230	0,230
$\omega_e y_e$	–3,7(–4)	–3,8(–4)	–3,9(–4)
$\omega_e z_e$	–3,7(–6)	–3,5(–6)	– 3,1(–6)
B_e	0,03815	0,03812	0,03813
α_e	1,21(–4)	1,20(–4)	1,20(–4)
γ_e	–7,3(–7)	–7,3(–7)	–7,4(–7)
D_e	3,85(– 8)	3,85(– 8)	3,86(–8)
H_e	3,7(–14)	3,7(–14)	3,7(–14)

Table 2 contains the results of calculation of molecular constants (cm^{-1}) for the $B^1\Pi$ (b) state of the KRb dimer

Table 2

The molecular constants (cm^{-1}) for for the $B^1\Pi$ (b) state of the KRb dimer: Experimantal data – Exp; Theory -our data

KRb	$B^1\Pi$	
	Theory	Exp
ω_e	61,258	61,256
$\omega_e x_e$	0,2095	0,2089
$\omega_e y_e$	2,88(– 3)	2,87(– 3)
$\omega_e z_e$	–1,034(–4)	–1,031(–4)
B_e	0,03287	0,03288
α_e	7,54(– 5)	7,41(– 5)
γ_e	–1,12(– 5)	–1,13(–5)
D_e	3,75(– 8)	3,79(–8)
H_e	5,5(– 14)	5,7(–14)

Tables 3 and 4 contains the same data for states of the rubidium dimer for the $^1\Sigma^+_g$ and $(1)^1\Pi_u$(B) states.

Table 3

The molecular constants (cm^{-1}) for the $^1\Sigma^+_g$ state of the Rb2 dimer: Experimantal data – Exp; Theory: a- [11]; b- our data

	[16]	Our data	Exp
ω_e	31,4883	31,4884	31,4880
$\omega_e x_e$	–0,1140(–1)	– 0,1142(–1)	–0,1144(–1)
$\omega_e y_e$	–4,255(–4)	– 4,263(–4)	–4,269(–4)
$\omega_e z_e$	7,20(–7)	7,31(–7)	7,40(–7)
B_e	0,13433(–1)	0,13435(–1)	0,13431(–1)
α_e	–1,449(–6)	– 1,468(–6)	–1,485(–6)
γ_e	–4,136(–7)	– 4,132(–7)	–4,122(–7)

Table 4

The molecular constants (cm^{-1}) for the $(1)^1\Pi_u$(B) state of the Rb2 dimer: Experimantal data – Exp; Theory: our data

Rb_2	Theory	Exp
ω_e	47,471	47,470
$\omega_e x_e$	0,1431	0,1430
$\omega_e y_e$	– 8,351(– 7)	-
B_e	0,19529(– 1)	0,19523(– 1)
α_e	1,02(– 4)	1,00(– 4)
γ_e	1,564(– 7)	1,561(– 7)

Analsysis of the listed data show a physically reasonable agreement beyween thepretical and experimental data. Further we present the accurate data on the probabilities for vibration-rotation-nuclear transitions from state with v_a=0, J_a=0 and state v_a=1, J_a=0 in a case of the emission and absorption spectrum of nucleus ^{127}I ($E^{(0)}_g$= 203 keV) linked with molecule $H^{127}I$ in the ground electron state X^1S (molecular parameters: R_o=1,61Å, n_e=2309 cm^{-1}, B=6,55cm^{-1}). The recoil energy for this molecule is 0,172 eV. Parameters which define excitation of vibrations and rotations for this molecule because of the recoil, are as follows: a_o=1.30 and e_o=5.29×10^{-2} It should be noted also that a width of the gamma lines are corresponding to temperature T=300K. In figure 1 we present the calculated spectrum of emission and adsorption of nucleus ^{127}I in the $H^{127}I$.

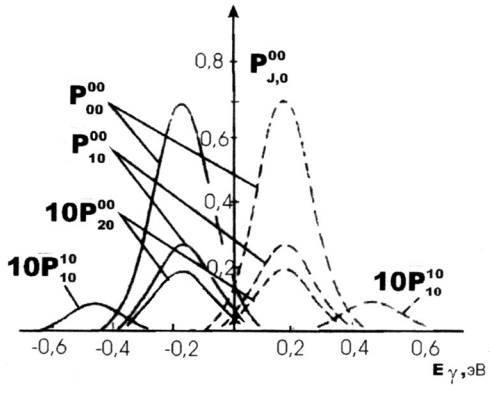

(a)

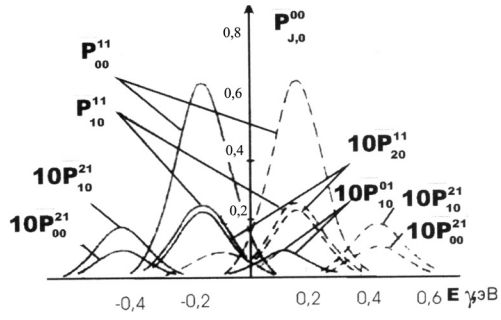

(b)

Fig. 1. Computed emission (solid curve) and absorption spectrum of nucleus ^{127}I ($E^{(0)}_g$ = 203 KeV) in the molecule $H^{127}I$. Initial state of molecule: a). above n_a=0, J_a=0 and b). below n_a=1, J_a=0 (our data)

We have made comparison of the corresponding vibration-rotation-nuclear transition parobailities from state with v_a=0, J_a=0 and state v_a=1, J_a=0 in a case of the emission and absorption spectrum of nucleus ^{127}I ($E^{(0)}_g$= 203 keV) in the $H^{127}I$ for different approximations of the for potential curves: the harmonic oscillator [4], the Dunham model [5,7] and presented approach. The values for probabilities, calculated within the present approach and Dunham model for potential curve [7,8], differ from the corresponding ones, calculated within the harmonic oscillator approximation [1], in average on 5-20%. A direct experimental observation of the cooperstive electron-ganna-nuclear effects represents a great fundamental interest. Finally let us note that the presented theory is related to usual molecular systems. At the same time in the last years a great attention is turn to the exotic (hadronic) atomic and molecular systems such pionic and kaonic atoms and molecules. The difference between the usual and exotic molecules at the theoretical level is obviously provided by using the Schrodinger equation in a case of usual molecules and the Klein-Gordon-Fock equation for the pionic and kaonic systems. Taking into accout the results of the last two decades on succseful solutions of the Klein-Gordon-Fock equation with the difeerent (for example, Morse etc) [18] potentials our theory is naturally generalized on a case of exotic diatomic molecules. All theoretical positions are remained the same. Simulteniuosly it is self-undrestood that the relatively quick radiative processes with

chartacteristic life less than the negative pion and kaon lifetime (~10^{-8}s) are of a direct theoretical and practical interest.

References

1. Letokhov V S, 1977 Laser Spectroscopy, Academic Press, N.-Y.
2. Letokhov V.S., Using lasers in Atomic, nuclear and molecular physics//In: Apllication of Lasers in Atomic, Nuclear and Molec. Phys.. Ed. Prokhorov A.M., Letokhov V.S.-Moscow: Nauka, 1979.-P.405-414.
3. Goldansky V.I., Letokhov V.S., On problem of g laser on nuclear transitions //JETP.-1994.-Vol.67.-P.513-524;
4. Letokhov V.S., Minogin V., Spectrum of gamma transitions in nuclei of a diatomic molecule//JETP.-1995-Vol.69.-P.1569-1582.
5. Glushkov A.V., Khetselius O.Yu., Malinovskaya S.V., Spectroscopy of cooperative laser-electron nuclear effects in multiatomic molecules// Molec. Physics (UK).-2008.-Vol.106.-N9-10.-P.1257-1260.
6. Glushkov A.V., Malinovskaya S.V., Shpinareva I.M., Kozlovskaya V.P., Gura V.I., Quantum stochastic modelling energy transfer and effect of rotational and V-T relaxation on multiphoton excitation and dissociation for CF_3Br molecules// Int. Journ.Quant. Chem.-2005.-Vol.104, N4 .-P. 512-516.
7. Glushkov A.V., Kondratenko P.A., Buyadzhi V., Kvasikova A., Shakhman A., Sakun T., Spectroscopy of cooperative laser electron-γ-nuclear processes in polyatomic molecules// Journal of Physics: C Series (IOP, London, UK).-2014.-Vol.548.-P. 012025.
8. Glushkov A.V., Kondratenko P.A., Lopatkin Yu., Buyadzhi V., Kvasikova A., Spectroscopy of cooperative laser electron-g-nuclear processes in diatomics and multiatomic molecules// Photoelec-tronics.-2014.-Vol.23.-P.142-146.
9. Kvasikova A.S., On probabilities of the vibration-nuclear transitions in spectrum of the R**u**O_4 molecule//Photoelectronics.-2015.-Vol.24.-P.141-145.
10. Smirnov A.D., Calculation of radiative parameters for electron transition B1Π−X1Σ+ in molecule of KRb//Herald of the Bauman Moscow State Tech. Univ., Nat. Sci.- 2015.-N6.-P.52-62.
11. Smirnov A.D., Calculation of spectroscopic constants for the electronic states (2)1Σ+ g , (1)1Πu(B), (1)1Πg, (2)1Πu(C) of the rubidium dimer//Herald of the Bauman Moscow State Tech. Univ., Nat. Sci.- 2010.-N4.-P.60-72.
12. Ph.Duranrd, J.P.Malriew, Ab initio methods of Quantum Chemistry. Ed. Lawley K.P.,Chichester B.etc., N.-Y.: Academic Press,2004.-550p.
13. Simons G., Parr R.G., Quantum Chemistry, Academic Press, N-Y.-2002.
14. Simons G., Parr R.G., Finlan J.M., New alternative to the Dunham potential for diatomic molecules//J.Chem. Phys.-1993.-Vol.59.-P.3229-3242.
15. Glushkov A.V., A new method of determining the molecular ionization potentials // J. Appl. Spectr.-1998-Vol.49, N5.-P.840-843.
16. Glushkov A.V., Spectroscopic factors of diatomic molecules // Opt. Spektr.-1999.-Vol.66, N6.-P.1298-1301.
17. Glushkov A.V., The perturbation theory with a model zeroth approximation for molecules // Zhurn.Fiz.himii.-1999-T.65, N11.-S.2970-2976.
18. Tao Chen, Shu-Rong Lin, and Chun-Sheng Jia, Solutions of Klein-Gordon equation with the improved Rosen-Morse potential energy model//Eur. Phys.J.Plus.-2013.-Vol.128.-P.69-76.
19. Radtsig A.A., Smirnov B.M., Handbook of atomic and molecular physics, M .: Energoatomisdat, 1996.- 240P.
20. Huber K.-P., Herzberg G., Conctants of Diatomic Molecules.-Voscow: Mir.-1994.-Vol.1,2.-408P., 360P.

The articles were received from 1.04 up to 30.05.2016

UDC 539.183

A. S. Kvasikova, V. F. Mansarliysky, A. A. Kuznetsova, Yu. V. Dubrovskaya, E. L Ponomarenko

NEW QUANTUM APPROACH TO DETERMINATION OF THE MOLECULAR SPECTRAL CONSTANTS AND PROBABILITIES FOR COOPERATIVE VIBRATION-ROTATION-NUCLEAR TRANSITIONS IN SPECTRA OF DIATOMICS AND THE HADRONIC MOLECULES

Abstract

It is proposed a new approach to construction of the potential function of diatomic molecules as a sum of the known perturbed Morse oscillator function, the Simons-Parr-Finlan molecular potential in the middle of the potential curve, function of the $-Cn/R^n$ type at the large internuclear distances. Within this approach it is presented a precise scheme for computing the molecular spectral parameters, namely, vibrational, rotational, centrifugal constants for the electronic states of diatomics. As application it was carried out calculation of the of molecular constants (cm^{-1}) for the $X^1\Sigma^+$ $B^1\Pi$ states of the KRb dimer and rubidium dimer and performed further comparison with experimental data. Within consistent approach to calculation of the electron-nuclear g transition spectra (set of vibration-rotational satellites in molecule) of molecule there are obtained the estimates for vibration-rotation-nuclear transition probabilities in a case of the emission and absorption spectrum of nucleus ^{127}I ($E^{(0)}_g$ = 203 keV) in the molecule of $H^{127}I$ for different approximations of the for potential curves: the hadmonic oscillator, the Dunham model and presented approach.

Key words: electron-g-nuclear transition spectrum, molecules, spectral parameters

УДК 539.183

А. С. Квасикова, В. Ф. Мансарлийский, А. А. Кузнецова, Ю. В. Дубровская, Е. Л. Пономаренко

НОВЫЙ КВАНТОВЫЙ ПОДХОД К ОПРЕДЕЛЕНИЮ МОЛЕКУЛЯРНЫХ СПЕКТРАЛЬНЫХ КОНСТАНТ И ВЕРОЯТНОСТЕЙ КООПЕРАТИВНЫХ КОЛЕБАТЕЛЬНО-ВРАЩАТЕЛЬНО-ЯДЕРНЫХ ПЕРЕХОДОВ В СПЕКТРАХ ДВУХАТОМНЫХ И АДРОННЫХ МОЛЕКУЛ

Резюме

Предлагается новый подход к построению потенциальной функции двухатомных молекул в виде суммы известного возмущенной функции осциллятора Морзе, молекулярного потенциала Simons-Парра-Finlan в средней части потенциальной кривой, функции типа $-C_n/R^n$ при больших межъядерных расстояниях. В рамках этого подхода развита прецизионная схема вычисления молекулярных спектральных параметров, а именно колебательных, вращательных, центробежных постоянных для электронных состояний двухатомных молекул. В качестве приложения проведено вычисление молекулярных констант ($см^{-1}$) для состояний $X^1\Sigma^+$ $B^1\Pi$ димера KRb и димера рубидия и выполнено сравнение с экспериментальными данными. В рамках последовательного подхода к расчету спектров электронно-гамма-ядерных переходов (набор колебательно-вращательных спутников в молекуле) в молекуле получены оценки для колебательно-

вращательных-ядерных вероятностей переходов в случае испускания и поглощения спектра ядро ^{127}I ($E^{(0)}_g$ = 203 keV)) в молекуле $H^{127}I$ для различных приближений для потенциальных кривых: модели гармонического осциллятора, модели на основе потенциала Данхэм и предложенного в работе нового подхода.

Ключевые слова: спектр электрон- g -ядерных переходов, молекулы, спектральные параметры

УДК 539.183

Г. С. Квасикова, В. Ф. Мансарлійський, А. О. Кузнецова, Ю. В. Дубровська, О. Л. Пономаренко

НОВИЙ КВАНТОВИЙ ПІДХІД ДО ВИЗНАЧЕННЯ МОЛЕКУЛЯРНИХ СПЕКТРАЛЬНИХ КОНСТАНТ І ІМОВІРНОСТЕЙ КООПЕРАТИВНИХ КОЛИВАЛЬНО- ОБЕРТАЛЬНО -ЯДЕРНИХ ПЕРЕХОДІВ У СПЕКТРІ ДВОАТОМНИХ І АДРОННИХ МОЛЕКУЛ

Резюме

Пропонується новий підхід до побудови потенційної функції двохатомних молекул у вигляді суми відомого обуреної функції осцилятора Морзе, молекулярного потенціалу Simons-Парра-Finlan в середній частині потенційної кривої, функції типу $-C_n / R^n$ при великих меж'ядерних відстанях. В рамках цього підходу розвинена прецизійна схема обчислення молекулярних спектральних параметрів, а саме коливальних, обертальних, відцентрових постійних для електронних станів двохатомних молекул. Як додаток проведено обчислення молекулярних констант (**см-1**) для станів $X^1\Sigma^+$ $B^1\Pi$ димера KRb і димера рубідію і виконано порівняння з експериментальними даними. В рамках послідовного підходу до розрахунку спектрів електронно-гамма-ядерних переходів (набір колебательно-обертальних супутників в молекулі) в молекулі отримані оцінки для колебательно-обертальних-ядерних ймовірностей переходів в разі випускання і поглинання спектра ядро ^{127}I ($E^{(0)}_g$ = 203 keV) в молекулі $H^{127}I$ для різних наближень для потенційних кривих: моделі гармонійного осцилятора, моделі на основі потенціалу Данхем і запропонованого в роботі нового підходу.

Ключові слова: спектр електрон- g -ядерних переходів, молекули, спектральні параметри

Інформація для авторів наукового збірника «Photoelectronics»

У збірнику "Photoelectronics " друкуються статті, що містять відомості про наукові дослідження і технічні розробки в напрямках:

*** фізика напівпровідників;**
*** гетеро- і низькорозмірні структури;**
*** фізика мікроелектронних приладів;**
*** лінійна і нелінійна оптика твердого тіла;**
*** оптоелектроніка та оптоелектронні прилади;**
*** квантова електроніка;**
*** сенсорика**

Збірник "Photoelectronics видається англійською мовою. Рукопис подається автором у двох примірниках англійською і російською мовами.

Електронна копія статті повинна відповідати наступним вимогам:
1. Для тексту дозволяються наступні формати - MS Word (rtf, doc).
2. Рисунки приймаються у форматах – EPS. TIFF. BMP, PCX, JPG. GIF, CDR. WMF, MS Word I MS Giaf, Micro Calc Origin (opj).

Рукописи надсилаються за адресою:
Відп. секр. Куталовій М. І., вул. Пастера, 42. фіз. фак. ОНУ, м. Одеса, 65082
E-mail: photoelectronics@onu.du.ua
тел. 0482 - 726 6356 .

Збірники "Photoelectronics" знаходяться на сайті: http://photoelectronics.onu.edu.ua

До рукопису додаються:
1. Коди PAC і УДК. Допускається використання декількох шифрів, що розділяються комами.
2. Прізвища і ініціали авторів.
3. Установа, повна поштова адреса, номер телефону, номер факсу, адреси електронної пошти для кожного з авторів.
4. Назва статті.
5. Резюме обсягом до 200 слів пишеться англійською, російською і (для авторів з України) – українською мовами.

Текст друкувати шрифтом 14 пунктів через два інтервали на білому папері формату А4. Назва статті, а також заголовки підрозділів друкуються прописними літерами. .
Рівняння необхідно друкувати в редакторі формул MS Equation Editor. Необхідно давати визначення величин, що з'являються в тексті вперше.
Посилання на літературу друкувати через два інтервали, нумеруватися в квадратних дужках послідовно, у порядку їхньої появи в тексті статті. Посилатися необхідно на літературу, що видана пізніше 2000 року.
Підписи до рисунків і таблиць друкуються в тексті рукопису в порядку їхньої ілюстрації.
Резюме обсягом до 200 слів друкується англійською, російською і українською мовами (для авторів з України). Перед текстом резюме відповідною мовою вказуються УДК, прізвища та ініціали всіх авторів, назва статті.

Информация для авторов
Научного сборника «Photoelectronics »

В сборнике "Photoelectronics " печатаются статьи, которые содержат сведения о научных исследованиях и технических разработках в направ-лениях:

*** физика полупроводников;**
*** гетеро- и низкоразмерные структуры;**
*** физика микроэлектронных приборов;**
*** линейная и нелинейная оптика твердого тела;**
*** оптоэлектроника и оптоэлектронные приборы;**
*** квантовая электроника;**
*** сенсорика**

Сборник"Photoelectronics издаётся на английском языке. Рукопись подается автором в двух экземплярах на английском и русском языках.

Электронная копия статьи должна отвечать следующим требованиям:
1. Для текста допустимы следующие форматы - MS Word (rtf, doc).
2. Рисунки принимаются в форматах – EPS. TIFF. BMP, PCX, JPG. GIF, CDR. WMF, MS Word И MS Giaf, Micro Calc Origin (opj).

Рукописи присылаются по адресу:
Отв. секр. Куталовой М. И., ул. Пастера. 42. физ. фак. ОНУ, г. Одесса, 65026
E-mail:photoelectronics@onu.du.ua тел. 0482 - 726 6356 .

Статьи сб."Photoelectronics " находятся на сайте: http://photoelectronics.onu.edu.ua

К рукописи прилагается:
1. Коды PAC и УДК. Допускается использование нескольких шифров, которые разделяются запятой.
2. Фамилии и инициалы авторов.
3. Учреждение, полный почтовый адрес, номер телефона, номер факса, адреса электронной почты для каждого из авторов.
4. Название статьи.
5. Резюме объемом до 200 слов пишется на английском, русском языках и (для авторов из Украины) – на украинском.

Текст должен печататься шрифтом 14 пунктов через два интервала на белой бумаге формата А4. Название статьи, а также заголовки подразделов печатаются прописными буквами и отмечаются полужирным шрифтом.

Уравнения необходимо печатать в редакторе формул MS Equation Editor. Необходимо давать определение величин, которые появляются в тексте впервые.

Ссылки на литературу должны печататься через два интервала, нумероваться в квадратных скобках последовательно, в порядке их появления в тексте статьи. Ссылаться необходимо на литературу, которая издана позднее 2000 года.

Подписи к рисункам и таблицам печатаются в тексте рукописи в порядке их иллюстрации.

Резюме объемом до 200 слов печатается на английском, русском языках и на украинском (для авторов из Украины). Перед текстом резюме соответствующим языком указываются УДК, фамилии и инициалы всех авторов, название статьи.

Information for contributors of «Photoelectronics» articles

"Photoelectronics" Articles publishes the papers which contain information about scientific research and technical designs in the following areas:

- Physics of semiconductors;
- Physics of microelectronic devices;
- Linear and non-linear optics of solids;
- Optoelectronics and optoelectronic devices;
- Quantum electronics;
- Sensorics.

"Photoelectronics" Articles is defined by the decision of the Highest Certifying Commission as the specialized edition for physical-mathematical and technical sciences and published and printed at the expense of budget items of Odessa I.I. Mechnikov National University.

«Photoelectronics» Articles is published in English. Authors send two copies of papers in English. The texts are accompanied by 3.5» diskette with text file, tables and figures. Electronic copy of a material can be sent by e-mail to the Editorial Board and should meet the following requirements:

1.The following formats are applicable for texts – MS Word (rtf, doc).

2. Figures should be made in formats – EPS, TIFF, BMP, PCX, JPG, GIF, WMF, MS Word I MS Giaf, Micro Calc Origin (opj). Figures made by packets of mathematical and statistic processing should be converted into the foregoing graphic formats.

The papers should be sent to the address:

Kutalova M.I., Physical Faculty of Odessa I.I. Mechnikov National University, 42 Pastera str, 65026 Odessa, Ukraine, e-mail: wadz@mail.ru, tel. +38-0482-7266356. Information is on the site:

http://www.photoelectronics.onu.edu.ua

The title page should contain:

1. Codes of PACS
2. Surnames and initials of authors
3. TITLE OF PAPER
4. Name of institution, full postal address, number of telephone and fax, electronic address

An abstract of paper should be not more than 200 words. Before a text of summary a title of paper, surnames and initials of authors should be placed.

Equations are printed in MS Equation Editor.

References should be printed in double space and should be numbered in square brackets consecutively throughout the text. References for literature published in 2000-2009 years are preferential.

Illustrations will be scanned for digital reproduction. Only high-quality illustrations will be taken for publication. Legends and symbols should be printed inside. Neither negatives, nor slides will be taken for publication. All figures (illustrations) should be numbered in the sequence of their record in text.

For additional information please contact with the Editorial Board.

Верстка – О. І. Карлічук

Підп.до друку 15.09.2016. Формат 60×84/8. Ум.-друк.арк. 17,67. Тираж 300 прим. Замов. № 1461.

Видавець і виготовлювач
«Одеський національний університет імені І. І. Мечникова»
Свідоцтво ДК № 4215 від 22.11.2011 р.

65082, м. Одеса, вул. Єлісаветинська, 12, Україна
Тел.: (048) 723 28 39, e-mail: druk@onu.edu.ua